

A Thesis Submitted for the Degree of PhD at the University of Warwick

Permanent WRAP URL:

<http://wrap.warwick.ac.uk/139730>

Copyright and reuse:

This thesis is made available online and is protected by original copyright.

Please scroll down to view the document itself.

Please refer to the repository record for this item for information to help you to cite it.

Our policy information is available from the repository home page.

For more information, please contact the WRAP Team at: wrap@warwick.ac.uk

**Structural Studies of Secondary and Multi-Centre Bonding
in Compounds of the Non-Metals**

By

Jeffery Frederick Sawyer

**A thesis submitted to the University of Warwick in
partial fulfilment of the requirements for the degree
of Doctor of Philosophy**

**Department of Molecular Sciences,
University of Warwick,
Coventry CV4 7AL,
Warwickshire.**

October, 1977



ACKNOWLEDGEMENTS

The work described here was carried out in the Department of Molecular Sciences at the University of Warwick. I would like to thank my supervisor, Dr N.W. Alcock, for his patient guidance, encouragement and much helpful discussion during the course of this work. My sincere thanks also go to Drs. R.M.C. Countryman, H.M. Colquhoun, T.J. Greenhough and Professor M.G.H. Wallbridge for many helpful comments. I would also like to acknowledge the contributions of Dr. S.E. Esperas who collected the data for and initially solved the structure of iodobenzene bis(dichloroacetate) and also collected the first data set for the compound $[\text{Me}_4\text{N}]^+ - [\text{Me}_2\text{N}(\text{ICl}_2)]^-$. Finally I would like to thank all those who supplied crystals, the staff of the Computer Centre who patiently processed my many jobs, and Mrs. J.I. McKeand for typing the thesis.

A postgraduate studentship from the Science Research Council is gratefully acknowledged.

Parts of the work contained in this thesis have been published or accepted for publication in the scientific literature with the following references:

N.W. Alcock and J.F. Sawyer, Acta Cryst., 1976, B32, 285.

N.W. Alcock and J.F. Sawyer, J. Chem. Soc. Dalton, 1977, 1090.

N.W. Alcock, B.T. Golding, P.V. Ioannu and J.F. Sawyer, Tetrahedron, in press.

N.W. Alcock, H.M. Colquhoun, G. Haran, J.F. Sawyer and M.G.H. Wallbridge, J. Chem. Soc. Chem. Comm., 1977, 368.

N.W. Alcock, S. Esperas, J.F. Sawyer, N.D. Cowan, C.J. Ludman and T.C. Waddington, J. Chem. Soc. Chem. Comm., 1977, 403.

Copies of the available papers are included in Appendix B.

To My Parents

My parents, I am writing this to you because I want to tell you how much I love you and how much I appreciate you. You have been my greatest support and my greatest source of strength. I am proud of you and I am grateful for everything you have done for me. I hope this letter finds you well and happy. I love you both very much.

I hope you are both well and happy. I love you both very much. I hope this letter finds you well and happy. I love you both very much. I hope this letter finds you well and happy. I love you both very much.

ABSTRACT

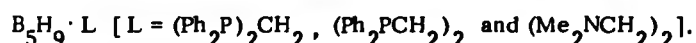
In this thesis the results of several crystal structure determinations are discussed in terms of their multi-centre inter- and intra-molecular bonding interactions. In Section 1 the structures reported form part of a systematic investigation into the importance of secondary bonding in determining the crystal packing and influencing primary geometry in compounds of the non-metals. In pursuance of this aim, the following crystal structures have been determined:-

- (1) The diethyl tin dihalides, Et_2SnX_2 ($\text{X} = \text{Cl}, \text{Br}, \text{I}$).
- (2) The solid solvate $\text{SeOCl}_2 \cdot \text{Dioxane}$ and the compound iodoxybenzene.
- (3) The compounds iodobenzene diacetate and iodobenzene bis-(dichloroacetate).
- (4) cis-3,5-Dibromo-4-oxo-2,2,6,6-tetramethylpiperidin-1-yloxy, a derived bis nitroxide and (Z, Z) 2,4-Dibromo-1,5-diphenylpenta-3-one.
- (5) The novel pseudo polyhalide anion $[\text{Me}_2\text{N}(\text{ICl})_2]^-$ as its tetramethylammonium salt.

Each of these structures is discussed in relation to similar examples. In some cases no secondary bonds were found, and possible reasons for this are given. In others, a three-centre overlap of a σ^* orbital with two lone pairs is proposed as a viable alternative to the principal linear arrangement $\text{X}-\text{A} \dots \text{Y}$ of primary and secondary bonds found in most examples. A discussion of the significance of these structures in relation to current stereochemical and bonding models, including charge transfer descriptions of the interactions, and possible methods to quantify the strengths of these interactions are given in Chapter VI.

In Section 2 the topological descriptions of the structures of the boron hydrides and related compounds are discussed in terms of their multi-centre bonding interactions, and the classification of the geometries of the boron polyhedra as closo, nido, arachno and

hypho. The hypho class is by far the least well-known, and the crystal structures have been determined of three new examples isoelectronic with the hypothetical hypho $B_5H_{11}^{2-}$ ion, viz.



The geometries of these compounds are significantly different, illustrating the diversity possible within such a related series. The structural relationships between these compounds are discussed in terms of the involvement of phosphorus 3d orbitals in the bonding of the phosphine adducts, and the contribution of vacant orbital valence structures to the structure of the tetramethylene diamine adduct.

CONTENTS

	<u>page</u>
Chapter I. <u>The crystal and molecular structures of the</u>	
<u>dialkyl tin dihalides; tetrahedral versus</u>	
<u>octahedral geometries.</u>	1
(I. 1) <u>Introduction</u>	1
(I. 2) <u>Structural Tin Chemistry</u>	2
(I. 2. 1) Three co-ordinate tin	2
(I. 2. 2) Four co-ordinate tin	2
(I. 2. 3) Five co-ordinate tin	3
(I. 2. 3) Six co-ordinate tin	4
(I. 2. 5) Higher co-ordination numbers (> 6)	4
(I. 2. 6) Structural and related work on the Group IV organometal halides and pseudohalides	5
(I. 3) <u>Experimental</u>	7
(I. 3. 1) General	7
(I. 3. 2) Data Collections	9
(I. 3. 2(i)) Et_2SnCl_2 , compound (1)	9
(I. 3. 2(ii)) Et_2SnBr_2 , compound (2)	9
(I. 3. 2(iii)) Et_2SnI_2 , compound (3)	10
(I. 3. 2(iv)) Me_2SnBr_2 and Bu_2SnCl_2	10
(I. 3. 3) Structure Solution	11
(I. 3. 3. 1) The diethyl tin dihalides, compounds (1-3)	11
(I. 3. 3. 2) Dibutyl tin dichloride	12
(I. 4) <u>Discussion of the diethyl tin dihalides</u>	13
(I. 4. 1) General	13
(I. 4. 2) Intermolecular Interactions	19
(I. 4. 3) Factors affecting Intermolecular Interactions	21
(I. 4. 4) Hybridisation models and other physical measurements	23
(I. 5) <u>References</u>	24

	<u>page</u>
<u>Chapter II. The crystal and molecular structures of the solid solvate Seleninyl Dichloride Dioxane and of Iodoxybenzene; Distorted octahedral arrangements of Primary and Secondary Bonds.</u>	29
(II. 1) <u>Introduction</u>	29
(II. 2) <u>The solid solvates of seleninyl dichloride</u>	29
(II. 3) <u>Iodoxybenzene</u>	31
(II. 4) <u>Experimental</u>	31
(II. 4. 1) <u>Preparations and Data Collections</u>	31
(II. 4.1.1) $\text{SeOCl}_2 \cdot \text{Dioxane}$	31
(II. 4.1.2) <u>Iodoxybenzene</u>	32
(II. 4. 2) <u>Structure solution and refinement</u>	33
(II. 4.2.1) $\text{SeOCl}_2 \cdot \text{Dioxane}$	34
(II. 4.2.2) <u>Iodoxybenzene</u>	34
(II. 5) <u>Discussion</u>	38
(II. 5. 1) $\text{SeOCl}_2 \cdot \text{Dioxane}$	38
(II. 5. 2) <u>Iodoxybenzene</u>	41
(II. 6) <u>Octahedral or distorted octahedral arrangements of primary and secondary bonds</u>	44
(II. 7) <u>References</u>	48
<u>Chapter III The Iodobenzene Acetates; planar pentagonal systems with three-centre overlaps</u>	56
(III. 1) <u>Introduction</u>	56
(III. 2) <u>Experimental</u>	57
(III. 3) <u>Data Collection and Structure Solution</u>	57
(III. 3. 1) <u>Iodobenzene diacetate (compound 1)</u>	57
(III. 3. 2) <u>Iodobenzene bis(dichloroacetate) (compound 2)</u>	59
(III. 4) <u>Discussion of Structures</u>	60
(III. 4. 1) <u>General</u>	60
(III. 4. 2) <u>Bonding Models</u>	70
(III. 4. 3) <u>Factors affecting intermolecular interactions</u>	73
(III. 4. 4) <u>Conclusions</u>	75
(III. 5) <u>References</u>	84

	<u>page</u>
<u>Chapter IV. The crystal and molecular structures of two new spin labels and of α-α dibromobenzylidene acetone; pyramidal distortions of the nitroxide group and the importance of Br...O secondary bonds in the packing of organic molecules</u>	86
(IV. 1) <u>Introduction</u>	86
(IV. 2) <u>Data Collection and Structure Solution</u>	89
(IV. 2. 1) 3, 5-dibromo-4-oxo-2, 2, 6, 6-tetramethylpiperidin-1-yloxy (compound 1)	89
(IV. 2. 2) 4-[(2', 2', 5', 5'-tetramethylpyrrolin-1'-yloxy)-3'-carbonyloxy]-2, 2, 6, 6-tetramethyl-3, 5-dibromo-3, 4-dehydropiperidin-1-yloxy (compound 2)	90
(IV. 2. 3) (Z, Z)2, 4-Dibromo-1, 5-diphenyl-penta-1, 4-dien-3-one (compound 3)	91
(IV. 3) <u>Discussion of Structures</u>	94
(IV. 3. 1) Compounds (1) and (2)	94
(IV. 3. 2) (Z, Z)2, 4-Dibromo-1, 5-diphenyl-penta-1, 4-dien-3-one	99
(IV. 4) <u>The Nitroxide Group; distortions due to non-bonded interactions</u>	101
(IV. 5) <u>Halogen-Oxygen Secondary Bonding</u>	103
(IV. 6) <u>References</u>	106
<u>Chapter V. The X-ray Structure of a novel pseudo-polyhalide Anion [Me₂N(ICI)₂]⁻</u>	119
(V. 1) <u>Introduction</u>	119
(V. 2) <u>Experimental</u>	119
(V. 3) <u>Structure Solution and Refinement; Crystal Twinning</u>	121
(V. 4) <u>Discussion</u>	124
(V. 5) <u>References</u>	132

	<u>page</u>
<u>Chapter VI. A Discussion of Secondary Bonding and other</u>	
<u>Intermolecular Forces.</u>	135
(VI. 1) <u>Introduction</u>	135
(VI. 2) <u>Stereochemical Bonding Models</u>	135
(VI. 2. 1) Valence Shell Electron Pair Repulsion (VSEPR)	
theory	135
(VI. 2. 2) Galy Model	136
(VI. 2. 3) 3c-4e MO's	137
(VI. 3) <u>Intermolecular Forces</u>	138
(VI. 3. 1) Van der Waals interactions	138
(VI.3.1(i)) What are van der Waals forces ?	139
(VI. 3. 2) Charge Transfer Bonding	142
(VI. 4) <u>Quantitative Analyses of Secondary Bond Strengths</u>	144
(VI. 5) <u>Correlations between distances A-X and A...Y</u>	148
(VI. 6) <u>Application of Secondary Bonds</u>	156
(VI. 6. 1) Reaction Routes	156
(VI. 6. 2) Stabilisation of unusual valence states	157
(VI. 6. 3) Other physical measurements	158
(VI. 7) <u>References</u>	161
<u>Chapter VII. <u>Hypho</u> Boranes</u>	165
(VII. 1) <u>Introduction; n centre-m electron bonding</u>	165
(VII. 2) <u>Topological Models</u>	168
(VII. 2. 1) Lipscomb's <u>styx</u> notation	168
(VII. 2. 2) Wade's rules (<u>Hypho</u> systems)	169
(VII. 3) <u>Experimental</u>	175
(VII. 3. 1) Preparation	175
(VII. 3. 2) Data collection	176
(VII.3.2(i)) $B_5H_9 \cdot dppm$	176
(VII.3.2(ii)) $B_5H_9 \cdot dppe$	177
(VII.3.2(iii)) $B_5H_9 \cdot tmed$	178

	<u>page</u>
(VII. 3. 3) Structure Solutions	180
(VII.3.3(I)) $B_5H_9 \cdot dppm$	180
(VII.3.3(II)) $B_5H_9 \cdot dppe$	182
(VII.3.3(III)) $B_5H_9 \cdot tmed$	184
(VII. 4) Discussion	188
(VII. 5) References	204
<u>Chapter VIII. Crystallographic Methods</u>	235
(VIII. 1) X-Ray Diffraction	235
(VIII. 2) Structure Determination	235
(VIII. 3) Data Collection	236
(VIII. 4) Structure Solution	242
(VIII. 4. 1) The Patterson method	242
(VIII. 4. 2) Direct methods	244
(VIII. 5) Electron Density Maps	247
(VIII. 6) Least Squares Refinement	249
(VIII. 7) Systematic Errors	251
(VIII. 7. 1) Absorption	251
(VIII. 7. 2) Extinction	252
(VIII. 7. 3) Other factors; weighting schemes	253
(VIII. 8) References	256
Appendix A	258
Appendix B	259

LIST OF TABLES [†]

		page
I. 1	Unit cell data for the dialkyl tin dihalides R_2SnX_2 (R = Me, X = Br and I; R = Et, X = Cl, Br and I; and R = Bu, X = Cl)	8
I. 2	Atomic co-ordinates ($\times 10^4$) and anisotropic temperature factors ($\times 10$) for the diethyl tin dihalides	14
I. 3	Bond distances (\AA) and bond angles ($^\circ$)	15
II. 1	Atomic co-ordinates ($\times 10^4$) and anisotropic temperature factors ($\times 10^3$) with standard deviations in parentheses for (a) $SeOCl_2 \cdot$ Dioxane; (b) Iodoxy- benzene	49
II. 2	Significant bond lengths (\AA), contact distances and related bond angles ($^\circ$) for (a) $SeOCl_2 \cdot$ Dioxane, (b) Iodoxybenzene	51
II. 3	Dihedral angles in dioxane molecule	53
II. 4	Equations of the least squares mean planes	53
III. 1	Atomic co-ordinates ($\times 10^4$) and anisotropic temperature factors ($\times 10^3$)	76
III. 2	Bond lengths (\AA) and bond angles ($^\circ$)	79
III. 3	Equations of least squares mean planes	82
IV. 1	Atomic co-ordinates ($\times 10^4$) and anisotropic temperature factors ($\times 10^3$) for (a) 3,5-dibromo- 4-oxo-2,2,6,6-tetramethylpiperidin-1-yloxy, (b) the ester (2) derived from (1), (c) Z, Z 2,4- Dibromo-1,5-diphenyl-penta-1,4-diene-3-one	107
IV. 2	Bond distances and bond angles [for same compounds]	111
IV. 3	Least squares planes for (2) and (3)	115
V. 1	Atomic co-ordinates and temperature factors for $[Me_4N]^+[Me_2N(ICI)_2]^-$	125
V. 2	Bond lengths (\AA) and bond angles ($^\circ$)	125
V. 3	Twinning factors for some equivalent hOl and $\bar{1}Oh$ reflections	126

	<u>page</u>
VI. 1 Van der Waals and single bond radii (\AA), after A. Bondi	141
VI. 2 Geometrical parameters for some <u>cis-cis</u> -tetra-phenylbutadienyl dimethyl tin complexes	153
VI. 3 Correlation of Dihedral Angles with Secondary Bonding in Square Planar Tellurium Compounds	154
VII. 1 Starting reflection sets for multisolution direct methods program MULTAN	179
VII. 2 Known or postulated structures for tetramethylene diamine adducts of the boron hydrides	200
VII. 3 Some B_5H_9 vacant orbital species	202
VII. 4 Atomic co-ordinates and temperature factors	207
VII. 5 Bond distances and bond angles	216
VII. 6 Equations of least squares mean planes	226
VII. 7 Torsion angles in chelate rings	229
VII. 8 Atomic co-ordinates, bond distances and bond angles for the disordered tetrahydrofuran solvent in compound (1)	230

† In some cases an abbreviated title has been given to indicate the subject of the Table only.

Introduction

1. Secondary Bonding In Non-Metal Complexes

The initial definition of the term secondary bonding and a collation of the majority of the known structures in which this type of bonding interaction is prominent was published in a review which appeared in *Advances in Inorganic Chemistry and Radiochemistry* in 1972. Prior to this review, the chemical and structural significance of the weaker of these solid state interactions were not discussed in much detail and, in a vast number of cases, was completely omitted from discussion or else confined to a few values in tables of non-bonded contact distances. The exceptions to this were amongst the stronger (shorter) examples of this type of interaction, and these were included under the all-embracing title of charge transfer interactions or else were described as weak acid-base interactions. Several reviews have, in fact, included many of the compounds in the secondary bonding review under these latter descriptions. Whilst the charge transfer nomenclature is not incorrect, the secondary bonding interactions can be more specifically defined.

Thus, in the original thesis, the secondary bonding model considers that in non-metal complexes containing intra-molecular distances longer than normal bonds and/or inter-molecular distances that are shorter than van der Waals distances, these interactions can be considered as secondary bonds if certain criteria are satisfied. These criteria are:-

- (a) the interacting neighbour(s) are not in the most favourable positions for non-directed forces, and/or
- (b) the interacting neighbour(s) are in stereochemically significant positions.

These criteria are the same as those used for recognising bonding interactions compared to non-directional interactions of the van der Waals type. The stereochemically significant arrangement that was found to be important in virtually all of the known interactions was a linear system $Y-A \cdots X$, where $Y-A$ is a normal bond and $A \cdots X$ is a short inter-molecular (or intra-molecular) distance. Since then a series of compounds have been recognised (Chapter III) in which a significantly different stereochemical

arrangement occurs. It has also been observed (Chapter I) that interactions are not always significantly shorter than the van der Waals distance.

Having given the criteria whereby a secondary bond can be defined, it is perhaps important at this stage to indicate briefly the theoretical bonding description of these interactions. As can perhaps be seen from the nature of the criteria, a simple electrostatic description can be relatively easily dismissed. In fact the favoured view of these interactions is in terms of three-centre four-electron (3c, 4e) molecular orbitals. In a system of the type Y-A...X, the secondary bond A...X is formed by donation from a lone pair on X into the σ^* orbital of the Y-A primary bond. Alternatively (and equivalently) the interaction of the three σ -symmetry atomic orbitals (on Y, A and X) gives a filled bonding molecular orbital concentrated between A and Y, a filled non-bonding or weakly bonding orbital concentrated between A and X, and an empty antibonding orbital. The overall scheme is identical to the MO description of the hydrogen bond.

It is the intention in the first section of this thesis to describe the results of recent crystallographic studies in several areas of non-metal chemistry which have formed part of a systematic investigation of secondary bonding. Several factors affecting the strength of these interactions have been found. These and other conclusions about the role of secondary bonding in non-metal compounds are discussed in the final chapter of the section.

2. The Hypo Boranes

Whilst the majority of the interactions described in Section 1 of the thesis can be explained using 3c-4e molecular orbitals, the bonding in the boron hydrides, their ions, the closely related carboranes and similar compounds must be described using well-established 3c-2e molecular orbitals (and, in a relatively few cases, higher n-centre m-electron M.O's) since there are too few valence electrons available to provide a pair of electrons between every pair of atoms close enough to be regarded as covalently bonded (that is, by 2-centre-2-electron single bonds). These 3c-2e molecular orbitals result in a few basic structural features such as

hydrogen bridge bonding and three-centre open (and closed) triangular BBB face bonding being common to the majority of the structures. Lipscomb has described a topological model in which all the various theoretical valence structures based on these structural features are obtained from a set of rules. Alternatively (or equivalently) a good idea of the structure can be obtained from another set of simple rules due to Wade (and separately to Rudolph). These rules allow the structural class, and hence the geometry, to be predicted from the number of skeletal electron pairs in the structure. These rules are described in detail in Chapter VII. The first three structural types resulting from these rules are closo, nido and arachno, representing closed polyhedra and closed polyhedra missing one and two vertices respectively. These descriptions cover the majority of the boron hydrides and related structures. However, an extension of Wade's rules allows a fourth class to be recognised which was given the name HYPHO from the Greek for net. HYPHO structures may be described as being based on closed polyhedra with three vertices missing. The application of these rules is seen from the description of the crystal structures of several hypho boranes in Chapter VII of this thesis.

SECTION 1

CHAPTER I

The crystal and molecular structures of the dialkyl tin dihalides; tetrahedral versus octahedral geometries

(I.1.) Introduction

There have been a wealth of physical measurements made on organotin compounds since tin is readily adaptable to many physical techniques and these compounds have immense commercial value. The two common oxidation states of tin are Sn(II) and Sn(IV), and although the structures of their compounds might be expected to be based on a simple tetrahedral arrangement of ligands and lone pairs, extensive X-ray crystallographic investigations have established a marked tendency for the co-ordination number of the tin atom in these compounds to increase above four so that wide variety of structural types are known. The description of some of the higher stereochemistries varied in the past depending on what significance was given to certain inter- and intra-molecular contact distances in the crystal which are less than the sum of the van der Waals radii for the atoms concerned and which appear to have significant effect on the primary geometry and also the packing in the crystal via dimers or polymeric lattice type arrangements. In the majority of cases these interactions can be included into the secondary bonding model.¹

In this chapter, the crystal structures of diethyl tin dichloride, -dibromide and di-iodide and some preliminary results on dimethyl tin dibromide and dibutyl tin dichloride are reported, and the significance of the secondary bonds in distorting the molecular structures so that they are intermediate between tetrahedral and octahedral is discussed in relation to other known examples. Some related organo Sn(II) systems will be briefly covered.

(I.2.) Structural Tin Chemistry

Several reviews of the crystal chemistry of tin up to ca. 1972 have been published.² Probably the best method of classifying these structures is in terms of the co-ordination number of the tin atom. The inclusion and importance of secondary bonds in describing the overall stereochemistry can then be discussed. In particular, two research groups - those of Harrison and co-workers and Pellizzi and co-workers - have published the majority of the recent structures of organotin compounds, those of Harrison et al. normally being complexes of the organotin halides with Schiff's bases³ whilst Pellizzi et al. have concentrated on a series of organotin complexes containing nitrate groups which have various stereochemistries depending on what other ligands are attached to tin.⁴

(I.2.1.) Three co-ordinate tin

A single example of three co-ordinate tin will be discussed. This is the structure of the monomeric stannylene derivative $[(\text{Me}_3\text{Si})\text{C}]_2\text{SnCr}(\text{CO})_5$ which from an X-ray analysis contains the Group IV atom in an unusual three co-ordinate trigonal environment, the two carbon atoms, Sn and Cr being coplanar with a surprising low CSnCr angle (98°). There are no further intermolecular contacts less than 5 \AA .⁵

(I.2.2.) Four co-ordinate tin

In the crystal, tetra-aryl and tetra-alkyl tin compounds all contain tetrahedral molecules separated by van der Waals forces only. A compilation of recent structural determinations of tetra-aryl tin compounds can be found in ref. 6 where it is noted that molecular symmetry S_4 is consistently observed despite considerable variation in the molecular packing due to the aryl substituents. This strongly suggests that in these crystals, which all have tetragonal symmetry, conformations with S_4 symmetry must be energetically favoured.⁶ A tetrahedral arrangement of bonds about tin is also

found in the majority of compounds with dialkyl- and trialkyl tin-groups bonded to transition metals (e.g. $\text{Me}_3\text{SnMn}(\text{CO})_5$ and $\text{Ph}_3\text{SnMn}(\text{CO})_5^{2c}$) although there are some unusual distortions in these compounds. Notably, in the transition metal carbonyl derivatives, the $\text{M}-\text{C}\equiv\text{O}$ axes are found to deviate from linearity so as to bring the carbonyl groups towards the tin atom in an "umbrella effect".^{2c}

(I.2.3.) Five co-ordinate tin

Perhaps the earliest example of five co-ordinate tin observed was the pyridine adduct of trimethyl tin chloride.⁷ The normal geometry for this co-ordination number is trigonal bipyramidal and virtually all examples have this geometry albeit distorted to varying degrees. The bond lengths to the more electronegative axial ligands may be symmetrical or unsymmetrical but tend to be longer than those to the equatorial ligands. An arrangement of planar SnR_3 ($\text{R} = \text{alkyl or aryl}$) groups linked into polymeric chains via the axial ligands is quite common and can be found in trimethyl tin formate,^{3c} methoxide⁸, fluoroacetate and acetate⁹ and glycinate¹⁰ to give but a few examples. In these complexes it is quite common for the axial bonds to be unsymmetrical.

Five co-ordinate structures can also be obtained by intramolecular interactions involving either unsymmetrically bidentate ligands or by the formation of long dative interactions involving chelate rings of various sizes. An example is C,N-{2[(dimethylamino)methyl]phenyl} diphenyl tin bromide in which penta co-ordination results from using a structured ligand. The dimethylamino group and bromine atoms are axial.¹¹ The structure of (1,3-diphenylpropane-1,3-dionato)triphenyl tin(IV) similarly achieves penta-co-ordination by intramolecular co-ordination.¹² In these two structures, the intramolecular co-ordinate bond is significantly shorter and the resulting geometry more regular than several other examples of systems containing a secondary bond to

complete the trigonal bipyramidal geometry, notably in 4-bromo cis cis tetraphenylbutadienyldimethyltin(IV) bromide.¹³ (see section I.5). Similarly dimethyl tin chloride N N-dimethyldithiocarbamate has been described as being distorted trigonal bipyramidal due to an axial intra-molecular Sn...S contact of 2.79(1) Å from the bidentate dithiocarbamate. The electronegative chlorine is also axial with an Cl-Sn...S angle of 154°. ¹⁴

The second way Sn can obtain penta-co-ordination is seen in a series of stannocanes where the fifth bond is intra-molecular involving an oxygen or sulphur atom in the backbone of a fairly large chelating ring. Examples of this type of co-ordination are summarised in ref. 15.

Finally for Sn(II) compounds trigonal bipyramidal structures appear to be extremely common although SnO is a rare example with a square pyramidal structure.¹⁶

(I.2.4.) Six co-ordinate tin

This stereochemistry is based on an octahedron or distorted octahedron, especially in complexes of the diorgano- and triorgano-tin halides with Lewis bases. Again in these compounds the degree of distortion of the octahedral arrangement can be related to the strength of the inter- and intra-molecular secondary bonding amongst other factors. In some cases there may be some ambiguity in the description of the overall geometry which may be intermediate between tetrahedral and octahedral. The dialkyl tin dihalides are a case in point.

(I.2.5.) Higher co-ordination numbers (> 6)

Examples of tin with co-ordination numbers of 7 or 8 are rare. A summary of the known seven co-ordinate structures and a description of their geometries can be found in ref. 17 where some of the factors affecting this structural class are discussed. Whilst three basic polyhedra possible for these seven co-ordinate structures are the 1:3:3 capped octahedron (C_{3v}), the 1:4:2 mono-

capped trigonal prism (C_{2v}) and the 1:5:1 pentagonal bipyramid (D_{5h}); with one exception all the known structures have the last D_{5h} structure. The exception does not fit either the C_{3v} or the C_{2v} descriptions.¹⁷

The known 8-co-ordinate structures are tin tetraacetate,¹⁸ tin tetranitrate and bis(phthalocyaninato)tin(IV).¹⁹ The geometries of these three structures are distorted dodecahedral, dodecahedral and square antiprismatic respectively.

(1.2.6.) Structural and related work on the Group IV organo-metal halides and pseudohalides

Of the four diorganotin(IV) dihalides whose crystal structures are known, Me_2SnF_2 has the Sn atoms octahedrally co-ordinated by forming two trans-bonds to methyl groups and four equal Sn-F bonds (2.14 \AA), giving a regular two-dimensional layer lattice.²⁰ In both Me_2SnCl_2 (ref. 21) and $(CH_2Cl)_2SnCl_2$ (ref. 22) the tin atoms can be regarded as being four-co-ordinate, but it is also possible to distinguish infinite chains in the crystal held together by weak inter-molecular interactions. The tin atoms are strongly distorted from the expected tetrahedrally co-ordinated arrangement by further secondary bonds to chlorine atoms of other molecules. In the crystal structure of Ph_2SnCl_2 the original authors described the structure in terms of isolated molecules without any inter-molecular tin-chlorine bridging.²³ This has been criticised by Bokil *et al.*²² who point out that the Sn-Cl bond lengths are different, and that the chlorine atoms involved in the longer of the Sn-Cl bonds are also involved in short inter-molecular interactions of $3.77 - 3.78 \text{ \AA}$ with the tin atoms of neighbouring molecules. These interactions produce linear groups of four molecules, the two terminal tin atoms remaining four-co-ordinate while the central tin atoms can be viewed as six-co-ordinate.

As well as the diorganotin(IV) dihalides, the crystal structures are known of several nominally four-co-ordinate dialkyltin(IV) compounds containing pseudohalides²⁴ and many trialkyl- and triaryl-

tin(IV) halides and pseudohalides.²⁵ Three review articles have²⁶ discussed the inter-molecular bonding in the organometallic pseudohalides of several heavy atoms including tin in terms of donor-acceptor bonding. Most of these compounds are also associated in the crystal and the secondary bonds to the O, S and N ligands appear to be much stronger than those to chlorine. It also appears that some compounds which are not associated by secondary bonding at room temperature may be associated at lower temperatures. This is seen in triphenyltin(IV) chloride whose room-temperature crystal structure shows discrete molecules with the valence angles about the tin being very close to normal tetrahedral values.²⁷ The authors suggested that the significant difference in the ³⁵Cl n.q.r. spectra at 303 and 77 K (ref. 28) was due to the appearance of a polymeric structure with trigonal bipyramidal tin and a weak secondary bond Sn...Cl (as has been suggested²⁹ for Me₃SnCl) at the lower temperature. However, a recent series of Mössbauer measurements over a range of temperatures has failed to discover any gross structural changes in Ph₃SnCl, whilst the association in Me₂SnCl₂ becomes stronger at lower temperatures.³⁰

In comparison, structural studies of the other Group IV di- and tri-organometal halides are sparse, although it appears that associated structures are likely to be found. In the case of lead, only diphenyllead dichloride has been investigated crystallographically[†] by means of 2D projections. Significantly the structure has been found to consist of infinite planar Cl₂PbCl₂ chains with equivalent Pb-Cl bonds (2.80 Å) mutually perpendicular. The phenyl rings are normal to the chain axis with the Pb-C bonds (2.12 Å) nearly perpendicular to the plane of the chain.³¹ The polymeric nature of the other tri-phenyl and trimethyl lead halides and the dimethyl and diphenyl lead dihalides

† Presumably because of the rapid photodecomposition shown by organo lead halides (ref. 32).

in the solid state has also been inferred from evidence including their low solubilities in non-polar solvents, high melting points and most significantly the lowering of the infra-red metal-halogen stretching vibrations in the solid state compared with the corresponding values in solution (when soluble). Furthermore, it appears from these measurements that the molecular association in the organo lead compounds is greater than in the corresponding tin compounds.³³

The majority of the organo germanium halides are liquids at room temperature. Gas phase electron diffraction studies on Me_2GeF_2 , MeGeF_3 , Me_2GeBr_2 and MeGeBr_3 have recently been published³⁴ but little crystallographic work has been performed with the exception of a few complexes of GeCl_2 ³⁵ and several organogermeryl complexes including the germanium analogues of the stannocanes mentioned above.¹⁵ A structure associated via Ge-F-Ge bridged interactions in the solid state has been deduced from i.r. and other measurements for bis(trifluoromethyl)germanium difluoride.³⁶

Crystallographic studies of organo silicon compounds are, however, more numerous, and have been the subject of several reviews. Of recent structures published, triphenyl silicon thiocyanate consists of isolated molecules, whilst bis(triphenyl silicon)carbo di-imide consists of a linear Si-N=C=N-Si chain along a three-fold axis.³⁷

(1.3.) Experimental Results

(1.3.1.) General

Crystal samples R_2SnX_2 ($\text{R} = \text{Me}$, $\text{X} = \text{Br}$ and I ; $\text{R} = \text{Et}$, $\text{X} = \text{Cl}$, Br and I ; and $\text{R} = \text{Bu}$, $\text{X} = \text{Cl}$) were kindly provided by Dr. D.A. Armitage. The crystal quality varied from sample to sample but was, however, somewhat poor even after recrystallisations from dry isopentane. The compounds were also sensitive to air-moisture hydrolysis and so handling and mounting of each compound was performed in a modified nitrogen 'dry box' fitted with a microscope and heating wire, using Lindemann capillary tubes which had been baked in vacuo for several hours. Even then, several crystals had to be mounted before one of sufficient quality for use on the diffractometer was found. Density measurements were not made because of the moisture sensitivity of the crystals and their solubility in most organic solvents, although calculated values, D_c , are in reasonable agreement with the values

TABLE I.1

Unit cell data for the dialkyltin dihalides R_2SnX_2 ($R = Me, X = Br$ and I ; $R = Et, X = Cl, Br$ and I ; and $R = Bu, X = Cl$)

Compound	System	Space group	a(Å)	b(Å)	c(Å)	$\beta(^{\circ})$	$\mu(\text{\AA}^3)$	Z	D_c g/cm ³	$\mu(\text{Mo-K}\alpha)$ cm ⁻¹
Me_2SnBr_2	Monoclinic	$C2/e(?)$	12.437(2)	9.212(1)	24.791(4)	91.95(1)	2838.5(9)	16	2.89	154.07
Me_2SnI_2	Monoclinic	—	14.433(6)	10.279(4)	22.351(9)	94.03(3)	3307.8(23)	16	3.23	105.40
Et_2SnCl_2	Monoclinic	$P2_1/c$	9.677(3)	9.835(2)	9.243(3)	102.73(2)	858.1(4)	4	1.92	35.35
Et_2SnBr_2	Orthorhombic	$C22_1$	9.786(2)	10.006(3)	9.494(2)	—	929.7(4)	4	2.40	117.70
Et_2SnI_2	Orthorhombic	$Pbcn$	13.469(4)	5.385(2)	13.733(4)	—	996.0(6)	4	2.87	87.61
Bu_2SnCl_2	Monoclinic	$P2_1(?)$	14.059(4)	9.407(2)	19.407(3)	96.79(2)	2548.8(10)	8	1.58	23.79

quoted for Me_2SnCl_2 and Ph_2SnCl_2 . The unit cell constants, their standard deviations and space group data (where known) for the compounds are listed in Table I.1. Unit cell constants were obtained from least-squares refinement of the diffracting positions of up to 15 reflections on a Syntex P2_1 diffractometer by use of

Mo-K_α radiation ($\lambda = 0.71069 \text{ \AA}$). No further work was performed on the crystal of Me_2SnI_2 used, and although data sets have been collected for both Me_2SnBr_2 and Bu_2SnCl_2 they have been of very poor quality and need recollection.

(I.3.2.) Data collections

(I.3.2(i)) Et_2SnCl_2 , compound (1)

Data were collected using a needle shaped crystal of dimensions $0.052 \times 0.052 \times 0.48 \text{ mm}$ bounded by the faces (00 ± 1) , (0 ± 10) , (± 100) . Systematic absences $h0l$, $l \neq 2n$; $0k0$, $k \neq 2n$, indicate space group $\text{P2}_1/c$. Reflections were measured using a $\theta - 2\theta$ scan and scan range $(K_{\alpha 1} - 0.95)$ to $(K_{\alpha 2} + 0.95)$ to a maximum 2θ of 50° . A variable scan-rate of $1.3^\circ/\text{min}$ to $29.5^\circ/\text{min}$ depending on the intensity of a preliminary 2 s count, was used. Background counts were recorded at each end of the scan. The intensities of three standard reflections were monitored every 80 reflections. These showed a steady loss of intensity and the collected data were rescaled according to the equation $F = F_0(1 + 0.00065t)(1 + 0.00254 \sin \theta/\lambda, t)$. The maximum rescale factor was 1.1458. 1709 data were collected, of which 811 were considered observed ($I/\sigma(I) \geq 3.0$).

(I.3.2(ii)) Et_2SnBr_2 , compound (2)

Data were collected using a crystal of dimensions $0.211 \times 0.260 \times 0.343 \text{ mm}$ bound by the faces (± 110) , (-1 ± 10) , (00 ± 1) . Systematic absences hkl , $h + k \neq 2n$, and $00l$, $l \neq 2n$ indicate space group C22_1 , with the Sn on special positions, symmetry 2. Reflections were measured using a $\theta - 2\theta$ scan over a range $(K_{\alpha 1} - 0.9)$ to $(K_{\alpha 2} + 0.9)$ and variable scan rate of $1.5^\circ \text{ min}^{-1}$ to $29.3^\circ \text{ min}^{-1}$.

to a maximum 2θ of 55° . The intensities of four standard reflections were recorded after every 50 reflections and again showed a steady loss in intensity. The collected data were rescaled according to the equation

$$F = F_0(1 + 0.0004024t)(1 + 0.0012724 \sin \theta/\lambda.t)$$

(Maximum rescale factor was 1.0524). 1263 data were measured including systematic absences due to the centering condition of which 289 were considered observed ($I/\sigma(I) \geq 3.0$).

(I.3.2(iii)) Et_2SnI_2 , compound (3)

Data were collected using a needle shaped crystal needle axis a , (dimensions unknown). Systematic absences $Ok1$, $k \neq 2n$; $h0l$, $l \neq 2n$; $hk0$, $h+k \neq 2n$; Indicates space group Pbcn with the Sn on special positions, symmetry 2. Reflections were measured using a $\theta - 2\theta$ scan over a range ($K_{\alpha 1} - 0.9$) to ($K_{\alpha 2} + 0.9$) and variable scan rate of 3° min^{-1} to $29.3^\circ \text{ min}^{-1}$ to a maximum 2θ of 52° . The intensities of three standard reflections were recorded after every 60 reflections and showed a steady drop in intensity. The collected data were rescaled in two sections according to the equations

$$F = F_0(1 + 0.007655t)(1 - 0.004628 \sin \theta/\lambda.t) \text{ for } t \leq 15.18$$

$$F = F_0(1 + 0.002832t)(1 - 0.0009608 \sin \theta/\lambda.t) \text{ for } t > 15.18$$

The maximum rescale factor was 1.0682. 1187 data were measured, of which 342 were considered observed ($I/\sigma(I) \geq 3.0$).

(I.3.2(iv)) Me_2SnBr_2 and Bu_2SnCl_2

Crystals of Me_2SnBr_2 are colourless needles. Several attempts were made to collect a complete 3-dimensional set of data for Me_2SnBr_2 using several different crystals. However, crystal decomposition and crystal movement at each attempt drastically limited the amount and quality of the data collected, and prevented the solution of the structure.

Crystals of dibutyl tin dichloride were thin colourless plates with poorly-defined edges. One reasonable-looking flake was mounted in a Lindemann capillary and used for data collection.

Crystal data:

Monoclinic, $a = 14.059(4)$, $b = 9.407(2)$, $c = 19.407(3)$ Å, $\beta = 96.79(2)^\circ$, $D_c = 1.58 \text{ g/cm}^3$ for $Z = 8$. Mo-K α radiation, $\lambda = 0.71069$ Å, $\mu(\text{Mo-K}\alpha) = 23.79 \text{ cm}^{-1}$.

Unit cell dimensions and standard deviations were obtained by least squares fit to 15 strong reflections collected after the data collection had finished. Data were collected using $\theta - 2\theta$ scans over a scan range ($K_{\alpha 1} - 1.1^\circ$) to ($K_{\alpha 2} + 1.1^\circ$) using scan speeds from 2.0 to 29.3 $^\circ/\text{min}$. Several shells of data were collected. Some of these were later recollected due to crystal movement and the crystal was frequently recentred. Including duplicated data and standards 6305 reflections were eventually collected which, when reduced, gave only 660 observed reflections ($I/\sigma(I) \geq 2.58$) due to the marked pseudo-absences in the data. The three standards collected every 100 reflections showed a gradual loss of intensity which was corrected for by rescaling the data in several sections, using several linear equations $F = F_0(1 + at)$.

(I.3.3.) Structure Solution

(I.3.3.1.) The diethyltin dihalides, compounds (1-3)

For compounds (1) and (2) Lorentz, polarisation and absorption corrections were applied, the last with the program ABSCOR. For (3), Lorentz and polarisation corrections were made, but crystal

decomposition prevented any measurement of the crystal for absorption correction. In all three cases, structure solution was attempted successfully using 3-dimensional Patterson maps to locate the heavy atoms and Fourier maps to locate the other non-hydrogen atoms. Block diagonal least squares refinement using anisotropic temperature factors for all atoms with correction for the effects of anomalous dispersion produced final R factors of 0.047(1), 0.058(2) and 0.049(3). The weights used were based on counting statistics.

Final co-ordinates and temperature factors are listed in Table I.2, significant bond lengths and angles in Table I.3. Structure factors for the three compounds are listed in Appendix

(I.3.3.2.) Dibutyl tin dichloride

The data contains several well marked pseudo-absences so that the choice of space group at this initial stage is somewhat arbitrary. The Patterson map reflects the pseudo I-centring of the heavy tin and chlorine atoms in the unit cell. Consistent with the observed pseudo-absences hkl , $k \neq 2n$, hkl , $l \neq 2n$ [and hence hkl , $k + l \neq 2n$, $h + k/2 + l/2 \neq 2n$] there are peaks at $(0, 0, 0)$; $(0, \frac{1}{2}, 0)$; $(0, 0, \frac{1}{2})$ and $(\frac{1}{2}, \frac{1}{4}, \frac{1}{4})$ of approximately equal weight. Hence a feasible set of tin positions which would fit this map are given by

$$\begin{array}{ll} (0, 0, 0) & (\frac{1}{2}, \frac{1}{4}, \frac{1}{4}) \\ (0, \frac{1}{2}, 0) & \text{and} \quad (\frac{1}{2}, \frac{3}{4}, \frac{1}{4}) \\ (0, 0, \frac{1}{2}) & (\frac{1}{2}, \frac{1}{4}, \frac{3}{4}) \\ (0, \frac{1}{2}, \frac{1}{2}) & (\frac{1}{2}, \frac{3}{4}, \frac{3}{4}) \end{array}$$

There are at present 8 monoclinic space groups available and with suitable origin shifts the above combination of Sn positions can be fitted to all of these space groups. In some, this would involve placing some or all of the Sn atoms on special positions. It is very unlikely that the molecules would have $\bar{1}$ symmetry which rules out some possibilities. This still leaves several

possibilities, all of which need to be tested. Several alternatives have been tried with similar progress in each space group: that is, the Sn and Cl atoms can be located and in refinement show large correlation effects. The R factor for Sn and Cl atoms is $\approx R = 12\%$ at which point the C atoms in the n-butyl groups can be observed in the difference Fourier with a strong suggestion that one chain is disordered at the α -position. However, due to the poor quality of the data and the problems of refining the C atoms in a acentric space group with a dominant centric distribution of heavy atoms, no reasonable bond distances and angles have yet been obtained. Even on reducing the data into the pseudo (primitive) cell (following a similar procedure to that in ref. 38, where disorder is blamed for the poor refinement in the true cell) no improvement was attained.

(I.4.) Discussion of the Diethyl Tin Dihalides

(I.4.1.) General

In the crystal structures of all three diethyl tin dihalides, Et_2SnX_2 (X = Cl, Br and I), the individual molecules interact to form chains. Probably as a result, there are significant angular distortions from tetrahedral values in the individual molecules. The values of the angles C-Sn-C and X-Sn-X are respectively 134.0(6) and 96.0(1) for (1), 135.9(10) and 98.5(1) for (2) and 130.2(11) and 104.0(2) $^\circ$ for (3).

Although there are few other Sn-C(Et) bond distances available for comparison, there should be little difference between Sn-C(Me) and Sn-C(Et). The Sn-C(Et) bond in dichloro(ethyl)hydroxotin³⁹ is 2.20(3) Å and a large number of Sn-C(Me) distances in the solid state for a variety of distorted geometries at tin give Sn-C from 2.07 to 2.22 Å.⁴⁰ The Sn-C distance in SnMe_4 has been determined most recently by gas-phase electron diffraction as 2.144(3) Å.⁴¹ The present values are quite close to those quoted, but they do seem to show a slight systematic increase from (1) to (3). For Sn-Cl

TABLE 1.2[†]

Atomic co-ordinate ($\times 10^4$) and anisotropic temperature factors ($\times 10^3$)[†] for the diethyl tin dihalides with standard deviations in parentheses. $\dagger \exp \left[-\frac{1}{2} (B_{11} h^2 a^2 + B_{22} k^2 b^2 + B_{33} l^2 c^2 + 2B_{12} hka^*b^* + 2B_{13} hla^*c^* + 2B_{23} klb^*c^*) \right]$

(1) Et₂SnCl₂

Atom	X	Y	Z	B ₁₁	B ₂₂	B ₃₃	B ₂₃	B ₁₃	B ₁₂
Sn	2788(1)	2312(1)	7006(1)	37.8(4)	43.8(5)	48.2(5)	-0.4(5)	8.3(3)	-0.9(5)
Cl(1)	2774(5)	705(4)	5071(4)	75.9(25)	47.0(20)	50.1(18)	-7.8(15)	10.4(17)	-1.5(17)
Cl(2)	2738(4)	672(4)	8898(4)	72.4(24)	48.7(19)	56.4(18)	7.4(15)	20.5(17)	1.0(17)
C(1)	751(14)	3238(15)	6542(16)	13(7)	74(9)	92(9)	1(7)	-2(6)	11(6)
C(2)	-413(20)	2217(25)	6152(34)	30(10)	135(15)	275(26)	-53(17)	0(13)	-9(11)
C(3)	4912(16)	3100(15)	7494(16)	40(7)	67(9)	74(8)	-1(6)	10(6)	-13(6)
C(4)	6028(16)	2021(18)	7800(20)	18(7)	90(11)	143(12)	8(9)	11(8)	10(8)

(2) Et₂SnBr₂

Sn	431(3)	0(0)	5000(0)	58.4(14)	63.2(14)	52.3(13)	-4.1(65)	0(0)	0(0)
Br	2100(3)	48(21)	3002(3)	68.4(18)	117.0(28)	57.6(17)	1.6(73)	11.3(13)	-19.0(62)
C(1)	-420(26)	1956(25)	4745(31)	51(11)	65(12)	13(19)	-10(11)	-7(12)	-11(13)
C(2)	393(28)	300(31)	5366(61)	56(13)	70(15)	108(49)	-27(20)	-45(23)	10(15)

(3) Et₂SnI₂

I	1245(1)	965(5)	1531(1)	56.6(10)	64.0(13)	55.5(9)	-6.5(14)	16.2(8)	2.0(18)
Sn	0(0)	4080(6)	2500(0)	43.6(11)	40.2(15)	37.9(10)	0(0)	-4.8(10)	0(0)
C(1)	904(19)	5829(54)	3644(15)	83(15)	20(12)	50(11)	1(17)	-30(11)	7(17)
C(2)	1501(21)	3739(77)	4220(17)	89(17)	118(27)	58(12)	-28(22)	-40(12)	18(27)

TABLE I.3

Bond distances (Å) and bond angles (°) with standard deviations in parentheses.

(a) Distances	Compound	Ref.	Sn-X	Sn-C	C-C	Sn...X	Δ^a	Sn...X ^b	X...X
	Me ₂ SnCl ₂	21	2.40(4)	2.21(8)		3.54(5)	1.14		
	(CH ₂ Cl) ₂ SnCl ₂	22	2.37(2)	2.18(7)		3.71(3.21) ^c	1.34(0.84)	3.85	
	Et ₂ SnCl ₂	d	2.385(3)	2.132(13)	1.452(25)	3.483(4)	1.08		3.544(6)
			2.384(4)	2.167(15)	1.471(22)	3.440(4)			
	Et ₂ SnBr ₂	d	2.505(4)	2.162(26)	1.456(46)	3.777(4)	1.27	3.95	3.795(4)
	Et ₂ SnI ₂	d	2.719(4)	2.178(27)	1.573(49)	4.284(5)	1.565	4.08	5.383
	Ph ₂ SnCl ₂ (1)	23	2.353(2)	2.119(5)		3.78			
			2.336(2)	2.105(5)				3.85	
	(2)		2.357(2)	2.118(5)		3.77			
			2.336(2)	2.112(6)					

^a $\Delta = (\text{Sn} \cdots \text{X}) - \text{Sn-X}$ ^b van der Waals distance from A. Bondi, J. Phys. Chem., 1964, 68, 441^c Values in parentheses in Sn...X are given in parentheses^d This work

Table I.3 continued

(b) Angles									
Compound	X-Sn-X	C-Sn-C	C-Sn-X	Sn-C-C	X...Sn-X	Sn...X-Sn			
Me_2SnCl_2	93.0(20)	123.5(45)	109.0(45)						
$(\text{CH}_2\text{Cl})_2\text{SnCl}_2$	97.0(20)	135.0(60)	105.0(20)						
Et_2SnCl_2	96.0(1)	134.0(6)	106.3(4)	112.1(12)	173.0(1)	104.0(1)			
Et_2SnBr_2	98.5(1)	135.9(10)	97.5(9)	113.6(10)	172.0(1)	102.8(1)			
Et_2SnI_2	104.0(2)	130.2(11)	105.6(8)	114.0(20)	179.5(5)	98.2(1)			
Ph_2SnCl_2 (1)	101.7(1)	123.9(2)	106.0(2)	110.0(21)	158.0(1)	98.0(1)			
(2)			106.5(2)	107.8(2)					
	97.8(1)	127.0(2)	110.1(2)	105.0(2)					
			107.1(2)	105.9(2)					

a $\Delta = (\text{Sn}...\text{X})$ minus $(\text{Sn}-\text{X})$

b van der Waals distance from A. Bondi, J. Phys. Chem., 1964, 68, 441.

c Value in parenthesis is $\text{Sn}...\text{Cl}$ intramolecular distance.

d This work

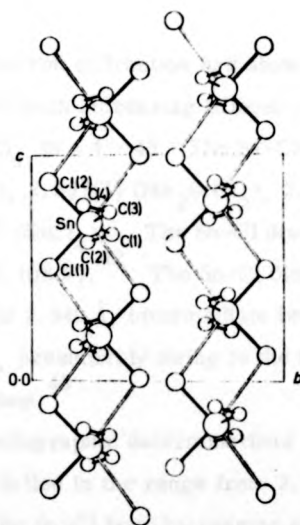


FIGURE 1 Et_2SnCl_2 projected down a ; primary bonds are shown closed; secondary bonds open

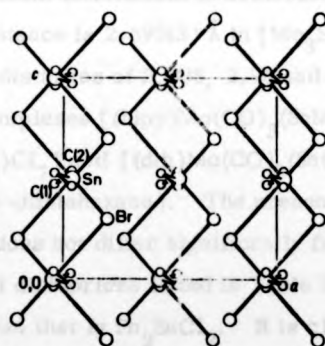


FIGURE 2 Et_2SnBr_2 projected down b

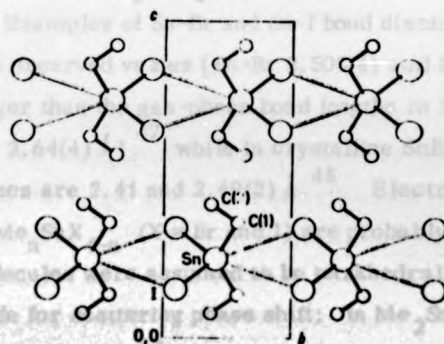


FIGURE 3 Et_2SnI_2 projected down a

Figs 1-1-3

bonds, electron diffraction has shown a regular contraction in the bond length with increasing halogen substitution in the series $\text{Me}_{4-n}\text{SnCl}_n$ ($n = 1 - 4$). The Sn-Cl distances are 2.351(7) (Me_3SnCl), 2.327(3) (Me_2SnCl_2), 2.304(3) (MeSnCl_3), and 2.281(4) Å (SnCl_4). The Sn-Cl distances are essentially constant (2.104 - 2.108 Å).⁴² The Sn-Cl distance in (chloromethyl)trichlorostannane is 2.340 Å, intermediate between those for Me_2SnCl and Me_2SnCl_2 , presumably owing to the inductive effect of the chloromethyl group.⁴³

Crystallographic determinations of the Sn-Cl bond length have generally fallen in the range from 2.318 to 2.584 Å,⁴⁴ with the length of the Sn-Cl bond increasing as the co-ordination of the tin changes from tetrahedral to octahedral. The longest recorded Sn-Cl distance is 2.693(3) Å in $[\text{Me}_3\text{SnCl}_2]^-$,⁴⁵ although bridging Sn...Cl distances of 2.805, 2.96 and 2.78 Å occur in transition-metal complexes $[(\text{bipy})\text{Mo}(\text{CO})_3(\text{SnMeCl}_2)\text{Cl}]$, $[(\text{dth})-\text{W}(\text{CO})_3-(\text{SnMeCl}_2)\text{Cl}_7]$ and $[(\text{dth})\text{Mo}(\text{CO})_3(\text{SnCl}_3)\text{Cl}]$ ⁴⁶ (bipy = $\alpha\alpha'$ -bipyridyl, dth = 2,5-dithiahexane). The present mean Sn-Cl bond length 2.384 Å does not differ significantly from those for the other two dialkyltin dichlorides listed in Table 3 although it is ca. 0.04 Å longer than that in Ph_2SnCl_2 . It is clearly considerably longer than that in Me_2SnCl_2 in the gas phase.⁴²

Examples of Sn-Br and Sn-I bond distances are less numerous. The observed values [Sn-Br 2.505(4) and Sn-I 2.719(4) Å] are again longer than the gas-phase bond lengths in SnBr_4 and SnI_4 [2.44(2) and 2.64(4) Å]⁴⁷ while in crystalline SnBr_4 and SnI_4 the respective values are 2.41 and 2.69(2) Å.⁴⁸ Electron-diffraction measurements on $\text{Me}_n\text{SnX}_{4-n}$ ($X = \text{Br}$ and I) are probably not very accurate as the molecules were assumed to be tetrahedral and no allowance was made for scattering phase shift; in Me_2SnX_2 , Sn-Br was 2.45(2) and Sn-I 2.69(3) Å, and for this series a contraction was reported

with increasing halogen substitution,⁴⁹ although the values quoted above for SnX_4 seem not to bear this out.

Considering solid state values, the observed Sn-Br value is in good agreement with that [2.504(5) Å] in (4-bromo-1,2,3,4-tetraphenyl-cis, cis-1,3-butadienyl)dimethyltin bromide which is also distorted from tetrahedral geometry by secondary bond interactions.¹³ In the two isomers of bis-[1,2-bis(ethoxycarbonyl)-ethyl]tin dibromide, Sn-Br distances of 2.516(6), 2.588(6) and 2.504(5) Å were found in distorted octahedral structures.⁵⁰ However, in the crystal structure of $\text{C}_6\text{H}_5\text{N}[\text{2}[(\text{dimethylamino})\text{methyl}]\text{phenyl}]_2$ diphenyl tin bromide, intra-molecular co-ordination from the dimethylamino group of the built-in ligand results in a penta-co-ordinate tin atom and a significantly longer axial Sn-Br bond of 2.630(2) Å [N-Sn-Br = 171.0(1)°].¹¹ The only other examples of solid state Sn-Br distances are for organotin-transition metal compounds, where more complex bonding and packing effects occur, e.g. $[(\text{Br}_3\text{Sn})\text{Fe}(\text{CO})_2(\pi\text{-C}_5\text{H}_5)]$ mean 2.501(2), $[(\text{Br}_2\text{Sn})\{\text{Mn}(\text{CO})_5\}_2]$ 2.548(2), and $[(\text{BrSn})\{\text{Co}(\text{CO})_4\}_3]$ 2.520(5) Å.⁵¹ The mean value for $[(\text{Br}_3\text{Sn})\text{Mo}(\pi\text{-C}_5\text{H}_5)\text{Br}]$ is 2.506(8) Å, but this compound also possesses a long bridging Sn-Br distance of 3.411 Å (cf. ref. 24) which results in trigonal bipyramidal geometry at the tin atom.^{51d}

The observed Sn-I for (3) also agrees with that of 2.729(3) Å in 1,4-bis(iododiphenylstanna)butane which contains a tetrahedral tin atom.⁵²

(I.4.2.) Inter-molecular Interactions

The strength of the inter-molecular interactions can be deduced from the length of the secondary bonds and the angles around tin (especially C-Sn-C). In Et_2SnCl_2 and Et_2SnBr_2 the lengths of the secondary bonds (see Table 3) are 0.39 and 0.17 Å less than the sum of their appropriate van der Waals radii. The weakest interaction occurs in Et_2SnI_2 , where the Sn...I secondary bond distance [4.284(5) Å] is greater than the sum of the tin and iodine

van der Waals radii. However, it can be argued that the interaction is still present since the value of the C-Sn-C angle [$130.2(11)^\circ$] is much larger than the tetrahedral value. Taking into account only the difference between the secondary bond distance and the sum of the van der Waals radii, it would appear that the strength of the secondary bonding is in the order $\text{Cl} > \text{Br} > \text{I}$. However, if the apparent difference in the C-Sn-C angle is genuine, then the order may be $\text{Cl} \approx \text{Br} > \text{I}$. It has also been suggested, from n.q.r. measurements, that bromine bridging is stronger than chlorine bridging.⁵³ Zahrobsky,⁵⁴ by use of a simple stereochemical model which optimises the van der Waals forces between the bonded and neighbouring atoms (regarded as spheres), has predicted inter-molecular distances of 3.81 and 4.11 Å for Me_2SnBr_2 and Me_2SnI_2 . The distances quoted are reasonable although the steric requirements of the larger ethyl group might affect these results. However, this model calculates the C-Sn-C angles as being only 125 and 124° respectively.

The mode of bridging in the Et_2SnCl_2 and Et_2SnBr_2 chains is also different from that in Et_2SnI_2 where both bridging secondary bonds $\text{Sn} \dots \text{I}$ involve the halogen atoms on the same neighbouring molecule (Fig. 3). In Et_2SnCl_2 and Et_2SnBr_2 the distorted octahedral arrangement around each tin is completed by two secondary bonds involving the halogen atoms of two neighbouring molecules (Figs. 1 and 2). Both $(\text{CH}_2\text{Cl})_2\text{SnCl}_2$ and Ph_2SnCl_2 associate in the same chelating manner as does Et_2SnI_2 ; Me_2SnCl_2 , however, has the second bridging type of association. It is not readily apparent which type of bridging arrangement a system containing secondary bonds will adopt, but the chelating bridges seems to be favoured with the longer weaker bonds. Brown and Shannon⁵⁵ have attempted to classify the bridging environments in certain inorganic structures using the bond valences of the bridging atoms, and this method may be applicable to secondary bonded systems.

The lengths of the Sn...Cl secondary bonds (Table 3) can be compared to that [3.486(7) Å] for quinuclidine trichlorodimethylstannane(IV) where this bond links two $\text{Me}_2\text{SnCl}_3^-$ ions into dimeric units.⁵⁶ The cation here is very important since in $[\text{Me}_2\text{Sn}(\text{terpyridyl})]^+ [\text{Me}_2\text{SnCl}_3]^-$ the anion shows no Sn...Cl contacts < 3.7 Å;⁵⁷ nor does the ion $[\text{Me}_3\text{SnCl}_2]^-$ in $[\text{Mo}_3(\eta^5\text{-C}_5\text{H}_5)_4]^+ [\text{Me}_3\text{SnCl}_2]^-$, although it does contain a very long Sn-Cl distance (2.696 Å).⁴⁵

The Sn...Br secondary bond in Et_2SnBr_2 has the same length [3.774(5) Å] as the intra-molecular interaction of bromine with tin in (4-bromo-1,2,3,4-tetraphenyl-cis, cis-1,3-butadienyl)dimethyltin bromide (resulting in an axially substituted trigonal bipyramid with equatorial organic groups).¹³ In that compound also, the C(butadienyl)-Sn-C(Me) angle has opened to 129.0° and C(Me)-Sn-Me to 112.7°. A series of analogous 4-chloro- and 4-bromo-compounds has been investigated in which Sn-Ph replaces Sn-Br. In these compounds, the interaction is drastically weakened so that the Sn...Cl (4.28) and Sn...Br distances (4.35 Å) are both greater than the sum of the two corresponding van der Waals radii. The difference in the two Sn...Br distances is 0.57 Å. Similarly the C(butadienyl)-Sn-C(Me) angles are reduced to 116.5 (4-chloro) and 117.1° (4-bromo).⁵⁸ Furthermore, in the crystal structures of triphenyltin 2-methylthiophenolate and -2,6-dibromo-4-fluorothiophenolate, the Sn-S-C angles involving the thiophenolate rings are the same [98.6(8) and 101(2)° respectively] indicating that no intra-molecular co-ordinative interactions are occurring. The resulting intra-molecular Sn...Br distances of 4.26 and 4.29 Å again show that a Sn...Br van der Waals contact distance of 4.1 (after Bondi) is essentially correct.⁵⁹

(I.4.3.) Factors affecting inter-molecular interactions

A CNDO calculation of the valence electron distribution in a series of Sn^{IV} compounds has shown that for isolated halogeno-(dimethyl)stannanes the 5s and 5p orbital occupancies are strongly

The lengths of the Sn...Cl secondary bonds (Table 3) can be compared to that [3.486(7) Å] for quinolinium trichlorodimethylstannane(IV) where this bond links two $\text{Me}_2\text{SnCl}_3^-$ ions into dimeric units.⁵⁶ The cation here is very important since in $[\text{Me}_2\text{Sn}(\text{terpyridyl})]^+ [\text{Me}_2\text{SnCl}_3]^-$ the anion shows no Sn...Cl contacts < 3.7 Å;⁵⁷ nor does the ion $[\text{Me}_3\text{SnCl}_2]^-$ in $[\text{Mo}_3(\eta^5\text{-C}_5\text{H}_5)_4]^+ [\text{Me}_3\text{SnCl}_2]^-$, although it does contain a very long Sn-Cl distance (2.696 Å).⁴⁵

The Sn...Br secondary bond in Et_2SnBr_2 has the same length [3.774(5) Å] as the intra-molecular interaction of bromine with tin in (4-bromo-1,2,3,4-tetraphenyl-cis, cis-1,3-butadienyl)dimethyltin bromide (resulting in an axially substituted trigonal bipyramid with equatorial organic groups).¹³ In that compound also, the C(butadienyl)-Sn-C(Me) angle has opened to 129.0° and C(Me)-Sn-Me to 112.7°. A series of analogous 4-chloro- and 4-bromo-compounds has been investigated in which Sn-Ph replaces Sn-Br. In these compounds, the interaction is drastically weakened so that the Sn...Cl (4.28) and Sn...Br distances (4.35 Å) are both greater than the sum of the two corresponding van der Waals radii. The difference in the two Sn...Br distances is 0.57 Å. Similarly the C(butadienyl)-Sn-C(Me) angles are reduced to 116.5 (4-chloro) and 117.1° (4-bromo).⁵⁸ Furthermore, in the crystal structures of triphenyltin 2-methylthiophenolate and -2,6-dibromo-4-fluorothiophenolate, the Sn-S-C angles involving the thiophenolate rings are the same [98.6(8) and 101(2)° respectively] indicating that no intra-molecular co-ordinative interactions are occurring. The resulting intra-molecular Sn...Br distances of 4.26 and 4.29 Å again show that a Sn...Br van der Waals contact distance of 4.1 (after Bondi) is essentially correct.⁵⁹

(I.4.3.) Factors affecting inter-molecular interactions

A CNDO calculation of the valence electron distribution in a series of Sn^{IV} compounds has shown that for isolated halogeno-(dimethyl)stannanes the 5s and 5p orbital occupancies are strongly

dependent on the electronegativity of the halogen.⁶⁰ Although the methyl groups donate electrons to the tin, they are unable to replace all the electron density removed by the halogen atoms, leaving a slightly electron-deficient tin atom which can then form secondary bonds. The decreasing electronegativity of the halogens and decreasing overlap with the more diffuse orbitals on bromine and iodine would then qualitatively explain the observed strengths of the secondary interactions. There is also a clear connection between secondary bond strength and the nature of the organic group.

In Me_2SnCl_2 , Et_2SnCl_2 and Et_2SnBr_2 the secondary bonding is considerably stronger than in Ph_2SnCl_2 . The effect of replacing methyl by ethyl in R_2SnCl_2 is to strengthen the inter-molecular bonding by shortening the secondary bond from 3.54(5) to 3.461(4) (mean) Å with the corresponding C-Sn-C angle opening out from 123(4) to 134.0(6)°. These angles are still considerably less than in the more associated dimethyltin pseudo-halide compounds $\text{Me}_2\text{Sn}(\text{CN})_2$ [148.7(3.5)°] and $\text{Me}_2\text{Sn}(\text{NCS})_2$ [145.9(1.4)°]. The phenyl group produces a significant weakening of the secondary interaction as can be seen from Table 3 and from the dimethyl-(tetraphenylbutadienyl)tin compounds already mentioned. This is presumably due to the ability of the phenyl group to involve available orbitals on the tin atom in inductive and mesomeric interactions so that they cannot overlap effectively with further orbitals. Similarly the chloro-methyl group, with a reasonably strong inductive effect, also weakens the secondary bonding. However, the C-Sn-C angle of 135(6)° in $(\text{CH}_2\text{Cl})_2\text{SnCl}_2$ compared with 123.9(2) and 127.0(2)° in the two crystallographically independent Ph_2SnCl_2 molecules suggests a stronger interaction in the former. If the viewpoint of Bokil *et al.*²² is accepted, the difference of 4° between the C-Sn-C angles in the two Ph_2SnCl_2 molecules is directly attributable to secondary bonding effects.

(I.4.4.) Hybridisation models and other physical measurements

The C-Sn-C angle is important when describing any tin hybridisation model and in interpreting other physical measurements made on tin. Sham and Bancroft⁴⁰ using a simple theoretical model, have correlated the Sn¹¹⁹ Mössbauer quadrupole splittings with the C-Sn-C angle in a number of distorted Me₂Sn^{IV} compounds. They find that Me₂SnCl₂ and Me₂Sn(NO₃)₂ lie in intermediate positions between the two predicted curves for Me₂SnL₂ and Me₂SnL₄. Recent Mössbauer results have also shown that the amount of tin 5s character in the bonds from tin to (transition) metals and organic groups in the series of compounds X_nR_{3-n}SnM [X = Cl, Br or C₆F₅; R = Me or Ph; M = Mn(CO)₅ or Fe(CO)₂-(π -C₅H₅)] decreases in the order: Sn-Fe(CO)₂(π -C₅H₅) > Sn-Mn(CO)₅ > Sn-Me > Sn-Ph > Sn-C₆H₅ > Sn-Cl \approx Sn-Br. By use of this series they have rationalised the known distortions from tetrahedral geometry in several tin compounds.⁶¹

The values of the coupling constants J¹¹⁹Sn-CH₃ also indicate that the s character in the Sn-Me bonds decreases substantially as the C-Sn-C angle decreases.⁶² There should be a corresponding increase in the Sn-C distance, which is not always readily seen owing to the difficulty of determining this distance accurately. The idea of a linear relationship between the J¹¹⁹Sn-Me values and the percentage s character in the Sn-C bonds was advanced by Holmes and Kaesz⁶³ but has been criticised by McFarlane.⁶⁴ Van den Berghe and van der Kelen⁶⁵ have since suggested that the coupling constants are proportional to the percentage s character of spⁿ hybrid orbitals only, since any d orbital involvement in bonding would increase orbital overlap and hence bond strength, whilst not increasing the amount of s character of the hybrid orbital.

In trans-octahedral complexes, the bonding may, therefore, be described in terms of sp₂ hybridisation of the tin with p_x and p_y orbitals used in the equatorial bonds.⁶⁶ The resulting equatorial bonds should then be longer than those observed for tetrahedral

compounds as is generally found (cf. Ph_2SnCl_2 and Et_2SnCl_2). In the present compounds (1) - (3), which are clearly intermediate between tetrahedral and trans-octahedral, the tin hybridisation must be intermediate between sp^3 and sp and involvement of the 3d orbitals is possible. The Mössbauer parameters and other physical measurements have been made on the present compounds as well as on a series of related mixed-halogen species.⁶⁷

(I.5.) References

1. N.W. Alcock, Advan. Inorg. Chem. Radiochem., 1972, **15**, 1.
2. The crystal chemistry of tin is reviewed in the following articles:
 - (a) R. Okawara and M. Wada, Advan. Organometal. Chem., 1967, **5**, 137.
 - (b) N.G. Bokil and Yu. T. Struchkov, J. Struct. Chem.(USSR), 1968, **9**, 663.
 - (c) B.Y.K. Ho and J.J. Zuckerman, J. Organometal. Chem., 1973, **49**, 1.
 - (d) P.J. Smith, A Bibliography of Organotin X-ray Crystal Structures, Publicn. No. 484, London: TR1, 1975.
3. P.G. Harrison, T.J. King and R.C. Phillips, J. Chem. Soc. Dalton, 1976, 2317 (Part XVI in a series of papers).
4. M. Nardelli, C. Pelizzi and G. Pelizzi, J. Organometal. Chem., 1977, **126**, 161; M. Nardelli, C. Pelizzi, G. Pelizzi and P. Tarasconi, Z. anorg. Chem., 1977, **431**, 250.
5. J.D. Cotton, P.J. Davison, D.E. Goldberg, M.F. Lappert and K.M. Thomas, J. Chem. Soc. Chem. Comm., 1974, 893.
6. A. Karipides and M. Oertel, Acta Cryst., 1977, **B33**, 683 and references therein.
7. R. Hulme, J. Chem. Soc., 1963, 1524.
8. A.M. Domingas and G.M. Sheldrick, Acta Cryst., 1974, **B30**, 519.
9. H. Chih and B.R. Penfold, J. Cryst. Mol. Str., 1974, **3**, 285.
10. B.Y.K. Ho and J.J. Zuckerman, J. Chem. Soc. Chem. Comm., 1975, 88.

11. G. van Koten, J.G. Noltes and A.L. Spek, J. Organometal. Chem., 1976, 118, 183.
12. M. Bancroft, B.W. Davies, N.C. Payne and T.K. Sham, J. Chem. Soc. Dalton, 1975, 973.
13. F.P. Boer, J.J. Flynn, jun., H.H. Freedman, S.V. McKinley and V.R. Sandel, J. Am. Chem. Soc., 1967, 89, 5068; F.P. Boer, G.A. Doorakian, H.H. Freedman and S.V. McKinley, ibid. 1970, 92, 1225.
14. K. Furue, T. Kimura, N. Yaskova, N. Kasal and H. Kakudo, Bull. Chem. Soc. Japan, 1970, 43, 1661. See also P.G. Harrison and A. Mangia, J. Organometal. Chem., 1976, 120, 211 for a comparison of valence bond distances and angles in similar dithiocarbamate tin(IV) compounds.
15. M. Dräger, Z. anorg. Chem., 1977, 428, 243.
16. J.D. Donaldson, D.R. Laughlin and D.C. Puxley, J. Chem. Soc. Dalton, 1977, 865.
17. L. Coghi, C. Pellizzi and G. Pellizzi, J. Organometal. Chem., 1976, 114, 53.
18. N.W. Alcock, unpublished results.
19. C.S. Harreld and E.O. Schlemper, Acta Cryst., 1971, B27, 1964 and refs. therein.
20. E.O. Schlemper and D. Britton, Inorg. Chem., 1966, 5, 995.
21. (a) J.D. Graybeal and D.A. Berta, Nat. Bur. Stand.(U.S.) Spec. Publ. No. 301,393 (1967). This structural analysis was based on an incorrect space group.
(b) A.G. Davies, H.J. Milledge, D.C. Puxley and P.J. Smith, J. Chem. Soc. (A), 1970, 2862.
22. N.G. Bokil, Yu. T. Struchkov and A.K. Prokof'ev, J. Struct. Chem. (USSR), 1972, 13, 619.
23. P.T. Greene and R.F. Bryan, J. Chem. Soc. (A), 1971, 2549.
24. (a) Y.M. Chow, Inorg. Chem., 1970, 9, 794; (b) Y.M. Chow, Inorg. Chem., 1971, 10, 673; (c) R.A. Forder and G.H. Sheldrick, J. Organometal Chem., 1970, 22, 611; (d) J. Konnert, D. Britton and Y.M. Chow, Acta Cryst., 1972, B28, 180.

25. (a) R.A. Forder and G.M. Sheldrick, J. Chem. Soc.(D), 1969, 1125;
 (b) R.A. Forder and G.M. Sheldrick, J. Organometal. Chem., 1970, 21, 115; (c) R. Hulme, J. Chem. Soc., 1963, 1524; (d) N. Kasal, K. Yasuda and R. Okawara, J. Organometal. Chem., 1965, 3, 172;
 (e) E.O. Schlemper and D. Britton, Inorg. Chem., 1966, 5, 507;
 (f) Y.M. Chow and D. Britton, Acta Cryst., 1971, B27, 856;
 (g) H.C. Clark, R.J. O'Brien and J. Trotter, J. Chem. Soc., 1964, 2332; (h) J.B. Hall and D. Britton, Acta Cryst., ¹⁹⁷²B28, 2133;
 (i) A.M. Domingos and G.M. Sheldrick, J. Organometal. Chem., 1974, 67, 257.
26. (a) J.S. Thayer and R. West, Advan. Organometal. Chem., 1967, 15, 169; (b) M.F. Lappert and H. Pyszora, Advan. Inorg. Chem. Radiochem., 1966, 9, 133; (c) D. Britton, Perspect. Struct. Chem., 1967, 1, 109.
27. N.G. Bokil, G.N. Zakharova and Yu. T. Struchkov, Zh. Strukt. Khim., 1970, 11, 895.
28. (a) P. Green and J. Graybeal, J. Am. Chem. Soc., 1967, 89, 4305;
 (b) T. Srivastava, J. Organometal. Chem., 1967, 10, 373.
29. (a) H.A. Stöckler, private communication quoted in J. Am. Chem. Soc., 1968, 90, 3234; (b) A.G. Davies, H.J. Milledge and D.C. Puxley, unpublished work, quoted in 'MTP International Review of Science', Vol. 4, ed. H.J. Emeléus, pg 280, ref. 31.
30. G.M. Bancroft, K.D. Butler and T.K. Sham, J. Chem. Soc. (A), 1975, 1483.
31. M. Mammi, V. Buseti and A. del Pra, Inorg. Chim. Acta, 1967, 1, 419.
32. G. Gruttner and E. Krause, Ber. Deut. Chem. Ges., 1916, 49, 1415.
33. R.J.H. Clark, A.G. Davies and R.J. Puddephatt, J. Am. Chem. Soc., 1968, 90, 6923; Inorg. Chem., 1969, 8, 457.
34. J.E. Drake, R.T. Hemmings, J.L. Hencher, F.M. Mustoe and Q. Shen, J. Chem. Soc. Dalton, 1976, 385; ibid., 1976, 811.
35. V.I. Kulishov, N.G. Bokil, Yu. T. Struchkov, O.M. Nefedov, S.P. Kolesnikov and B.L. Perl'mutter, Zh. Strukt. Khim., 1970, 11, 71.

36. R. Eujen and H. Bürger, J. Organometal. Chem., 1975, 88, 165.
37. G.M. Sheldrick and R. Taylor, J. Organometal Chem., 1975, 87, 145; 1975, 101, 19.
38. P.G. Harrison, T.J. King and J.A. Richards, J. Chem. Soc. Dalton, 1976, 1414.
39. P.C. Lecomte, J. Protas and M. Davaud, Acta Cryst., 1976, B32, 923.
40. T.K. Sham and G.M. Bancroft, Inorg. Chem., 1975, 14, 2281.
41. M. Nagashima, H. Fujii and M. Kimura, Bull. Chem. Soc. Japan, 1973, 46, 3708.
42. (a) B. Beagley, K. McAloon and J.M. Freeman, Acta Cryst., 1974, B30, 444; (b) H. Fujii and M. Kimura, Bull. Chem. Soc. Japan, 1971, 44, 2643.
43. I.A. Ronova, N.A. Suritsyna, Yu. T. Struchkov and A.K. Prokof'ev, Zh. Strukt. Khim., 1972, 13, 15.
44. P.G. Harrison, T.J. King and J.A. Richards, J. Chem. Soc. Dalton, 1974, 1723.
45. P.J. Vergamini, H. Vahrenkamp and L.F. Dahl, J. Am. Chem. Soc., 1971, 93, 6237.
46. (a) M. Elder and D. Hall, Inorg. Chem., 1969, 8, 1268, 1273; (b) R.A. Anderson and F.W.B. Einstein, Acta Cryst., 1976, B32, 966.
47. M. W. Lister and L.E. Sutton, Trans. Faraday Soc., 1941, 37, 393.
48. P. Brand and H. Sackmann, Acta Cryst., 1963, 16, 446; F. Mellow and I. Fankuchen, Acta Cryst., 1955, 8, 343.
49. H.A. Skinner and L.E. Sutton, Trans. Faraday Soc., 1944, 40, 164.
50. (a) T. Kimura, T. Ueki, N. Yasuoka, N. Kasai and M. Kakudo, Bull. Chem. Soc. Japan, 1969, 42, 2479; (b) N. Yoshida, T. Ueki, N. Yasuoka, N. Kasai, M. Kakudo, I. Omae, S. Kikkawa and S. Matsuda, Bull. Chem. Soc. Japan, 1968, 41, 1113.
51. (a) H. Preut, W. Wolfes and H.J. Haupt, Z. anorg. Chem., 1975, 412, 121; (b) G.A. Melson, P.F. Stokely and R.F. Bryan, J. Chem. Soc. (A), 1970, 2247; (c) R.D. Hall and D. Hall, J. Organometal Chem., 1973, 52, 293; (d) T.S. Cameron and C.K. Prout, J. Chem. Soc. Dalton, 1972, 1447.

36. R. Eujen and H. Bürger, J. Organometal. Chem., 1975, 88, 165.
37. G.M. Sheldrick and R. Taylor, J. Organometal Chem., 1975, 87, 145; 1975, 101, 19.
38. P.G. Harrison, T.J. King and J.A. Richards, J. Chem. Soc. Dalton, 1976, 1414.
39. P.C. Lecomte, J. Protas and M. Davaud, Acta Cryst., 1976, B32, 923.
40. T.K. Sham and G.M. Bancroft, Inorg. Chem., 1975, 14, 2281.
41. M. Nagashima, H. Fujii and M. Kimura, Bull. Chem. Soc. Japan, 1973, 46, 3708.
42. (a) B. Beagley, K. McAloon and J.M. Freeman, Acta Cryst., 1974, B30, 444; (b) H. Fujii and M. Kimura, Bull. Chem. Soc. Japan, 1971, 44, 2643.
43. I.A. Ronova, N.A. Suritsyna, Yu. T. Struchkov and A.K. Prokof'ev, Zh. Strukt. Khim., 1972, 13, 15.
44. P.G. Harrison, T.J. King and J.A. Richards, J. Chem. Soc. Dalton, 1974, 1723.
45. P.J. Vergamini, H. Vahrenka, p and L.F. Dahl, J. Am. Chem. Soc., 1971, 93, 6237.
46. (a) M. Elder and D. Hall, Inorg. Chem., 1969, 8, 1268, 1273; (b) R.A. Anderson and F.W.B. Einstein, Acta Cryst., 1976, B32, 966.
47. M. W. Lister and L.E. Sutton, Trans. Faraday Soc., 1941, 37, 393.
48. P. Brand and H. Sackmann, Acta Cryst., 1963, 16, 446; F. Mellow and I. Fankuchen, Acta Cryst., 1955, 8, 343.
49. H.A. Skinner and L.E. Sutton, Trans. Faraday Soc., 1944, 40, 164.
50. (a) T. Kimura, T. Ueki, N. Yasuoka, N. Kasai and M. Kakudo, Bull. Chem. Soc. Japan, 1969, 42, 2479; (b) M. Yoshida, T. Ueki, N. Yasuoka, N. Kasai, M. Kakudo, I. Omae, S. Kikkawa and S. Matsuda, Bull. Chem. Soc. Japan, 1968, 41, 1113.
51. (a) H. Preut, W. Wolfes and H.J. Haupt, Z. anorg. Chem., 1975, 412, 121; (b) G.A. Melson, P.F. Stokely and R.F. Bryan, J. Chem. Soc. (A), 1970, 2247; (c) R.D. Hall and D. Hall, J. Organometal Chem., 1973, 52, 293; (d) T.S. Cameron and C.K. Prout, J. Chem. Soc. Dalton, 1972, 1447.

52. V. Cody and E.R. Corey, J. Organometal. Chem., 1969, 19, 359.
53. D.F. van de Vordel, H. Willeman and G.P. van der Kelen, J. Organometal. Chem., 1973, 63, 205.
54. R.F. Zahrobsky, J. Solid State Chem., 1973, 8, 101.
55. I.D. Brown and R.D. Shannon, Acta Cryst., 1975, A29, 266; I.D. Brown, J. Solid State Chem., 1974, 11, 214.
56. A.J. Buttenshaw, M. Duchene and M. Webster, J. Chem. Soc. Dalton, 1975, 2230.
57. F.W.B. Einstein and B.R. Penfold, J. Chem. Soc. (A), 1968, 3019.
58. F.P. Boer, F.P. van Remoortere, P.P. North and G.N. Reeke, Inorg. Chem., 1971, 10, 529.
59. N.G. Bokil, Yu. T. Struchkov, D.N. Krartsov and E.M. Rokhlina, Zh. Strukt. Chim., 1974, 15, 497. (C.A. 81:69697).
60. P.G. Perkins and D.H. Wall, J. Chem. Soc. (A), 1971, 3620.
61. G.M. Bancroft, K.D. Butler, A.T. Rake and B. Dale, J. Chem. Soc. Dalton, 1972, 2025.
62. R.C. Poller, 'Chemistry of Organotin Compounds', Academic Press, New York, 1970.
63. J.R. Holmes and H.D. Kaesz, J. Am. Chem. Soc., 1961, 83, 3903.
64. W. McFarlane, J. Chem. Soc. (A), 1967, 528.
65. E.V. van den Berghe and G.P. van der Kelen, J. Organometal. Chem., 1968, 11, 479.
66. First suggested by M.M. McGrady and R.S. Tobias, J. Amer. Chem. Soc., 1965, 87, 1909, although equatorial bonding has been discussed in terms of 3c-4e orbitals by e.g. E.O. Schlemper, Inorg. Chem., 1967, 6, 2012 and E.O. Schlemper, Inorg. Chem., 1973, 12, 677.

See also E.M. Shustorovich and Yu. A. Buslaev, Inorg. Chem., 1976, 15, 1142 and ref. 8 therein for a discussion of the mutual cis/trans influences of ligands and the application of hypervalent bonding theory in the main group co-ordination compounds. This paper also contains an energy level diagram showing the relative energy positions organo and halogen atoms adopt in relation to the energy levels of the main group elements.

CHAPTER II

The Crystal and Molecular Structures of the Solid Solvate Seleninyl Dichloride, Dioxane and of Iodoxybenzene; Distorted Octahedral Arrangements of Primary and Secondary Bonds

II.1. Introduction

In the previous chapter, the central tin atoms of the diethyl tin dihalides were regarded as distorting under the influence of secondary bonds from neighbouring molecules so that the resultant geometries are intermediate between tetrahedral and octahedral. In this chapter it is intended to discuss further octahedral and distorted octahedral arrangements of primary and secondary bonds, and perhaps show considerable variance in the role of any lone pairs in affecting the secondary bonds and hence the resultant structures. In particular two systems will be used to illustrate these points. The first involves the several known solid solvates of seleninyl dichloride and in particular the crystal structure of the 1:1 solvate with dioxane. The second will involve a discussion of the crystal structure of iodoxybenzene in relation to these solvates and other compounds, all of which have considerably more distorted arrangements of primary and secondary bonds.

V.2. The Solid Solvates of Seleninyl Dichloride[†]

The non-aqueous solvent seleninyl dichloride has for some time been known to form solid solvates with a variety of metal halides and organic acids and bases.¹ Wise² performed much of the original work back in 1923, but he found that, apart from the problems of excluding all traces of moisture, the resulting solvates often form gelatinous melts from which it is very difficult to isolate pure (crystalline) materials. Single crystals suitable for X-ray work have been isolated for a few of the solvates by conventional or zone-melting techniques, and the results of these studies have been reviewed by Hermodsson³ and Cordes.⁴ The interest in the structural properties of these solvates concerns the multi-functional role

[†] Also known as selenium oxychloride or dichloro selenium(IV) oxide.

of the seleninyl dichloride molecules and the importance in identifying specific solute-solvent interactions. In $\text{SnCl}_4 \cdot \text{SeOCl}_2$ ⁵ and $\text{SbCl}_5 \cdot \text{SeOCl}_2$ ⁶ the solvent acts as a Lewis base using a lone pair of electrons on oxygen in the co-ordination bond, whilst in the adduct $\text{SeOCl}_2 \cdot 2\text{C}_5\text{H}_5\text{N}$ ⁷, the seleninyl dichloride behaves as a Lewis acid, expanding its valence shell to give a distorted square pyramidal structure with trans chlorine and nitrogen atoms. Finally, in the complex $(\text{CH}_3)_4\text{N}^+\text{Cl}^- \cdot 5\text{SeOCl}_2$ there is a centrosymmetric cluster $(2\text{Cl} \cdot 10\text{SeOCl}_2)^{2-}$ in which the seleninyl dichloride solvates chloride ions via a variety of weak inter-molecular contacts.⁸ In fact, in all of the solvates of seleninyl dichloride studied so far, the selenium atoms have been found to form $\text{Se} \dots \text{O}$ and $\text{Se} \dots \text{Cl}$ contacts which may be described as secondary bonds. Inclusion of these contacts results in the geometry about the selenium atoms being based on an octahedral arrangement of three primary and three secondary bonds, although in some cases the third secondary bond opposite the $\text{Se}-\text{O}$ bond may be significantly longer than the other two secondary bonds. The geometry in those cases has been described in terms of a square pyramid with the lone pair assumed to point in the direction of the third longer contact, although the octahedral description of the primary and secondary bonds is more complete. Furthermore there are other examples where a secondary bond has been replaced by two longer contacts, and it may be inferred from these results that the steric role of the lone pair of electrons on SeOCl_2 varies in importance. In those cases where an octahedron can be observed, the angles $\text{X}-\text{Se} \dots \text{Y}$ ($\text{X}, \text{Y} = \text{O}$ or Cl) have been found to lie in the range $142 - 173^\circ$, and there appears to be no clear way of deciding which atoms, chlorine or oxygen, are going to form the secondary bonds.⁹ The present structure of $\text{SeOCl}_2 \cdot \text{dioxane}$ is, however, the first in which SeOCl_2 is involved in three secondary bonds to oxygen with the SeOCl_2 being classed as amphoteric. The octahedral environment of selenium in this compound will be compared to several analogous systems of 3 primary and 3 (or 4) secondary bonds in Section (II.5.).

II.3. Iodoxybenzene

The preparation of many organotervalent iodine compounds proceeds via iodosobenzene, which is most conveniently prepared by reacting iodosobenzene dichloride with aqueous sodium hydroxide.¹⁰ During one such preparation, using an excess of water, several thin crystalline plates were noticed amongst the yellow powdery product. In the belief that these were crystalline iodosobenzene which would be expected from previous studies of organotervalent iodine compounds to have extensive inter-molecular interactions or secondary bonds (Chapter III), a low temperature data set was collected. The structure solution, however, showed the compound to be another possible product, namely iodoxybenzene. Nonetheless, the structure of this compound again contains several important intermolecular interactions which are described as being part of a more strongly distorted octahedral arrangement of primary and secondary bonds due to the more prominent importance of the iodine lone pair. Again, analogous systems will be quoted, and the inter-relation between these two diverse systems will be qualitatively discussed.

II.4. Experimental

II.4.1. Preparations and Data Collections

(II.4.1.(1)) $\text{SeOCl}_2 \cdot \text{Dioxane}$

Dropwise addition of a carbon tetrachloride (dried over CaCl_2) solution of seleninyl dichloride (BDH Chemicals Ltd.) to a carbon tetrachloride solution of dioxane (dried over sodium) gave immediate precipitation of clear, colourless needle-shaped crystals of the 1:1 solvate. These crystals are extremely moisture sensitive and needed to be mounted in Lindemann capillaries baked for several hours in vacuo to minimize crystal decomposition.

Crystal data: $\text{C}_4\text{H}_8\text{Cl}_2\text{SeO}_3$, orthorhombic, $a = 8.884(2)$, $b = 12.066(3)$, $c = 8.410(3)$ Å, $U = 901.5(5)$ Å³, $D_c = 1.870$ g/cm³ for $Z = 4$. Mo K_α radiation, $\lambda = 0.71069$ Å, $\mu(\text{Mo-K}_\alpha) = 50.10$ cm⁻¹, $F(000) = 496.0$.

Systematic absences $0k1$, $k+1 \neq 2n$ and $h0l$, $h \neq 2n$ indicate space groups Pnam (No. 62 non-standard) or $\text{Pna}2_1$ (No. 33).

Unit cell dimensions and data were collected using the diffractometer, and a crystal of size $0.194 \times 0.104 \times 0.093$ mm. Reflections were measured using θ - 2θ scans to a maximum 2θ of 55° . A variable scan rate of $3.0^\circ/\text{min}$ to $29.3^\circ/\text{min}$ depending on the intensity of a preliminary 2 sec count was used. Background counts were recorded at each end of the scan, each for one quarter of the scan time. The intensities of four standard reflections were recorded every 55 reflections. These showed gradual crystal decomposition complicated by slight movements of the crystal in the capillary. The effects of the crystal movement were reduced by recentering at frequent intervals and increasing the scan range of $(K_{\alpha_1} - 1.0^\circ)$ to $(K_{\alpha_2} + 1.0^\circ)$ to $(K_{\alpha_1} - 2.0^\circ)$ to $(K_{\alpha_2} + 2.0^\circ)$ after 480 reflections had been collected. A correction for crystal decomposition was obtained by scaling the collected data in small sections, using several linear equations of the form $F = F_0 (1 + at)$ where a = a linear scaling coefficient and t = time.

1190 unique reflections were collected of which 640 were considered observed, $(I/\sigma(I) \geq 3.0)$, and used in refinement.[†] Lorentz, polarisation and absorption corrections were applied, the last with the program ABSCOR.

(II. 4. 1. (II)) Iodoxybenzene

As mentioned above, during the standard preparation of Iodosobenzene by the hydrolysis of Iodobenzene dichloride,¹⁰ an excess of water was used and the product was left overnight to react. Amongst the expected Iodosobenzene product, a fine yellow powder normally, was a small amount of thin, clear, approximately hexagonal crystalline platelets. Several of these crystals were separated and extinguished sharply under polarised light. Many were too thin, however, to scatter X-rays well. A much thicker, roughly hexagonal crystal of size ca. 0.19×0.16 mm and thickness 0.021 mm was eventually found and used for the data collection. As a precaution

[†] Two reflections (01-1) and (200) were later removed because of large extinction effects.

against the known tendency of organolodine compounds to undergo rapid photo-decomposition in X-rays (see Chapter III) it was decided to cool the crystal down to -100°C using the Syntex LT-1 attachment to the diffractometer.

Crystal data:

$\text{C}_6\text{H}_5\text{IO}_2$, M.W. = 236.0, monoclinic, $a = 12.9041(23)$, $b = 6.4023(14)$, $c = 4.0115(7)$ Å, $\beta = 99.018(14)^{\circ}$, $V = 327.32(11)$ Å³, at -100°C $D_c = 2.394$ g/cm³ for $Z = 2$. Mo K_{α} radiation, $\lambda = 0.71069$ Å, $\mu(\text{Mo}-K_{\alpha}) = 48.66$ cm⁻¹, $F(000) = 220.0$. Systematic absence $0k0$, $k \neq 2n$ indicates space group $P2_1$ (No. 4).

Unit cell dimensions and data were collected using the diffractometer. Reflections were measured using θ - 2θ scans to 2θ of 60° in three shells, using a scan range ($K_{\alpha 1} - 0.75$) to ($K_{\alpha 2} + 0.75$) and scan speed $0.7 - 29.3^{\circ}/\text{min}$. Other conditions were the same as in (II.4.1.(1)). Four standards collected every 60 reflections showed only statistical fluctuations throughout the data collection. 1080 reflections were eventually processed (thus excluding several blocks of data recollected using a better orientation matrix and a block of reflections with low values due to problems with the generator (also recollected)). Of these, 801 were observed ($I/\sigma(I) \geq 3.0$); averaging symmetry equivalent reflections reduced this further to a final set of 775 data.

II.4.2. Structure Solution and Refinement

(II.4.2.(1)) $\text{SeOCl}_2 \cdot \text{Dioxane}$

Initially the centric space group $Pnam$ was assumed but was rejected at an early stage. The co-ordinates of the selenium atom were located in a Patterson map and Fourier maps revealed the remaining light atoms. Hydrogen atoms in the dioxane molecule were placed in calculated positions ($\text{C-H} = 0.95$ Å) with temperature factors of 0.06. In the final cycles of least squares refinement, anisotropic temperature factors were used for all non-hydrogen atoms with the hydrogen atom parameters fixed. The weights used were given by $w = X \cdot Y$ where, if $\sin \theta < 0.35$, $X = \sin \theta / 0.35$ otherwise $X = 1$ and if $F_{\text{obs}} > 27.0$ then $Y = 27.0 / F_{\text{obs}}$ otherwise $Y = 1$. This scheme gave unit weights to most

reflections, but downweights those reflections with large F_{obs} and/or low $\sin \theta$.

The refinement, including corrections for anomalous dispersion, converged to a final R of 0.052 and weighted R of 0.064; in the final cycle no parameter shift was greater than 12% of its standard deviation. The final difference Fourier was featureless except for residual peaks near the selenium. There was virtually no difference in refinement with the two alternative 'hands' of the molecule, with negligible differences in bond distances and bond angles.

(II. 4. 2. (ii)) Iodoxybenzene

The co-ordinates of the iodine atom were readily located from the Harker plane $U\frac{1}{2}V$ in the Patterson. In space group $P2_1$, with a single heavy atom, the y co-ordinate can be arbitrarily fixed ($y = 0$) to define the position of the molecule with respect to the polar 2_1 axis. As a consequence the phases based on this iodine have the centrosymmetric values 0 and 180° , and the resulting Fourier contained a mirror plane at $y = \frac{1}{2}$ relating different images of the true molecule. The immediate observation from the original Fourier was that the compound was not iodosobenzene as expected, but iodoxybenzene, another likely reaction product. However, the normal process in locating all the atoms in the correct mirror image of the molecule is to break the pseudosymmetry in the map by including a second heavy atom in the calculation. In the present case, there were some difficulties encountered before the present atomic arrangement was obtained, because the positions of the carbons in the phenyl ring did not help discriminate between the alternative oxygen positions, all of which gave similar R-factors when refined. However, of the alternatives, two sets of oxygen positions resulted in a bad O...O contact of $\sim 1.75 \text{ \AA}$ and a third resulted in a close C...O contact, leaving the present arrangement as the most chemically reasonable.

Hydrogen atoms for the phenyl ring were included in calculated positions with fixed temperature factors. In the final cycles of least squares refinement, anisotropic temperature factors were used for the iodine and

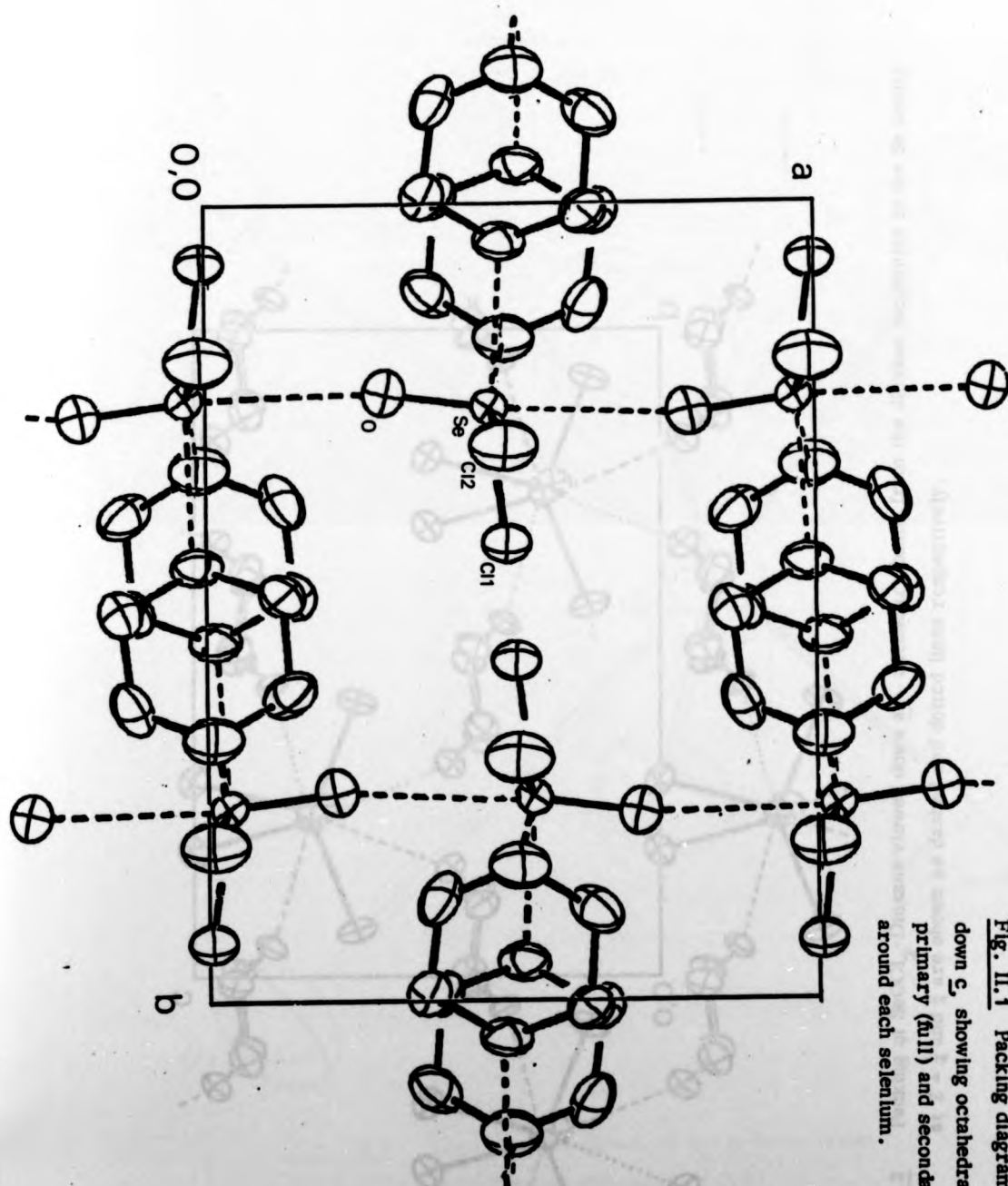


Fig. II. 1 Packing diagram for $\text{SeOCl}_2 \cdot \text{Dioxane}$ down c , showing octahedral arrangement of primary (full) and secondary (broken) bonds around each selenium.

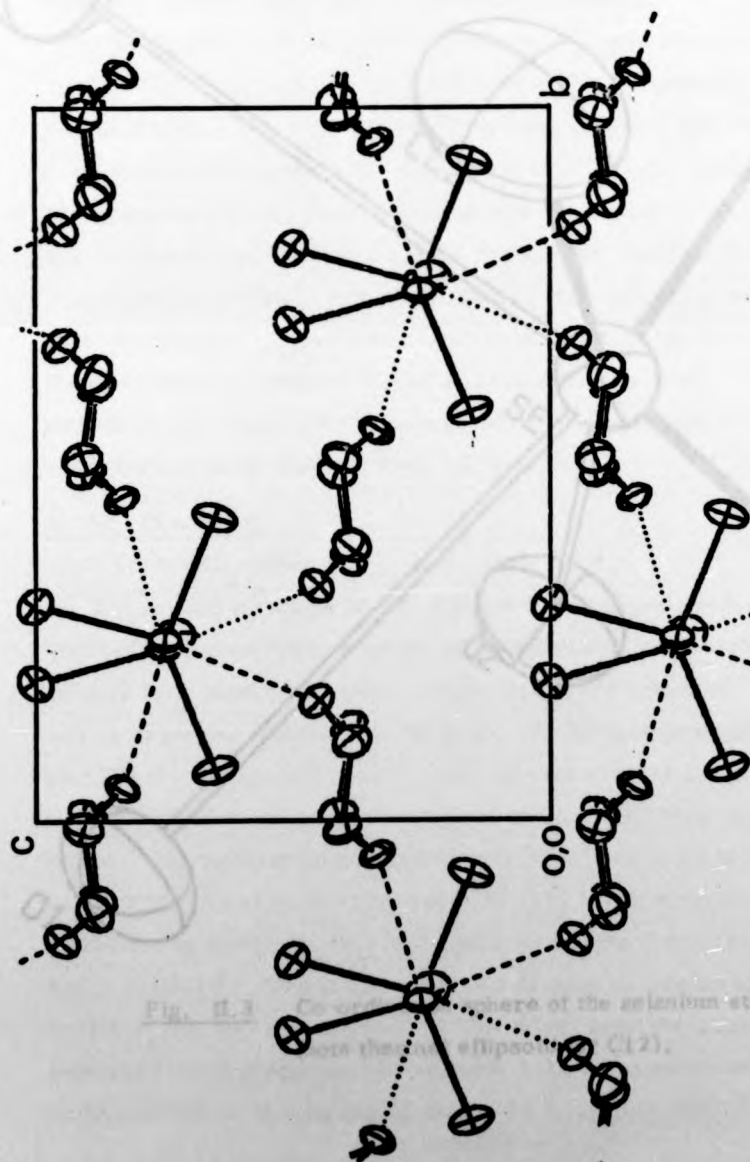


Fig. II. 2 Packing of $\text{SeOCl}_2 \cdot \text{Dioxane}$ viewed down a. Secondary bonds from the dioxane molecules to the Se atoms at $Z = \frac{1}{4}$ and $\frac{3}{4}$ are shown as dashed and dotted lines respectively.

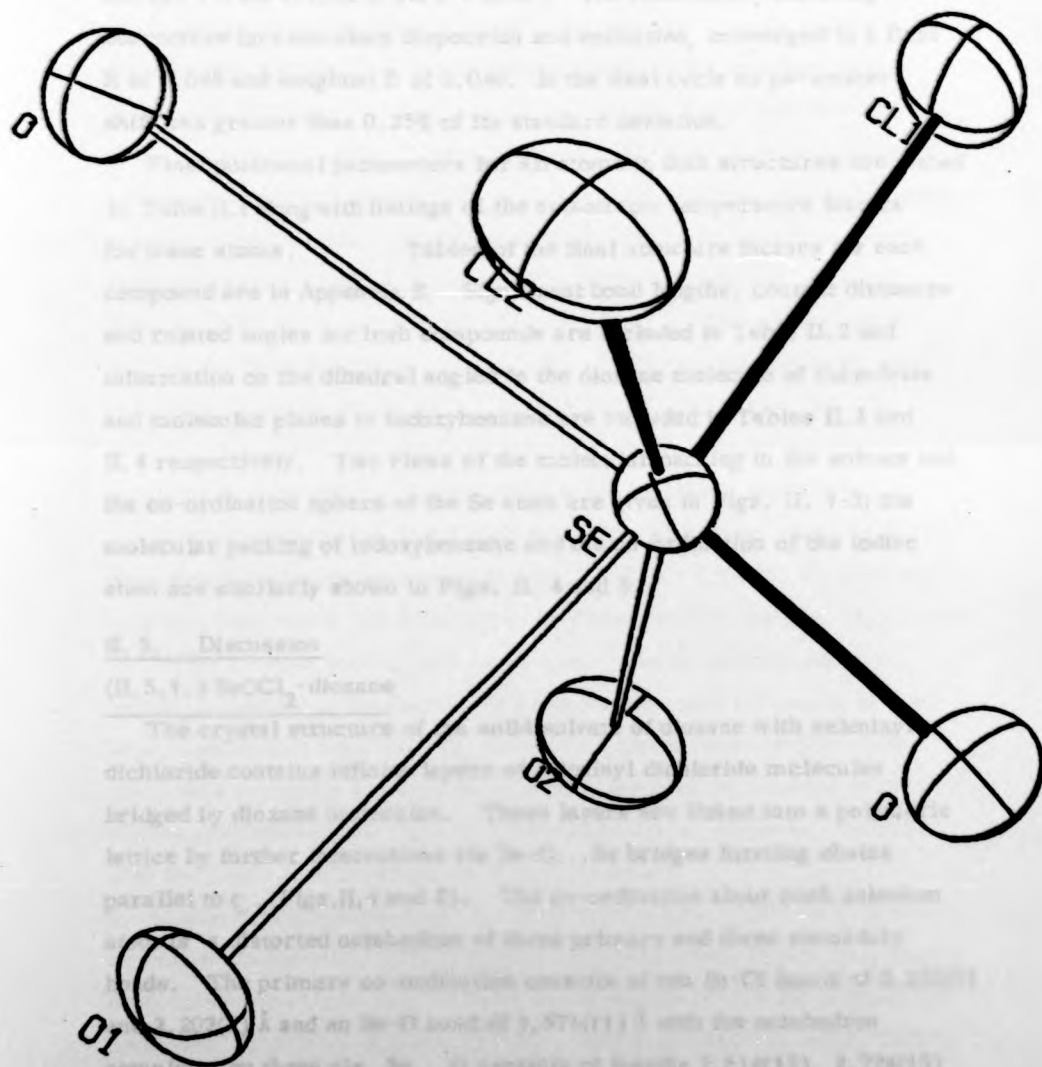


Fig. II.3 Co-ordination sphere of the selenium atom
(note thermal ellipsoid for Cl 2).

oxygen atoms and the reflections were given weights given by $w = X \cdot Y \cdot (1/\sigma(F))^2$ where (1) $X = F/10.0$ if $F < 10.0$, otherwise $X = 1$ and (2) $Y = \sin \theta / 0.30$ if $\sin \theta < 0.30$. The refinement, including corrections for anomalous dispersion and extinction, converged to a final R of 0.048 and weighted R of 0.046. In the final cycle no parameter shift was greater than 0.25% of its standard deviation.

Final positional parameters for all atoms in both structures are listed in Table II.1 along with listings of the anisotropic temperature factors for these atoms. Tables of the final structure factors for each compound are in Appendix B. Significant bond lengths, contact distances and related angles for both compounds are included in Table II.2 and information on the dihedral angles in the dioxane molecule of the solvate and molecular planes in iodoxybenzene are included in Tables II.3 and II.4 respectively. Two views of the molecular packing in the solvate and the co-ordination sphere of the Se atom are given in Figs. II. 1-3; the molecular packing of iodoxybenzene and the co-ordination of the iodine atom are similarly shown in Figs. II. 4 and 5.

II. 5. Discussion

(II. 5. 1.) $\text{SeOCl}_2 \cdot \text{dioxane}$

The crystal structure of the solid solvate of dioxane with seleninyl dichloride contains infinite layers of seleninyl dichloride molecules bridged by dioxane molecules. These layers are linked into a polymeric lattice by further interactions via Se-O...Se bridges forming chains parallel to c . (Figs. II. 1 and 2). The co-ordination about each selenium atom is a distorted octahedron of three primary and three secondary bonds. The primary co-ordination consists of two Se-Cl bonds of 2.235(5) and 2.202(7) Å and an Se-O bond of 1.571(11) Å with the octahedron completed by three *cis* Se...O contacts of lengths 2.614(13), 2.724(15) and 2.902(11) Å. Two involve different dioxane molecules with Cl-Se...O angles of 168.1(4) and 167.5(4)°. The third, from the oxygen atom of an adjacent selenenyl oxychloride molecule links the layers together with the O-Se...O and Se-O...Se angles being 168.6(12)° and 166.2(14)°. (Fig. II. 3).

The Se...O contact distances should be compared with the sums of the covalent and van der Waals radii for oxygen and selenium (1.80 and 3.42 Å respectively).

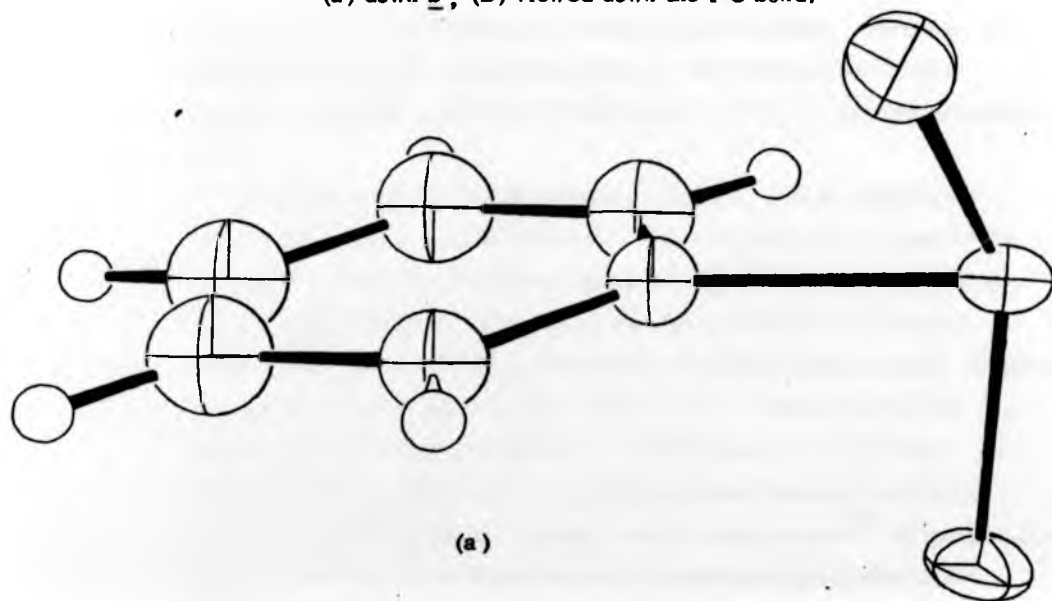
In the seleninyl dichloride moiety, the two Se-Cl bonds appear to be significantly different but this is almost certainly due to anisotropy of the thermal motion of Cl(2). No corrections for this effect has been made. The average Se-Cl bond length of 2.22 Å should be compared to a value of 2.204(5) Å determined in a gas-phase electron-diffraction study of seleninyl dichloride. In the same study, the Se-O bond length was determined as 1.612(5) Å and the angles Cl-Se-Cl and Cl-Se-O were found to be 96.8(7)° and 105.8(7)° respectively.¹¹ The present study has found a Se-O bond length of 1.571(11) Å, Cl-Se-Cl angle of 95.6(3)° and Cl-Se-O angles of 101.6(7)° and 103.6(12)°. Clearly, the differences between the seleninyl dichloride in the solvate with the parameters observed for the molecule in the gas phase are slight.

In other solvates the Se-Cl bond length has an average value of 2.123 Å (based on 6 measurements ranging from 2.09(1) - 2.141(9) Å) when SeOCl₂ acts as a base and 2.235 Å (based on 16 measurements ranging from 2.17(1) - 2.251(6) Å) when SeOCl₂ acts as an acid.⁴ In the present case, the SeOCl₂ is somewhat amphoteric in using the lone pair on oxygen in one Se...O secondary bond (that is, acting as a Lewis base) whilst at the same time accepting electron density from the bridging dioxane molecules (Lewis acid behaviour). The Se-Cl distance would, however, indicate that the Lewis acid behaviour is more significant.

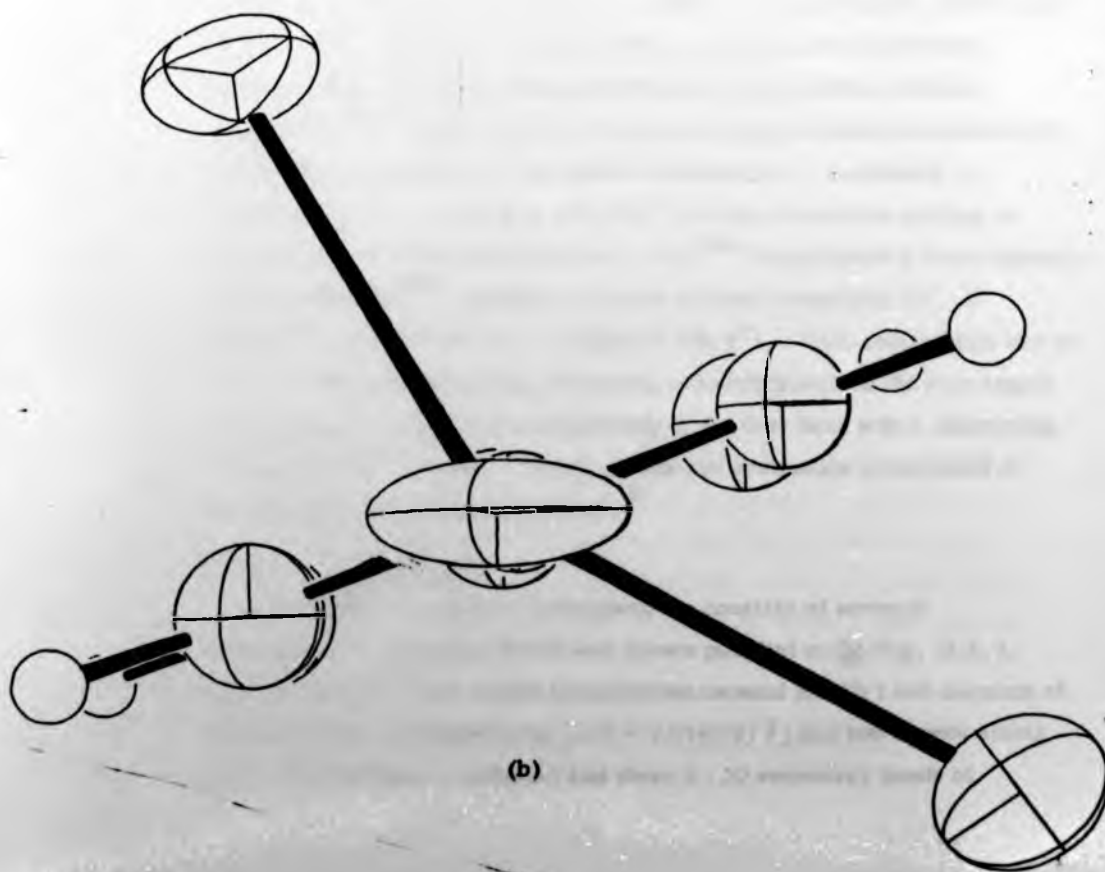
In other solvate structures the Se-O bond lengths in the SeOCl₂ moiety depend on its function. Thus, in those solvates where it acts as a Lewis base forming a co-ordinate bond via the oxygen atom, the Se-O bonds are lengthened (1.67(1) Å in SnCl₄·2SeOCl₂⁵ and 1.685(24) Å in SbCl₅·SeOCl₂⁶) compared with other solvates where lengths of 1.57 - 1.62 Å* have been observed. It is difficult to see further correlations between the individual values and the strength of the other inter-molecular contacts, partly

* The anomalous Se-O value of 1.82 found in [SeOCl₂·(C₆H₅)₃PO]₂ is due to rotational disorder.³

Fig. II. 4 Two views of isolated molecule of Iodoxybenzene.
(a) down \underline{b} , (b) viewed down the I-C bond.



(a)



(b)

because of the limited accuracy of some of these values. However, in the present structure, considering that the Se-O bond is involved in bridging interactions, the Se-O bond length (1.57(1) Å) appears somewhat short.

The dihedral angles for the dioxane molecule, which exists in the chair conformation, are in Table II.3. The distances and angles in the molecules are similar to those of dioxane itself.¹² The bridging role of the dioxane giving polymeric layers here has similarly been noted in several other structures of dioxane with molecules such as iodine, bromine and oxalyl chloride where infinite chains occur. Similar behaviour also occurs with the related molecules 1,4-dithiane and 1,4-diselenane, and the short contacts involving the oxygen, sulphur or selenium atoms have generally been described as charge transfer interactions.¹³ In the present example, the Se...O contacts involve the equatorial lone pairs of the oxygen atoms.

The Se...O distances in $\text{SeOCl}_2 \cdot \text{dioxane}$ fall in the middle of the range (2.47 - 3.14 Å) observed in other SeOCl_2 solvates, and in the intra-molecular Se...O contact distances found in several other selenium compounds.^{14, 15} Examples of the latter are bis(o-nitrobenzeneselenenyl) sulfide, in which there are two intra-molecular Se...O contacts of 2.574(8) Å (S-Se...O angle is 171.9(2)°) and the molecular packing is further dictated by Se-S contacts of 3.48 Å;^{14a} structure of o-formylphenyl-selenenyl bromide^{14b} similarly contains an intra-molecular Se...O contact of 2.31(2) Å (Br-Se...O angle is 176.8°). This contact also has an effect on the o-formyl group, producing a downfield shift of the nmr signal of the aldehyde proton and a lengthening of the C=O bond with a shortening of the adjacent C-C bond. These effects are even more pronounced in the analogous tellurenyl compounds.¹⁶

(II.5.2.) Iodoxybenzene

The crystal structure of iodoxybenzene consists of strongly distorted ClO_5 octahedra linked into layers parallel to bc (Fig. II.5.). The arrangement about iodine is somewhat unusual for I(V) and consists of primary bonds to a phenyl ring [I-C = 2.014(12) Å] and two oxygen atoms [I-O = 2.021(9) and 1.924(9) Å] and three I...O secondary bonds of

lengths 2.578(8), 2.660(10) and 2.733(9) Å. (Fig. II.5.). The distortion produced by these secondary bonds is shown in the angles between the primary bonds. Instead of a tetrahedral AX_3E arrangement typical of I(V) structures (as found in iodates¹⁷) the O-I-O angle has opened to $147.8(4)^\circ$ with the C-I-O closing to $91.1(4)$ and $76.3(4)^\circ$ so that the geometry is intermediate between AX_3E and a typical AX_3E_2 trigonal bipyramidal arrangement normally associated with I(III).[†]

In chemical terms the present geometry should perhaps be regarded as polymeric. Then the I-O bond lengths, which are long compared with other IO_3^- structures based on an octahedron of 3 primary and 3 secondary bonds, would be similar in length to bridging I-O distances in other polymeric ions such as HI_3O_8 .¹⁸

The deviation of the present geometry from an ideal T-shaped arrangement can be seen from the difference between the angle O-I-O [147.8°] and the sum of the two C-I-O angles [167.4°] and the displacement [1.83 Å] of C(1) from the OIO plane. The considerable distortion in the primary geometry also forces a close intra-molecular I...C(2) repulsive contact. Other evidence of this repulsive contact can be seen from the I-C-C angles which are significantly different [$116(1)$ cf. $122(1)^\circ$].

As a result of the pseudosymmetry present in the refinement, the other distances and angles in the phenyl ring are less accurate and no conclusions can be drawn although the effect of the iodine atom would be expected to slightly alter some of the ring angles. (See discussion of dppm and dppe ligands in Chapter VII).

If the present geometry is regarded as distorted trigonal bipyramidal, the phenyl ring being less electronegative than oxygen would be expected to be equatorial. The observed I-C distance is very close to normal I-C distances observed in other complexes (see Chapter III), and the sum of the covalent radii [2.10 Å]. The I-C distance in the closely related

[†] The normal geometry of an AX_3E_2 arrangement is T-shaped with the lone pairs and the least electronegative ligand in the equatorial plane, since this minimises lone pair-bonding pair repulsions (cf. Chapter III).

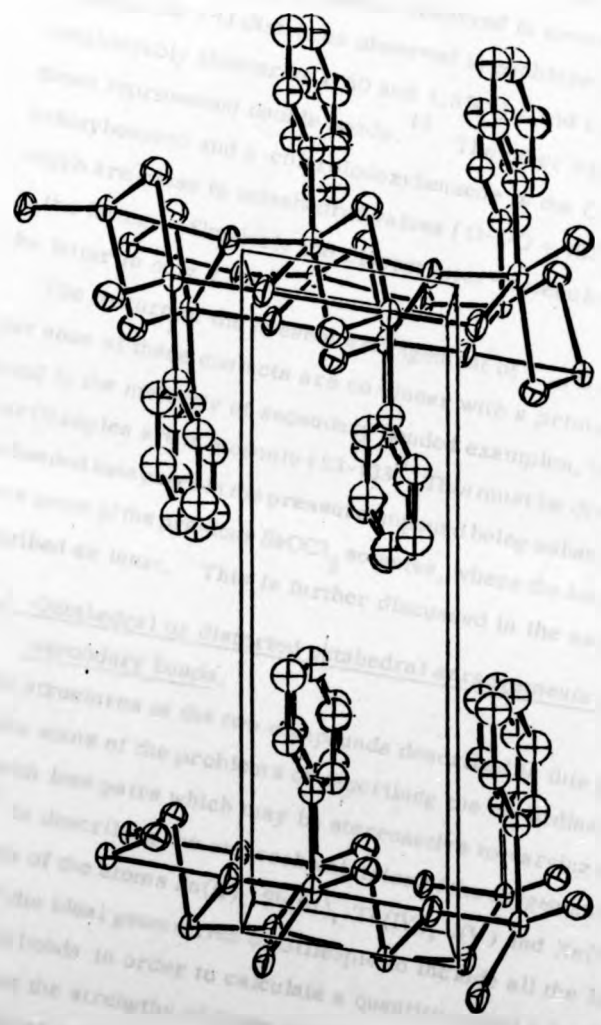


Fig. II.5 Packing diagram for iodoxybenzene viewed down b.

p-chlorolodoxybenzene¹⁹ is 1.93(5) Å. However, this determination is probably of limited accuracy. The I-O distances are also close to single bond distances observed in several other complexes although the I-O distances observed in p-chlorolodoxybenzene are considerably shorter at 1.60 and 1.65(5) Å and it was suggested that these represented double bonds.¹⁹ The other significant difference between lodoxybenzene and p-chlorolodoxybenzene is the O-I-O and C-I-O angles which are close to tetrahedral values [O-I-O = 103°; C-I-O = 94 and 95°] in the latter. Similarly the closest inter-molecular I...O contact in the latter is only 2.72 Å.

The feature of the present arrangement of I...O secondary bonds is that none of these contacts are co-linear with a primary bond as has been found in the majority of secondary bonded examples. The largest A-I...O (A = C or O) angles are in fact only 125-133°. This must be directly attributable to the non-bonded lone pairs in the present compound being substantially more important than in some of the previous SeOCl₂ solvates, where the lone pairs should be described as inert. This is further discussed in the next section.

(II.6.) Octahedral or distorted octahedral arrangements of primary and secondary bonds.

The structures of the two compounds described in this chapter illustrate some of the problems of describing the co-ordination around atoms with lone pairs which may be stereoactive to varying degrees. Brown¹⁷ in describing the stereochemistries of the oxygen and fluorine complexes of the atoms Sn(II), Sb(III), Te(IV), I(V) and Xe(VI) redefined the ideal geometries of Gillespie to include all the longer (secondary) bonds in order to calculate a quantity called a bond valence to represent the strengths of these additional interactions. All five of these redefined geometries are shown in Figure II.6 and can be described as follows:-

- A = AX₂Y₂E + two secondary bonds of ~ equal strength (bonds X5 and X6) = AX₂Y₂a₂E overall.
- C = AX₃E + three secondary bonds of ~ equal strength = AX₃a₃E overall.
- E = AX₄E + one secondary bond if E stereoinactive = AX₄CE overall, otherwise AX₄E.

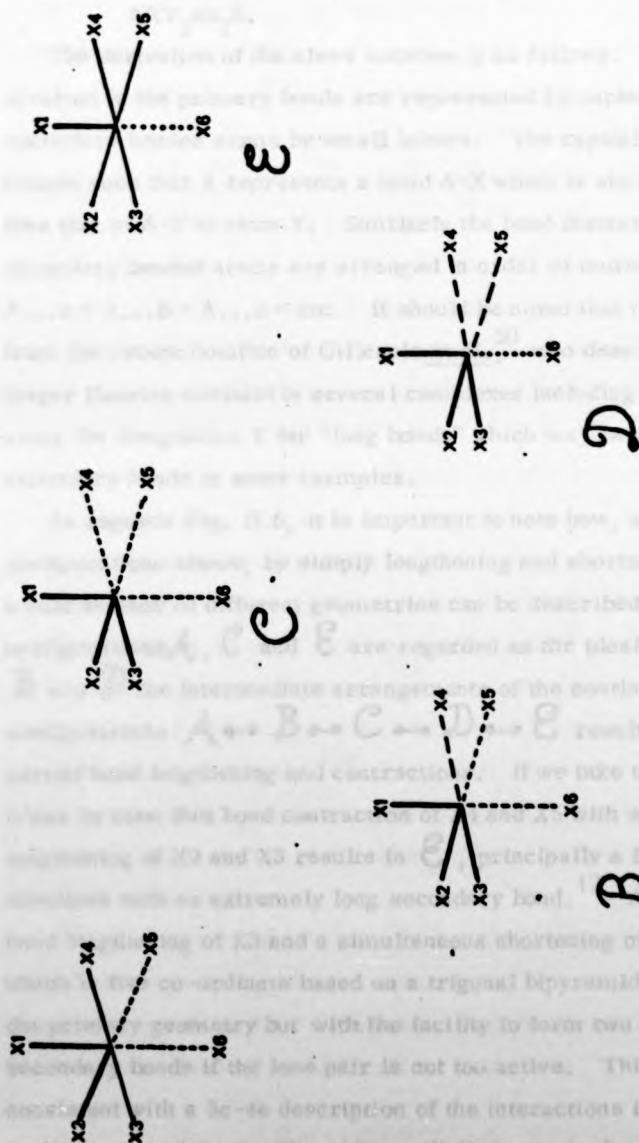
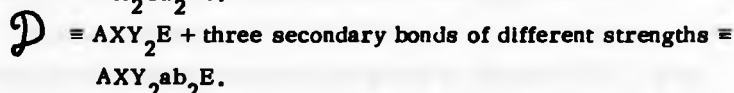
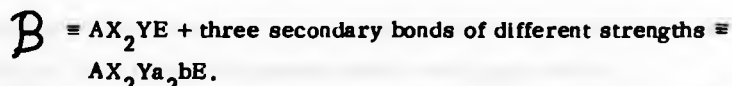


Fig. II.6
Characteristic arrangements of bonds around Sn(II), Sb(III), Te(IV), I(V) and Xe(VI)
according to Brown.¹⁷



The derivation of the above notation is as follows. The atoms involved in the primary bonds are represented by capital and the secondary bonded atoms by small letters. The capital letters are chosen such that X represents a bond A-X which is shorter (stronger) than that of A-Y to atom Y. Similarly the bond distances to the secondary bonded atoms are arranged in order of increasing length:- $A...a < A...b < A...c < \text{etc.}$ It should be noted that the above differs from the recent notation of Gillespie *et al.*,²⁰ who described the longer fluorine contacts in several complexes including the ion $[Sb_2F_4]^{2+}$ using the designation Y for "long bonds" which may be equivalent to secondary bonds in some examples.

As regards Fig. II.6, it is important to note how, using the configurations shown, by simply lengthening and shortening trans bonds a vast number of different geometries can be described. The three configurations \mathcal{A} , \mathcal{C} and \mathcal{E} are regarded as the ideal geometries with \mathcal{B} and \mathcal{D} the intermediate arrangements of the continuous set of configurations $\mathcal{A} \leftrightarrow \mathcal{B} \leftrightarrow \mathcal{C} \leftrightarrow \mathcal{D} \leftrightarrow \mathcal{E}$ resulting from partial bond lengthening and contractions. If we take the arrangement \mathcal{C} it can be seen that bond contraction of X4 and X5 with simultaneous lengthening of X2 and X3 results in \mathcal{E} , principally a five co-ordinate structure with an extremely long secondary bond.¹⁷ Alternatively, a bond lengthening of X3 and a simultaneous shortening of X4 results in \mathcal{A} which is five co-ordinate based on a trigonal bipyramid as regards the primary geometry but with the facility to form two additional secondary bonds if the lone pair is not too active. This idea is consistent with a 3c-4e description of the interactions involved. Cordes⁴ in discussion of the Se-Cl and Se...Cl distances in the $SeOCl_2$ solvates has already commented that there are three types of Se-Cl bonds "short",

"long" and "intermediate" - arranged short-long, intermediate-intermediate, etc. to give a constant sum to the trans-bonds.

Further discussion of the bond valence calculations associated with these co-ordination polyhedra are given in Chapter VI.3. It is sufficient to say that there are many examples available in the literature of other complexes of the non-metals bonded to ligands other than O and F whose co-ordination polyhedra can reasonably be assigned one of the descriptions *A*, *B*, *C*, *D* and *E* from a simple qualitative analysis of individual bond distances and angles.²² Those complexes in which more than six primary and secondary bonds are involved have higher co-ordination polyhedra which may be seen to be related to the octahedral arrangements by simple deformation mechanisms in which one or more of the secondary bonds in the octahedral arrangement are replaced by several weaker interactions. The normal cause of this change octahedral \rightarrow higher co-ordination is an increased stereoactivity of a lone pair of electrons which are defined as non-bonding rather than inert²¹ (see Chapter VI.). This appears to be the case with iodoxybenzene. The arrangement about the iodine in this compound is not very easily defined using any of these octahedral arrangements, and is probably defined as $AX_3a_3E_2$.

The other complex described in this chapter has a regular[†] octahedral arrangement of three primary and secondary bonds which has been found in a number of other examples.^{22a} The primary geometry in each case is based on a tetrahedral AX_3E arrangement of ligands *X* and lone pair *E*, although the overall geometry about the selenium could be described either as AX_3Y_3E or AX_3a_3E .

A feature of the present octahedral arrangement is that the angles Y-Se-Y between the cis oxygen contacts are less than 90° . This is somewhat surprising as the lone pair, if stereochemically active, would point in a direction bisecting the three Y contacts, and as a consequence

[†] Regular in the sense that secondary bonds are virtually co-linear with the primary.

the cis angles Y-Se-Y would be expected to be greater than 90° because of repulsive interactions. Furthermore, as the Cl-Se-Cl and Cl-Se-O angles are also intermediate between tetrahedral angles of 109.5° and angles of 90° based on an octahedron, the stereochemical role of the lone pair may be reduced in the present example and should be defined as inert.²¹

From a qualitative analysis it can readily be seen that the solid solvates of seleninyl dichloride contain selenium co-ordination polyhedra which range from *A* to *E*. The present geometry of the dioxane solvate is probably best described as *C*. Interestingly, the crystal structure of trifluoromethylselenium trichloride²³ contains a *D* type configuration about each selenium, the structure contrary to its original description can be regarded as $(\text{CF}_3)\text{SeCl}_2^+$ ions interacting via extensive Se...Cl interactions. The arrangement in SeOCl_3^- "dimers" of $\text{C}_5\text{H}_7\text{N}_2\text{SeOCl}_3$ is very similar (*B*)⁴; an *E* configuration can be found in $\text{SeOCl}_2 \cdot 2\text{py}$.⁷

Although the SeOCl_2 moiety has been extensively investigated in the other known solvates, no low temperature crystal structure of SeOCl_2 itself has yet been determined, although Hermoddson attempted a determination without success.³ However, the analogous seleninyl difluoride structure was recently determined at -35°C . As expected, the SeOF_2 is pyramidal [Se-O = 1.62 Å mean, Se-F = 1.70 Å] but forms a layer arrangement through secondary bonds to two oxygens (mean Se...O 2.76 Å) and a fluorine (Se...F 3.03 Å) so that the overall arrangement about the selenium is a distorted octahedron which is very similar to the SeF_3^+ complexes [SeF_3][Nb_2F_{11}], [SeF_3][NbF_6] and the SeOF_2 solvate with NbF_5 .²⁴ Again these appear to have *C* configurations.

(II.6.) References

1. I. Lindqvist, 'Inorganic Adduct Molecules of Oxo-Compounds', Springer-Verlag, 1963; J. Jackson and G.B.L. Smith, *J. Am. Chem. Soc.*, 1940, **62**, 544; M.J. Frazer, *J. Chem. Soc.*, 1961, 3165; J.C. Sheldon and S.Y. Tyree, *J. Am. Chem. Soc.*, 1959, **81**, 2290; B. Edgington and J.B. Firth, *J. Chem. Ind.*, 1936, 192.

TABLE II.1

Atomic co-ordinates ($\times 10^4$) with standard deviations in parentheses.

(a) <u>SeOCl₂·Dioxane</u>	<u>X</u>	<u>Y</u>	<u>Z</u>
Atom			
Se	5350(1)	2554(1)	7500(0)
Cl(1)	5070(7)	4263(4)	6522(9)
Cl(2)	5111(10)	3039(5)	10011(8)
O	7090(12)	2370(11)	7300(40)
O(1)	5152(18)	474(10)	8342(18)
O(2)	4905(22)	-1692(12)	9519(18)
C(1)	6426(22)	-95(17)	9102(29)
C(2)	6236(22)	-1283(18)	8881(31)
C(3)	3653(25)	-1126(17)	8833(32)
C(4)	3773(21)	104(16)	9019(28)
H(11)	6347	10	10364
H(12)	7324	174	8854
H(21)	6225	-1384	7754
H(22)	7075	-1681	9309
H(31)	2762	-1408	9322
H(32)	2653	-1260	7749
H(41)	2913	458	8668
H(42)	3748	246	10259

(b) Iodoxybenzene

ATOM	X	Y	Z
I	572.3(5)	0.0	3182.2(14)
O(1)	1097(7)	2586(15)	5807(21)
O(2)	468(7)	-1561(17)	-955(18)
C(1)	2053(9)	-968(21)	3098(28)
C(2)	2268(11)	-2952(26)	4128(35)
C(3)	3263(12)	-3761(32)	4200(38)
C(4)	4023(13)	-2502(28)	3065(41)
C(5)	3804(11)	-506(25)	1995(34)
C(6)	2800(8)	331(29)	1973(24)
H(2)	1728	-3810	4791
H(3)	3440	-5157	5000
H(4)	4716	-3036	3080
H(5)	4334	320	1225
H(6)	2640	1750	1277

TABLE II. 1 (cont.) Anisotropic temperature factors \dagger ($\times 10^3$) with standard deviations

in parentheses

(a) SeOCl₂·Dioxane

	U ₁₁	U ₂₂	U ₃₃	U ₁₂	U ₁₃	U ₂₃
Se	29.0(5)	27.7(5)	45.1(6)	-1.5(7)	-0.3(15)	1.2(11)
Cl(1)	52(3)	36(2)	86(4)	-1(2)	1(3)	19(2)
Cl(2)	103(6)	59(3)	50(3)	-1(3)	4(3)	-11(2)
O	38(5)	51(7)	72(14)	3(5)	-3(9)	3(10)
O(1)	61(9)	33(5)	50(8)	-2(5)	8(8)	13(6)
O(2)	80(13)	50(7)	50(8)	-2(7)	5(9)	13(6)
C(1)	42(10)	51(10)	67(15)	5(9)	-1(11)	5(10)
C(2)	43(10)	67(12)	59(12)	20(9)	-3(10)	15(11)
C(3)	60(12)	51(10)	64(13)	-16(10)	-21(10)	10(10)
C(4)	45(10)	43(9)	63(14)	6(8)	-16(10)	15(9)

Atoms H(11)-H(42) all have U = 0.07

(b) Iodoxybenzene

ATOM	U ₁₁	U ₂₂	U ₃₃	U ₁₂	U ₁₃	U ₂₃
I	26.3(3)	91.6(7)	14.9(3)	-1.6(18)	2.9(2)	0.5(16)
O(1)	31(4)	35(6)	32(4)	1(4)	5(3)	-5(4)
O(2)	39(5)	48(7)	16(3)	-9(5)	8(3)	-8(4)
ATOM	U	ATOM	U	ATOM	U	ATOM
C(1)	26(2)	C(2)	42(3)	C(3)	48(3)	C(4)
C(5)	46(4)	C(6)	32(3)	H(2)	52	H(3)
H(4)	61	H(5)	56	H(6)	42	
						51(4)
						57

\dagger In the form $\exp\{-2\pi^2(U_{11}h^2 + U_{22}k^2 + U_{33}l^2 + 2U_{12}hk + 2U_{13}hl + 2U_{23}kl)\}$

TABLE II.2

Significant bond lengths (\AA), contact distances and related
bond angles ($^\circ$) with standard deviations in parentheses

(a) SeOCl₂-DioxaneBond lengths[†]

Se-Cl(1)	2.235(5)	O(1)-C(1)	1.47(3)
Se-Cl(2)	2.202(7)	O(1)-C(4)	1.42(3)
Se-O	1.571(11)	O(2)-C(2)	1.39(3)
Se...O	2.902(11)	O(2)-C(3)	1.43(3)
Se...O(1)	2.614(13)	C(1)-C(2)	1.46(3)
Se...O(2)	2.724(15)	C(3)-C(4)	1.50(3)

Bond angles ($^\circ$)[†]

Cl(1)-Se-Cl(2)	95.6(3)	Se-O...Se	166.2(14)
Cl(1)-Se-O	101.6(7)	Se...O(1)-C(1)	121.0(11)
Cl(2)-Se-O	103.6(12)	Se...O(1)-C(4)	117.9(11)
		Se...O(2)-C(4)	124.2(14)
Cl(1)-Se...O(1)	168.1(4)	Se...O(2)-C(3)	119.3(14)
Cl(2)-Se...O(2)	167.5(4)	C(1)-O(1)-C(4)	110.0(15)
O-Se...O	168.6(12)	C(2)-O(2)-C(3)	109.7(16)
O-Se...O(1)	87.7(7)	O(1)-C(1)-C(2)	108.3(17)
O-Se...O(2)	85.9(12)	C(1)-C(2)-O(2)	113.5(18)
O(1)...Se...O(2)	82.9(4)	O(2)-C(3)-C(4)	112.2(18)
O...Se...O(1)	88.8(5)	C(3)-C(4)-O(1)	109.3(16)
O...Se...O(2)	82.9(7)		

[†] The C-H bond lengths range from 0.89 \AA to 1.07 \AA ; C-C-H angles range from 103.6 $^\circ$ to 115.8 $^\circ$, OCH angles from 107.5 $^\circ$ to 116.0 $^\circ$ and HCH angles from 103 $^\circ$ to 111 $^\circ$.

(b) Iodoxybenzene ^{*}Bond lengths (Å)

Around iodine

I - O(1)	2.021(9)	I...O(1')	2.733(9)
I - O(2)	1.924(8)	I...O(2'')	2.578(8)
I - C(1)	2.014(12)	I...O(2''')	2.660(10)
I...C(2)	2.872(15)		

Phenyl ring

C(1)-C(2)	1.351(21)	C(2)-H(2)	0.96
C(2)-C(3)	1.380(22)	C(3)-H(3)	0.96
C(3)-C(4)	1.400(26)	C(4)-H(4)	0.96
C(4)-C(5)	1.364(24)	C(5)-H(5)	0.95
C(5)-C(6)	1.400(19)	C(6)-H(6)	0.96
C(6)-C(1)	1.401(19)		

Bond angles (°)

Around iodine

O(1)-I-C(1)	91.1(4)	C(1)-I-O(1')	126.9(4)
O(1)-I-O(2)	147.9(4)	C(1)-I-O(2'')	94.7(4)
O(1)-I-O(1')	126.4(3)	C(1)-I-O(2''')	132.8(4)
O(1)-I-O(2'')	84.5(3)	O(1')-I-O(2'')	59.4(3)
O(1)-I-O(2''')	66.9(3)	O(1')-I-O(2''')	98.6(3)
O(2)-I-C(1)	76.4(4)	O(2'')-I-O(2''')	122.1(3)
O(2)-I-O(1')	83.3(3)	I-O(1)-I ^{IV}	109.5(3)
O(2)-I-O(2'')	125.4(4)	I-O(2)-I ^V	125.4(5)
O(2)-I-O(2''')	100.2(3)	I-O(2)-I ^{VI}	133.1(4)
		I ^V -O(2)-I ^{VI}	96.3(2)

Phenyl ring

I-C(1)-C(2)	115.7(10)	C(2)-C(3)-C(4)	118.3(17)
I-C(1)-C(6)	121.7(10)	C(3)-C(4)-C(5)	121.3(16)
C(6)-C(1)-C(2)	122.6(13)	C(4)-C(5)-C(6)	120.5(15)
C(1)-C(2)-C(3)	120.3(15)	C(5)-C(6)-C(1)	116.9(15)

^{*} Symmetry transformations are:

- | | |
|---------------------------------|----------------------------------|
| (i) $-x, -\frac{1}{2} + y, -z$ | (iv) $-x, \frac{1}{2} + y, 1-z$ |
| (ii) $x, y, 1+z$ | (v) $x, y, -1+z$ |
| (iii) $-x, \frac{1}{2} + y, -z$ | (vi) $-x, -\frac{1}{2} + y, 2-z$ |

TABLE II.3

Dihedral angles in dioxane molecule

C(1)-O(1)-C(4)-C(3)	+ 57.5
O(1)-C(4)-C(3)-O(2)	-56.4
C(4)-C(3)-O(2)-C(2)	+55.0
C(3)-O(2)-C(2)-C(1)	-57.5
O(2)-C(2)-C(1)-O(1)	+59.1
C(2)-C(1)-O(1)-C(4)	-58.5

TABLE II.4

Equations of the least squares mean planes $PI + QJ + RK = S^\dagger$ in
orthogonal angstrom space for iodoxybenzene.

Plane	Defining Atoms	P	Q	R	S
1	I, C(1-6)	0.1290	0.3342	0.9336	1.2487
2	I, O(1), O(2)	0.8111	-0.4698	0.3485	0.8761
3	C(1), I, O(1)	-0.1448	-0.4937	0.8575	1.0031
4	C(1), I, O(2)	0.2609	0.8330	-0.4879	-0.4746

Angles between planes

(1)-(2)	74.16	(2)-(3)	65.58
(1)-(3)	51.91	(2)-(4)	69.53
(1)-(4)	81.75	(3)-(4)	29.84

Atomic displacements from these planes:-*

Plane 1. O(1) by 1.59 Å
O(2) by -1.85 Å
O(1') by -0.43 Å
O(2'') by 1.77 Å
O(2''') by -0.24 Å

Plane 2. C(1) by 1.83 Å
O(1') by 0.87 Å
O(2'') by -0.93 Å
O(2''') by -2.32 Å

Plane 3. O(2) by -0.93 Å
O(1') by 1.43 Å
O(2'') by 2.56 Å
O(2''') by -1.67 Å

Plane 4. O(1) by 1.01 Å
O(1') by -2.06 Å
O(2'') by -2.10 Å
O(2''') by 1.95 Å

[†] The orthogonal unit vector I is parallel to a, K is perpendicular to a in the ac plane and J is perpendicular to the ac plane.

* Symmetry transformations are:

- (i) $-x, -\frac{1}{2} + y, -z$ (ii) $x, y, 1 + z$ (iii) $-x, \frac{1}{2} + y, -z$
(iv) $-x, \frac{1}{2} + y, 1 - z$ (v) $x, y, -1 + z$ (vi) $-x, -\frac{1}{2} + y, 2 - z$

2. C.R. Wise, J. Am. Chem. Soc., 1923, 45, 1233.
3. Y. Hermoddson, Arkiv. Kemi., 1970, 31, 199.
4. A.W. Cordes, 'The Structural Aspects of Selenium Chemistry'.
Chap. 6 of 'Selenium', Eds. R.A. Zingaro and W.C. Cooper,
Van Nostrand-Reinhold.
5. Y. Hermoddson, Acta Cryst., 1960, 13, 656.
6. Y. Hermoddson, Acta Chem. Scand., 1967, 21, 1313.
7. I. Lindquist and G. Nahringsbauer, Acta Cryst., 1959, 12, 638.
8. Y. Hermoddson, Acta Chem. Scand., 1967, 21, 1328.
9. See for example R.S. Drago and K.F. Purcell, Prog. Inorg. Chem.,
1964, 6, 271.
10. F.G. Mann and B.C. Saunders, 'Practical Organic Chemistry',
Longmans (London), 1936.
11. D. Gregory, I. Hargittai and M. Kolonits, J. Mol. Structure, 1976,
31, 261.
12. M. Davies and O. Hassel, Acta Chem. Scand., 1963, 17, 1181.
13. H.A. Bent, Chem. Rev., 1968, 68, 587; O. Hassel, Science, 1970,
170, 497. Also Chapter 7 of ref. 4.
14. (a) R. Eriksen, Acta Chem. Scand., 1975, A29, 517; (b) M. Baiwir,
G. Llabres, O. Dideberg, L. Dupont and J.L. Plette, Acta Cryst.,
1975, B31, 2188.
15. A. Atkinson, A.G. Brewster, S.V. Ley, R.S. Osborn, D. Rogers,
D.J. Williams and K.A. Woode, J.C.S. Chem. Comm., 1977, 325.
16. M. Baiwir, G. Llabres, O. Dideberg, L. Dupont and J.L. Plette,
Acta Cryst., 1974, B30, 139.
17. I.D. Brown, J. Solid State Chem., 1974, 11, 214.
18. Y.D. Felkema and A. Vos, Acta Cryst., 1966, 20, 769.
19. E.M. Archer, Acta Cryst., 1948, 1, 64.
20. R.J. Gillespie, D.R. Slim and J.E. Vekris, J. Chem. Soc. Dalton,
1977, 971.
21. P.J. Durrant and B. Durrant, 'General and Inorganic Chemistry',
Longmans Green and Co. Ltd., p. 647, 1962.
22. (a) J.C. Jumas, M. Ribes, M. Maurin and E. Philippot, Acta Cryst.,
1976, B32, 444; B. Ducourant, R. Fourcade, E. Philippot and
G. Mascherpa, Rev. Chim. Minér., 1975, 12, 485;

- (b) Less regular arrangements of primary and secondary bonds due to more prominent lone pairs are to be found in P. Maraine and G. Pérez, Acta Cryst., 1977, B33, 1158; M. Palazzi and S. Jaulmes, Acta Cryst., 1977, B33, 908; G.B. Johansson and O. Lindquist, Acta Cryst., 1976, B32, 2720; A.A. Udovenko, R.L. Davidovich, L.V. Samarets, L.A. Zemnukhova, Koord. Khim., 1975, 1, 1419 (Abstr. only available C.A. 86:63900); R. Mercier, J. Douglade and J. Bernard, Acta Cryst., 1976, B32, 2787.
23. C.J. Marsden, G.M. Sheldrick and R. Taylor, Acta Cryst., 1977, B33, 139.
24. J.C. Dewan and A.J. Edwards, J. Chem. Soc. Dalton, 1976, 2433 and refs. therein.

CHAPTER III

The Iodobenzene Acetates; planar pentagonal systems with three
centre overlaps(III.1.) Introduction

Before 1970, crystallographic studies of compounds containing organo-tervalent iodine were restricted to iodobenzene dichloride (PhICl_2)¹ and the diphenyl iodonium compounds.² However, recently many more structures containing this oxidation state of iodine have been published.³⁻⁵ In particular, complexes containing the benziodoxoline heterocyclic ring have been investigated by Gougoutas and others to understand the solid state topotactic transformations displayed by these compounds.⁶ In all of these compounds the trivalent iodine atoms form three covalent bonds to other atoms in slightly distorted T-shaped geometries as predicted for five electron pairs.⁷ As well as covalent bonds, virtually all of the known structures also contain weak inter- and intra-molecular co-ordination bonds of remarkably constant orientation around the iodine atoms. The lengths of these co-ordination interactions are all less than the sum of the van der Waals radii for the atoms concerned, and again may be described as secondary bonds.⁸

There is some importance in considering these interactions in some detail as one suggested explanation of the extensive molecular re-organisations necessary for the polymorphic phase transformations in the benziodoxoline compounds involves intermolecular bond delocalisation with the weakening of the covalent bonds and strengthening of the weak inter-molecular bonds.⁶

In this chapter, the crystal structures of iodobenzene diacetate and iodobenzene bis(dichloroacetate) determined at -60°C are reported, and the secondary bonding in these compounds is described in terms of a possible three centre overlap of a σ^* antibonding orbital. After the completion of these structural studies, the structure of iodobenzene diacetate was reported independently although without any discussion of the longer intramolecular I---O contacts.⁹

(III.2.) Experimental

As mentioned above with the compounds of Gougoutas, there are some experimental difficulties when working with these organo tervalent iodine systems in that solid state topotactic transformations between reactant and preferentially orientated single crystal product phases can occur. A knowledge of the geometrical comparisons between the reactant and product phases can then be of some importance. However, in other examples, changes on irradiation of the crystals at room temperature are normally facile and complex. In the present examples, the crystals rapidly decomposed in the X-ray beam at room temperature, but on cooling the crystals to -60°C using a Syntex LT-1 attachment to the diffractometer, the problem of crystal decomposition was effectively solved. Curiously, in ref. 9, no decomposition was reported.

Both iodobenzene diacetate and iodobenzene bis(dichloroacetate) were prepared by reacting iodobenzene with the appropriate acid, the iodosobenzene having been prepared by hydrolysis of iodobenzene dichloride with aqueous sodium hydroxide.¹⁰ In a typical reaction, 2 g iodosobenzene (as a yellow powder) is added to 6 cc of glacial acetic acid and the iodobenzene diacetate precipitated by the addition of ether. Both acetates occur as colourless needle shaped crystals. The diacetate can be recrystallised from benzene, the bis(dichloroacetate) from carbon tetrachloride or ethanol.

(III.3.) Data Collection and Structure Solution

(III.3.1.) Iodobenzene diacetate (Compound 1)

For the data collection, the crystal used was obtained by cleaving a long thick needle perpendicular to the needle axis. At room temperature, the crystals rapidly decompose in the X-ray beam. However, by cooling the crystal to -60°C using a Syntex LT-1 attachment to the diffractometer, the problem of crystal decomposition was solved.

Crystal data:

$\text{C}_{10}\text{H}_{11}\text{IO}_4$, orthorhombic, $a = 15.693(3)$, $b = 8.477(2)$, $c = 8.762(2)$, $U = 1165.5(5) \text{ \AA}^3$, $D_c = 1.835 \text{ g/cm}^3$ for $Z = 4$. MoK_α radiation, $\lambda = 0.71069 \text{ \AA}$, $\mu(\text{Mo-K}_\alpha) = 27.75 \text{ cm}^{-1}$, $F(000) = 624.0$, $T = -60^{\circ}\text{C}$.

Systematic absences $Ok1$, $k+1 \neq 2n$ and $h0l$, $h+1 \neq 2n$ indicate space groups Pn \bar{m} (No. 58) or Pnn2 (No. 34).

Unit cell dimensions and data were collected using a Syntex P2₁ diffractometer. Reflections were measured using θ - 2θ scans over a scan range ($K_{\alpha_1} - 1.0^\circ$) to ($K_{\alpha_2} + 1.0^\circ$) to a maximum 2θ of 51° . A variable scan rate of $1^\circ/\text{min}$ to $29.3^\circ/\text{min}$, depending on the intensity of a preliminary 2 sec count, was used. Background counts were recorded at each end of the scan, each for one quarter of the scan time. The intensities of three standard reflections were monitored every 55 reflections. These reflections showed no significant loss in intensity. 1306 data were collected, of which 1063 were considered observed ($I/\sigma(I) \geq 3.0$) and used in refinement.[†]

Lorentz, polarisation and absorption corrections were applied, the last with the program ABSCOR. A Patterson synthesis revealed the position of a single iodine atom. In space group Pn \bar{m} this position would impose mirror symmetry on the molecule. However, in a subsequent Fourier phased by this heavy atom, possible light atom positions were too close to their mirror images. The space group symmetry was relaxed to Pnn2 whereupon all light atom positions were located and successfully refined. Hydrogen atoms in the methyl groups were located in a difference Fourier, whilst the ring hydrogen atoms were placed in calculated positions ($C-H = 0.95 \text{ \AA}$). In the final cycles of least squares refinement, anisotropic temperature factors were used for all non-hydrogen atoms with the hydrogen atom parameters fixed. The weighting scheme used was $w = [1 + \{(F-31)/19\}^2]^{-1}$. The refinement, including corrections for anomalous dispersion and extinction, converged to a final R of 0.021 and weighted R of 0.026; in the final cycle no parameter shift was greater than 20% of its standard deviation. The final difference Fourier was featureless except for residual peaks up to 0.7 e/\AA^3 near the iodine. The alternative 'hand' of the molecule was

[†] Two reflections (002) and (020) were too intense to be measured.

rejected because $R = 0.022$ and $wR = 0.026$, and distances around the iodine which should be expected to be equivalent differed significantly, (e.g. I-O(1) and I-O(3) were 2.191(5) and 2.130(5) Å respectively). The independent determination of (1) gives very similar dimensions (at room temperature), but the co-ordinates have been reported with the opposite hand (1-x, 1-y, z) relative to those in Table 1.⁹

(III.3.2.) Iodobenzene bis(dichloroacetate) (Compound 2)

A thin needle crystal was used for the data collection. Again, by cooling the crystal to -60°C , the crystal decomposition was minimal.

Crystal data:

$\text{C}_{10}\text{H}_7\text{Cl}_2\text{IO}_4$, triclinic, $a = 10.462(3)$, $b = 4.870(2)$, $c = 15.445(5)$ Å, $\alpha = 101.03(3)^{\circ}$, $\beta = 99.89(3)^{\circ}$, $\gamma = 94.40(3)^{\circ}$, $V = 756.0(5)$ Å³, $D_c = 2.02$ g/cm³ for $Z = 2$, $D_m = 1.96$ g/cm³ (floatation). MoK_{α} radiation, $\lambda = 0.71069$ Å; $\mu(\text{MoK}_{\alpha}) = 28.49$ cm⁻¹, $F(000) = 440$; $T = -60^{\circ}\text{C}$.

Possible space groups $\overline{P}1$ and $P1$.

Unit cell dimensions and data were collected using a Syntex P2₁ diffractometer. Reflections were measured using θ - 2θ scans over a scan range ($K_{\alpha_1} - 1.2^{\circ}$) to ($K_{\alpha_1} + 1.1^{\circ}$) to a maximum 2θ of 50° in two shells. The scan rate varied from 1.5°/min to 29.3°/min and three standards were monitored every 100 reflections. The crystal was recentred after the first shell of data was completed. Towards the end of the data collection, the crystal showed signs of decomposition and the data were rescaled in groups using the equations

$$F = F_0 \text{ for } t \leq 15.42 \text{ hrs} \quad (1)$$

$$F = F_0 * (1 + 0.0044985 * t) \text{ for } 15.43 < t \leq 30.59 \text{ hrs} \quad (2)$$

$$\text{and } F = F_0 * (1 + 0.00053 * t) * (1 + 0.0180 * t * \sin \theta / \lambda) \text{ for } 30.59 \leq t \text{ hrs} \quad (3)$$

2685 data were collected, of which 1580 were considered observed ($I/\sigma(I) \geq 3.0$) and used in refinement.

Lorentz and polarisation corrections were applied. The absorption correction for the block-shaped crystal used is small and, because of the effects of crystal decomposition, no absorption corrections was performed. The centrosymmetric space group $\overline{P}1$ was initially assumed

and confirmed by a satisfactory refinement. From a Fourier phased by an iodine atom located in a Patterson map, all remaining heavy atoms were located. In the final cycles of least squares, anisotropic temperature factors were used for all non-hydrogen atoms. Hydrogen atoms were included in calculated positions, but were not refined. The weights used were $(1/\sigma(F))^2$ for reflections within the ranges $10.0 \leq F \leq 21.5$ and $0.29 \leq \sin \theta \leq 0.65$. Reflections outside these ranges are given weights $w = X \cdot Y \cdot \left(\frac{1}{\sigma(F)}\right)^2$ where (1) $X = (\sin \theta / 0.29)$ if $\sin \theta < 0.29$ or $X = (0.65 / \sin \theta)$ if $\sin \theta > 0.65$ and (2) $Y = (F / 10.0)$ if $F < 10.0$ or $Y = (21.5 / F)$ if $F > 21.5$. Four reflections with bad $w \cdot (\Delta F)^2$ values after the application of this weighting scheme were rejected from subsequent refinement cycles. The refinement, including corrections for anomalous dispersion, converged to a final R of 0.058 and weighted R of 0.054.

Final positional parameters for all atoms in both (1) and (2) are listed in Table III. 1, bond lengths and angles are in Table III. 2, and information on molecular planes in Table III. 3. Table III. 1 also contains listings of the anisotropic temperature factors for the atoms in (1) and (2). Final structure factors for both compounds are included in Appendix 3A. Views of the isolated molecular units are shown in Figures III. 1 and 2, whilst the different crystal packing is given in Figures III. 3 and 4.

(III. 4) Discussion of Structures

(III. 4. 1.) General

In both (1) and (2) the primary geometry of the trivalent iodine is the familiar T-shaped arrangement with covalent bonds to a phenyl ring and two oxygen atoms of the acetate groups. In (1) the I-O distances are the same (2.156 Å av.) whilst in (2) they differ significantly (2.136(6) and 2.163(7) Å). The I-C distances in (1) and (2), however, are the same (2.08-2.09 Å). These bond lengths should be compared with values of 1.99 Å (I-O) and 2.10 Å (I-C) from the sum of the covalent radii. The corresponding C-I-O angles are 81.4(2) and 82.6(2)° for (1); 86.0(3) and 82.5(3)° for (2) so that the O-I-O angles are 164.0(2)° (1) and 167.1(4)° (2). This T-shaped arrangement of covalent bonds has been

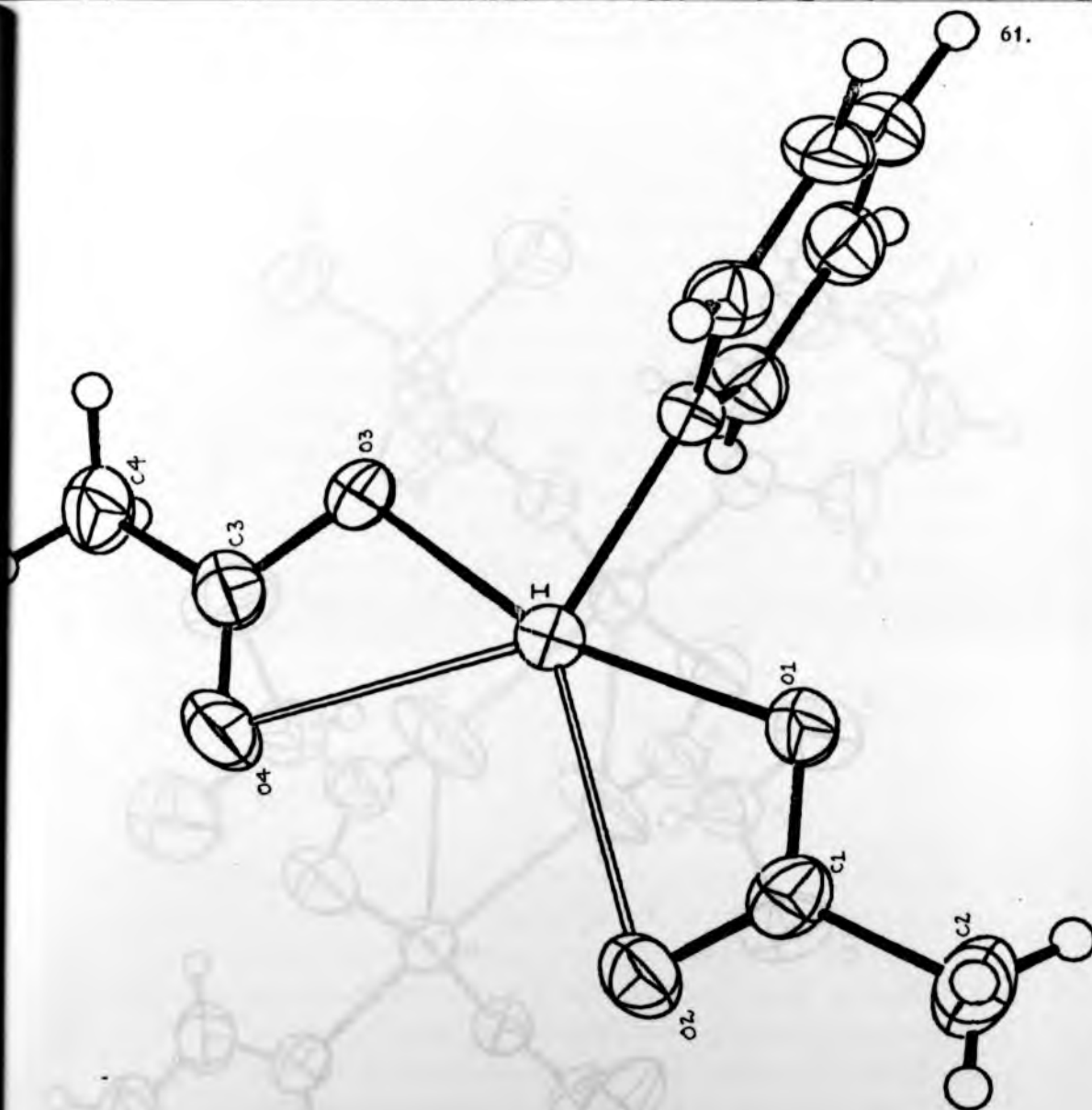


Fig. III-1 ORTEP View of molecule 1 down b rotated 20° about c showing the pentagonal planar arrangement of primary(shaded) and secondary bonds.

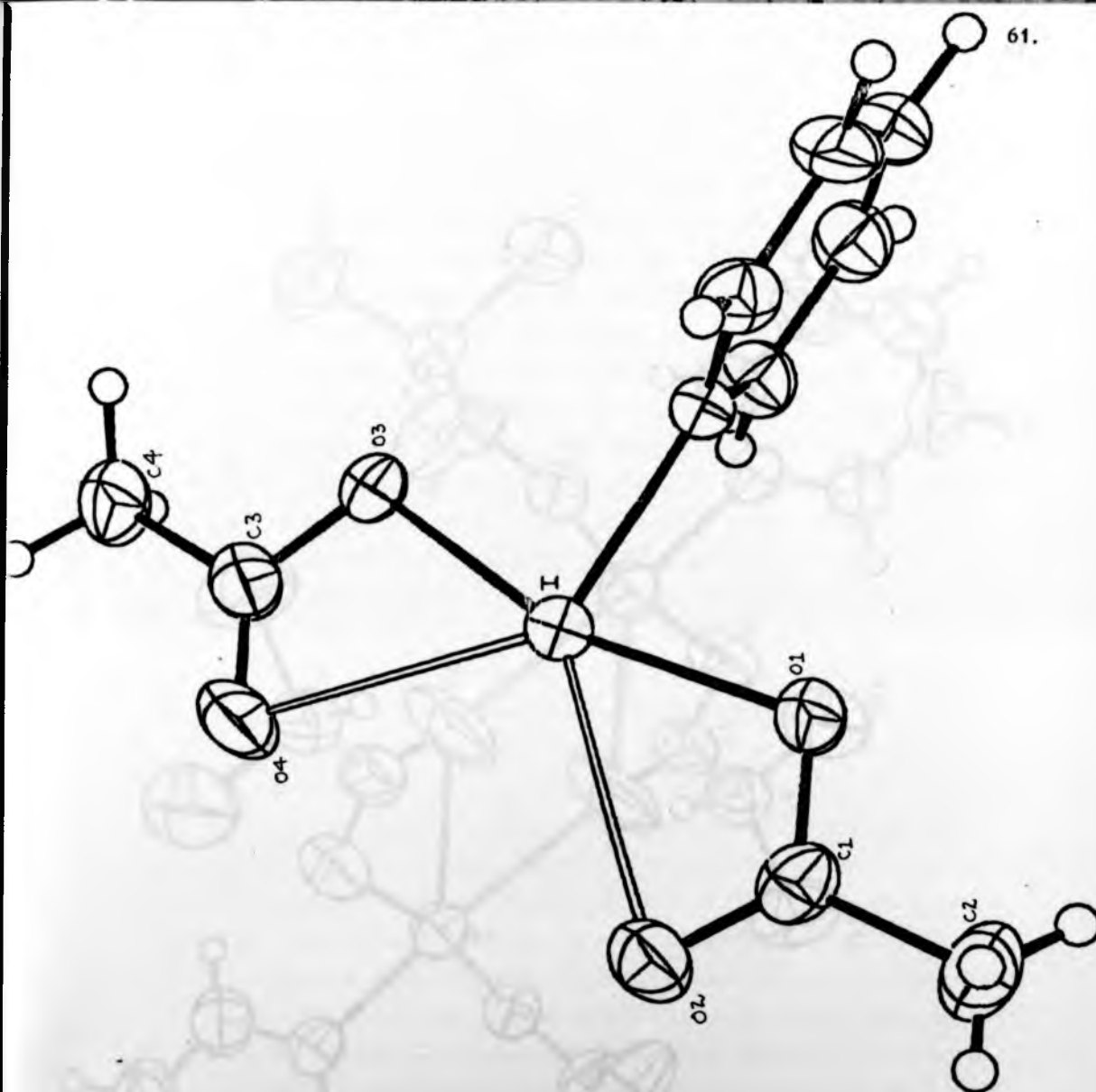
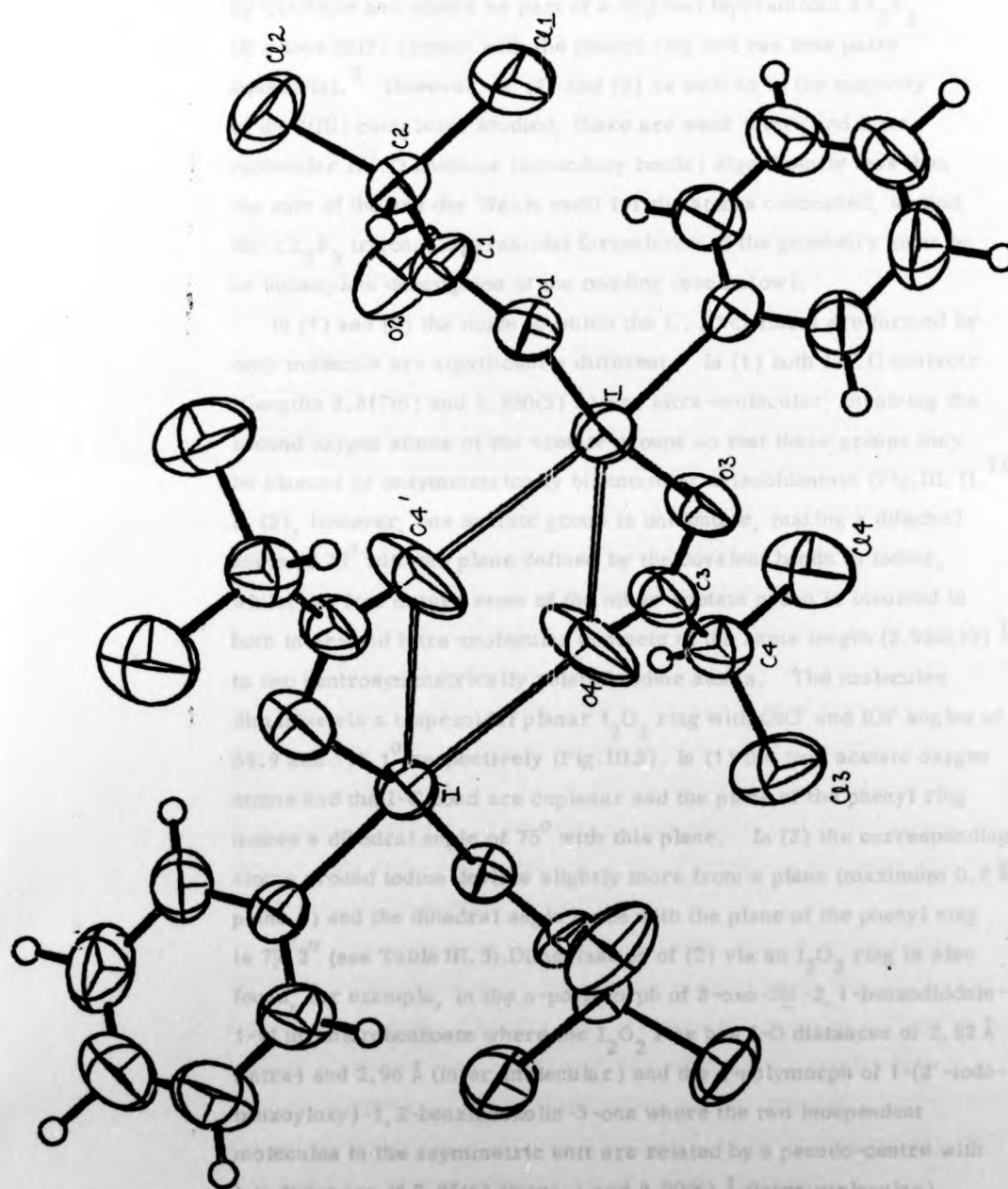


Fig.III-1 ORTEP View of molecule 1 down b rotated 20° about c showing the pentagonal planar arrangement of primary(shaded) and secondary bonds.



FigIII-2 ORTEP View of molecule 2 down b showing bimolecular units linked by secondary bonds.

found in most compounds of I(III) investigated, and has been described by Gillespie and others as part of a trigonal bipyramidal AX_3E_2 (E = lone pair) system with the phenyl ring and two lone pairs equatorial.⁷ However, in (1) and (2) as well as in the majority of the I(III) complexes studied, there are weak inter- and intra-molecular I...O contacts (secondary bonds) significantly less than the sum of the van der Waals radii for the atoms concerned, so that the AX_3E_2 trigonal bipyramidal formulation of the geometry must be an incomplete description of the bonding (see below).

In (1) and (2) the mode in which the I...O contacts are formed by each molecule are significantly different. In (1) both I...O contacts (lengths 2.817(6) and 2.850(5) Å) are intra-molecular, involving the second oxygen atoms of the acetate groups so that these groups may be classed as unsymmetrically bidentate or anisobidentate (Fig.III. 1).¹¹ In (2), however, one acetate group is unidentate, making a dihedral angle of 78° with the plane defined by the covalent bonds to iodine, whilst the free oxygen atom of the other acetate group is involved in both inter- and intra-molecular contacts of the same length (2.936(10) Å) to two centrosymmetrically related iodine atoms. The molecules dimerise via a trapezoidal planar I_2O_2 ring with OIO' and IOI' angles of 68.9 and 111.1° respectively (Fig.III.2). In (1) the four acetate oxygen atoms and the I-C bond are coplanar and the plane of the phenyl ring makes a dihedral angle of 75° with this plane. In (2) the corresponding atoms around iodine deviate slightly more from a plane (maximum 0.5 Å - plane 4) and the dihedral angle made with the plane of the phenyl ring is 79.2° (see Table III.3). Dimerisation of (2) via an I_2O_2 ring is also found, for example, in the α -polymorph of 3-oxo-3H-2,1-benzodiodole-1-yl m chlorobenzoate where the I_2O_2 ring has I-O distances of 2.82 Å (intra-) and 2.96 Å (inter-molecular) and the α -polymorph of 1-(2'-iodo-benzoyloxy)-1,2-benziodoxolin-3-one where the two independent molecules in the asymmetric unit are related by a pseudo-centre with I-O distances of 2.85(6) (intra-) and 2.90(6) Å (inter-molecular).

In the corresponding β -polymorph of the latter compound there is a conformational change in the molecule and the two weak co-ordination bonds to the trivalent iodine involve an oxygen atom intramolecularly and a further unique contact to the monovalent iodine atom in the iodo-benzoyloxy group of a centro-symmetrically related molecule $I(III) - I(I)$ is 3.70 \AA .⁶

The structures of (1) and (2) are furthermore very similar to the recently solved structure of 'iodobenzene dinitrate' which again contains a pentagonal planar geometry. The structure consists of two iodines linked by an oxygen bridge with all the oxygen atoms of the two nitrate groups involved in primary and secondary interactions to the iodines. The primary geometry of each iodine is again T-shaped, with bonds to the phenyl ring, the bridging oxygen and one oxygen of a nitrate group. The pentagonal planar arrangement about each iodine is then completed by two $I \dots O$ contacts, one of which is intramolecular and the other involves an oxygen atom of the nitrate group attached to the other iodine which is not involved in any interactions with that iodine. Individual distances and angles involved are contained in Figure III.5.¹²

Apart from the pentagonal planar arrangement of three primary and two secondary bonds described above, trivalent iodine also forms a square planar arrangement of three covalent and one secondary bond. In iodobenzene dichloride¹ and *N*-chloro-3-aza-3H, 2,1-benzodiodol-1-yl chloride⁶ the $I \dots Cl$ secondary bonds of 3.40 and 3.36 \AA respectively complete the square arrangement of bonds giving dimeric units and chains of co-ordinated molecules respectively.

Etter has noted four basic packing modes in crystals containing trivalent iodine covering the two bonding arrangements described above.⁶ Packing modes a and d are the square planar arrangement of three strong and one secondary bond whilst packing modes b and c involve the pentagonal planar system of three strong and two secondary bonds. Both (1) and (2) are of the latter type although (1) uniquely involves two intramolecular $I \dots O$ weak bonds and is in a class of its own.

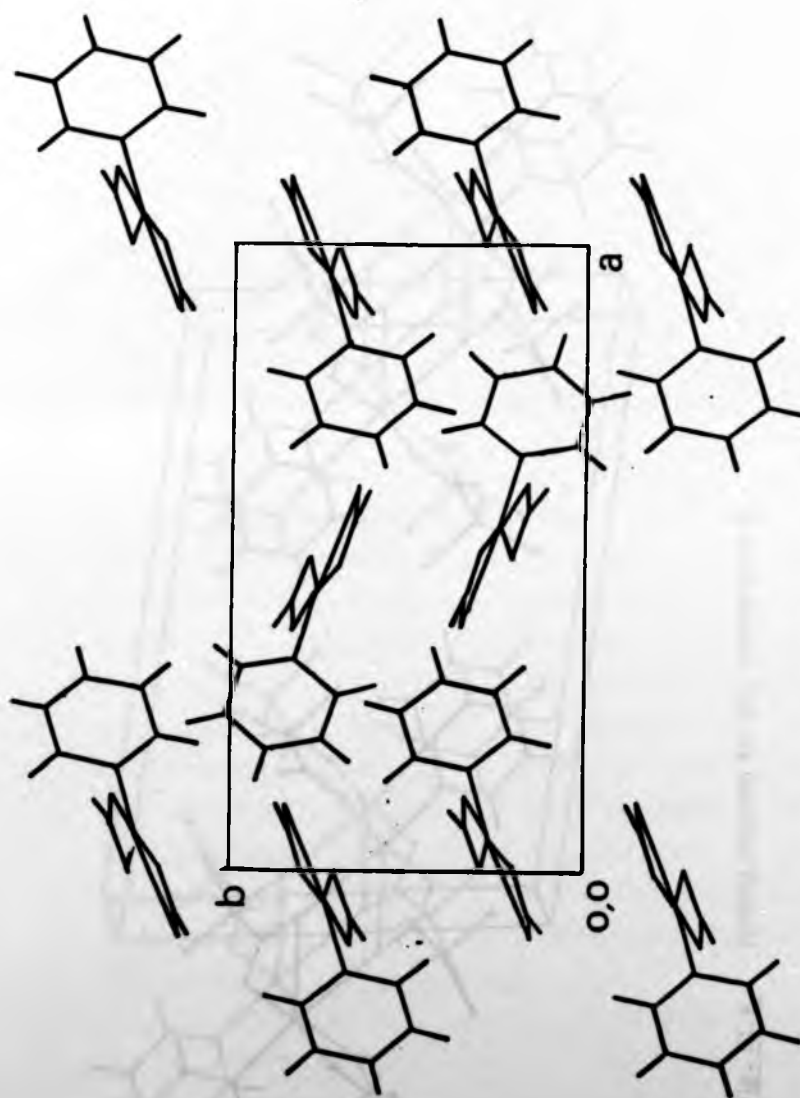
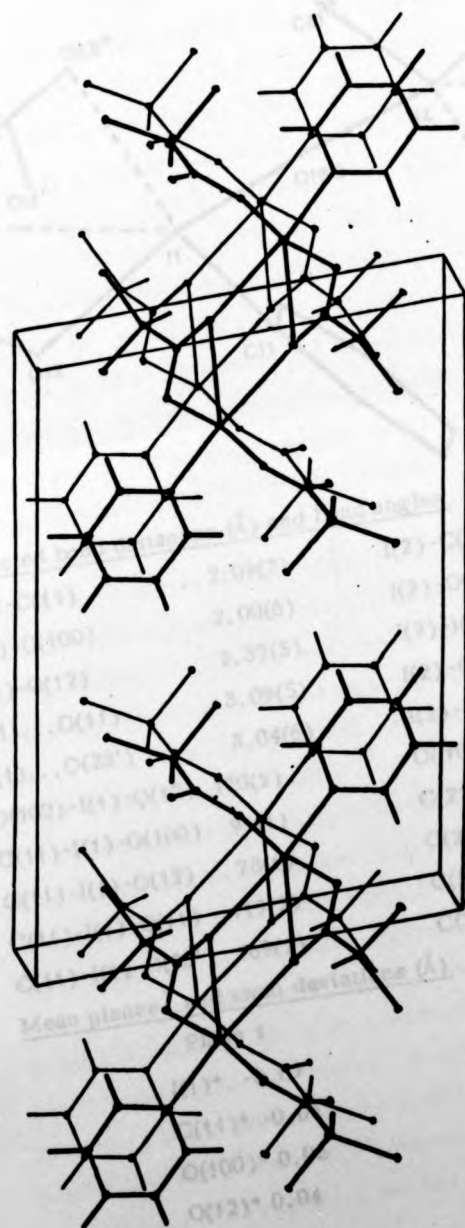


Fig. III. 3. Packing diagram for (1), viewed down c.

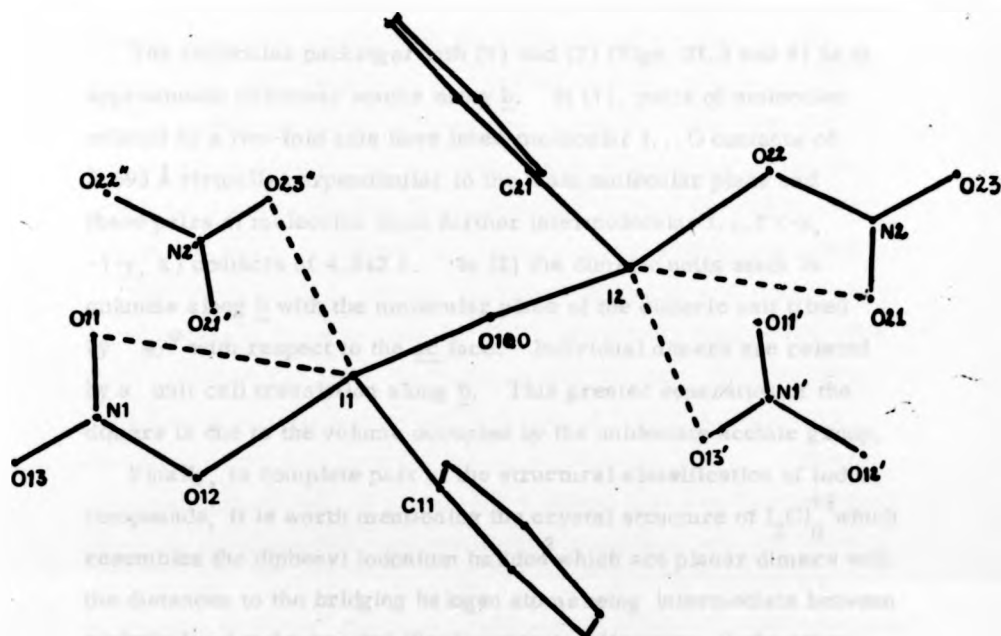


Packing diagram for (2), viewed down \bar{b} .

Fig. III. 4.

* Atoms defining plane marked with asterisks.

Fig. III.5 Structural parameters for "iodobenzene dinitrate".

Selected bond distances (\AA) and bond angles

I(1)-C(11)	2.09(2)	I(2)-C(21)	2.05(2)
I(1)-O(100)	2.00(6)	I(2)-O(100)	2.02(6)
I(1)-O(12)	2.37(5)	I(2)-O(22)	2.27(5)
I(1)...O(11)	3.09(5)	I(2)-O(21)	2.88(5)
I(1)...O(23')	3.04(6)	I(2)-O(13'')	2.99(4)
O(100)-I(1)-O(12)	170(2)	O(100)-I(2)-O(22)	166(2)
C(11)-I(1)-O(100)	96(1)	C(21)-I(2)-O(100)	88(1)
C(11)-I(1)-O(12)	78(1)	C(21)-I(2)-O(22)	79(1)
C(11)-I(1)-O(11)	119(2)	C(21)-I(2)-O(21)	126(2)
C(11)-I(1)-O(23')	169(2)	C(21)-I(2)-O(13'')	163(2)

Mean planes[†] and atom deviations (\AA)

Plane 1	Plane 2
I(1)* -0.09	I(2)* 0.08
C(11)* -0.01	C(21)* 0.01
O(100)* 0.05	O(100)* -0.05
O(12)* 0.04	O(22)* -0.04
O(11) -0.84	O(21) 0.52
O(23) -0.58	O(13'') 0.66

[†] Atoms defining plane marked with asterisks.

The molecular packing of both (1) and (2) (Figs. III.3 and 4) is in approximate columnar stacks along \underline{b} . In (1), pairs of molecules related by a two-fold axis have inter-molecular I...O contacts of 3.693 Å virtually perpendicular to the main molecular plane and these pairs of molecules form further intermolecular I...I' (-x, -1-y, z) contacts of 4.342 Å. In (2) the dimeric units stack in columns along \underline{b} with the molecular plane of the dimeric unit tilted by 46° with respect to the \underline{ac} face. Individual dimers are related by a unit cell translation along \underline{b} . This greater separation of the dimers is due to the volume occupied by the unidentate acetate group.

Finally, to complete part of the structural classification of iodine compounds, it is worth mentioning the crystal structure of I_2Cl_6 ¹³ which resembles the diphenyl iodonium halides² which are planar dimers with the distances to the bridging halogen atoms being intermediate between a single bond and a van der Waals contact. However, in the other closely related diphenyl iodonium structures, diphenyl iodonium tetrafluoroborate consists of separated diphenyliodonium and tetrafluoroborate ions whilst the structure of diphenyl iodonium nitrate consists of infinite zig-zag chains, -I-O-I'-O', with the square planar arrangement about the diphenyl iodonium group being completed by the I-O and I-O' contacts of 2.768(8) and 2.877(8) Å respectively; (C-I-O angles are 170.6 and 168.3° respectively).¹⁴

The bonding arrangements described above for iodine also occur with other non-metals as the central atom. The square planar arrangement is quite common, either with three primary and one secondary bond, or two primary and two secondary bonds.⁸ The square planar arrangement of three primary and one secondary bond has been found, for example, in one crystalline form of bromo(ethylene thiourea) phenyl tellurium(II) and bromo(ethylene selenourea) phenyl tellurium(II) where the Te...Br secondary bonds are of lengths 3.821(1) and 3.849(2) Å (the C-Te...Br angles are 162.3° and 163.3° respectively).¹⁵ The square planar arrangement of two primary and two secondary bonds is also found in

several examples, particularly the structures of the interhalogen cations ICl_2^+ , BrF_2^+ and ClF_2^+ with the anions AsF_6^- and SbF_6^- .^{8, 16}

The pentagonal planar geometry is, however, much rarer for non-metal complexes. An equatorial plane of five bonds of varying strengths is known to occur in compounds with axial (or pseudo-axial) lone pairs, and also with the axial lone pair(s) replaced by a ligand(s).

With three primary and two secondary bonds, the pentagonal planar arrangement of bonds is found for Te(II) and Xe(IV) compounds. The XeF_3^+ cation in $\text{XeF}_3^+\text{SbF}_6^-$ is T-shaped with two axial Xe-F bonds of 1.91 Å and a shorter equatorial Xe-F bond of 1.84 Å and was again described as trigonal bipyramidal AX_3E_2 (E = lone pair).¹⁷ However, there are further Xe...F contacts of 2.49 and 2.71 Å to fluorine atoms in two neighbouring SbF_6^- cations which are coplanar with the primary Xe-F bonds; the F-Xe...F angles are 153° and 143° respectively. In the case of Te(II), the anion $[\text{Te}(\text{EtXan})_3]^-$ (EtXan = O^- -ethylxanthate) is pentagonal planar with three strong and two weaker bonds involving two unsymmetrically bidentate and one unidentate ligands.¹⁸ Other Te(II) compounds are known with two strong covalent bonds and three weaker intra- and inter-molecular bonds coplanar with the covalent bonds. Thus in $\text{Te}[(\text{S}_2\text{CNEt}_2)_2]$ there is a planar TeS_4 group formed by the unsymmetrically bidentate ligands and the fifth Te...S contact of length 3.579(5) Å is made by a sulphur atom in a centrosymmetrically related molecule with this atom 0.5 Å out of the plane defined by the TeS_4 group.¹⁹ The crystal structures of tellurium(II)(dimethylxanthate) and tellurium(II) di(ethylxanthate)²¹ are similar: planar TeS_4 groups with unsymmetrical Te-S distances and a fifth inter-molecular contact (Te...S distances 3.51 and 3.61 Å respectively). The deviations of the S atoms forming these contacts from the planes defined by the TeS_4 groups are 1.10 and 0.65 Å respectively.

An equatorial arrangement of five pentagonal bonds of widely different strengths can also be found with axial substituents so that the geometry is derived from a pentagonal bipyramid. To give a few

examples, in big(1-oxopyridine-2-thiolato)phenylbismuth there is an intermolecular Bi...O of 3.37 Å completing the equatorial pentagonal plane of bonds and results in dimeric units. The phenyl group and a lone pair are in axial positions.²¹ In $[\text{Pb}(\text{O-ethylxanthate})_3]^-$ an equatorial plane of two strong and three weak Pb-S distances occur with a further Pb-S bond and a lone pair presumed to be axial. A further even longer Pb-S inter-molecular contact close to the direction of the lone pair results in dimeric units again.²² Even in dimethylthallium(I) dimethylxanthate three inter-molecular contacts appear to be in the same plane as the primary Te-S bonds with the methyl groups axial.²³

(III.4.2.) Bonding Models¹⁹

Three possible bonding models can be considered for these planar pentagonal systems involving bonds of very different lengths. The simplest treats the primary covalent bonds as 2 centre-2 electron bonds and any additional interactions are considered to be electrostatic. This model, however, fails to explain why the primary and secondary bonds in these systems are, within reasonable limits, coplanar.

Secondly, it has been proposed for the anion $[\text{Te}(\text{EtXan})_3]^-$ that it might represent an AX_5E_2 system on the Gillespie-Nyholm model.¹⁸ With two lone pairs, the expectation of the geometry would presumably be the pentagonal planar arrangement. The two lone pairs would be in axial positions perpendicular to the plane, minimising lone pair bond pair interactions since the alternative of equatorial lone pairs would give (with all bonds equal) lone pair-bond pair angles of 72° in the plane. The drawback to this model is the difference in strength between the strong and weak bonds. One explanation for this, advanced to explain the asymmetric dithiolate ligands in $[\text{Te}(\text{EtXan})_3]^-$ and related complexes, suggests that the repulsion between the bonding electrons of the short Te-S bond to the unidentate ligand and the axial lone pairs is stronger than other bond pair-lone pair interactions; this forces the lone pairs into an off-axial position away from the unidentate ligand.

The two Te-S bonds furthest from the unidentate ligand lengthen as a consequence of the increased repulsion from these off-axial lone pairs.¹⁸ The asymmetry in the shorter Te-S bond lengths (one of 2.50 Å and two of 2.66 Å) seems, however, too modest to account for the substantial lengthening of the two other Te...S bonds.

Overcrowding might offer an alternative explanation for the difference in the bond lengths and a useful comparison is with uranyl complexes which often have pentagonal planar co-ordination around the axial UO_2^{2+} group. The geometrical constraints of these compounds are fairly well understood and it appears that non-bonded O...O contacts of 2.6 - 2.8 Å are the minimum to avoid distortions due to overcrowding which, if sufficiently strong, will cause the expulsion of a ligand.²⁴ In (1) the non-bonded O...O contacts in the AX_5 plane is 4.2 Å, whilst in (2) it is 3.32 Å. These will clearly not impose any steric constraints.

A third approach describes the longer I...O and Te...S interactions using the secondary bonding model.

In its normal form (Introduction) it normally predicts a linear X-A...Y system. However, in the pentagonal planar examples, the long inter- and intra-molecular contacts are far from being collinear with a covalent bond; typically O-I...O, C-I...O or S-Te...S angles are in the range 140-150°.

It is, however, possible to modify the secondary bonding model to account for this geometry by considering the overlap of the I-C σ^* orbital not with one filled orbital (e.g. a p orbital on chlorine in PhICl_2) but with two. Thus, two "unco-ordinated" oxygen atoms of two acetate groups give two filled non-bonding or weakly bonding orbitals concentrated between the heavy atom and the oxygen atoms (Fig. III.6). The resulting molecular orbitals resemble the three centre bonding orbital description found in the triangular faces in boranes.²⁵ In the alternative case of the Te(II) compounds with two strong and three weak bonds, the secondary bonding description requires the formation of two separate three centre systems involving three lone pairs on sulphur atoms overlapping with the σ^* orbitals of the strong covalent Te-S bonds (Fig. III.6).

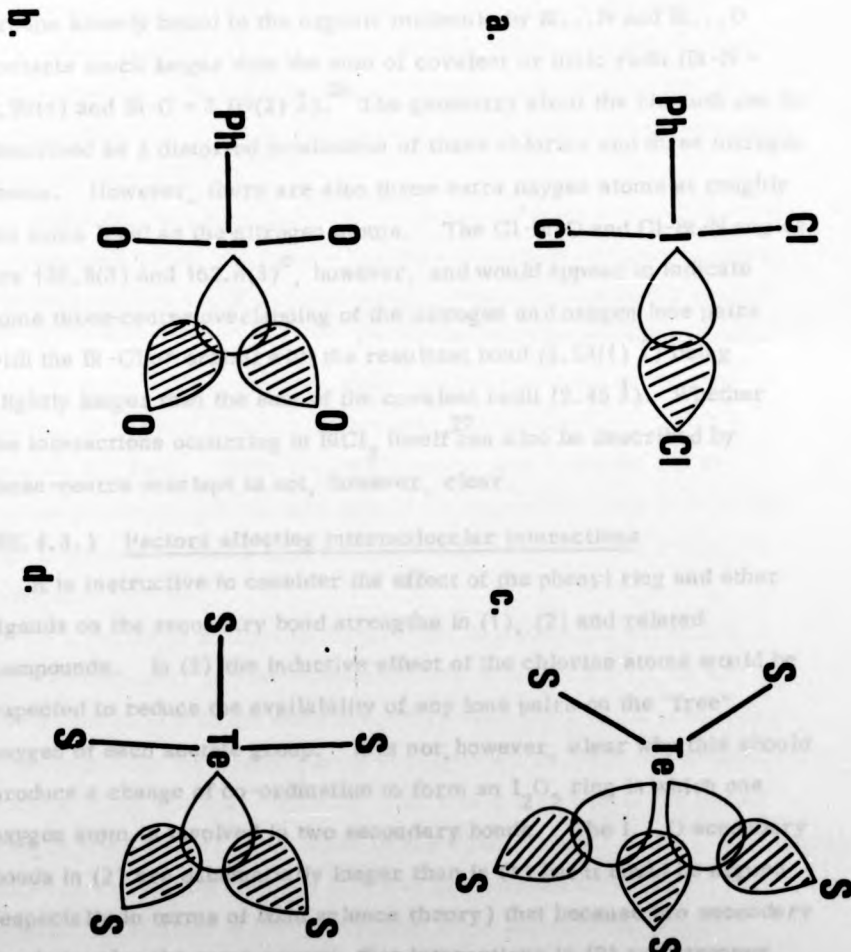


Fig. III.6.

Two and three centre secondary bonding overlaps in (1), (2) (a. and b.) and related Te compounds (c. and d.). Shaded orbitals are filled.

This three-centre overlap model can be used to rationalise several other examples of anomalously long interactions. For example, the crystal structure of the pharmaceutically important molecule trichloro-tris(3-sulfanilamide-6-methoxy-pyridazine)bismuth(III) has three-fold symmetry, lying on the axis in space group $\bar{R}3$, and contains BiCl_3 groups loosely bound to the organic molecule by $\text{Bi}\dots\text{N}$ and $\text{Bi}\dots\text{O}$ contacts much longer than the sum of covalent or ionic radii ($\text{Bi-N} = 2.90(1)$ and $\text{Bi-O} = 3.09(2)$ Å).²⁶ The geometry about the bismuth can be described as a distorted octahedron of three chlorine and three nitrogen atoms. However, there are also three extra oxygen atoms at roughly the same level as the nitrogen atoms. The Cl-Bi-O and Cl-Bi-N angles are $139.8(3)$ and $162.6(3)^\circ$, however, and would appear to indicate some three-centre overlapping of the nitrogen and oxygen lone pairs with the $\text{Bi-Cl } \sigma^*$ orbital with the resultant bond ($2.53(1)$ Å) being slightly longer than the sum of the covalent radii (2.45 Å). Whether the interactions occurring in BiCl_3 itself²⁷ can also be described by three-centre overlaps is not, however, clear.

(III.4.3.) Factors affecting intermolecular interactions

It is instructive to consider the effect of the phenyl ring and other ligands on the secondary bond strengths in (1), (2) and related compounds. In (2) the inductive effect of the chlorine atoms would be expected to reduce the availability of any lone pairs on the "free" oxygen of each acetate group. It is not, however, clear why this should produce a change of co-ordination to form an I_2O_2 ring in which one oxygen atom is involved in two secondary bonds. The $\text{I}\dots\text{O}$ secondary bonds in (2) are substantially longer than in (1) but it could be argued (especially in terms of bond valence theory) that because two secondary bonds involve the same oxygen, that interactions in (2) are stronger overall. Why only the oxygen atom O3 is so co-ordinated is difficult to explain. Clearly there should be observable differences in the solid state i.r. between the vibrations of the two acetate groups in (2).

An alternative way of affecting the strength of the secondary bonds would be to reduce the availability of the $\text{I-C } \sigma^*$ orbital with which the

lone pairs overlap. This will be affected by inductive and other interactions with substituents on the phenyl ring. Interactions involving the phenyl ring can also be observed cis as well as trans to the I-C(Ph) bond. In phenylhydroxytosyloxylodine, the phenyl group occurs in the bar of the T so that there are no further atoms trans to the equatorial I-O bond (cis to the phenyl) which would complete a square planar arrangement (cf. PhICl_2). Furthermore, there appears to be a lengthening of the equatorial bond so that the I-O distance of 2.473 Å is significantly longer than in other compounds (e.g. (1) and (2)).⁵

Although, in a brief report of the crystal structure of p-chlorolodibenzenedichloride, the system has been described as having a square planar arrangement of 3 primary and 1 secondary bond very similar to that of PhICl_2 , the actual I...Cl distance and atomic co-ordinates are not given.^{1b, 2} The inductive withdrawal of electrons by chlorine through the phenyl ring would, however, be expected to produce a weaker I-C bond. Hence the small energy gain when the I-C σ^* orbital interacts with the lone pair of Cl intermolecularly will be less and one could predict a longer I...Cl secondary bond in ClPhICl_2 as compared to PhICl_2 .

In a series of phenyltellurium(II) halide complexes PhTeLX (L = ethylenethiourea, ethyleneselenourea and thiourea; X = Cl, Br and I), the presence of a fourth weak secondary bond trans to the phenyl ring and completing the square planar arrangement of bonds can be apparently related to the dihedral angles made by either the plane of the phenyl ring (a trans effect) or the plane of the ligand L (a cis effect), with the plane containing the primary covalent bonds to the tellurium.²⁸ A similar correlation of phenyl dihedral angle and secondary bond formation is not so easy for I(III). In PhICl_2 ^{1a} the phenyl ring is perpendicular to the Cl-I-Cl line whilst in complexes containing the benziodoxoline nucleus the phenyl ring is forced to be coplanar with the bonds to iodine. In this latter case, there may be π -interactions

with any lone pair orbitals perpendicular to the plane of the molecule; with the phenyl ring perpendicular there may be repulsion between the ring π -orbitals and the I-Cl orbitals.

In comparing compounds (1) and (2) it is again clear that the secondary bonds are very sensitive to slight changes in ligands and the resulting conformational effects can be considerable. Similar conclusions have been reached on the basis of i.r. and Mössbauer evidence particularly for organotellurium compounds.²⁹

(III.4.4.) Conclusions

In selecting between the alternative explanations of the present geometries of (1) and (2) in terms of an AX_5E_2 system with axial lone pairs, or an AX_3E_2 system with two secondary bonds (forced into the same plane as the primary bonds by repulsion from the pseudo-axial lone pairs) the balance appears to lie towards the latter. In particular, it appears to offer a more satisfactory explanation for the essentially undisturbed T-shaped geometry of the primary bonds, and the large difference in bond length between the primary and secondary bonds. For the Te(II) compounds mentioned, a single bonding description cannot be used to cover both $[Te(Etxan)_3]_3$ and the two examples of tellurium(II) di(methylxanthate) and di(ethylxanthate). The former is again best described as AX_3E_2 plus secondary bonds, whilst the latter examples with two strong and three weak secondary bonds are probably classified as AX_2E_2 systems with the two lone pairs approximately tetrahedrally disposed with respect to the bonding pairs forcing the Te...S contacts into the same plane as the primary bonds. The alternative AX_3E_2 classification would have one of the weak secondary bonds in the same direction as one of the lone pairs. The XeF_3^+ examples are again best described as AX_3E_2 with two secondary bonds.

Table III-1 Atomic co-ordinates ($\times 10^4$) with standard deviations in parentheses(1) Iodobenzene diacetate

<u>Atom</u>	<u>X</u>	<u>Y</u>	<u>Z</u>
I	9508.5(2)	7393.9(3)	0(0)
O(1)	8791(3)	6610(5)	1960(5)
O(2)	10023(4)	7127(7)	3069(6)
O(3)	9911(3)	7959(5)	-2285(6)
O(4)	11106(3)	8549(5)	-1072(6)
C(1)	8875(5)	6155(9)	4626(7)
C(2)	9294(4)	6664(8)	3160(8)
C(3)	11069(5)	8786(9)	-3820(9)
C(4)	10705(4)	8424(6)	-2268(8)
C(5)	8381(4)	6768(7)	-1114(7)
C(6)	7846(4)	7971(7)	-1643(8)
C(7)	7111(4)	7513(8)	-2397(8)
C(8)	6933(4)	5955(10)	-2641(8)
C(9)	7466(5)	4811(8)	-2117(8)
C(10)	8205(4)	5210(7)	-1318(8)
H(11)	8243	6532	4569
H(12)	9188	6660	5452
H(13)	8908	4989	4672
H(31)	10981	9757	-3937
H(32)	10860	8291	-4524
H(33)	11524	8985	-3802
H(1)	7980	9043	-1546
H(2)	6733	8313	-2815
H(3)	6426	5665	-3219
H(4)	7335	3736	-2347
H(5)	8567	4434	-984

(2) Iodobenzene bis(dichloroacetate)

<u>Atom</u>	<u>X</u>	<u>Y</u>	<u>Z</u>
I	4256,8(8)	119,0(16)	1405,9(5)
Cl(1)	8639(3)	4349(9)	4122(2)
Cl(2)	6143(4)	5816(12)	4407(2)
Cl(3)	1289(4)	-5061(9)	-1741(2)
Cl(4)	1093(4)	-8047(8)	-325(2)
O(1)	5429(7)	3393(13)	2413(5)
O(2)	6831(10)	394(21)	2708(7)
O(3)	2825(8)	-3217(16)	585(5)
O(4)	3869(12)	-2677(31)	-495(6)
C(1)	7120(10)	5071(24)	3614(7)
C(2)	6441(12)	2669(25)	2880(7)
C(3)	2141(12)	-6380(27)	-832(8)
C(4)	3042(13)	-3886(30)	-212(8)
C(5)	3053(11)	-110(21)	2340(7)
C(6)	3413(13)	-1547(27)	3006(9)
C(7)	2662(19)	-1637(32)	3613(9)
C(8)	1578(19)	-495(38)	3547(10)
C(9)	1195(14)	932(36)	2888(12)
C(10)	1942(14)	1129(28)	2260(9)
H(11)	7248	6724	3350
H(31)	2710	-7749	-1049
H(1)	4211	-2396	3041
H(2)	2884	-2556	4107
H(3)	983	-541	4013
H(4)	335	1704	2823
H(5)	1694	2073	1752

TABLE III. 1 (cont.)

78.

Anisotropic temperature factors U_{ij} ($\times 10^3$) with standard deviations in parentheses. *In the form $\exp[-2\pi^2(U_{11}h^2a^* + U_{22}k^2b^* + U_{33}l^2c^* + 2U_{12}hka^*b^* + 2U_{13}hla^*c^* + 2U_{23}k lb^*c^*)]$

(1) Iodobenzene diacetate

Atom	U(11)	U(22)	U(33)	U(12)	U(13)	U(23)
I	27.6(2)	36.1(2)	30.3(2)	-0.5(1)	-0.8(3)	-1.5(4)
O(1)	34(2)	53(2)	28(2)	-3(2)	6(2)	2(2)
O(2)	47(3)	108(4)	34(3)	-27(3)	-10(3)	1(3)
O(3)	37(2)	62(2)	26(2)	-12(2)	0(2)	1(2)
O(4)	43(2)	48(2)	38(2)	-10(2)	-6(2)	-1(2)
C(1)	58(4)	76(4)	31(4)	-11(4)	3(3)	1(3)
C(2)	44(4)	51(3)	34(4)	-5(3)	-3(3)	-3(3)
C(3)	61(5)	67(4)	36(4)	-19(4)	16(4)	-7(3)
C(4)	41(3)	33(3)	38(4)	-3(2)	8(3)	1(2)
C(5)	25(3)	42(3)	27(3)	-3(2)	0(2)	-5(2)
C(6)	35(3)	37(3)	40(3)	-1(2)	2(3)	5(3)
C(7)	29(3)	62(4)	44(4)	9(3)	-6(3)	8(3)
C(8)	32(3)	80(5)	38(4)	-11(3)	-3(3)	-11(3)
C(9)	46(3)	55(4)	46(4)	-14(3)	-0(3)	-15(3)
C(10)	43(3)	37(3)	42(4)	0(2)	-3(3)	-3(3)

Atoms H(11, 12, 13, 31, 32, 33) have $U = 0.07$ Atoms H(1, 2, 3, 4, 5) have $U = 0.05$

(2) Iodobenzene bis(dichloroacetate)

Atom	U(11)	U(22)	U(33)	U(12)	U(13)	U(23)
I	51.0(8)	51.3(6)	48.8(6)	0.0(3)	7.7(3)	5.1(3)
Cl(1)	64(2)	128(3)	83(2)	27(2)	-15(2)	11(2)
Cl(2)	91(3)	204(5)	58(2)	53(3)	18(2)	6(2)
Cl(3)	120(4)	115(3)	80(2)	-12(3)	-13(2)	21(2)
Cl(4)	118(3)	98(3)	93(3)	-42(2)	15(2)	14(2)
O(1)	55(5)	46(4)	48(4)	5(4)	9(4)	2(3)
O(2)	97(7)	57(6)	128(8)	12(5)	-29(6)	23(5)
O(3)	76(6)	69(5)	53(5)	23(4)	21(4)	-7(4)
O(4)	128(9)	212(13)	72(6)	-105(9)	54(6)	-23(7)
C(1)	46(7)	74(8)	48(6)	8(6)	1(6)	18(6)
C(2)	47(8)	45(7)	53(7)	4(6)	-8(6)	19(6)
C(3)	71(9)	86(9)	57(7)	-1(7)	13(7)	6(7)
C(4)	65(9)	97(10)	47(8)	-22(8)	12(7)	1(7)
C(5)	47(8)	42(6)	51(7)	0(6)	3(6)	5(5)
C(6)	84(10)	83(9)	68(8)	38(8)	24(8)	30(7)
C(7)	107(14)	97(11)	82(10)	28(10)	39(10)	40(9)
C(8)	85(12)	105(12)	75(10)	-12(10)	35(9)	5(9)
C(9)	56(10)	118(12)	106(12)	28(9)	17(9)	12(10)
C(10)	54(9)	84(9)	87(9)	11(8)	18(8)	33(7)

All hydrogen atoms have $U = 0.08$

Table III-2 Bond lengths (\AA) and bond angles ($^{\circ}$) with standard deviations in parentheses*.

(1) Iodobenzene diacetate

(a) Bond lengths

(i) Around iodine

I-O(1)	2.159(5)
I-O(3)	2.153(5)
I-C(5)	2.090(6)
I...O(2)	2.817(6)
I...O(4)	2.850(5)

(ii) Acetate groups

C(1)-C(2)	1.506(10)	C(3)-C(4)	1.507(10)
C(2)-O(1)	1.316(8)	C(4)-O(3)	1.307(8)
C(2)-O(2)	1.211(9)	C(4)-O(4)	1.227(8)
C(1)-H(11)	1.04	C(3)-H(31)	0.84
C(1)-H(12)	0.97	C(3)-H(32)	0.82
C(1)-H(13)	0.99	C(3)-H(33)	0.73

(iii) Phenyl ring

C(5)-C(6)	1.400(8)	C(6)-H(1)	0.94
C(6)-C(7)	1.384(9)	C(7)-H(2)	0.97
C(7)-C(8)	1.368(11)	C(8)-H(3)	0.97
C(8)-C(9)	1.361(10)	C(9)-H(4)	0.96
C(9)-C(10)	1.396(10)	C(10)-H(5)	0.92
C(10)-C(5)	1.361(8)		

(b) Bond angles

(i) Around iodine

O(1)-I-O(3)	164.0(2)	C(5)-I-O(2)	131.9(2)
O(1)-I-C(5)	81.4(2)	C(5)-I-O(4)	132.7(2)
O(3)-I-C(5)	82.6(2)	O(1)-I-O(4)	145.8(2)
O(2)-I-O(4)	95.2(2)	O(3)-I-O(2)	145.2(2)

(ii) Acetate groups

I-O(1)-C(2)	108.1(4)	I-O(3)-C(4)	109.6(4)
O(1)-C(2)-O(2)	121.7(6)	O(3)-C(4)-O(4)	121.7(6)
O(1)-C(2)-C(1)	114.1(6)	O(3)-C(4)-C(3)	114.4(6)
O(2)-C(2)-C(1)	124.2(7)	O(4)-C(4)-C(3)	124.0(6)
I-O(2)-C(2)	79.6(4)	I-O(4)-C(4)	78.5(4)

(iii) Phenyl ring

I-C(5)-C(6)	118.5(4)
I-C(5)-C(10)	118.7(4)
C(5)-C(6)-C(7)	116.9(6)
C(6)-C(7)-C(8)	121.1(6)
C(7)-C(8)-C(9)	120.6(6)
C(8)-C(9)-C(10)	120.5(6)
C(9)-C(10)-C(5)	118.0(6)

(2) Iodobenzene bis(dichloroacetate)(a) Bond lengths(i) Around iodine

I-O(1)	2.136(6)
I-O(3)	2.163(7)
I...O(2)	3.049(10)
I...O(4)	2.936(10)
I-C(5)	2.083(12)

(ii) Acetate groups

Cl(1)-C(1)	1.740(11)	Cl(3)-C(3)	1.784(13)
Cl(2)-C(1)	1.731(12)	Cl(4)-C(3)	1.696(14)
C(1)-C(2)	1.499(14)	C(3)-C(4)	1.533(16)
C(2)-O(1)	1.288(14)	C(4)-O(3)	1.275(16)
C(2)-O(2)	1.208(16)	C(4)-O(4)	1.199(20)
C(1)-H(11)	0.98	C(3)-H(31)	0.98

(iii) Phenyl ring

C(5)-C(6)	1.369(18)	C(6)-H(1)	0.96
C(6)-C(7)	1.328(24)	C(7)-H(2)	0.96
C(7)-C(8)	1.298(28)	C(8)-H(3)	1.03
C(8)-C(9)	1.361(27)	C(9)-H(4)	1.00
C(9)-C(10)	1.358(25)	C(10)-H(5)	0.99
C(10)-C(5)	1.348(19)		

(b) Bond angles(i) Around iodine

O(1)-I-O(3)	167.1(4)	O(1)-I-O(4)	143.3(3)
O(1)-I-C(5)	86.0(3)	O(3)-I-O(4')	116.8(3)
O(3)-I-C(5)	82.5(3)	I-O(4)-I'	111.1(4)
O(4)-I-O(4')	68.9(3)		
C(5)-I-O(4)	157.8(4)		
C(5)-I-O(4')	130.0(4)		

* O(4') is related to O(4) by $\frac{1}{2}-x, -y, -z$.

(ii) Acetate groups

Cl(1)-C(1)-Cl(2)	110.0(6)	Cl(3)-C(3)-Cl(4)	111.4(7)
Cl(1)-C(1)-C(2)	112.1(9)	Cl(3)-C(3)-C(4)	106.7(10)
Cl(2)-C(1)-C(3)	109.2(8)	Cl(4)-C(3)-C(4)	114.7(9)
O(1)-C(2)-O(2)	123.8(9)	O(3)-C(4)-O(4)	124.5(11)
O(1)-C(2)-C(1)	111.4(10)	O(3)-C(4)-C(3)	115.8(12)
O(2)-C(2)-C(1)	124.7(11)	O(4)-C(4)-C(3)	119.7(12)
I-O(1)-C(2)	116.2(6)	I-O(3)-C(4)	111.5(8)
I-O(4)-C(4)	75.8(7)	I-O(2)-C(2)	73.3(7)

(iii) Phenyl ring

I-C(5)-C(6)	118.7(9)
I-C(5)-C(10)	119.0(9)
C(10)-C(5)-C(6)	122.3(13)
C(5)-C(6)-C(7)	118.7(14)
C(6)-C(7)-C(8)	120.3(16)
C(7)-C(8)-C(9)	122.1(18)
C(8)-C(9)-C(10)	119.8(16)
C(9)-C(10)-C(5)	116.7(14)

Table III-3 Equations of the least squares mean planes $PI + QJ + RK = S^{(a)}$
in orthogonal angstrom space

(1) Iodobenzene diacetate

Plane 1	<u>P</u>	<u>Q</u>	<u>R</u>	<u>S</u>
	0.4926	0.0197	-0.8700	-0.4418
Atom, dev. (Å)				
I*	0.018	C(7)*	-0.006	C(10)* -0.021
C(5)*	-0.015	C(8)*	0.017	O(1) -2.044
C(6)*	-0.005	C(9)*	0.010	O(3) 2.081
Plane 2	<u>P</u>	<u>Q</u>	<u>R</u>	<u>S</u>
	-0.2989	0.9387	0.1717	-1.8387
Atom, dev. (Å)				
O(1)*	0.003	C(2)*	-0.10	O(4) 0.005
O(2)*	0.004	I	-0.004	C(5) -0.141
C(1)*	0.003	O(3)	-0.087	
Plane 3	<u>P</u>	<u>Q</u>	<u>R</u>	<u>S</u>
	-0.3024	0.9493	0.0865	-1.7736
Atom, dev. (Å)				
O(3)*	0.000	C(4)*	-0.001	O(2) -0.316
O(4)*	0.000	I	-0.090	C(5) -0.143
C(3)*	0.000	O(1)	-0.232	
Plane 4	<u>P</u>	<u>Q</u>	<u>R</u>	<u>S</u>
	-0.3226	0.9350	0.1471	-1.8555
Atom, dev. (Å)				
I*	0.039	C(1)	-0.027	C(6) 1.126
O(1)*	0.033	C(2)	-0.025	C(7) 1.038
O(2)*	-0.038	C(3)	-0.140	C(8) -0.139
O(3)*	-0.012	C(4)	-0.043	C(9) -1.248
O(4)*	0.008	C(5)*	-0.030	C(10) -1.203
Angles between planes (°)				
(1)-(2)	73.85	(1)-(3)	78.14	(1)-(4) 74.43
(2)-(3)	4.93	(2)-(4)	1.97	(3)-(4) 3.75

(III.5.) References

1. (a) E.M. Archer and T.G.D. van Schalkwyk, Acta Cryst., 1953, 6, 88.
 (b) p-chlorobenzene dichloride is apparently similar to PhCl_2 , although the I...Cl distance was not specified, D.A. Bekoe and R. Hulme, Nature, 1956, 177, 1230.
2. (a) N.W. Alcock and R.M. Countryman, J. Chem. Soc. Dalton, 1977, 217; (b) T.G. Khotsyanova, T.A. Babushkina and V.V. Saatsazov, Izv. Akad. Nauk. SSSR, Ser. Fiz., 1975, 12, 2530 and refs. therein.
3. E. Schefter and W Wolf, J. Pharm. Sci., 1965, 54, 104; Nature, 1964, 203, 513.
4. K. Prout, M.N. Stevens, A. Coda, V. Tazzoli, R.A. Shaw and T. Demir, Z. Naturforsch., 1976, 31b, 687.
5. G.F. Koser, R.H. Wettach and J.M. Troup, J. Org. Chem., 1976, 41, 3609.
6. M.C. Etter, J. Solid State Chem., 1976, 16, 399, and references cited there.
7. R.J. Gillespie, 'Molecular Geometry', Van Nostrand Reinhold, London, 1972.
8. N.W. Alcock, Advanc. Inorg. Chem. Radiochem., 1972, 15, 1.
9. C-K. Lee, T.C.W. Mak, W-K. Li and J.F. Kirner, Acta Cryst., 1977, B33, 1620.
10. F.G. Mann and B.C. Saunders, 'Practical Organic Chemistry', Longmans (London), 1936.
11. (a) The term anisobidentate was first used by J.L.K.F. de Vries and R.H. Herber, Inorg. Chem., 1972, 11, 2458, but is not common usage.
 (b) For a classification of acetate co-ordination modes, see N.W. Alcock, V.M. Tracy and T.C. Waddington, J. Chem. Soc. Dalton, 1976, 2243.
12. N.W. Alcock, unpublished results.
13. K.H. Boswijk and E.H. Wiebenga, Acta Cryst., 1954, 7, 417.
14. W.B. Wright and E.A. Meyers, Cryst. Str. Comm., 1972, 1, 95.
15. O. Vlkane, Acta Chem. Scand., 1975, A29, 738.
16. 'Comprehensive Inorganic Chemistry', ed. A.F. Trotman-Dickenson, Pergamon, Vol. 2, p. 1350 ff.

(2) Iodobenzene bis(dichloroacetate)

<u>Plane 1</u>	<u>P</u>	<u>Q</u>	<u>R</u>	<u>S</u>
	0.3372	0.8468	0.4114	2.2930
Atom, dev. (Å)				
I*	0.004	C(7)*	0.015	C(10)* -0.002
C(5)*	0.001	C(8)*	-0.005	
C(6)*	-0.015	C(9)*	0.002	
<u>Plane 2</u>	<u>P</u>	<u>Q</u>	<u>R</u>	<u>S</u>
	-0.6477	-0.3145	0.6940	-1.3723
Atom, dev. (Å)				
O(1)*	-0.007		I 0.191	
O(2)*	-0.009		C(5) 2.197	
C(1)*	-0.006			
C(2)*	0.023			
<u>Plane 3</u>	<u>P</u>	<u>Q</u>	<u>R</u>	<u>S</u>
	0.6542	-0.6223	0.4298	3.3859
Atom, dev. (Å)				
O(3)*	-0.002		I 0.160	
O(4)*	-0.003		O(1) 0.256	
C(3)*	-0.002		O(2) 2.447	
C(4)*	0.007		C(5) -0.132	
<u>Plane 4</u>	<u>P</u>	<u>Q</u>	<u>R</u>	<u>S</u>
	0.5352	-0.6784	0.5033	3.2121
Atom, dev. (Å)				
I*	0.002	C(8)	0.079	O(2) 2.147
O(1)*	-0.001	C(2)	1.142	O(4) -0.302
O(3)*	-0.001	C(4)	-0.711	O(4)' -0.523 ^(b)
C(5)*	0.000			
<u>Angles between planes (°)</u>				
(1)-(2)	78.51	(1)-(3)	82.55	(1)-(4) 79.22
(2)-(3)	85.97	(2)-(4)	77.53	(3)-(4) 8.64

(a) The orthogonal unit vector I is parallel to a, K is perpendicular to a in the ac plane and J is perpendicular to the ac plane.

(b) Related to O(4) by a centre of symmetry.

(III.5.) References

1. (a) E.M. Archer and T.G.D. van Schalwyk, Acta Cryst., 1953, 6, 88.
 (b) p-chlorobenzene dichloride is apparently similar to PhICl_2 , although the I...Cl distance was not specified, D.A. Bekoe and R. Hulme, Nature, 1956, 177, 1230.
2. (a) N.W. Alcock and R.M. Countryman, J. Chem. Soc. Dalton, 1977, 217; (b) T.G. Khotsyanova, T.A. Babushkina and V.V. Saatsazov, Izv. Akad. Nauk. SSSR, Ser. Fiz., 1975, 12, 2530 and refs. therein.
3. E. Scheffter and W Wolf, J. Pharm. Sci., 1965, 54, 104; Nature, 1964, 203, 513.
4. K. Prout, M.N. Stevens, A. Coda, V. Tazzoli, R.A. Shaw and T. Demir, Z. Naturforsch., 1976, 31b, 687.
5. G.F. Koser, R.H. Wettach and J.M. Troup, J. Org. Chem., 1976, 41, 3609.
6. M.C. Etter, J. Solid State Chem., 1976, 16, 399, and references cited there.
7. R.J. Gillespie, 'Molecular Geometry', Van Nostrand Reinhold, London, 1972.
8. N.W. Alcock, Advanc. Inorg. Chem. Radiochem., 1972, 15, 1.
9. C-K. Lee, T.C.W. Mak, W-K. Li and J.F. Kirner, Acta Cryst., 1977, B33, 1620.
10. F.G. Mann and B.C. Saunders, 'Practical Organic Chemistry', Longmans (London), 1936.
11. (a) The term anisobidentate was first used by J.L.K.F. de Vries and R.H. Herber, Inorg. Chem., 1972, 11, 2458, but is not common usage.
 (b) For a classification of acetate co-ordination modes, see N.W. Alcock, V.M. Tracy and T.C. Waddington, J. Chem. Soc. Dalton, 1976, 2243.
12. N.W. Alcock, unpublished results.
13. K.H. Boswijk and E.H. Wiebenga, Acta Cryst., 1954, 7, 417.
14. W.B. Wright and E.A. Meyers, Cryat. Str. Comm., 1972, 1, 95.
15. O. Vikane, Acta Chem. Scand., 1975, A29, 738.
16. 'Comprehensive Inorganic Chemistry', ed. A.F. Trotman-Dickenson, Pergamon, Vol. 2, p. 1350 ff.

17. P. Boldrini, R.J. Gillespie, P.R. Ireland and G.J. Schrobilgen, Inorg. Chem., 1974, 13, 1693.
18. B.F. Hoskins and C.D. Pannan, Chem. Commun., 1975, 408; Aust. J. Chem., 1976, 29, 2337.
19. C. Fabiani, R. Spagna, A. Vaciago and L. Zambonelli, Acta Cryst., 1971, B27, 1499 and refs. cited there.
20. H. Graver and S. Husebye, Acta Chem. Scand., A29, 14 (1975); S. Husebye, Acta Chem. Scand., 21, 42 (1967).
21. J.D. Curry and R.J. Jandacek, J. Chem. Soc. Dalton, 1972, 1120.
22. W.G. Mumme and G. Winter, Inorg. Nucl. Chem. Letters, 1971, 7, 505; see also S.L. Lawton and G.T. Kokotailo, Nature, 1969, 221, 550.
23. W. Schwarz, G. Mann and J. Weidlein, J. Organometal. Chem., 1976, 122, 303.
24. N.W. Alcock, J. Chem. Soc. Dalton, 1973, 1616; four O...O contacts of 2.75 - 2.92 Å and an O...O of 2.17 Å for a nitrate group have been found in a pentagonal bipyramidal Sn complex, tris(dimethylsulphoxide)-nitrate diphenyl tin(IV) nitrate, L. Coghi, C. Pellizzi and G. Pellizzi, J. Organometal. Chem., 1976, 114, 53. See also ref. 11b for a discussion of the relation of O...O contacts to the acetate co-ordination mode.
25. W.N. Lipscomb, 'Boron Hydrides', Benjamin (New York), 1963 and also Section II.
26. M.B. Ferrari, L.C. Capacchi, L. Cavalca and G.F. Gasparri, Acta Cryst., 1972, B28, 1169.
27. S.C. Nyburg, G.A. Ozln and J.T. Szymanski, Acta Cryst., 1971, B27, 2298.
28. See Section (VI.5).
29. F.J. Berry and C.H.W. Jones, Can. J. Chem., 1976, 54, 3737; R.F. Ziolo and D.T. Pritchett, J. Organometal. Chem., 1976, 116, 211; H. Siebert and M. Handrich, Z. anorg. Chem., 1976, 426, 173.

CHAPTER IV

The crystal and molecular structures of two new spin labels and of α - α dibromobenzylidene acetone; pyramidal distortions of the nitroxide group and the importance of Br...O secondary bonds in the packing of organic molecules

(IV.1.) Introduction

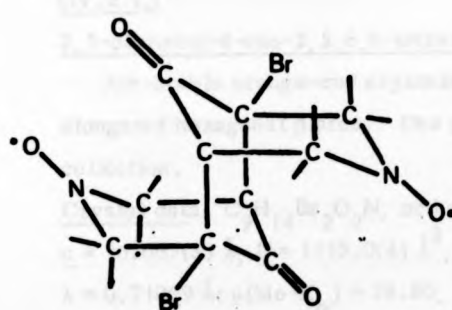
Among the better known examples of relatively stable free radicals (i.e. $\tau_{1/2} > \text{days}$) are a group of compounds known as nitroxides.¹ These compounds are readily prepared by oxidation of the corresponding secondary amine. Nitroxides have secured an important place in biochemistry as spin labels.² The technique of spin labelling entails covalent attachment of the nitroxide to a biologically active molecule whereupon the resulting biological system can then be probed by electron spin resonance spectroscopy. In this way valuable information about conformational change accompanying binding of a substrate to an enzyme can be deduced. Since e.s.r. spectroscopy is such a sensitive technique (concentrations of paramagnetic species down to 10^{-14} M can be detected) extremely small quantities of a nitroxide-labelled substrate suffice for biochemical investigations. As part of a research program into adenosylcobalamin-dependent enzymatic reactions, several spin-labelled probes for studying the biochemistry of β -lactam antibiotics were prepared by other workers. One objective was to prepare a stereo-specific spin-labelled penicillin from 6-aminopenicillanic acid and an achiral nitroxide such as 3-carboxy-2,2,5,5-tetramethyl-3-pyrrolin-1-yloxy. Both 3,5-dibromo-4-oxo-2,2,6,6-tetramethyl-piperidin-1-yloxy (compound 1) and its monobromo analogue were similarly investigated as potential precursors of 3-(N-substituted)-amino carbonyl-2,2,5,5-tetramethyl-3-pyrrolidin-1-yloxy radicals also of use in such coupling reactions.

Whilst (1) was highly suitable for its intended purpose, the monobromo analogue could not be readily prepared in pure form, and in any case was found to be too unreactive for the direct acylation of primary and secondary amines to give the 3-(N-substituted) radicals.

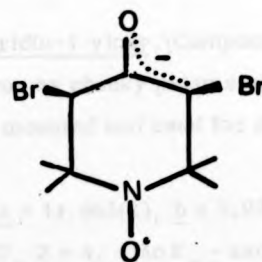
The 3, 5-dibromo-4-oxo-2, 2, 6, 6-tetramethyl-pyrrolin-1-yloxy was prepared by oxidation of 3, 5-dibromo-4-oxo-2, 2, 6, 6-tetramethyl-piperidine using m-chloroperbenzoic acid and details of this preparation are given elsewhere.³ The radical (1) is a highly reactive acylating agent converting amines, amino-acid esters and amino-alcohols to crystalline amides. It is, however, quite unreactive towards hydroxyl groups and reaction with ethanolamine leads to selective acylation of the amino function. During one reaction of (1) with propan-2-ol in dichloromethane containing triethylamine, a compound of molecular formula $C_{18}H_{26}Br_2N_2O_4$ (compound 2) was obtained. This substance also arises from treatment of (1) with triethylamine alone and is also a by-product from reactions between (1) and amino compounds of relatively low basicity. The structure of this compound was originally tentatively given as a dimer of the putative intermediate (3) with the suggested structure (4). X-ray analysis, however, has rigorously established this compound to be a bis-nitroxide 4-[(2', 2', 5', 5'-tetramethylpyrrolin-1'-yloxy)-3'-carbonyloxy]-2, 2, 6, 6-tetramethyl-3, 5-dibromo-3, 4-dehydropiperidin-1-yloxy.⁴

In this chapter, the details of the X-ray analysis on compounds (1) and (2) will be described. Apart from establishing the structure of (2) as the bis-nitroxide, the analysis has given further valuable information on the pyramidal distortions that occur at the nitrogen atom of the nitroxide group. Furthermore, the packing in (2) is determined by Br...O secondary bonds which was another important consideration in attempting these structural analyses.

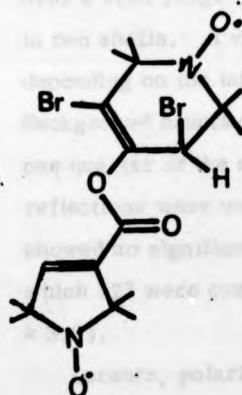
Also reported is the crystal structure of (Z, Z) 2, 4-dibromo-1, 5-diphenyl-penta-1, 4-dien-3-one which has similarly been determined to gain information on Br...O secondary bonds, and secondly to establish the molecular conformation. However, in both this compound and (1) above, the molecular packing is that of a molecular crystal with no secondary bonding involved. These three structures show a little of the difficulty of establishing a priori whether secondary bonds will be found in a particular structure.



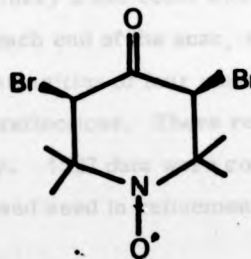
4



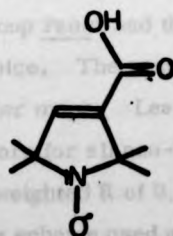
3



2



1



1a

(IV.2.) Data Collection and Structure Solution

(IV.2.1.)

3,5-dibromo-4-oxo-2,2,6,6-tetramethylpiperidin-1-yloxy. (Compound 1)

Air-stable orange-red crystals of (1) occur as chunky prisms or as elongated hexagonal plates. One prism was mounted and used for data collection.

Crystal data: $C_9H_{14}Br_2O_2N$, orthorhombic, $a = 11.665(2)$, $b = 5.938(1)$, $c = 16.067(3)$ Å, $V = 1113.0(4)$ Å³, $D_c = 1.957$, $Z = 4$. MoK_{α} - radiation, $\lambda = 0.71069$ Å; $\mu(Mo-K_{\alpha}) = 76.85$, $F(000) = 644$. Systematic absences $hk0$, $h \neq 2n$, $0kl$, $k + 1 \neq 2n$ indicate space groups $Pnma$ or $Pn2_1a$ (non-standard setting of $Pna2_1$ (No. 33)).

Unit cell dimensions and data were measured using $\theta - 2\theta$ scans over a scan range ($K_{\alpha_1} - 0.65$) to ($K_{\alpha_2} + 0.65$) to a maximum 2θ of 55° in two shells. A variable scan rate of $1.0^\circ/\text{min}$ to $29.5^\circ/\text{min}$ depending on the intensity of a preliminary 2 sec count was used. Background counts were recorded at each end of the scan, each for one quarter of the scan time. The intensities of four standard reflections were monitored every 70 reflections. These reflections showed no significant loss in intensity. 1527 data were collected, of which 823 were considered observed and used in refinement ($I/\sigma I \geq 3.0$).

Lorentz, polarisation and absorption corrections were applied. With four molecules in the unit cell, space group $Pnma$ requires mirror symmetry in the molecule. A Patterson synthesis was successfully interpreted for the vectors generated by a single bromine atom in space group $Pnma$ and the subsequent satisfactory refinement confirms this choice. The remaining atoms were located in subsequent Fourier maps. Least squares refinement with anisotropic temperature factors for all non-hydrogen atoms produced a final R factor of 0.026 (weighted R of 0.025).

The weighting scheme used gives reflections within the ranges $15.0 \leq F \leq 45.0$ and $0.265 \leq \sin \theta \leq 0.50$ weights of $(1/\sigma(F))^2$. Other reflections are weighted by the equation $W = X \cdot Y \cdot (1/\sigma(F))^2$ where $X =$

$\sin \theta / 0.265$ if $\sin \theta < 0.265$ or $X = 0.50 / \sin \theta$ if $\sin \theta > 0.50$ and $Y = F / 15.0$ if $F < 15.0$ or $Y = 45.0 / F$ if $F > 45.0$. Using this weighting scheme, one reflection with a very bad $\omega^* \Delta s_q$ was rejected from the refinement.

(IV.2.2.)

4-[(2',2',5',5'-tetramethylpyrrolidin-1'-yloxy)-3'-carbonyloxy]-2,2,6,6-tetramethyl-3,5-dibromo-3,4-dehydropiperidin-1-yloxy
(Compound 2)

Air-stable orange-red crystals of (2) slowly recrystallised from boiling n-hexane as thin plates. One such plate was found to extinguish under crossed polars along the diagonal of the plate.

Crystal data: $C_{18}H_{26}Br_2O_4N_2$, orthorhombic, $a = 11.089(2)$, $b = 30.477(6)$, $c = 12.970(2)$ Å, $V = 4383.3(14)$ Å³, $D_c = 1.498$, $Z = 8$, Mo K_α -radiation, $\lambda = 0.71069$ Å, $\mu(\text{Mo}-K_\alpha) = 39.41 \text{ cm}^{-1}$, $F(000) = 2000$. Systematic absences $Ok1$, $k \neq 2n$; hOl , $l \neq 2n$; hkO , $h \neq 2n$ indicate space group Pbca (No. 61).

Unit cell dimensions and data were measured using the diffractometer. Reflections were measured using $\theta - 2\theta$ scans over a scan range $(K_{\alpha_1} - 0.7)$ to $(K_{\alpha_2} + 0.7)$ to a maximum 2θ of 50° . The intensities of three standard reflections were monitored every 100 reflections. These reflections showed no significant loss in intensity. Other conditions were the same as in (IV.2.1.). 4399 data were collected, of which 1104 were considered observed and used in refinement ($I/\sigma(I) \geq 3.0$).

Lorentz, polarisation and absorption corrections were applied. The two bromine atoms were readily located on a Patterson synthesis and the remaining light atoms found by Fourier methods. Least squares refinement, using three blocks with anisotropic temperature factors for all non-hydrogen atoms and including a correction for the effects of anomalous dispersion, produced a final R factor of 0.048 (weighted R of 0.035). The weights used were based on counting statistics.

Final co-ordinates and temperature factors are in Table IV.1. Significant bond lengths, bond angles and torsion angles are given in Table II. 2, and molecular planes in Table IV.3. Structure factors are in Appendix A

(IV.2.3.)

(Z, Z) 2,4-Dibromo-1,5-diphenyl-penta-1,4-dien-3-one. (Compound 3)

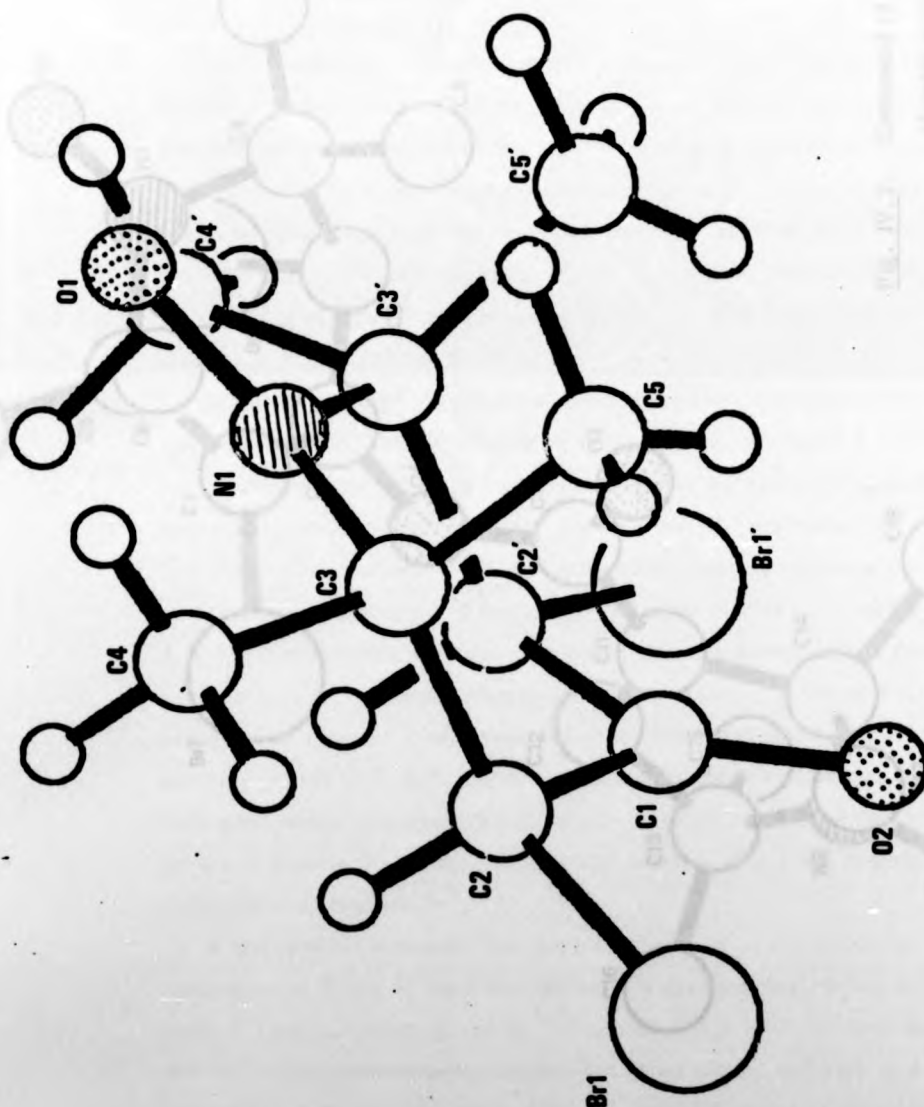
The sample of (Z, Z)^{2,4}-Dibromo-1,5-diphenyl-penta-1,4-dien-3-one were prepared and supplied by Professor Shoppee. The crystals (m.p. 97-98°C), recrystallised slowly from ethanol, form chunky needles (needle axis c). One needle was mounted and used for all subsequent work.

Crystal data: C₁₇H₁₂Br₂O, monoclinic, a = 41.080(11), b = 6.527(2), c = 11.118(3) Å, β = 97.767(23)°, V = 2953.7(16) Å³ at 18°C, Z = 8, D_c = 1.71 g/cm⁻³. MoK α - radiation, λ = 0.71069 Å; μ (MoK α) = cm⁻¹. Systematic absences, h0l, l ≠ 2n, and 0k0, k ≠ 2n indicate space group P2₁/c.

Unit cell dimensions and data were measured on the diffractometer and the long a axis was confirmed by Weissenberg photographs. There are two independent molecules in the asymmetric unit and also a marked pseudo-absence hk0, h ≠ 2n in the data. However, there is no evidence from the Syntex autoindexing program or more particularly from the Weissenberg photographs of an orthorhombic system with a single molecule in the asymmetric unit. Reflections were measured using θ - 2 θ scans over a scan range (K α ₁ - 0.9) to (K α ₂ + 0.8)° to a maximum 2θ of 50° in two shells. In the first shell ($0 < 2\theta \leq 35^\circ$) all reflections were collected whilst in the second shell ($35 < 2\theta \leq 50^\circ$) a reflection was only collected if the intensity of a 8 sec preliminary count was greater than 40 counts per sec. A variable scan rate of 1.0 - 29.3°/min depending on the intensity of the preliminary count was used.

The positions of the four Br atoms were located by applying the direct methods programs NORMAL and MULTAN (Germain and Woolfson, 1968) to the 274 reflections with E > 1.50 in the first shell of data. Fourier and least squares refinement using the 1865 observed (I/ σ (I) > 3.0) reflections in both shells located the remaining non-hydrogen atoms. The final refinement was with Br, C and O with anisotropic temperature factors to an R factor of 0.081. The

Fig. IV.1. General view of Compound (1). Primed and unprimed atoms are related by the mirror plane.



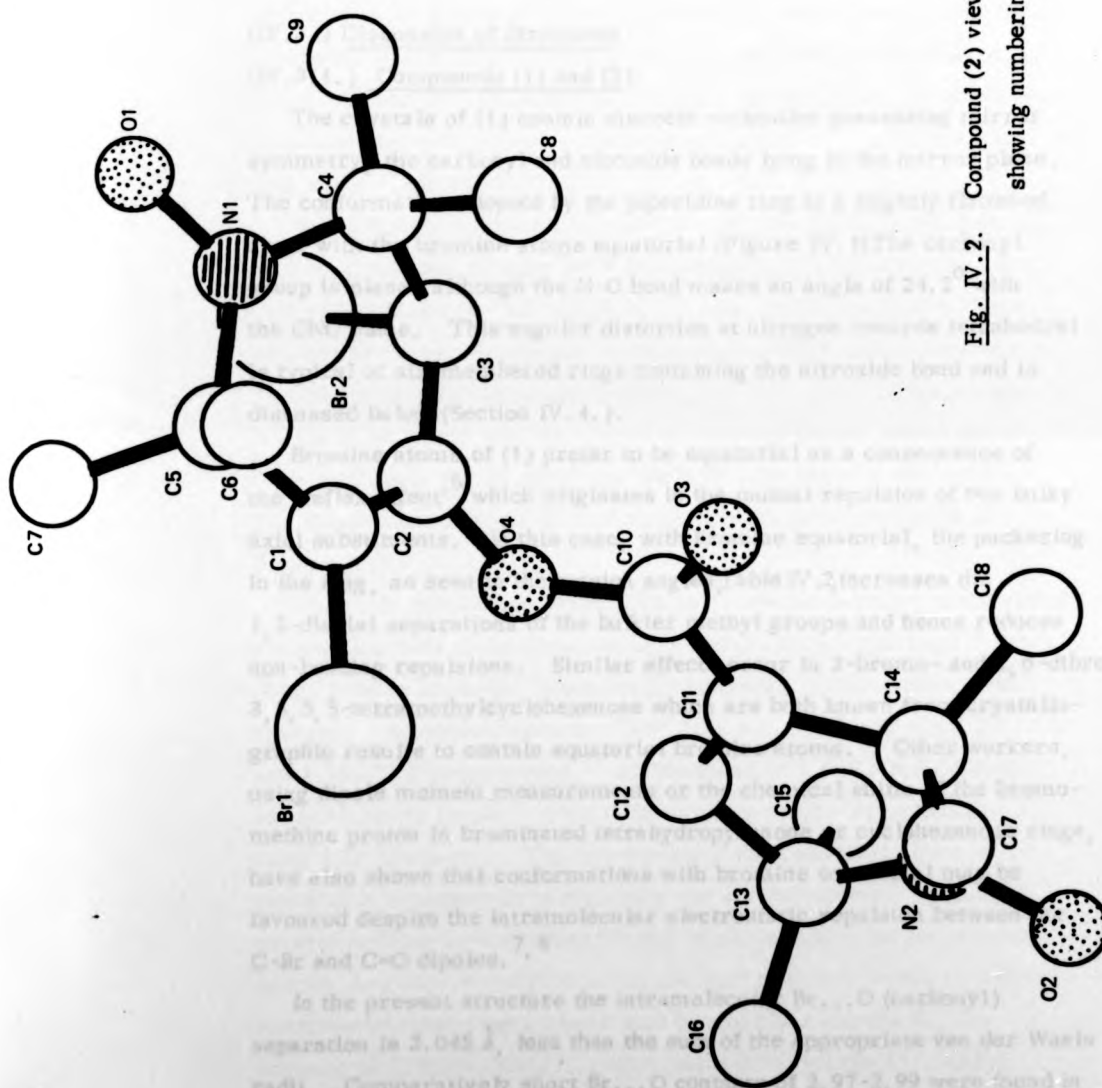


Fig. IV. 2. Compound (2) viewed down b , showing numbering of atoms.

weighting scheme used was $\sqrt{w} = 1.0/(186-335 \sin \theta)$. Hydrogen atoms were not included and no correction for absorption was performed.

(IV.3.) Discussion of Structures

(IV.3.1.) Compounds (1) and (2)

The crystals of (1) contain discrete molecules possessing mirror symmetry, the carbonyl and nitroxide bonds lying in the mirror plane. The conformation adopted by the piperidine ring is a slightly flattened chair with the bromine atoms equatorial (Figure IV.1). The carbonyl group is planar although the N-O bond makes an angle of 24.2° with the CNC plane. This angular distortion at nitrogen towards tetrahedral is typical of six-membered rings containing the nitroxide bond and is discussed below (Section IV.4.).

Bromine atoms of (1) prefer to be equatorial as a consequence of the 'reflex effect'⁵ which originates in the mutual repulsion of two bulky axial substituents. In this case, with bromine equatorial, the puckering in the ring, as seen in the torsion angles, Table IV.2, increases the 1,3-diaxial separations of the bulkier methyl groups and hence reduces non-bonding repulsions. Similar effects occur in 2-bromo- and 2,6-dibromo-3,3,5,5-tetramethylcyclohexanone which are both known from crystallographic results to contain equatorial bromine atoms.⁶ Other workers, using dipole moment measurements or the chemical shifts of the bromomethine proton in brominated tetrahydropyranone or cyclohexanone rings, have also shown that conformations with bromine equatorial may be favoured despite the intramolecular electrostatic repulsion between the C-Br and C=O dipoles.^{7,8}

In the present structure the intramolecular Br...O (carbonyl) separation is 3.045 \AA , less than the sum of the appropriate van der Waals radii. Comparatively short Br...O contacts of 2.97 - 2.99 were found in the two bromocyclohexanone structures noted above, and also in 2,4-dibromo-1,5-diphenyl penta-1,4-dien-3-one (Compound 3) which has the ZZ configuration about the two double bonds, due again to the steric requirements of other bulkier groups, resulting in adjacent Br and O and Br...O of 2.93 - 2.95 \AA . Other evidence of strain in the piperidine

ring is the small C(2)-C(1)-C(2') angle ($108.2(6)^{\circ}$) which reduces the repulsion between the C-Br and C=O dipoles.

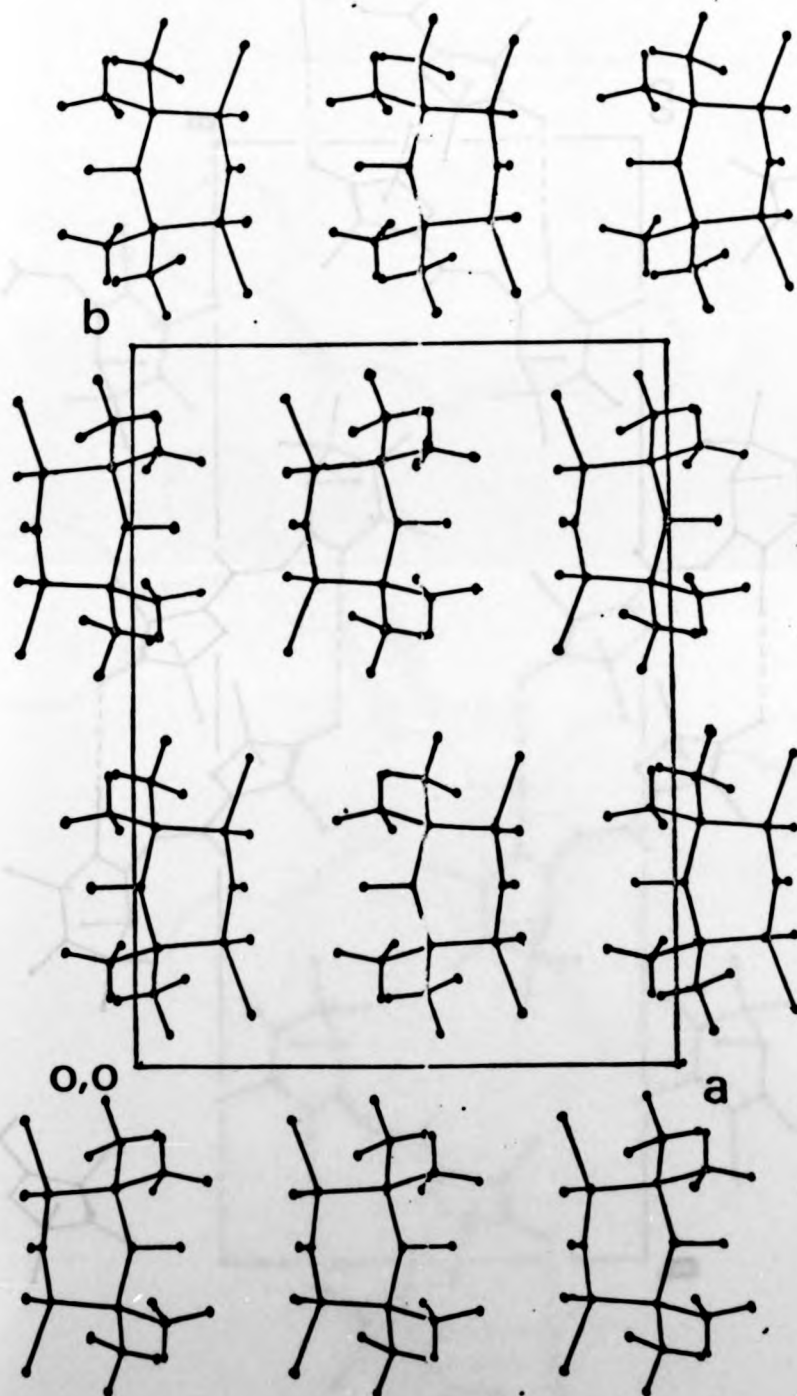
The packing of the individual molecules of (1) is dictated by normal van der Waals forces (Figure IV.3). There appears to be no close intermolecular interactions involving the nitroxide bond (In contrast to 9-aza-bicyclo[3,3,1]nonan-3-one-8-oxyl, for example, in which two nitroxide bonds lie around a centre of symmetry forming a rectangle with sides 1.289 and 2.278 Å).⁹

In (2) individual molecules contain nitroxide bonds in two different ring environments (Figure IV.2). In contrast to (1) the crystal packing (Figure IV.4) does seem to involve Br...O secondary bonds of 3.086(8) Å between Br(1) and the oxygen of the pyrrolin-yloxy ring, resulting in dimeric units about inversion centres. This secondary bond is 0.28 Å less than the sum of the van der Waals radii[†]; the C-Br...O angle is $178.4(4)^{\circ}$ and the N-O...Br angle is $114.2(6)^{\circ}$. The importance of these Br...O secondary bonds is discussed in Section IV.5.

The C-Br distance in (1) is 1.941(3) Å whilst in ring 1 of (2) there are two different C-Br distances of 1.988(12) (C(sp³)-Br) and 1.916(11) Å (C(sp²)-Br) as expected, since the hybridisation of the carbon atom changes. Accepted values for C(sp²)-Br and C(sp³)-Br are 1.89(1) Å and 1.937(3) Å respectively,¹⁰ but the value of 1.988 Å for C(3)-Br(2) is significantly longer. (The C-Br distance in (1) is typical of C(sp³)-Br however). The lengthening of the C(3)-Br(2) bond is probably a consequence of repulsive non-bonded contacts, although several authors have commented that Sutton's values¹⁰ for these bond lengths may be under-estimated in the light of recent results. The conformation that ring 1 adopts also forces close intramolecular contacts of 3.361(8) (Br(2)...O(2)) and 3.008(8) Å (Br(1)...O(2)) involving the bromine atoms. The remaining distances and angles in (1) and (2) are within normal ranges.

[†] After H. Bondi, *J. Phys. Chem.*, **68**, 441, (1964).

Fig. IV.3. Packing diagram for (1), viewed down c .



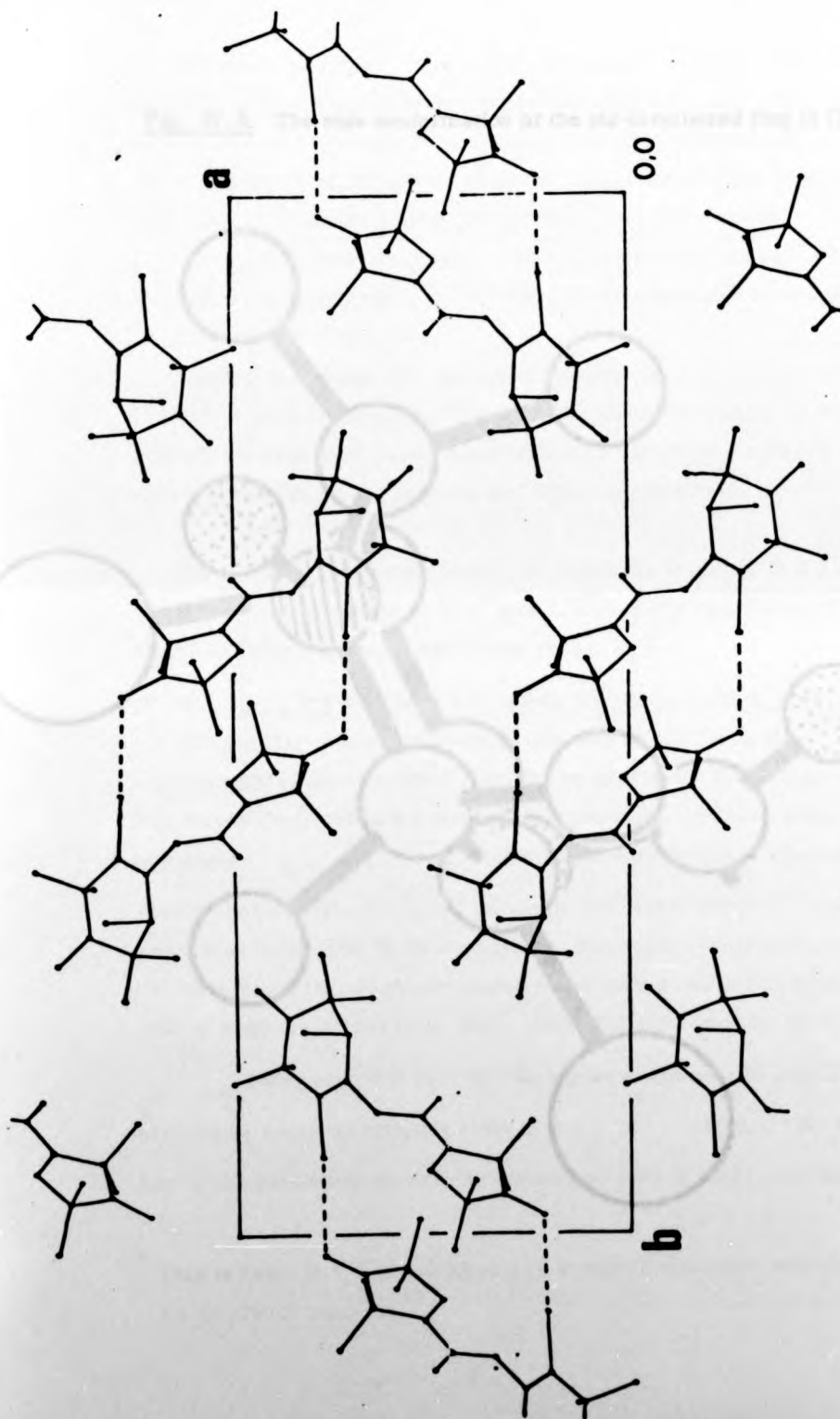
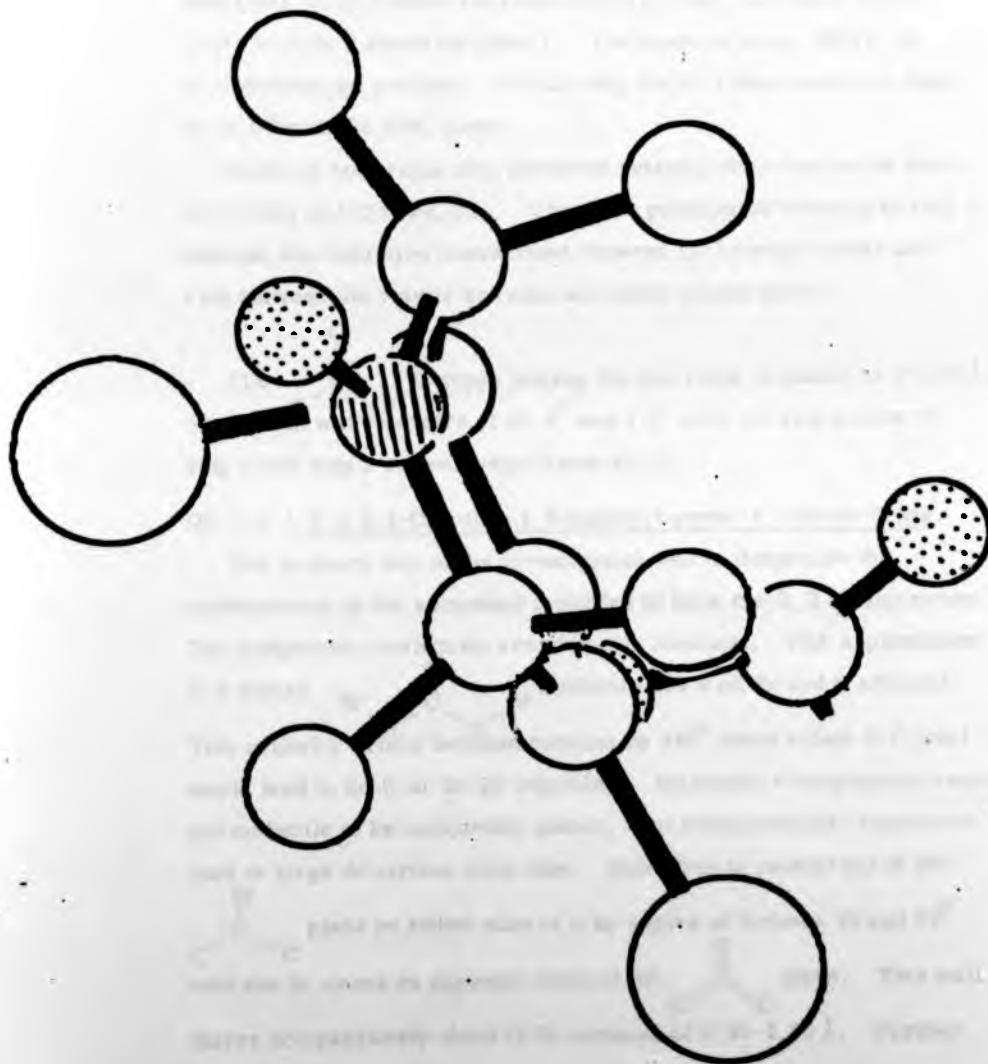


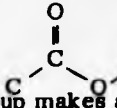
Fig. IV.4. Packing diagram for (2), viewed down c , showing dimeric units associated by Br...O secondary bonds (dashed). 97.

Fig. IV.5. The sofa conformation of the six-membered ring in (2).

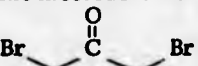
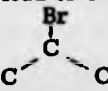
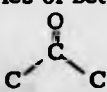


The pyrrolin-yloxy ring is virtually planar with atom C(13) deviating from the plane of the ring by only 0.025 Å. The nitroxide bond makes an angle of 0.5° with the CNC plane. The second six-membered ring, however, adopts a 'sofa' conformation (Figure IV.5) with C(4), 0.60 Å above the plane of N(1), C(2), C(3) and C(5). [C(1) is 0.08 Å above the plane]. The bromine atom, Br(2), is in a pseudoaxial position. In this ring the N-O bond makes an angle of 16.04° with the CNC plane.

Strain in both rings also produces twisting about the double bonds C(1)=C(2) and C(11)=C(12). The more pronounced twisting in ring 1 reduces the repulsive interactions between its bromine atoms and also between the vinylic bromine and ester oxygen atoms.

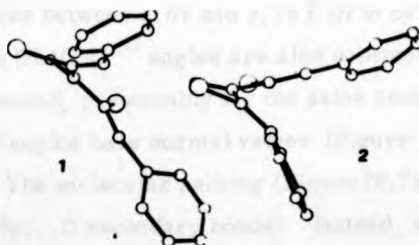
The  group linking the two rings is planar to ± 0.02 Å. This group makes angles of 87.3° and 1.9° with the ring planes of ring 1 and ring 2 respectively (Table IV.3).

(IV.3.2.) Z-Z 2,4-Dibromo-1,5-diphenyl-penta-1,4-diene-3-one.

The primary aim of the investigation was to determine the conformation of the compound regarded to have the Z, Z configuration.¹¹ The independent molecules are virtually identical. Both approximate to a planar  conformation with Br and O adjacent. This probably arises because rotation by 180° about either C-C bond would lead to Br-H or Br-Br repulsion. Maximum π -conjugation requires the molecule to be completely planar,* but intramolecular repulsions lead to large deviations from this. Each C=O is twisted out of the  plane on either side of it by angles of between 22 and 32°, with the Br atoms on opposite sides of the  plane. This still leaves comparatively short O-Br contacts of 2.93-2.95 Å. Further,

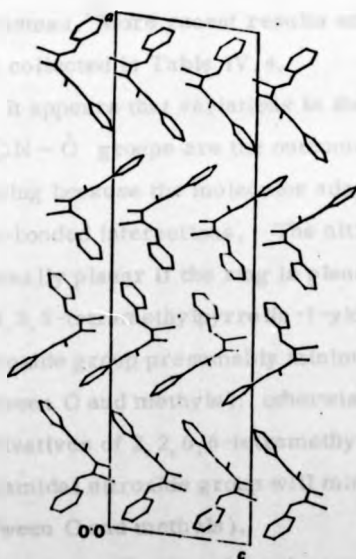
* This is found in 1,5-diphenylpenta-1,4-dien-3-one itself, (investigated as its uranyl complex).¹²

Fig. IV.6.



Views of the two molecules showing the deviations from planarity.

Fig. IV.7.

Packing diagram, viewed down b . The rows contain respectively (from the bottom) molecules 1,2,1,2, those in each row being related by the glide plane.Figs. for *Z-Z* 2,4-Dibromo-1,5-diphenyl-penta-1,4-diene-3-one

the phenyl rings are twisted out of plane by between 24 and 32° to increase the Br-H (ortho) contact distances resulting in values between 2.61 and 2.78 \AA (H in calculated positions) (Figure IV.6). The $(\text{Ph})\text{C}-\text{C}=\text{C}$ angles are also substantially larger than expected, presumably for the same reason. Other bond lengths and angles have normal values (Figure IV.8).

The molecular packing (Figure IV.7) proved not to be controlled by Br...O secondary bonds. Instead, the phenyl rings take up the typical herring-bone arrangement.

(IV.4) The Nitroxide Group; distortions due to non-bonded interactions

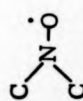
A tabulation of relevant distances and angles in molecules containing the nitroxide group has been given by Lajzerowicz-Bonnetau.¹³ More recent results and data for acyclic nitroxides are collected in Table IV.4.

It appears that variations in the dimensions and angles of the $\text{C} \begin{smallmatrix} \nearrow \\ \searrow \end{smallmatrix} \text{N}-\dot{\text{O}}$ groups are the outcome of geometrical constraints arising because the molecules adopt conformations which minimise non-bonded interactions. The nitroxide group in ring systems is normally planar if the ring is planar (e.g. in derivatives of 2,2,5,5-tetramethylpyrrolin-1-yloxy where planarity of the nitroxide group presumably minimises repulsive interactions between O and methyls); otherwise it may be pyramidal (e.g. in derivatives of 2,2,6,6-tetramethylpiperidin-1-yloxy where a pyramidal nitroxide group will minimise repulsive interactions between O and methyls).

With acyclic nitroxides the non-bonded contact distances involving the oxygen atom may force the nitroxide group to be planar. For example, in Bu_2^tNO the O...C distance is already short and any deviation at N would decrease this distance even further. Packing arrangements, especially when hydrogen bonds are formed, can also alter the shapes of nitroxide groups.

TABLE IV.4

Structural Data on Nitroxides from Refs. (26-37)^a

Nitroxide	N-O(Å)	CNC(°)		Δ† Conformation of 5-membered ring	Ref.
2, 2, 5, 5-Tetramethyl-3-hydroxypyrrolidin-1-yloxy	1.265(5)	115.3	Planar	-	26
2, 2, 5, 5-Tetramethylpyrrolidin-3-on-1-yloxy oxime ^b	1.272(5)	117.1(4)	Virtually planar	-	27
3-Aminocarbonyl-2, 2, 5, 5-tetramethylpyrrolidin-1-yloxy	1.268(3)	115.0(2)	Virtually planar	-	28
2, 2, 6, 6-Tetramethyl-4-(hydroxyimino)piperidine-1-oxyl	1.27	125	Non-planar	25.8	29
exo-6-tetramethyl-3-azabicyclo(3, 3, 1)nonan-7-on-3-oxyl	1.28(1)	123.2(4)	Non-planar	17°	30
bis(2, 2, 6, 6-tetramethylpiperidin-1-oxyl)carbonate	1.287	d	Non-planar	19.4°	31
2, 2, 6, 6-tetramethylpiperidine-1-iminoxyl-4-(N, 2-hydroxy-1-naphthaldehydimine	1.28	d	d	22°	32
2, 2, 6, 6-tetramethyl-1-piperidine-1-oxyl	1.283(9)	123.6(3)	Non-planar	e	33
bis(p-Anisyl)nitroxide	1.23(5)	124(5)	Planar	-	34
bis(t-Butyl)nitroxide	1.28(2)	124(5)	Probably planar	-	35
bis(Trifluoromethyl)nitroxide	1.26(3)	121(2)	Non-planar	-	35
Fremy's salt (K nitrosodisulphonate, triclinic form)	1.28(4)	c	Small deviation from planarity	-	36
t-Butylferrocenyl nitroxide	1.20	not given	not given	-	37

^a Other data on nitroxides in ref. 13.^b Data for optically active form. This molecule also crystallises as a racemate with two independent molecules in the asymmetric unit. The N-O bond lengths are 1.261(5) and 1.276(5) Å and the corresponding CNC are 115.3(4)° and 116.5(3)°.^c Corresponding angle SNS is 118(2)°.^d Δ is the angle the N-O bond makes with the CNC plane.^e Abstract only available; information not included in abstract.^f Molecule is disordered.

The theoretical geometry of the nitroxide group has been investigated by a CNDO calculation on bis (trifluoromethyl) nitroxide which found that $r(\text{N-O}) = 1.26(1) \text{ \AA}$, and a minimum energy for the molecule occurs with an angle of 10° between the N-O bond and the CNC plane. However, very little energy is required to change this angle in the range 0° to 30° .¹⁴ An ab initio calculation on H_2NO reached similar conclusions: the out-of-plane angle is 26° , HNH is 116° and the N-O bond length is 1.34 \AA .¹⁵

The observed N-O bond lengths are $1.285(9) \text{ \AA}$ for (1), $1.286(15) \text{ \AA}$ (ring 1) and $1.252(13) \text{ \AA}$ (ring 2) for (2). The corresponding CNC angles are $125.1(3)^\circ$ for (1), $121.7(10)^\circ$ (ring 1) and $113.1(10)^\circ$ (ring 2) for (2). The N-O distances are within the ranges quoted in ref. 13 and Table IV.4. The angles between the N-O bonds and the CNC planes in the six-membered rings are also within the observed range ($15.8 - 30.5^\circ$).^{† 13}

The two N-O distances in the six-membered rings are very similar, but the shorter N-O distance in the five-membered ring 2 of (2) is not significantly different. The deviation from planarity of a nitroxide group would be expected to decrease π -overlap between the N and O and hence slightly lengthen the N-O bond. Similarly the CNC would be expected to decrease and the C-N distance to increase. The evidence here and in other nitroxide structures, however, is not sufficiently accurate to prove these points conclusively.

(IV.5.) Halogen - Oxygen Secondary Bonding

In the last few years the successful introduction of direct methods programs such as MULTAN, LSAM, SINGEN and PHASE and others has meant that, for organic molecules especially, it is no longer a necessity to have a heavy atom in the structure for its solution by

[†] The value of 30.5° is for 9-azabicyclo[3,3,1]nonan-3-one-9-oxyl,⁹ where there is a repulsive interaction between the nitroxide and carbonyl bonds and a more reasonable range is perhaps 15.8 to 24.9° .

Patterson methods. However, there have been and there still are a large number of organic and inorganic molecules being published in which the structures have been phased by the use of a heavy halogen atom in the structure. Principally this is due to the relative ease of producing relatively strong carbon-halogen bonds or by crystallising an organic molecule as a halide. Whilst the use of the halogen derivatives does ensure a relatively easy structure solution, the introduced halogen atoms can drastically affect the molecular packing arrangements in the crystal, and it is the intention of this section to summarise some of the specific interactions that are likely to involve the halogen atom, emphasising some secondary bonded examples.

All three of the compounds in this chapter were investigated in the hope that they might contain Br...O secondary bonds. Only compound (2) has been found to contain this type of interaction, although in both the other compounds the repulsive intra-molecular Br...O contacts do have significant effects on the molecular conformation. Apart from their involvement in secondary bonding interactions it is also well documented that halogen substituents on organic bases (in particular purine and pyrimidine bases) can considerably affect the solid state base-stacking patterns and it has been suggested that specific stacking interactions involving these halogen substituents are contributing to the unusual physical and biological properties of nucleic acids which contain halogenated pyrimidines.¹⁶ These latter interactions are however different from linear secondary bonded systems since they normally involve the molecules stacking in layers with partial base overlap so that the halogen atom normally rests over the centre of a nucleotide ring, and hence is involved in several close contacts to carbon and nitrogen atoms (see also Section VI.3.2). In some cases crystal structures may be found with both columnar stacking of approximately planar molecules with short halogen contacts and also with the halogen involved in lateral secondary bonds providing some cohesion between the molecular stacks.¹⁷

As regards the secondary bonds in (2) they result in dimeric units about centres of symmetry which are tilted with respect to the *ab* face and are related by unit cell translations. Similar Br...O secondary bonds to those in (2) have been found to be important in determining the packing of several brominated steroids,¹⁸ certain acid-base structures involving Watson-Crick pairs of molecules and several other organic and inorganic structures.¹⁹ A typical range of distances for the Br...O contact in these structures are from 2.91 to 3.35 Å (compared to the sum of van der Waals radii of 3.37 Å) and all involve nearly linear C-Br...O groups. They thus represent the simplest examples of secondary bonds and can be directly compared to hydrogen bonding in determining the crystal packing. In fact, both hydrogen and secondary bonds may occur together. Not only are the C-Br...O angles $\approx 180^\circ$ but the angles Br-O...X also suggest that the lone pair on oxygen involved in the interaction occurs in an sp^2 or sp^3 hybrid orbital.

Whilst C-Br...O interactions have been principally mentioned, these linear interactions are also found for the other halogen atoms (Cl and I) with oxygen and other electronegative donor atoms. However, there is as yet no comprehensive review of all structures containing the type of secondary bonds briefly covered in this section. A few examples will perhaps show how vast this particular area is likely to be.

In a series of structural determinations of 5-halo-benzofurazan-1-oxide structures, the molecular packing is dictated by C-Br...N secondary bonds for the chloro and bromo complexes, but C-I...O secondary bonds for the iodo compound. Whilst the contact distances are not too accurate [N...Cl 3.20 Å, N...Br 3.14 Å and O...I 3.1 Å] due to the poor quality of the data sets collected, resulting in rigid group refinements, the trend towards shorter distances (I > Br > Cl) and the change from nitrogen to oxygen interactions is quite interesting (attributed to differences in atomic size).²¹ In 2,3-dibromo-1,4-naphthoquinone C-Br...O secondary bonding again stabilises the

structure; the Br...O contacts are 3.15 and 3.22 Å with C-Br...O angles of 166-168° and C-O...Br angles close to 130°. Again these are lateral contacts and the molecules still stack in columns.²⁷ In 2,4-dibromo-*o*-cresyl-3',5'-dinitro salicylate the Br...O contacts are slightly longer at 3.34 and 3.19 Å.²² Whilst the above examples are examples of linear interactions, it is worth mentioning a rare example of a square planar arrangement of 2 primary and 2 secondary bonds at this point. This occurs in 4,5-dicyano-2-imidazolyl(phenyl)bromonium ylide where the two Br...N secondary bonded distances are 2.912(6) Å and 3.094(6) Å [C-Br...N angles are 175.5° and 159.9°] whilst the (Ph)CBrC(imidazolyl) angle is only 99.3(3)°.²³ Some other examples of linear C-Br...N interactions are compared in ref. 24.

A linear C-S...Br[S...Br 3.49 Å; C-S...Br 171°] secondary bond between a bromide ion which is almost in the same plane as a thiazolium ring is again an important component of the crystal packing of thiamine bromide hydrobromide hemihydrate (HThiBr₂·½H₂O). In comparison, the same S atom in the related HThiCl₂·H₂O and HThiI₂ structures forms totally different contacts; to a water molecule in the hydrochloride and to the β-hydroxy ethyl OH group in the hydroiodide.²⁵ The difference in these packing arrangements are presumably a consequence of the size of the halogen atom and the number of water molecules present (and hence the number of hydrogen bonds).

In compound (III) there are no secondary bonds because the molecular packing appears to be determined by the volumes occupied by the phenyl rings. This 'herringbone' arrangement which can be seen in Fig. IV.7 is a common feature of aromatic hydrocarbons and other simple organic molecules such as ethylene. The importance of this particular arrangement is that it minimises H...H repulsions.³⁸

IV.6. References

1. 'Free Nitroxyl Radicals', E.G. Rosantsev, Plenum Press, London (1970).
'Organic Chemistry of Stable Free Radicals', A.R. Forrester, J.M. Hay and R.H. Thomson, Academic Press, London (1968). Chap. 5.

TABLE IV

Atomic co-ordinates ($\times 10^4$) and anisotropic temperature factors* ($\times 10^3$) with standard deviations in parentheses.* In the form $\exp \{ -2\pi^2 (U_{11}h^2a^{*2} + U_{22}k^2b^{*2} + U_{33}l^2c^{*2} + 2U_{12}hka^*b^* + 2U_{13}hla^*c^* + 2U_{23}k lb^*c^*) \}$

(a) 3,5-dibromo-4-oxo-2,2,6,6-tetramethylpiperidin-1-yl-oxo (1)

Atom	\bar{X}	\bar{Y}	\bar{Z}	U_{11}	U_{22}	U_{33}	U_{12}	U_{13}	U_{23}
Br(1)	2127.1(3)	736.0(2)	-961.5(6)	40.6(2)	29.1(2)	59.3(3)	6.8(2)	8.8(2)	-4.5(2)
O(1)	-776(3)	2500(0)	3776(7)	43(2)	45(2)	45(2)	0(0)	24(2)	0(0)
O(2)	1998(3)	2500(0)	-2817(6)	52(2)	38(2)	34(2)	0(0)	14(2)	0(0)
N	106(3)	2500(0)	2499(7)	23(2)	28(2)	28(2)	0(0)	1(2)	0(0)
C(1)	1821(3)	2500(0)	-835(10)	21(2)	28(2)	42(3)	0(0)	0(2)	0(0)
C(2)	1654(3)	1735(2)	627(6)	25(1)	25(1)	33(2)	2(1)	-2(1)	-3(1)
C(3)	405(3)	1666(2)	1486(5)	28(2)	26(1)	28(2)	-1(1)	2(1)	-2(1)
C(4)	337(4)	1027(2)	3390(7)	60(3)	32(2)	36(2)	-1(2)	8(2)	6(2)
C(5)	-450(3)	1463(3)	-371(7)	29(2)	44(2)	40(3)	-5(2)	-1(2)	-8(2)
Atom	\bar{X}	\bar{Y}	\bar{Z}	U_{11}	U_{22}	U_{33}	U_{12}	U_{13}	U_{23}
H(1)	2169(29)	1777(20)	2009(56)	26(8)					
H(41)	583(36)	502(30)	2745(76)	63(13)					
H(42)	841(38)	1181(28)	4709(79)	61(13)					
H(43)	-479(41)	924(27)	3985(69)	62(12)					
Atom	\bar{X}	\bar{Y}	\bar{Z}	U_{11}	U_{22}	U_{33}	U_{12}	U_{13}	U_{23}
H(51)	2169(29)	1777(20)	2009(56)	26(8)					
H(52)	583(36)	502(30)	2745(76)	63(13)					
H(53)	841(38)	1181(28)	4709(79)	61(13)					
H(54)	-479(41)	924(27)	3985(69)	62(12)					

(b) The ester (2) derived from (1)

TABLE IV (continued)

Table I

Atom	X	Y	Z	U ₁₁	U ₂₂	U ₃₃	U ₁₂	U ₁₃	U ₂₃
Br(1)	2182.9(13)	761.1(5)	1120.8(11)	83.4(11)	43.1(9)	78.1(11)	12.1(11)	3.5(12)	19.8(10)
Br(2)	1733.2(17)	1967.8(6)	-1660.5(12)	131.1(16)	85.1(13)	50.9(9)	25.9(13)	-5.0(13)	15.5(11)
O(1)	511(9)	2366(3)	1186(8)	76(8)	61(9)	100(10)	30(7)	21(8)	-8(7)
O(2)	7801(7)	209(2)	-1806(6)	21(6)	48(6)	69(6)	14(5)	9(6)	3(5)
O(3)	5067(8)	1325(3)	418(6)	69(8)	99(8)	49(6)	31(6)	-32(6)	-50(6)
O(4)	3507(7)	1186(3)	-640(6)	30(6)	57(6)	45(6)	22(5)	4(5)	-18(5)
N(1)	1317(10)	2097(4)	859(8)	36(10)	32(9)	52(8)	9(7)	12(7)	17(7)
N(2)	6817(9)	401(3)	-1665(7)	31(7)	37(7)	43(6)	11(6)	9(7)	-8(6)
C(1)	2132(13)	1360(4)	678(11)	42(11)	13(8)	51(9)	16(9)	-8(9)	-6(8)
C(2)	2801(13)	1489(5)	-94(9)	26(10)	54(12)	18(8)	-1(10)	4(9)	-16(8)
C(3)	2851(11)	1956(4)	-462(9)	50(10)	29(9)	54(9)	10(10)	-12(9)	0(8)
C(4)	2441(13)	2260(4)	411(11)	53(13)	20(9)	76(12)	7(8)	17(10)	1(8)
C(5)	1200(11)	1639(4)	1243(9)	62(11)	36(10)	32(9)	5(9)	15(8)	5(8)
C(6)	1444(12)	1637(5)	2413(11)	93(12)	83(12)	58(10)	-23(10)	11(11)	-2(10)
C(7)	-74(11)	1473(4)	1014(11)	42(10)	78(10)	97(12)	17(8)	23(10)	-15(9)
C(8)	3449(12)	2257(5)	1134(12)	77(11)	85(14)	110(15)	-25(10)	-14(12)	-33(11)
C(9)	2209(13)	2727(4)	-45(12)	117(13)	31(9)	150(14)	-11(10)	21(13)	-6(9)
C(10)	4659(11)	1139(4)	-306(8)	35(10)	40(8)	35(8)	15(8)	-7(8)	-10(7)
C(11)	5306(13)	827(4)	-978(10)	46(12)	32(10)	26(10)	13(9)	9(9)	-7(8)
C(12)	4845(11)	633(4)	-1802(12)	45(11)	24(9)	47(12)	5(8)	17(10)	-10(8)

TABLE IV.1

Table 1

continued/

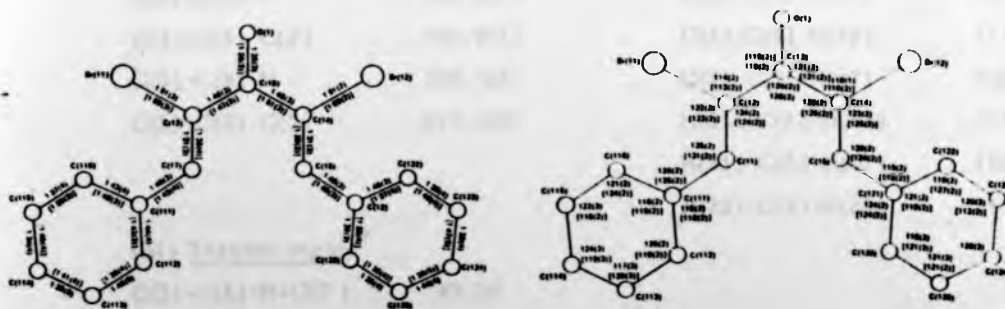
Atom	\bar{X}	\bar{Y}	\bar{Z}	\bar{U}	Atom	\bar{X}	\bar{Y}	\bar{Z}	\bar{U}
C(13)	5762(11)	355(4)	-2342(11)	32(10)	32(9)	35(11)	0(9)	-16(9)	-10(9)
C(14)	6612(13)	700(4)	-804(10)	38(10)	49(10)	46(10)	8(9)	2(9)	-5(8)
C(15)	6036(13)	531(5)	-3424(12)	82(13)	77(13)	55(12)	-4(10)	-10(11)	-1(10)
C(16)	5435(10)	-128(4)	2425(12)	11(9)	64(11)	111(11)	7(9)	-4(9)	-23(12)
C(17)	6817(13)	463(4)	199(10)	89(13)	67(11)	42(9)	26(10)	-15(10)	-4(8)
C(18)	7472(12)	1103(5)	-886(10)	60(12)	53(10)	91(12)	5(9)	-4(10)	-28(10)
Atom	\bar{X}	\bar{Y}	\bar{Z}	\bar{U}	Atom	\bar{X}	\bar{Y}	\bar{Z}	\bar{U}
H(31)	3863(58)	2020(23)	-1073(52)	68(27)	H(151)	6831(133)	456(52)	-3722(105)	84(64)
H(61)	1002(54)	1422(21)	2518(54)	-6(19)	H(152)	6369(80)	784(33)	-3307(69)	46(31)
H(62)	684(76)	1812(27)	2666(66)	64(30)	H(153)	5353(68)	444(23)	-376(55)	5(25)
H(63)	204(64)	1797(19)	2664(48)	6(21)	H(161)	6123(54)	-255(19)	-263(49)	-5(20)
H(71)	-87(65)	1468(23)	312(56)	3(25)	H(162)	4670(64)	-161(21)	-2724(56)	11(24)
H(72)	-607(58)	1649(22)	1396(50)	15(23)	H(163)	5097(57)	-189(20)	-1714(54)	-11(21)
H(73)	68(75)	1126(30)	1225(65)	28(32)	H(171)	6280(111)	-221(41)	356(96)	163(47)
H(81)	4373(84)	2403(31)	933(79)	74(36)	H(172)	6791(81)	680(34)	716(67)	101(33)
H(82)	3381(79)	2474(35)	1611(70)	66(31)	H(173)	7804(95)	378(33)	239(73)	103(38)
H(83)	3599(73)	2124(29)	1498(61)	78(28)	H(181)	8058(76)	964(27)	-839(62)	20(31)
H(91)	1543(101)	2706(34)	-320(93)	108(42)	H(182)	7335(63)	1195(21)	-1611(53)	45(23)
H(92)	3201(156)	2792(50)	-265(123)	215(73)	H(183)	7296(83)	1321(30)	-400(70)	48(34)
H(93)	1846(83)	2888(27)	587(67)	27(31)					
H(121)	3909(87)	587(35)	-2029(76)	114(46)					

TABLE IV.1 (continued)

(c) Z-Z 2,4-Dibromo-1,5-diphenyl-penta-1,4-diene-3-one

	x	y	z	U ₁₁	U ₂₂	U ₃₃	U ₁₂	U ₁₃	U ₂₃
Br(11)	1573 (1)	-1534 (4)	3388 (3)	88 (2)	30 (2)	78 (2)	19 (2)	27 (2)	4 (2)
Br(12)	917 (1)	4886 (5)	5324 (2)	124 (3)	75 (2)	39 (1)	56 (2)	32 (2)	10 (2)
O(1)	1190 (4)	776 (24)	4988 (14)	74 (13)	29 (9)	42 (9)	1 (9)	18 (9)	10 (8)
C(11)	1581 (5)	2553 (34)	2564 (20)	18 (14)	26 (10)	39 (13)	6 (11)	-5 (11)	-15 (11)
C(12)	1449 (6)	1279 (39)	3262 (20)	20 (14)	50 (17)	42 (13)	12 (12)	-12 (11)	10 (13)
C(13)	1223 (6)	1899 (35)	4102 (20)	42 (15)	34 (13)	49 (14)	4 (12)	23 (12)	-32 (13)
C(14)	1024 (5)	3721 (30)	3849 (18)	23 (13)	20 (12)	28 (11)	16 (10)	8 (10)	-10 (10)
C(15)	894 (5)	4363 (32)	2773 (16)	40 (16)	31 (14)	11 (10)	0 (11)	14 (10)	14 (9)
C(111)	1825 (5)	2373 (39)	1725 (21)	4 (13)	53 (15)	51 (14)	12 (12)	1 (11)	-5 (14)
C(112)	2025 (7)	4138 (39)	1561 (21)	40 (18)	64 (16)	37 (14)	-8 (14)	-7 (13)	6 (12)
C(113)	2264 (9)	4079 (59)	701 (30)	65 (28)	113 (29)	60 (20)	4 (21)	14 (20)	-19 (20)
C(114)	2292 (7)	2315 (52)	94 (22)	55 (19)	76 (23)	41 (15)	-7 (17)	-1 (13)	-5 (16)
C(115)	2124 (7)	610 (39)	276 (23)	43 (19)	60 (16)	47 (15)	27 (14)	16 (15)	-6 (13)
C(116)	1894 (6)	575 (43)	1063 (22)	46 (18)	70 (20)	35 (14)	4 (14)	-4 (13)	-10 (14)
C(121)	660 (5)	6054 (33)	2421 (20)	7 (12)	42 (13)	38 (13)	6 (10)	-8 (10)	21 (11)
C(122)	445 (6)	5732 (40)	1282 (23)	43 (16)	56 (17)	53 (16)	10 (14)	18 (13)	25 (14)
C(123)	201 (8)	7149 (44)	922 (28)	45 (22)	53 (19)	67 (21)	5 (15)	23 (17)	15 (16)
C(124)	169 (6)	8876 (46)	1625 (29)	24 (16)	71 (20)	90 (22)	14 (13)	24 (16)	37 (18)
C(125)	395 (7)	9236 (42)	2716 (27)	57 (20)	61 (18)	66 (20)	13 (16)	28 (17)	23 (15)
C(126)	643 (7)	7840 (41)	3096 (21)	84 (24)	37 (17)	49 (14)	4 (15)	22 (14)	-10 (13)
Br(21)	4084 (1)	9898 (5)	4436 (2)	119 (3)	70 (2)	28 (1)	-46 (2)	1 (1)	-6 (2)
Br(22)	3445 (1)	3329 (4)	1931 (3)	96 (3)	35 (2)	69 (2)	-16 (2)	-9 (2)	7 (2)
O(2)	3804 (5)	5763 (24)	3900 (13)	107 (15)	34 (10)	31 (8)	-15 (9)	15 (9)	6 (7)
C(21)	4112 (6)	9277 (44)	1912 (23)	19 (19)	56 (20)	61 (16)	16 (14)	6 (14)	-24 (14)
C(22)	3970 (5)	8677 (34)	2892 (20)	10 (12)	48 (14)	37 (13)	13 (11)	1 (10)	-6 (12)
C(23)	3776 (6)	6793 (36)	2928 (21)	32 (14)	24 (12)	59 (15)	-4 (11)	13 (12)	-15 (13)
C(24)	3542 (6)	6133 (30)	1830 (22)	49 (18)	6 (10)	59 (15)	-9 (10)	26 (14)	-2 (11)
C(25)	3401 (6)	7260 (35)	1013 (20)	60 (20)	35 (12)	24 (12)	11 (12)	-4 (12)	-25 (12)
C(211)	4344 (6)	10955 (31)	1752 (20)	40 (16)	16 (11)	38 (12)	-22 (11)	-9 (12)	-6 (10)
C(212)	4549 (6)	10647 (38)	824 (19)	17 (14)	65 (16)	43 (12)	23 (13)	11 (11)	3 (12)
C(213)	4791 (7)	12076 (42)	697 (22)	39 (19)	68 (19)	46 (16)	-4 (15)	32 (14)	17 (15)
C(214)	4823 (8)	13850 (38)	1428 (23)	89 (25)	42 (16)	37 (16)	9 (14)	-14 (16)	24 (14)
C(215)	4593 (7)	14167 (39)	2339 (24)	53 (19)	35 (16)	75 (18)	-3 (14)	32 (15)	12 (13)
C(216)	4379 (5)	12745 (31)	2455 (18)	2 (12)	29 (13)	37 (12)	-5 (9)	-6 (10)	0 (10)
C(221)	3166 (6)	7070 (39)	-71 (19)	21 (14)	52 (19)	35 (13)	7 (12)	5 (11)	16 (13)
C(222)	2987 (7)	8737 (42)	-531 (27)	31 (19)	61 (19)	90 (22)	13 (14)	10 (17)	21 (16)
C(223)	2753 (7)	8807 (40)	-1569 (27)	50 (18)	56 (18)	80 (20)	10 (14)	-38 (17)	-9 (16)
C(224)	2701 (7)	6778 (62)	-2137 (23)	45 (20)	110 (29)	32 (15)	-16 (22)	-4 (14)	-17 (20)
C(225)	2896 (8)	5114 (44)	-1717 (25)	73 (21)	51 (17)	62 (17)	-44 (17)	-4 (16)	14 (17)
C(226)	3115 (8)	5260 (38)	-663 (28)	49 (22)	36 (15)	60 (22)	-15 (14)	-17 (18)	-2 (16)

Fig. IV.8



(c) Z-Z 2,4-Dibromo-1,5-diphenyl-penta-1,4-diene-3-one

Atomic numbering, bond lengths and angles (in square brackets for the second molecule) with standard deviations in parentheses. For the second molecule, the initial digit in each atom's number is (2) instead of (1).

Bond distances (\AA), bond and torsion angles ($^\circ$) with standard deviations in parentheses.

(a) 3, 5-dibromo-4-oxo-2, 2, 6, 6-tetramethylpiperidin-1-yloxy

(I) Distances

Br(1)-C(2)	1.941(3)	C(2)-H(2)	1.02(3)
N-O(1)	1.278(5)	C(4)-H(41)	0.97(5)
N-C(3)	1.510(4)	C(4)-H(42)	1.01(5)
O(2)-C(1)	1.195(7)	C(4)-H(43)	1.03(5)
C(1)-C(2)	1.518(5)	C(5)-H(51)	0.87(5)
C(2)-C(3)	1.548(5)	C(5)-H(52)	0.92(4)
C(3)-C(4)	1.529(5)	C(5)-H(53)	0.98(4)
C(3)-C(5)	1.522(5)		

(II) Angles

Br(1)-C(2)-C(1)	110.8(3)	Br(1)-C(2)-H(2)	106.2(18)
Br(1)-C(2)-C(3)	111.6(2)	C(1)-C(2)-H(2)	109.3(18)
O(1)-N-C(3)	115.0(2)	C(3)-C(2)-H(2)	107.1(19)
C(3)-N-C(3')	125.1(3)	C(3)-C(4)-H(41)	106.1(27)
O(2)-C(1)-C(2)	125.8(2)	C(3)-C(4)-H(42)	112.2(26)
C(2)-C(1)-C(2')	108.2(4)	C(3)-C(4)-H(43)	114.2(24)
C(1)-C(2)-C(3)	111.5(3)	H(41)-C(4)-H(42)	110.3(36)
C(2)-C(3)-N	106.6(3)	H(41)-C(4)-H(43)	105.6(35)
C(4)-C(3)-C(5)	111.0(3)	H(42)-C(4)-H(43)	108.2(35)
C(4)-C(3)-N	106.8(3)	C(3)-C(5)-H(51)	109.9(28)
C(4)-C(3)-C(2)	109.9(3)	C(3)-C(5)-H(52)	111.5(27)
C(5)-C(3)-N	109.1(3)	C(3)-C(5)-H(53)	106.3(22)
C(5)-C(3)-C(2)	113.1(3)	H(51)-C(5)-H(52)	107.6(39)
		H(51)-C(5)-H(53)	110.0(36)
		H(52)-C(5)-H(53)	111.5(35)

(III) Torsion angles[†]

C(2)-C(3)-N-C(3')	42.58
C(1)-C(2)-C(3)-N	-50.53
C(3)-C(2)-C(1)-C(2')	65.51

[†] Primed numbers refer to the atom related by the mirror plane.

TABLE IV. 2 (continued)

b. The Ester [2] Derived From [1].

(i) Distances Ring 1		Ring 2	
Br(1)-C(1)	1.916(11)	N(2)-O(2)	1.252(13)
Br(2)-C(2)	1.988(12)	N(2)-C(13)	1.468(16)
N(1)-O(1)	1.286(15)	N(2)-C(14)	1.461(16)
N(1)-C(4)	1.462(18)	C(11)-C(12)	1.325(20)
N(1)-C(5)	1.489(17)	C(11)-C(14)	1.517(20)
C(1)-C(2)	1.306(19)	C(12)-C(13)	1.496(19)
C(1)-C(5)	1.525(18)	C(13)-C(15)	1.533(21)
C(2)-C(3)	1.502(20)	C(13)-C(16)	1.519(18)
C(3)-C(4)	1.532(18)	C(14)-C(17)	1.505(18)
C(4)-C(8)	1.461(20)	C(14)-C(18)	1.560(19)
C(4)-C(9)	1.562(17)	<u>Ester linkage</u>	
C(5)-C(6)	1.541(18)	C(2)-O(4)	1.403(16)
C(5)-C(7)	1.529(18)	C(10)-O(3)	1.188(14)
		C(10)-O(4)	1.356(14)
		C(10)-C(11)	1.476(18)
<u>Hydrogen atoms</u>			
C(3)-H(31)	1.39(6)	C(15)-H(151)	0.99(15)
C(6)-H(61)	0.83(6)	C(15)-H(152)	0.87(10)
C(6)-H(62)	1.05(8)	C(15)-H(153)	0.92(8)
C(6)-H(63)	0.89(7)	C(16)-H(161)	0.90(6)
C(7)-H(71)	0.91(7)	C(16)-H(162)	0.94(7)
C(7)-H(72)	0.94(7)	C(16)-H(163)	1.01(7)
C(7)-H(73)	1.10(9)	C(17)-H(171)	0.97(12)
C(8)-H(81)	1.11(10)	C(17)-H(172)	0.94(10)
C(8)-H(82)	0.84(10)	C(17)-H(173)	1.13(11)
C(8)-H(83)	0.71(8)	C(18)-H(181)	0.78(9)
C(9)-H(91)	0.82(11)	C(18)-H(182)	0.99(7)
C(9)-H(92)	1.15(17)	C(18)-H(183)	0.94(9)
C(9)-H(93)	1.04(9)		
C(12)-H(121)	1.08(9)		

/continued

TABLE IV. 2 (continued)

continued/

Table 2 - (3)

(ii) AnglesRing 1

Br(1)-C(1)-C(2)	120.0(10)
Br(1)-C(1)-C(5)	114.0(9)
Br(2)-C(3)-C(2)	104.0(9)
Br(2)-C(3)-C(4)	112.5(9)
O(1)-N(1)-C(4)	120.5(11)
O(1)-N(1)-C(5)	115.3(10)
C(4)-N(1)-C(5)	121.7(10)
C(5)-C(1)-C(2)	125.9(11)
C(1)-C(2)-C(3)	123.3(12)
C(2)-C(3)-C(4)	109.1(10)
C(3)-C(4)-N(1)	109.9(10)
C(1)-C(5)-N(1)	107.6(10)
C(8)-C(4)-C(9)	108.6(11)
C(6)-C(5)-C(7)	110.6(10)
C(6)-C(5)-N(1)	108.5(10)
C(6)-C(5)-C(1)	110.6(11)
C(7)-C(5)-N(1)	109.0(10)
C(7)-C(5)-C(1)	110.4(10)
C(8)-C(4)-N(1)	114.6(12)
C(8)-C(4)-C(3)	106.3(11)
C(9)-C(4)-N(1)	108.6(11)
C(9)-C(4)-C(3)	108.6(11)

Ring 2

O(2)-N(2)-C(13)	124.3(10)
O(2)-N(2)-C(14)	122.6(10)
C(13)-N(2)-C(14)	113.1(10)
C(12)-C(11)-C(14)	112.0(12)
C(11)-C(12)-C(13)	111.6(12)
C(12)-C(13)-N(2)	102.0(11)
C(11)-C(14)-N(2)	101.2(10)
C(15)-C(13)-C(16)	108.7(12)
C(17)-C(14)-C(18)	110.2(11)
C(15)-C(13)-N(2)	110.8(10)
C(15)-C(13)-C(12)	111.5(11)
C(16)-C(13)-N(2)	108.9(10)
C(16)-C(13)-C(12)	114.8(11)
C(17)-C(14)-N(2)	109.8(11)
C(17)-C(14)-C(11)	113.3(11)
C(18)-C(14)-N(2)	110.2(10)
C(18)-C(14)-C(11)	111.8(11)

Water linkage

O(3)-C(10)-O(4)	124.1(11)
O(3)-C(10)-C(11)	126.1(12)
O(4)-C(10)-C(11)	109.7(10)
O(2)-O(4)-C(10)	115.7(9)
C(1)-C(2)-O(4)	120.3(12)
C(3)-C(2)-O(4)	116.3(10)
C(10)-C(11)-C(12)	125.2(13)
C(10)-C(11)-C(14)	122.8(11)

TABLE IV. 2 (continued)

Methyl groups

H(61)-C(6)-H(62)	83(6)	H(151)-C(15)-H(152)	84(11)
H(61)-C(6)-H(63)	145(6)	H(151)-C(15)-H(153)	118(10)
H(62)-C(6)-H(63)	102(6)	H(152)-C(15)-H(153)	134(8)
H(71)-C(7)-H(72)	122(6)	H(161)-C(16)-H(162)	127(6)
H(71)-C(7)-H(73)	104(6)	H(161)-C(16)-H(163)	120(6)
H(72)-C(7)-H(73)	120(6)	H(162)-C(16)-H(163)	91(6)
H(81)-C(8)-H(82)	92(8)	H(171)-C(17)-H(172)	112(9)
H(81)-C(8)-H(83)	99(8)	H(171)-C(17)-H(173)	114(9)
H(82)-C(8)-H(83)	90(10)	H(172)-C(17)-H(173)	99(7)
H(91)-C(9)-H(92)	140(12)	H(181)-C(18)-H(182)	111(7)
H(91)-C(9)-H(93)	92(10)	H(181)-C(18)-H(183)	121(8)
H(92)-C(9)-H(93)	104(7)	H(182)-C(18)-H(183)	114(7)
H(121)-C(12)-C(11)	130(5)	Br(2)-C(3)-H(31)	93(3)
H(121)-C(12)-C(13)	117(6)	C(2)-C(3)-H(31)	110(3)
		C(4)-C(3)-H(31)	125(3)

(III) Torsion anglesRing 1

C(5)-C(1)-C(2)-C(3)	+7.60
C(1)-C(2)-C(3)-C(4)	+21.92
C(2)-C(3)-C(4)-N(1)	-48.33
C(3)-C(4)-N(1)-C(5)	+53.73
C(4)-N(1)-C(5)-C(1)	-24.38
N(1)-C(5)-C(1)-C(2)	-7.99

Ring 2

C(14)-C(11)-C(12)-C(13)	+1.88
C(11)-C(12)-C(13)-N(2)	-2.89
C(12)-C(13)-N(2)-C(14)	+2.93
C(13)-N(2)-C(14)-C(11)	-1.93
N(2)-C(14)-C(11)-C(12)	0.0

* As defined by R. Bucourt, "Topics in Stereochemistry", Vol.8, p.159, Interscience-Wiley

TABLE IV 3

Least squares planes for (2)

Equations of the least-squares mean planes are given as $PI + QJ + RK = S^\dagger$ in orthogonal space. Deviations of certain atoms from these planes are shown and atoms defining the plane are marked with an asterisk.

<u>Plane 1</u>	P	Q	R	S
	0.7153	0.1862	0.6736	2.9757

Atom. deviation (Å)

Br(1)	0.167		C(3)*	-0.009
Br(2)	-1.935		C(4)	0.602
O(1)	-0.192		C(5)*	-0.009
O(4)	-0.080		C(6)	1.206
N(1)*	0.009		C(7)	-1.313
C(1)	0.079		C(8)	2.049
C(2)*	0.008		C(9)	0.284

<u>Plane 2</u>	P	Q	R	S
	0.2974	0.7482	-0.5931	4.3751

Atom. deviation (Å)

O(3)*	-0.003		C(10)*	-0.005
O(4)*	-0.022		C(11)*	0.013
C(2)*	0.017		C(12)	0.052
N(2)	0.068		C(13)	0.136
O(2)	0.063		C(14)	0.020

<u>Plane 3</u>	P	Q	R	S
	0.2947	0.7690	-0.5673	4.3917

Atom. deviation (Å)

O(2)	-0.025		C(14)*	0.000
N(2)*	0.000		C(15)	1.344
C(11)*	0.000		C(16)	-1.131
C(12)*	0.000		C(17)	-1.226
C(13)	0.046		C(18)	1.287

Angles between planes:- (1)-(2) 87.28° (1)-(3) 88.38° (2)-(3) 1.90°

TABLE IV.3

Least squares planes for (3). Deviations of atoms forming these planes are insignificant and are not shown.

Plane No.	Defining atoms	P	Q	R	S
1.	Br(11), C(11), C(12), C(13)	.6583	.2039	.7246	6.4071
2.	Br(12), C(13), C(14), C(15)	.8072	.5902	.0019	4.3591
3.	Br(21), C(21), C(22), C(23)	.7768	-.5879	.2257	13.6357
4.	Br(22), C(23), C(24), C(25)	.8316	-.1868	-.5230	11.2415
5.	C(12), C(13), C(14), O(1)	.6604	.5265	.5354	5.9584
6.	C(22), C(23), C(24), O(2)	.7835	-.5312	-.3223	11.8726
7.	C(111) - C(116)	.6055	-.2893	.7414	5.3629
8.	C(121) - C(126)	.7137	.4736	-.5161	2.1855
9.	C(211) - C(216)	.5654	-.4721	.6764	10.9384
10.	C(221) - C(226)	.7973	.2218	-.5614	10.0034

(b)

Angles ($^{\circ}$) between planes or lines

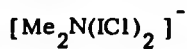
(1) - (2)	48.7	(3) - (4)	50.4
(1) - (5)	21.6	(3) - (6)	32.0
(1) - (7)	28.7	(3) - (9)	29.6
(2) - (5)	31.8	(4) - (6)	23.2
(2) - (8)	31.8	(4) - (10)	23.8

[†] With the orthogonal unit vector I parallel to a, K perpendicular to a in the ac plane and J perpendicular to the ac plane.

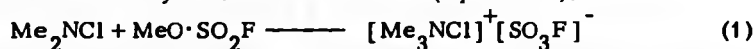
2. O.W. Griffith and A.S. Waggoner, Accounts Chem. Res., 1969, 2, 17.
W. Snipes and A. Keith, Research Development, Feb. 1970.
3. B.T. Golding, P.V. Ioannou and M.M. O'Brien, Synthesis, 1975, 462.
4. Details of the preparative routes, identification and chemistry of (1), (2) and related compounds, along with crystallographic details of (1) and (2) are contained in the paper by N.W. Alcock, B.T. Golding, P.V. Ioannou and J.F. Sawyer, submitted for publication in Tetrahedron, 1977.
5. C. Sandris and G. Ourisson, Bull. Soc. Chim. France, 1958, 1524;
J-F. Biellmann, R. Hanna, G. Ourisson, C. Sandris and B. Waegell, Bull. Soc. Chim. France, 1960, 1429.
6. L.C.G. Goaman and D.F. Grant, Acta Cryst., 1964, 17, 1604.
7. A. Baretta, J.P. Zahra, B. Waegell and C.W. Jefford, Tetrahedron, 1970, 26, 15.
8. B. Waegell and G. Ourisson, Bull. Soc. Chim. France, 1963, 503.
9. A. Caplomont, B. Chlon and J. Lajzerowicz, Acta Cryst., 1971, B27, 322.
10. Chem. Soc. Special Publ., No. 11, London (1958), Ed. L.E. Sutton.
11. C.W. Shoppee and B.J.A. Cooke, J. Chem. Soc. Perkin I, 1973, 2197.
12. N.W. Alcock, N. Herron, T.J. Kemp and C.W. Shoppee, J. Chem. Soc. Chem. Comm., 1975, 785.
13. J. Lajzerowicz, Chap. 6 in "Spin Labelling: Theory and Applications", ed. L.J. Berliner (Academic Press, London, 1976).
14. G.R. Underwood and V.L. Vogel, Mol. Phys., 1970, 19, 621.
15. A.W. Salotto and L. Burnelle, J. Chem. Phys., 1970, 53, 333.
16. See H. Sternglanz, J.M. Thomas and C.E. Bugg, Acta Cryst., 1977, B33, 2097; H. Sternglanz, G.R. Freeman and C.E. Bugg, Acta Cryst., 1975, B31, 1393 and refs. therein, especially C.E. Bugg, J.M. Thomas, M. Sundaralingam and S.T. Rao, Biopolymers, 1971, 10, 175.
17. M. Breton-Lacombe, Acta Cryst., 1967, 23, 1031.
18. D.N. Peck, W.L. Duax, C. Eger and D.A. Norton, Amer. Cryst. Assoc. Abstracts, Summer, 1970, 71 (L6); D.N. Peck, D.A. Langa, C. Eger and W.L. Duax, Cryst. Str. Comm., 1974, 3, 451, 573.

19. H-S. Shieh and D. Voet, Acta Cryst., 1976, B32, 2354.
20. K. Ollc and F.C. Mijlhoff, Acta Cryst., 1969, B25, 974; (see also L.K. Templeton and D.H. Templeton, ibid., 1971, B27, 1678 for an alternative refinement); P. Groth and O. Hassel, Acta Chem. Scand., 1962, 16, 2311.
21. R.C. Gehrz and D. Britton, Acta Cryst., 1972, B28, 1126 and previous 3 papers.
22. S.C. Kokkon and P.J. Rentzeperis, Acta Cryst., 1975, B31, 1564.
23. J.L. Attwood and W.A. Sheppard, Acta Cryst., 1975, B31, 2638.
24. J. Silverman, A.P. Krukons and N.F. Yannoni, Acta Cryst., 1973, B29, 2022.
25. D.M. Thompson and M.F. Richardson, Acta Cryst., 1977, B33, 324.
26. B. Chlon, J. Lajzėrowicz, A. Collet and J. Jacques, Acta Cryst., 1976, B32, 339.
27. B. Chlon and J. Lajzėrowicz, ibid., 1975, B31, 1430.
28. B. Chlon and M. Thomas, ibid., 1975, B31, 472.
29. D. Bordeaux and J. Lajzėrowicz, ibid., 1977, B33, 1837.
30. P. Murray-Rust, ibid., 1974, B30, 1368.
31. R.P. Shibaeva, R.M. Lobkovskaya and L.P. Rosenberg, Zh. Strukt. Khim., 1976, 17, 876. (C.A. 86:121125).
32. S.D. Mamedov, A.D. Khalilov and M.K. Guseinova, ibid., 1974, 15, 103. (C.A. 81:7173).
33. D. Bordeaux, A. Caplomont, J. Lajzėrowicz, M. Jouve and M. Thomas, Acta Cryst., 1974, B30, 2156 and following paper.
34. A.W. Hansen, ibid., 1953, 6, 32.
35. B. Anderson and P. Anderson, Acta Chem. Scand., 1966, 20, 2728; C. Gildewell, D.W.H. Rankin, A.G. Roblette, G.M. Sheldrick and S. Williamson, J. Chem. Soc. (A), 1971, 478.
36. R.A. Howle, L.S.D. Glaser and W. Moser, J. Chem. Soc. (A), 1968, 3043 and refs. therein.
37. A.R. Forrester, S.P. Hepburn, R.S. Dunlop and H.H. Mills, J. Chem. Soc. Chem. Comm., 1969, 698.
38. A. Kitaigorodskii, 'Molecular Crystals and Molecules', Academic Press, 1973.

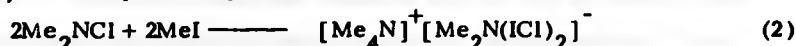
CHAPTER V

The X-ray Structure of a novel pseudo-polyhalide AnionV.1. Introduction

During studies on the halogen-substituted ammonium cations, the reactions of dimethyl chloramine with a series of potential alkylating agents were investigated by workers at the University of Durham. They found that powerful alkylating agents such as methyl fluorosulphate gave salts of the colourless trimethylchloroammonium ion (equation 1).



In contrast to this, when dimethylchloramine was dissolved in an excess of iodomethane at room temperature, a fine yellow solid slowly precipitated. The elemental analysis showed this compound to have the empirical formula $\text{C}_3\text{H}_9\text{ClIN}$ and the product was formed quantitatively on the dimethylchloramine taken, with respect to equation (2).¹



The compound represented an isomer of the known adduct of trimethylamine with iodine monochloride² but the i.r. spectrum clearly showed that the compound was of a different structure.¹ Clear demonstration that the compound $\text{C}_3\text{H}_9\text{ClIN}$ was in fact the ionic compound $[\text{Me}_4\text{N}]^+ [\text{Me}_2\text{N}(\text{ICl})_2]^-$ as indicated in equation (2) only came with the results of a low temperature X-ray analysis at -60°C . Details of this analysis will be described in this chapter. The bonding in the novel pseudo polyhalide anion $[\text{Me}_2\text{N}(\text{ICl})_2]^-$ will be compared to other polyhalides and to other iodine monochloride adducts which have been described as charge transfer adducts but could be regarded equally well as examples of linear secondary bonds.

V.2. Experimental

Crystals of the compound $\text{C}_3\text{H}_9\text{ClIN}$ were obtained by its slow preparation in tetrahydrofuran at 243 K (-30°C) over a number of months.¹ Crystals are pale yellow chunky plates or rhombs, generally with poorly defined faces.

The crystals decompose in a few hours at 20° C but can be stored indefinitely at lower temperatures. Due to this fact, crystal selection, examination under polarised light and mounting has to be performed in a minimal time and the mounted crystal rapidly transferred to the diffractometer where, with the use of the Syntex LT-1 attachment, the crystal can be cooled to the required temperature. All photographic examination and data collections were performed at -60° C. Several crystals were investigated and although on some crystals the reflections appear to centre well, the autoindexing results indicate twinning.³ Eventually a block-shaped crystal was found with a monoclinic cell 11.237 x 5.762 x 23.347 Å with a β of 110.20(3)° and a data collection was started using this crystal. It soon became clear that the chosen cell might be B-centred; there were a significant number of exceptions to this absence, although some of these could be rejected because of their faulty backgrounds.[†] The structure was, however, solved with this data set, but refinement did not proceed below an R-factor of \approx 15%. Taking the large number of observed systematic absences and the high R-factor it was decided to try and improve the data set using another crystal. The following crystal data and experimental conditions refer to this second data collection.

The crystal for the second data collection was again rapidly selected from a second sample of the compound, mounted using a large amount of hardener in the Araldite glue and was being cooled to -60° C on the diffractometer within ca. 30 min. The reflections from this crystal centre well and $2\theta/\omega$ and ω scans of several reflections give no indication of any twinning, although one reflection in the low angle centering did have an h index of 0.95.³ Using 15 high angle ($29 < 2\theta < 35^\circ$) reflections, a monoclinic B-centred cell 11.233(3) x 5.773(1) x 23.376(5) Å with a β angle of 110.15(2)° and volume of 1423.2(5) Å³ was calculated, and the data was collected using an orientation matrix based on this cell. The following crystal data, however, contains the reduced primitive cell based on the angular co-ordinates of the high angle reflections but with transformed hkl indices for each reflection

[†] Preliminary work and initial data set collected by Dr. S. Esperas.

given by

$$h' = h, k' = -k \text{ and } l' = -h/2 - l/2 \quad (3)$$

Crystal data:

$C_6H_{18}Cl_2I_2N_2$, $M = 442.92$, monoclinic, $a = 11.233(3)$, $b = 5.7734(10)$, $c = 11.087(2)$ Å, $\beta = 98.24(2)^\circ$, $V = 711.6(3)$ Å³ at -60° C, $D_c = 2.067$ g/cm³ for $Z = 4$, $D_m = 2.08$ g/cm³. Mo K_α radiation, $\lambda = 0.71069$ Å, $\mu(\text{Mo } K_\alpha) = 48.07$ cm⁻¹. Space group $P2$ or $P2/c$ (see below).

Data were collected out to a maximum 2θ of 60° in several shells, using the B-centred cell referred to above.⁵ Reflections were measured using θ - 2θ scans over a scan range ($K_{\alpha 1} - 0.85$) to ($K_{\alpha 2} + 0.85$) and variable scan rate of $1.2 - 29.3^\circ/\text{min}$ depending on the intensity of a preliminary 2 sec count. Background counts were recorded at each end of the scan, each for one quarter of the scan time. The intensities of 3 standard reflections collected every 100 reflections showed a gradual loss of intensity, and collected data were rescaled according to the equation $F = F_0(1 + 0.0006655t)$, t = time in hours. The maximum rescale factor was 1.0626.

Of 2363 collected data (excluding standards and 299 systematically absent reflections due to the B-centering), 1855 were considered observed ($I/\sigma(I) > 3.0$). Lorentz and polarisation factors were applied, and all data were transformed into the primitive cell using the transformation equations (3) above. Absorption corrections were applied at a later stage in the refinement using the program ABSCOR. The crystal was described using measured dplane parameters for this calculation, since the use of hkl indices for the crystal faces gives a much inferior description of the crystal.

V.3. Structure Solution and Refinement; Crystal Twinning

The structure of the compound was initially solved by applying Patterson methods to the first data set collected. Using the B-centred cell, the space groups assumed in the analysis were in fact the primitive monoclinic space groups Pm , $P2$, $P2/m$. The absence on any large peaks on the Harker plane $V = \frac{1}{2}$ ruled out $P2/m$. However, there were several large peaks on $V = 0$ and $V = \frac{1}{2}$ consistent with 8 iodine atoms in $P2$, such that their y co-ordinates are 0 and $\frac{1}{2}$ with their x and z co-ordinates related by $x' = x + \frac{1}{2}$, $z' = z + \frac{1}{2}$, to give the assumed pseudo-B-centred absence.

In fact, from the Harker peaks ($2x$, 0 , $2z$) and those on $V = \frac{1}{4}$, a feasible set of iodine positions appeared to be given by

$$\begin{array}{l} x, 0, Z \\ \frac{1}{2} + x, 0, \frac{1}{2} + Z \\ \frac{1}{4} + x, \frac{1}{4}, \frac{1}{4} + Z \\ \frac{3}{4} + x, \frac{1}{4}, \frac{3}{4} + Z \end{array} \quad \text{with } x \approx 0.07 \text{ and } Z \approx 0.443.$$

Using these positions an R of 0.274 was obtained, and in subsequent Fouriers the missing Cl, C and N atoms were located, enabling the compound to be formulated as $[\text{NMe}_4]^+ [\text{Me}_2\text{N}(\text{ICl})_2]^-$. However, refinement with the original data set was not possible below $R = 0.15$ and the bond distances and angles and some atomic temperature factors were unacceptable.

The second data set, transformed, along with the previous iodine co-ordinates, into the correct primitive cell eventually gave after several refinement cycles an R factor of 6.7% with the iodine and chlorine atoms anisotropic. However, even with this low R -factor there were several unsuitable features of the present model. Notably, the temperature factors of the chemically similar atoms N(1) and N(2) had $U = 0.014$ and $U = 0.0988$ respectively, the bond lengths and angles between the independent ions were markedly dissimilar and the agreements for certain reflection classes ($h0l$ and $00l$) were very poor.⁶ In fact, by a suitable origin shift, the co-ordinates of the present solution could be transformed into $P2_1/c$ so that independent ions become equivalent. When this possibility was tested, the R -factor improved slightly but more importantly the refinement resulting in chemically more reasonable bond distances and angles. Space group $P2_1/c$ requires the systematic absence $h0l$, $l \neq 2n$ to which there are a significant number of exceptions. However, inspection shows that the groups of reflections $h0l$, $l0h$, $h0\bar{l}$ and $\bar{l}0h$ contains particular inter-relationships very indicative of crystal twinning such that $a' = c$ with b reversed. The effects of this form of twinning are shown in Fig. V.1 where the $h0l$ lattice points associated with each orientation of the twin are shown very nearly superimposed. From an inspection of $h0l$ and the equivalent $\bar{l}0h$ reflection, a twinning factor of ca. 0.4 is observed for several sets of reflections, although the inconsistencies between equivalent pairs of

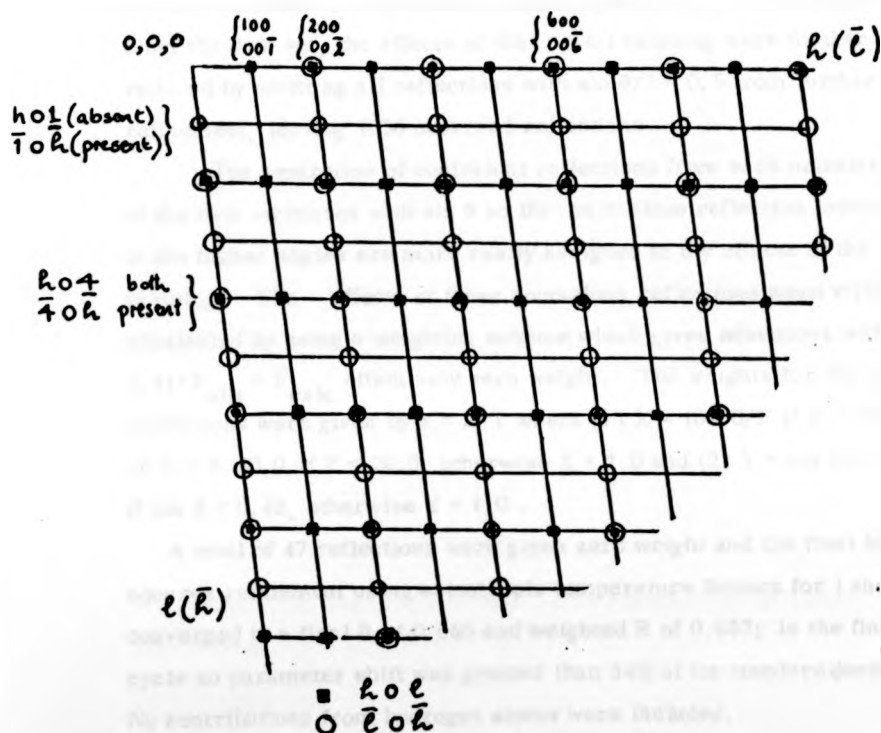


Figure V.1 Diagram showing the twinning of the hOl reciprocal lattice layers in $[\text{Me}_4\text{N}]^+[\text{Me}_2\text{N}(\text{ICI})_2]^-$. Some typical indices of reflections for the two components ($\blacksquare \equiv hOl$; $\circ \equiv hOl$) are shown. The twinning ($h' \equiv \bar{h}$, $l' \equiv \bar{l}$, $k' \equiv k$) is perfect as regards angle, but the difference in axial lengths leads to resolution between each pair of lattice points (not shown here) at high angles.

reflections prevented an accurate correction of the twinning effects.⁷

Therefore, it seems certain that space group $P2_1/c$ is correct, since it gives better bond distances and angles and that the missing $h0l$ absence is due to crystal twinning although no clear signs of twinning were seen in the data collection. Apart from removing all $h0l$, $l \neq 2n$ reflections from the data set, the effects of the crystal twinning were further reduced by omitting all reflections with $\sin \theta / \lambda < 0.5$ from further refinement, leaving 1056 observed reflections.

The separation of equivalent reflections from each orientation of the twin increases with $\sin \theta$ so that anomalous reflection intensities at the higher angles are more easily assigned to the effects of the twinning. The effects of these anomalous reflections were virtually eliminated by using a weighting scheme which gives reflections with $0.41 \cdot F_{\text{obs}} \geq F_{\text{calc}}$ effectively zero weight. The weights for the other reflections were given by $w = X \cdot Y$ where (1) $X = 100.0/F$ if $F > 100.0$, or $X = F/20.0$ if $F < 20.0$, otherwise $X = 1.0$ and (2) $Y = \sin \theta / 0.42$ if $\sin \theta < 0.42$, otherwise $Y = 1.0$.

A total of 47 reflections were given zero weight and the final least squares refinement using anisotropic temperature factors for I and Cl converged to a final R of 0.066 and weighted R of 0.057; in the final cycle no parameter shift was greater than 34% of its standard deviation. No contributions from hydrogen atoms were included.

Final positional parameters and temperature factors for all atoms are listed in Table V.1, bond lengths and angles in Table V.2. Table V.3 contains some equivalent $h0l$ and $l0h$ reflections indicating the twinning factors. The novel $[\text{Me}_2\text{N}(\text{ICl})_2]^-$ anion is shown in Fig. V.2 and the molecular packing in Fig. V.3. Final structure factors are listed in Appendix V.

V.4. Discussion

The crystal structure analysis of the compound with empirical formula $\text{C}_3\text{H}_9\text{ClIN}$ has shown that it consists of the ions $[\text{NMe}_4]^+$ and $[\text{Me}_2\text{N}(\text{ICl})_2]^-$, each with crystallographic two-fold symmetry

TABLE V.1.

Atomic co-ordinates and temperature factors for $[\text{Me}_4\text{N}]^+[\text{Me}_2\text{N}(\text{ICl})_2]^-$
with standard deviations in parentheses

Atom	X	Y	Z	U		
I(1)	0.36985(5)	0.11952(9)	0.13486(5)	**		
Cl(1)	0.2062(3)	-0.1522(5)	0.0057(3)	**		
N(1)	0.5000	0.3452(19)	0.2500	0.043(2)		
N(2)	0.0000	-0.4644(19)	0.2500	0.040(2)		
C(1)	0.5657(10)	0.4928(18)	0.1718(9)	0.049(2)		
C(2)	-0.0737(9)	-0.6114(21)	0.3191(9)	0.052(2)		
C(3)	-0.0807(11)	-0.3127(20)	0.1656(11)	0.054(2)		
**	U ₁₁	U ₂₂	U ₃₃	U ₁₂	U ₁₃	U ₂₃
I(1)	0.0405(4)	0.0348(4)	0.0411(4)	0.0042(2)	0.0020(1)	0.0015(2)
Cl(1)	0.0628(12)	0.0548(12)	0.0571(11)	-0.0131(10)	-0.0089(9)	-0.0007(9)

TABLE V.2.

Bond lengths (Å) and bond angles (°) with standard deviations in parentheses

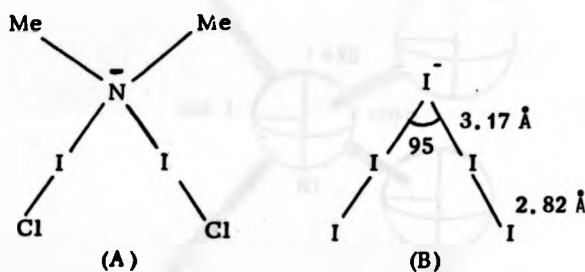
Bond lengths (Å)			
I(1) - Cl(1)	2.672(3)	N(2) - C(2)	1.475(13)
I(1) - N(1)	2.220(7)	N(2) - C(3)	1.491(13)
N(1) - C(1)	1.486(13)		
Bond angles (°)			
N(1)-I(1)-Cl(1)	177.02(7)	C(2)-N(2)-C(2')	109.7(9)
I(1)-N(1)-I(1')	108.1(5)	C(2)-N(2)-C(3)	110.4(6)
I(1)-N(1)-C(1)	110.0(4)	C(2)-N(2)-C(3')	109.1(6)
C(1)-N(1)-C(1')	110.0(9)	C(3)-N(2)-C(3')	108.0(9)
C(1)-N(1)-I(1')	109.3(4)		

TABLE V.3

Twinning Factors for some equivalent hOl and $\bar{1}O\bar{h}$ Reflections

hOl	F_1	$\bar{1}O\bar{h}$	F_2	F_1/F_2	hOl	F_1	$\bar{1}O\bar{h}$	F_2	F_1/F_2
20 $\bar{7}$	26	70 $\bar{2}$	56	.47	80 $\bar{5}$	9	50 $\bar{8}$	20	.42
20 $\bar{5}$	33	50 $\bar{2}$	78	.42	80 $\bar{3}$	22	30 $\bar{8}$	60	.36
20 $\bar{3}$	15	30 $\bar{2}$	34	.43	80 $\bar{1}$	5	10 $\bar{8}$	15	.31
20 $\bar{1}$	58	10 $\bar{2}$	139	.42	100 $\bar{9}$	13	90 $\bar{10}$	32	.41
40 $\bar{7}$	28	70 $\bar{4}$	70	.40	100 $\bar{5}$	15	50 $\bar{10}$	42	.37
40 $\bar{5}$	16	50 $\bar{4}$	14	.92	100 $\bar{1}$	8	10 $\bar{10}$	65	.12
40 $\bar{3}$	58	30 $\bar{4}$	142	.41	120 $\bar{11}$	7	110 $\bar{12}$	13	.53
40 $\bar{1}$	30	10 $\bar{4}$	87	.35	120 $\bar{7}$	10	70 $\bar{12}$	25	.40
60 $\bar{9}$	20	90 $\bar{6}$	53	.38	120 $\bar{3}$	8	30 $\bar{12}$	41	.20
60 $\bar{5}$	43	50 $\bar{6}$	105	.41	20 $\bar{5}$	39	50 $\bar{2}$	131	.30
60 $\bar{3}$	20	30 $\bar{6}$	50	.40	40 $\bar{1}$	6	10 $\bar{4}$	117	.05
60 $\bar{1}$	18	10 $\bar{6}$	85	.21	20 $\bar{9}$	5	90 $\bar{2}$	49	.10
80 $\bar{11}$	10	110 $\bar{8}$	31	.33	20 $\bar{7}$	14	70 $\bar{2}$	41	.34
80 $\bar{7}$	26	70 $\bar{8}$	64	.41	60 $\bar{1}$	4	10 $\bar{6}$	52	.07

(Fig. V.2). The only possible analogues to the extremely novel anion are the polyhalide anions, in particular $[I_5]^-$ which exists as a nearly planar V-shaped ion.⁸ This latter ion can be regarded as I^- interacting with two iodine molecules with the distances shown in (B). This seems to be a dominant feature in iodine polyatomic anions.⁸ In parallel with this, the present anion can be regarded as having the structure (A) with $[Me_2N]^-$ considered as a new pseudohalide. It is perhaps surprising to regard $[Me_2N]^-$ as acting as a pseudohalide in its interactions with iodine monochloride, although conventional pseudohalides have been found to form pseudopolyhalide anion analogues, for example in $(NCS \cdot I_2)^-$.⁹



In the anion, the N-I and I-Cl distances are 2.220(7) and 2.672(3) Å respectively, and the N-I-Cl system is very nearly linear $[N-I-Cl \text{ is } 177.02(7)^\circ]$. The N-C(Me) distance is 1.486(13) Å compared to N-C distances of 1.475(13) and 1.491(13) Å in the cation. In anion and cation the angles about nitrogen have values close to the tetrahedral value (Table V.2).

The I-Cl bond length in the anion is considerably longer than that in gaseous ICl (2.321 Å)¹⁰ or that found in the two polymorphic forms (α and β) of ICl in the solid state (2.44 and 2.37 (α); 2.440 and 2.351 Å (β)). The differences in these last two values are directly attributable to the different crystal packing arrangements resulting in slightly different inter-molecular contacts. Iodine monochloride has also been characterised in several charge transfer adducts with a variety of bases. The ICl distances in the adducts with pyridine,¹² 2-chloroquinoline¹³ and trimethylamine² are 2.510, 2.446 and 2.52 Å respectively. The I-Cl distance in the ICl adduct with 1-oxa-4-selenacyclohexane is even longer

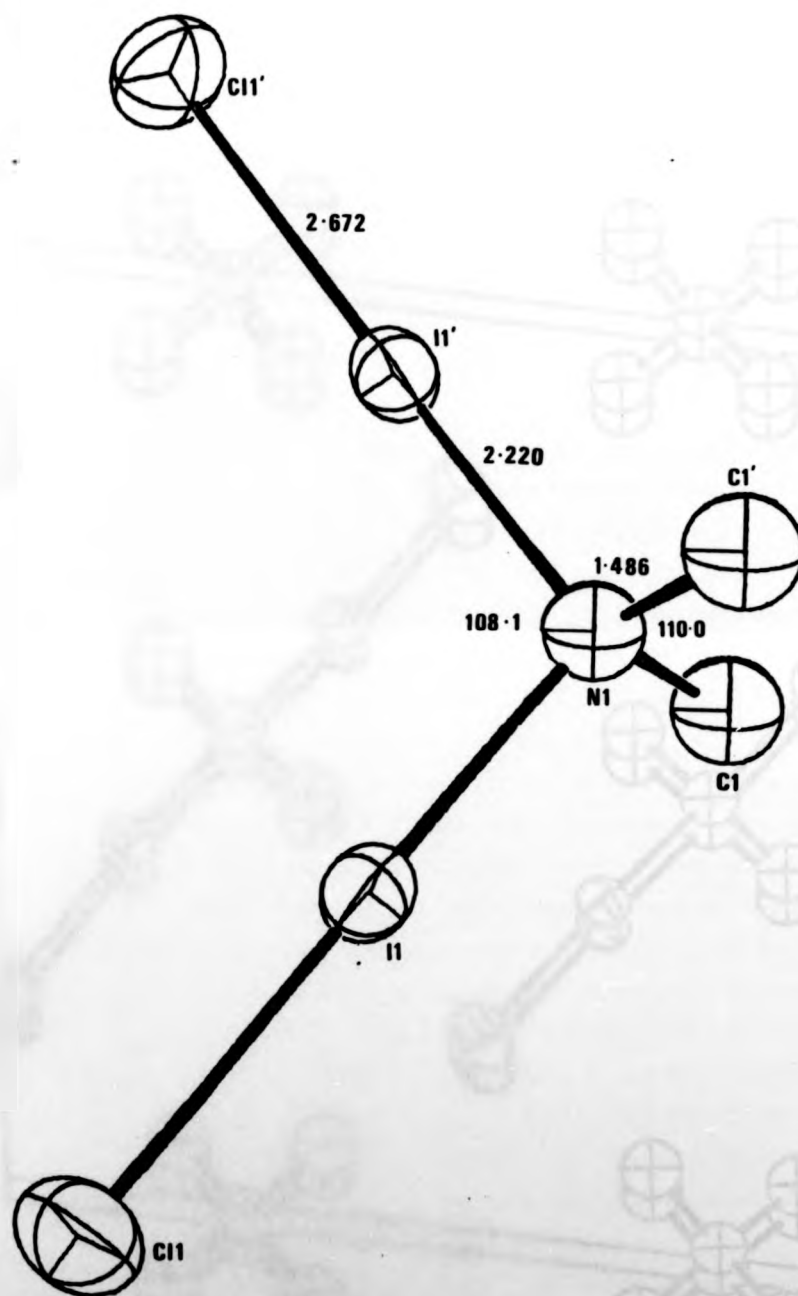


Figure V.2 The structure of the anion $[\text{Me}_2\text{N}(\text{ICl})_2]^-$

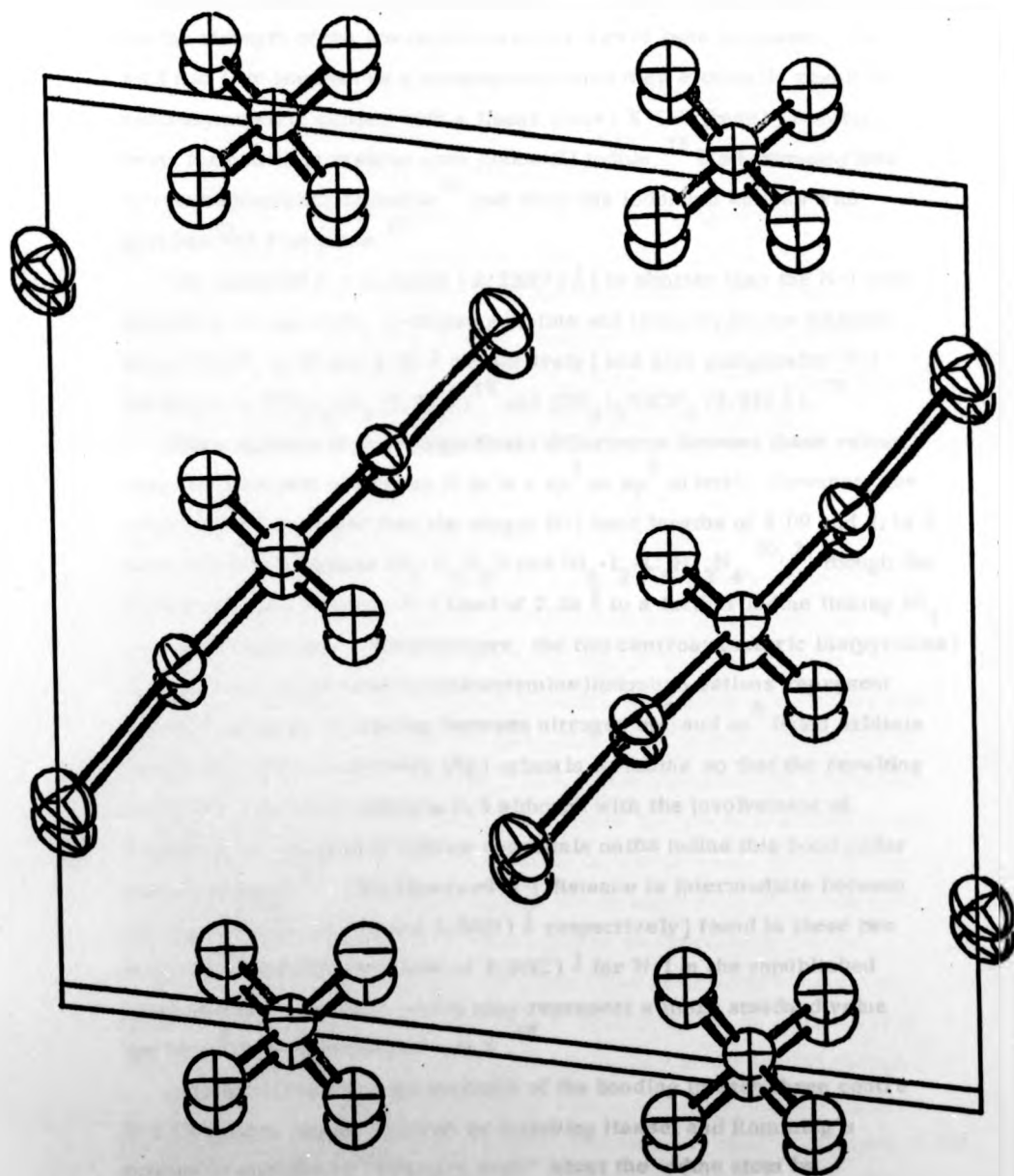


Fig. V.3 Packing arrangement in $[\text{Me}_4\text{N}^+][\text{Me}_2\text{N}(\text{ICl})_2]^-$ viewed down b .

(2.73(1) Å) which, with the short Se-I distance (2.630(5) Å), suggests the formation of the selenonium salt $[\text{C}_4\text{H}_8\text{OSeI}]^+\text{Cl}^-$.¹⁴ This behaviour is typical of adducts of iodine and the inter-halogen compounds ICl and IBr. As the strength of the interaction with the Lewis base increases, the I-I, I-Cl and I-Br lengths as a consequence until they eventually result in centrosymmetric cations with a linear (base) X-I-X (base) grouping being formed as in bis(thio urea)iodine(I) iodide,¹⁵ bis(hexamethylene tetramine)iodonium triiodide¹⁶ and other bis iodonium cations with pyridine¹⁶ and 3-picoline.¹⁷

The observed N-I distance [2.220(7) Å] is shorter than the N-I bond lengths in the pyridine, 2-chloroquinoline and trimethylamine adducts above [2.29, 2.43 and 2.30 Å respectively] and also comparable N-I distances in $(\text{CH}_3)_3\text{NI}_2$ (2.27 Å)¹⁸ and $(\text{CH}_3)_3\text{NICF}_3$ (2.932 Å).¹⁹

There appears to be no significant differences between these values when the lone pair orbital on N is in a sp^2 or sp^3 orbital. However, the observed N-I is longer than the single N-I bond lengths of 2.09 and 2.14 Å observed in the adducts $\text{NI}_3 \cdot \text{C}_5\text{H}_5\text{N}$ and $\text{NI}_3 \cdot \text{I}_2 \cdot \text{C}_6\text{H}_{12}\text{N}_4$.^{20, 21} though the former also has a longer N-I bond of 2.36 Å to a further iodine linking NI_4 tetrahedra together. Furthermore, the two centrosymmetric bis(pyridine) iodonium and bis(hexamethylenetetramine)iodonium cations represent examples with 3c-4e bonding between nitrogen sp^2 and sp^3 filled orbitals interacting with σ -symmetry (5p) orbitals on iodine so that the resulting N-I bonds have bond orders ≈ 0.5 although with the involvement of π -orbitals on the ligands and/or d-orbitals on the iodine this bond order would increase.¹⁶ The observed N-I distance is intermediate between the distances [2.16(10) and 2.30(1) Å respectively] found in these two compounds although the value of 2.24(2) Å for N-I in the unpublished bis(3-picoline) iodonium cation may represent a more standard value for $\text{N}(sp^2)\text{-I}$ with bond order ≈ 0.5 .¹⁷

Another measure of the strength of the bonding in each three centre N-I-Cl system can be obtained by following Hassel and Romming's method in calculating "effective radii" about the iodine atom by subtracting the covalent radii of the nitrogen [0.70 Å] and chlorine

[0.99 Å] atoms from the evaluated N-I and I-Cl bond lengths.²² The resultant values for the effective radii R_1 and R_2 in the present anion are 1.52 and 1.68 Å respectively which, if plotted on Hassel and Romming's graph of R_1 versus R_2 values for a series of polyiodide and IX(Y=Cl, Br) complexes, falls very close to the least squares straight line through all these points. The equation for this straight line is, in fact, $R_2 = 4.59 - 1.97 R_1$ from which the calculated R_2 for $R_1 = 1.52$ is 1.60 Å compared to an observed value of 1.68 Å. The strongest interactions are, therefore, for those complexes with $R_1 \approx R_2$. A similar attempt to correlate the bond lengths in the linear two-fold co-ordination of iodine which has been found to be an essential structural element in the crystal structures of several $NI_3 : I_2$: base [N, O and I] and NI_3 : base adducts or their analogues is not always obvious for, as yet, undefined reasons.²¹

The bonding in the present anion and the majority of the complexes described above has been described in terms of charge transfer interactions.^{22,23} However, as will be further explained in chapter VI, the orbital overlaps already defined in the secondary bonding model can equally well be applied to the present example of a σ - σ charge transfer complex. There are, therefore, two separate 3-centre-4-electron systems formed in the present anion when the two lone pairs in sp^3 orbitals on the Me_2N^- group interact with the σ -orbitals of both iodine monochloride molecules. The short N-I and long I-Cl distances indicate that the interactions in the present anion are among the strongest so far observed for iodine monochloride adducts. As a consequence of the strength of these interactions, the two chlorine atoms in each anion possess an appreciable partial negative charge which acts to prevent any close inter anion contacts so that the packing is that of discrete ions. Furthermore, no chlorine NQR signal is detected from the anion again as a result of the partial charge.¹ The absence of any inter-anion interactions is somewhat surprising as an essential structural feature of the polyiodide ions and other complexes of the X-I-I (X = base) type, e.g. (iodine adducts of 1-oxa-4-selenacyclohexane and 1,4-diselenacyclohexane) is that the compounds invariably form into polymeric arrangements via several weaker intermolecular contacts

which are possibly described as secondary bonds.^{8, 23} Even iodine adducts of such compounds as NI_3 ,²¹ and the transition metal complexes iodo tris (N, N-dimethyldithiocarbamate)ruthenium(IV),²⁴ $\text{Pt}(\text{phen})\text{I}_6$ and $\text{Pt}_2(\text{phen})_2\text{I}_{10}$ (phen = 1, 10 phenanthroline)²⁵ all form zigzag or helical chains with the iodine molecules bridging the directly bonded iodine atoms. In these latter complexes an adequate picture of the bonding might use semi-metallic bands of delocalised multi-centre orbitals formed by interacting p-orbitals of each iodine along the polymeric chain of iodine atoms.

V.5. References

1. The chemical reactions and physical measurements on the halogen-substituted ammonium cations are part of the research of N.D. Cowan, C.J. Ludman and T.C. Waddington at the University of Durham.
2. O. Hassel and H. Hope, *Acta Chem. Scand.*, 1960, **14**, 391.
3. Twinned crystals normally cause problems in either the centering or autoindexing routines or else are visible on axial photographs. Sometimes the reciprocal lattice points from the various members of the twinned crystal do not exactly fall on top of one another, and the centering routine will take many iterations and can often be observed to be oscillating between two close reflections. These will sometimes be clearly seen on plotting the peaks. Sometimes the centering routine behaves normally, but the autoindexing routine produces very few solutions all with very long axial lengths, yet the original rotation photograph may not have had a high density of reflections indicative of a large unit cell. Increasing the integer tolerance for accepting an axial vector will give a larger number of vectors and hence enable the reflections associated with the twin to be identified (normally one or two reflections will be calculated in the least squares routine with bad h, k, l indices). Finally, axial photographs may contain reflections which do not fall on the layer lines which are normally much less intense than the layer line reflections. In all these cases it is advisable to search for a better crystal before continuing with an obvious twin. Source: Syntex Analytical Instruments, Technical Notes, 1974.

4. Alternative transformations such as $a' = a/2 - c/2$; $b' = b$; $c' = a/2 + c/2$ OR $a' = a/2 - c/2$; $b' = b$; $c' = c$ give larger β -angles. The transformation matrix for the reflection indices is given by Matrix (I) whilst the atom co-ordinates are transformed into the primitive cell by the inverse matrix (II).

$$\begin{pmatrix} 1 & 0 & 0 \\ 0 & 1 & 0 \\ -\frac{1}{2} & 0 & -\frac{1}{2} \end{pmatrix} \text{ (I)} \qquad \begin{pmatrix} 1 & 0 & -1 \\ 0 & -1 & 0 \\ 0 & 0 & -2 \end{pmatrix} \text{ (II)}$$

5. After collecting 613 reflections, of which none with $h + l = 2n + 1$ were observed, the program was coded to exclude systematically absent reflections due to the B-centering condition. As a final check on this absence, after completion of the data collection out to 60° , a shell of data was collected containing only B-centred reflections, none of which were again found to be observed.
6. Marked variation in anion geometry is also the feature of several other complexes where pseudo symmetry and other factors are blamed. See, for example, M. Webster, K.R. Mudd and D.J. Taylor, Inorg. Chim. Acta, 1976, 20, 231.
7. Need to solve the simultaneous equations
- $$f_1 = f_a + af_b$$
- $$f_2 = f_b + af_a \qquad \text{to obtain the true intensities of}$$
- reflections 1 and 2 (f_a and f_b) from the observed values f_1 and f_2 (a = twinning factor).
8. E.H. Wiebenga, E.E. Havinga and K.H. Boswijk, Adv. Inorg. Chem. Radiochem., 1961, 3, 148; F.H. Herbststein and M. Kapon, Nature, 1972, 239, 153.
9. H. Hartl and S. Steidl, Z. Naturforsch., 1977, 32b, 6.
10. B. Hulten, N. Johansson and U. Pllsäter, Arkiv. Fysik., 1959, 14, 31.
11. 'Comprehensive Inorganic Chemistry', ed. A.F. Trotman-Dickenson, Pergamon, Vol. 2, p. 1509.
12. C. Rømming, Acta Chem. Scand., 1972, 26, 1555; G. Eia and O. Hassel, Ibid., 1956, 10, 139.

13. G. Bernardelli and R. Gerdil, Acta Cryst., 1976, B32, 1906.
14. C. Knobler and J.D. McCullough, Inorg. Chem., 1968, 7, 365.
15. G. H-Y. Lin and H. Hope, Acta Cryst., 1972, B28, 643.
16. H. Pritzkow, Acta Cryst., 1975, B31, 1505, 1589 and refs. therein. See also G.A. Bowmaker and R.J. Knappstein, Aust. J. Chem., 1977, 30, 1123.
17. R.S. Osborn, unpublished results, quoted in ref. 16.
18. K.O. Strömme, Acta Chem. Scand., 1959, 13, 268.
19. A.C. Legan, D.J. Millen and S.C. Rogers, J. Chem. Soc. Chem. Comm., 1975, 580.
20. H. Hartl and D. Ullrich, Z. anorg. Chem., 1974, 409, 228; H. Pritzkow, ibid., 1974, 409, 237.
21. J. Jander, Adv. Inorg. Chem. Radiochem., 1976, 19, 1.
22. O. Hassel and C. Rømming, Acta Chem. Scand., 1967, 21, 2659.
23. 'Selenium', Eds. R.A. Zingaro and W.C. Cooper, Van Nostrand-Reinhold, Chap. 7, esp. p. 361.
24. M. Mattson and L.H. Pignolet, Inorg. Chem., 1977, 16, 488.
25. K.D. Buse, H.J. Keller and H. Pritzkow, Inorg. Chem., 1977, 16, 1072.

CHAPTER VI

A Discussion of Secondary Bonding and Other Intermolecular Forces

VI.1. Introduction

In the previous chapters of this section of the thesis the idea of a secondary bond was introduced and discussed with reference to the crystal structures determined. In each chapter the significance of these structures in relation to other physical measurements made on these or related compounds was briefly discussed. It is the purpose of this chapter to expand these remarks and attempt to draw some conclusions on the importance of the secondary bonding model in comparison to other theories of inter-molecular interactions.

VI.2. Stereochemical Bonding Models

Before discussing this influence of secondary bonds on molecular geometry, it is important to have a general idea of the factors which affect the bonding in the unperturbed structures. What follows is therefore a general summary of a few of the currently accepted stereochemical bonding models.

(VI.2.1) Valence Shell Electron Pair Repulsion (VSEPR) theory

Perhaps the single most important stereochemical model in use in structural chemistry is the valence shell electron pair repulsion model of Nyholm and Gillespie¹ in which the molecular stereochemistry is derived from a simple consideration of lone pair-lone pair (lp-lp), lone pair-bonded pair (lp-bp) and bonded pair-bonded pair (bp-bp) electron pair repulsions. There are two basic principles involved in the application of this scheme:

- (i) Valence shell electron pairs repel one another so that the system adopts a minimum repulsion-energy configuration, and
- (ii) lone pair-lone pair (lp-lp) repulsions are greater than lone pair-bonded pair (lp-bp) repulsions which in turn are greater than bonded pair-bonded pair (bp-bp) repulsions.

By considering octahedral and trigonal bipyramidal arrangements with two or more lone pairs, Jenkins and Waddington² have extended the arguments of Nyholm and Gillespie and formulate two further axioms:

- (iii) the lone pair-bonded pair repulsion is less than the arithmetic mean of the lone pair-lone pair and bonded pair-bonded pair repulsions, and
- (iv) in trigonal bipyramidal arrangements, the electron pair interactions at 120° to each other are less than half the corresponding interactions at 90° to each other. (Electron pair interactions at 180° to each other are ignored since they exert no component of force perpendicular to the bond axis).

Together these four rules enable the primary geometries of a vast number of complexes to be rationalised. However, in chapter II it has already been stated that the primary geometry in the solid state may be considerably affected by the varying strengths of any secondary bonds which reflected the fact that in some systems the stereochemical activity of lone pairs may be over-estimated. Due to the weakness and variable lengths of secondary bonds, their inclusion into this stereochemical model is difficult. However, stereotypical arrangements such as those of Brown (Chapter II) are useful in classification.³

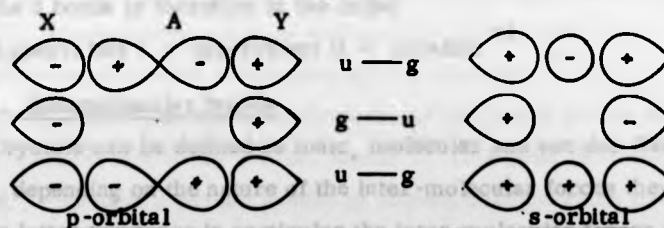
(VI.2.2.) Galy Model⁴

Secondly, the theoretical model of Galy et al.⁴ will be described. Starting from similar basic principles to those of Nyholm and Gillespie, the authors have developed a simple stereochemical model using data on the oxides, fluorides and oxyfluorides of various non-metals in which the distances between the bonded atoms are used to calculate the displacement of the central atom away from the centre of the co-ordination sphere towards the position occupied by a lone pair. The calculation also defines the centroid of the volume occupied by this lone pair. The co-ordination polyhedra resulting from this calculation are very similar to those used by Brown in his bond valence calculations.

(Some of the structures used are common to both models).³ Again, deformation mechanisms for the passage of a structure between polyhedra are readily predicted from structural results.⁵ Finally, the calculations enable the lone pair electrons to be defined as an inert pair (i.e. the electron pair is in a non-hybridised atomic orbital) or a non-bonding pair (i.e. the lone pair occupies a hybrid orbital) since the calculated distance between bonded atoms and the lone pair will be greater for the non-bonding case.⁶

(VI.2.3.) 3c-4e MO's

The 3c-4e MO's used to explain the interactions in hydrogen and secondary bonded systems are a natural extension of the arguments of Rundle who proposed delocalised 3c-4e bonds involving only s and p orbitals to explain the bonding in trihalide ions and related species.⁷ This view was different to that of Gillespie and others who attributed the stability of the chemical bonds formed between filled shell species to outer d-orbital participation⁸ although other bonding propositions explaining the stability of these bonds have also been given.⁹ The theoretical treatment of 3c-4e bonding as related to nitrenes and thiothiophenes has been investigated by Gleiter and Hoffmann.¹⁰ In forming the 3c-4e MO's, two cases may be distinguished, depending on the nature of the central orbital (s or p) participating.



The symmetry designations u (antisymmetric) and g (symmetric) refer to reflection through the plane bisecting the 3 centre system. Generally 3c-4e MO's with the middle orbital strictly non-bonding are restricted to the interhalogen and xenon and other rare gas compounds.¹⁰ In other cases the system tends to be asymmetric, the distance A-X shortening

as $A \dots Y$ increases until with very long $A \dots Y$ distances the orbital overlaps are best described as a lone pair on Y interacting with the σ^* orbital of a $2c-2e$ A-X bond, i.e. the secondary bonding model. The results of the calculations on the thiophenes again do not help to discriminate against the involvement of d-orbitals in the $3c-4e$ interactions. The potential energy curve produced on displacing the central S from a symmetrical situation show a preference for an unsymmetrical structure when 3d orbitals are not utilised and a nearly symmetrical structure (very flat minimum energy) when 3d orbitals are included.¹⁰ Calculations on other more extended linear arrays of S atoms constrained by π systems favour the viewpoint that the 3d orbitals should be treated as polarising functions only.¹¹

In general, therefore, the role of d-orbitals in the bonding of complexes of the non-metals is still ambiguous. According to Musher,¹² however, the bonding in virtually all non-metal compounds should be described without d-orbital participation. Instead, a mixture of "orbitally deficient hypervalent" $3c-3$ orbital and covalent ($2c-2e$) bonds should be used. His 'hypervalent' bonds are virtually identical to $3c-4e$ MO's above and the bond type is designated hypervalent I and II, depending on whether the central atom of linear L-A-L fragments uses either a p orbital or s and p orbitals in the bonding. The bond strengths for the 3 bonds is therefore in the order

$$\text{hypervalent I} < \text{hypervalent II} < \text{covalent}^{12}$$

VI.3. Intermolecular forces

Crystals can be defined as ionic, molecular and van der Waals in type, depending on the nature of the inter-molecular forces they contain. In the latter two types in particular the inter-molecular forces can be described using either van der Waals, charge transfer and/or secondary bonding descriptions.

(VI.3.1.) Van der Waals interactions

The definition of a secondary or charge transfer interaction relies on defining a limiting inter- or intra-molecular contact distance (van der Waals) contact. Distances shorter than this value but longer than

single bond distances can then be described as secondary or charge transfer interactions. Before attempting to discuss any general factors associated with secondary bonding, it is therefore important to ask some basic questions. In particular, what are van der Waals forces? Associated with this is the very important question: at what point does an inter- or intra-molecular contact distance cease to be a van der Waals contact and become a secondary bond?

(VI.3.1(i)) What are van der Waals forces?

These forces originate from the quantum mechanical behaviour of the electrons which are part of an atomic or molecular system. If the system is considered as positively charged nuclei (or nucleus) each surrounded by a negatively charged electron cloud which can only have certain permitted energies, then this electron cloud is not rigidly distributed around the nuclei but can be deformed by both external and internal electromagnetic influences. This occurs either when a permanent dipole exists or when temporary dipoles are induced by either an external field, a neighbouring dipole or even the mutual interaction of spherically symmetric non-dipole molecules (when localised fluctuations in charge density of the electron clouds occur). Such polarisation effects can, in fact, rapidly propagate through the solid and are known collectively as London dispersion forces. These localised fluctuations can be represented as a simple exchange of photons between neighbouring particles without emission of radiation.¹³

Overall, these forces are known as van der Waals forces after their initial treatment by van der Waals.¹⁴ Like most inter-molecular forces, they have a certain sphere of influence inside which the discussion of these forces involve more directional character - ionic or MO models - and outside which the influence of the forces steadily decreases. These effects can be conveniently represented in an interaction curve called a Morse curve.¹⁵ For each element the radius of the sphere of influence is represented by a van der Waals radius.

The determination of these radii can be obtained from an analysis of the atomic and molecular packing distances in as many compounds as possible. The most significant values of these radii would be for structures near the close packing limits. The most reliable values are therefore given particularly for the elements of Group VII and neutral spherically symmetrical molecules which can achieve close packing without any of the semi-polar interactions that occur between the dipoles of other asymmetrically shaped molecules being involved.

It is quite common for several values of the van der Waals radius ($r_{v.d.w.}$) of a particular element to appear in the literature, depending on the structures used in the analysis. For example, in Chapter I the van der Waals radius of tin has separately been given as 2.10 and 2.17 Å.

The two values are due to Bondi¹⁶ and Pauling¹⁷ who have both published fairly comprehensive tabulations of $r_{v.d.w.}$ for several atoms. Although Bondi's values are generally similar to Pauling's values, they are based on a more thorough examination of experimental evidence, so that the choice between the two sets of values is somewhat arbitrary. Therefore, the values of $r_{v.d.w.}$ of Bondi have consistently been used in the discussion of the secondary bonded systems in this section of the thesis. In fact, since covalent radii are more accurately known, it has been proposed that neither Pauling's nor Bondi's values should be used, but in fact the van der Waals radii should be obtained by the simple relationship that

$$r_{v.d.w.} \approx r_{\text{covalent}} + .75 \text{ Å}$$

since r_{covalent} values are more accurately known.

Irrespective of which van der Waals radii are used, the simple observation that, in an interaction A...X, if the distance A...X for an interaction is shorter than the same interaction with A of lower atomic number, the interaction is stronger. However, once it has been decided that an intra- or inter-molecular contact distance satisfies the criteria for a secondary bond, it is important to have some quantitative measure of the strength of the secondary bond and its effect on the primary geometry. This aspect is relatively complex because, unlike the

TABLE VI.1

Van der Waals and single bond radii, Å after A. Bondi.¹⁶

	H	He			
	1.20	1.40			
C	N	O	F	Ne	
r_w	1.70	1.55	1.52	1.47	1.54
r_c	0.77	0.70	0.66	0.64	
Si	P	S	Cl	Ar	
r_w	2.10	1.80	1.80	1.75	1.88
r_c	1.17	1.10	1.04	0.99	
Ge	As	Se	Br	Kr	
r_w	1.95	1.85	1.90	1.85	2.02
r_c	1.22	1.18	1.14	1.11	
Sn	Sb	Te	I	Xe	
r_w	2.10	2.05	2.06	1.98	2.16* [2.00]*
r_c	1.40	1.36	1.32	1.28	1.29
	Bi				
r_w	2.15				
r_c	1.55				

hydrogen bond¹⁸ there are a large number of other factors, steric as well as electronic, which significantly affect the orbitals on the central atom of the secondary bonded system and hence affect any correlations between the distances A-X and A...Y.

(VI.3.2) Charge Transfer Bonding

In the Introduction, it has already been stated that a number of secondary bonded systems have been previously described as examples of charge transfer (C.T) complexes. The term charge transfer complex is, however, somewhat imprecise unless qualified by some description of the orbital interactions involved. Prout and Wright¹⁹ in reviewing the crystal structures of several electron donor-acceptor (or C.T. complexes) sub-divided the compounds into three classes dependent on the symmetry of the orbitals involved in the charge transfer process. The three types of complex are σ - σ , σ - π and π - π . Secondary bonded complexes can clearly be classified as examples of σ - σ complexes and since the orbital overlaps involved in a secondary bond are more precisely defined, Prout and Wright's observation that, in σ - σ complexes, inter-molecular bonds become shorter and intra-molecular bonds become longer as charge transfer increases, immediately follows from the increased overlap of the donor orbital (on Y) with the σ^* orbital of A-X. It is this orbital overlap picture which is perhaps the strength of the secondary bond model.

As regards the σ - π and π - π classes, Prout and Wright also noted some other simple correlations. Thus, for σ - π complexes, the trends in the inter-molecular bond lengths are similar to those in the σ - σ complexes, although there are other factors compromising the situation. Similarly, the π - π complexes were found to contain stacks of alternate plane-to-plane donor and acceptor molecules arranged in 3 characteristic ways, although there is little correlation between the interplanar spacings in these stacks and charge transfer properties.^{19, 20} This is perhaps not surprising since π - π complexes are again very susceptible to other crystal packing forces, especially H...H repulsions within and between layers preventing maximum orbital overlaps.¹³

In an ideal situation, however, the stacks in the π - π complexes tend to form with the aromatic rings of the donor and acceptor molecules displaced by half a ring diameter (maximising C.T. interactions) and with polar bonds of one molecule overlapping a polarisable region of another (maximising dipole-induced dipole interactions).²⁰

Whether the σ - π and π - π C.T. complexes can be considered to be formed by similar bonding-antibonding orbital overlaps as in the σ - σ secondary bonded examples is not at present clear. Certainly, apart from the secondary bond examples, there are several other theories which in essence rely on bonding-antibonding orbital interaction to explain molecular properties. Notably, the Dewar-Chatt model, as used to describe the interactions in complexes of the transition metals with such small molecules as ethylene, CO, NO, etc. involves donation of electron density from occupied d-orbitals on the metal into antibonding π^* orbitals with the result that there should be a lengthening of the C-O distance as this interaction increases in strength.²¹ Effects of this can be observed by other physical measurements (i.r. etc.) normally. Similarly, the effects of this synergic bonding has been noted to activate other small molecules, e.g. CS_2 and butadiene, so that their molecular parameters when co-ordinated are consistent with those of an excited state.²²

One of the original theoretical treatments of donor-acceptor or charge transfer complexes was due to Mulliken who defined the ground state wave function ψ_N to be a linear combination of the wave functions of a no-bond structure [$\psi_0(\text{DA})$] with that of a structure with complete charge transfer [$\psi_1(\text{D}^+\text{A}^-)$].

$$\psi_N = a\psi_0(\text{DA}) + b\psi_1(\text{D}^+\text{A}^-) \quad (1)$$

However, this function is only approximate and in systems where three-centre σ -delocalisation bonding occurs, the wave functions for the complex should take account of the polarisation of the donor and acceptor molecule [equation (2)].

$$\psi_N = a\psi_0(N_3X_2) + b\psi_1(N^+XX^-) + c\psi_2(N^+X^-X^+) + d\psi_3(NX^+X^-) \quad (2)$$

Therefore, the difference between the secondary bond examples, the different charge transfer complexes and metal complexes is then the relative significance of each of the wave functions $\psi_1, 2, 3, \dots$ for the excited valence states. These can be treated as perturbation of the neutral separated wave function ψ_N .²³

(VI. 4.) Quantitative Analyses of Secondary Bond Strengths

The treatment of the majority of the structures described in the previous chapters has been only qualitative. The most rigorous treatment of secondary bonds would be to calculate molecular wave functions for the whole system. However, at present there are considerable difficulties in performing accurate calculations for all but the simplest molecules. Part of the difficulty is in obtaining accurately parameters for the d-orbitals. Where calculations have been performed for examples with the 3 centre systems nearly symmetrical, calculations by LCAO and other methods have produced some semi-quantitative correlations.

Apart from such relatively simple ideas as using the difference in A...X differences for bidentate ligands,²⁴ the ratio $(A-X_{\text{bridge}})/(A-X_{\text{terminal}})$ or differences $(A...X_{\text{observed}}) - (A-X_{\text{covalent}})$ to quantify the strength of a secondary bond,²⁵ recourse normally has to be made to semi-qualitative models in an attempt to quantify some of the secondary bond interactions and their effect on the primary geometries. The calculations attempting to model these bonding interactions can be subdivided into two types; (a) those molecular packing models in which the limitation on the interactions of non-bonded atoms is the contact of spheres with radii given by the van der Waals radii or by repulsion energy calculations; (b) those valence models which base the strength of any inter- or intra-molecular interaction on a comparison of the actual distances involved with reference distances, either single bond lengths or single bond radii.

All the following sections are based simply on intermolecular

Examples of each type of model are given in the following paragraphs.

Of the former type, the molecular packing model of Zahrobsky has already been mentioned in connection with the diethyl tin dihalides in Chapter I.²⁶ A criticism of this model and packing models in general is that no allowance is made for the interpenetration of the van der Waals surfaces. From Zahrobsky's model the calculated C-Sn-C angle is significantly lower than the experimental value, and although the calculated inter-molecular distances are of the right order, this is perhaps not surprising since the length of the secondary bonds are near the van der Waals limit. The C-Sn-C angle must be considered as a better indication of whether or not the model is successful. However, in comparison the distortion of the expected trans octahedral stereochemistry of several dimethyl tin complexes containing two bidentate ligands to a skew-trapezoidal bipyramidal stereochemistry has been demonstrated to be compatible with the results of simple ligand-ligand repulsion energy calculations. These calculations are based on minimising the repulsion energy U given by

$$U = \sum_{ij} u_{ij} = \sum_{ij} a_n d_{ij}^{-n} = a_n X \quad (i > j)$$

where U_{ij} is the repulsive energy between any 2 donor atoms i and j , a_n is a proportionality constant and d_{ij} is the inter-atomic distance between atoms i and j . The usual value of n is $n \sim 6$ where $n = 1$ would represent a purely Coulombic interaction. The calculations are performed as a function of the normalised bite of the bidentate ligands. However, in this type of calculation the predicted angles are again not very meaningful because of the chemical differences between the unidentate and bidentate ligands.²⁷ Again, although the bidentate ligands are predicted to be asymmetric and this asymmetry is a function of the metal-unidentate bond length, no weight can be given to these correlations. An example of this effect and a three-centre secondary bond overlap has already been postulated for related structures in Chapter III with the methyl groups in the structures above replaced by lone pairs (especially $\text{Te}(\text{Me}_2\text{Xan})_2$).

All the following measures are based simply on inter-molecular

distances. Zefirov and Zorkii* have suggested that a contracted inter-molecular contact radii r_{ij} may be a useful criteria for separating inter-molecular contacts into weak and strong contacts. The contracted inter-molecular contact radii are defined as $r_{ij} < 2(R_i R_j)^{\frac{1}{2}} - \delta$, where R_i and R_j are the statistical means of van der Waals radii of atoms i and j and δ is 0.15 Å for contacts without H atom participation and 0.30 Å with H participation. The boundary between weak and strong contacts is defined as $r_{ij} = 2(R_i R_j)^{\frac{1}{2}} - \delta - 0.1$ Å.²⁸ Zefirov* similarly uses weighted mean van der Waals radii R_{ij} in establishing criteria for the existence of hydrogen bonds as well. The general form of this criterion is that in the contact X-H...Y the distance $d(H...Y)$ must be $< 2.15\sqrt{R_{ij}} - 0.35$ Å for a hydrogen bond to exist. For Y = O, N, S and Cl, a hydrogen bond exists, provided $d(H...Y)$ are less than 2.1, 2.3, 2.56 and 2.6 Å respectively.²⁹ (cf. Table VI.1.)

Finally, there are two closely related valence bond models based solely on inter-atomic distances. Both are completely general in their application with only a few constants being required in their implementation. Pauling's model makes use of equation (1) where the bond order n' is related to bond length $D(n')$ of that bond and $D(1)$, the reference value, is the bond length of a single bond. The best values of $D(1)$ are those from gas-phase measurements.¹⁷ Summation of individual bond orders for the contacts around an atom should be very nearly integral, and it is this principle which is used considerably in the closely related bond valence model of Brown.^{3,30} The basis of

$$D(n') = D(1) - 0.71 \log(n') \quad (1)$$

this empirical model is that the chemical bonding in the crystal can be considered as a sum of two-body interactions. In some cases it has been stated that an a priori prediction of the bond valences and hence the bond lengths in a crystal may be possible by describing a network

* Unfortunately only the abstracts of these papers were available, so no critical appraisal is possible.

of two body contacts or 'bonds'. Then, using an equal valence principle that the sum of (bond) valences at a node (atom) in the above network is equal to the atomic valence at that node (atom).³⁰

The basic principle of bond valence theory is that for each two-body interaction/contact/bond a bond valence (S) can be calculated by either equation (1) or (2) which contain the purely empirical constants R_0 , N and A calculated for each atom pair, R is the contact

$$S = (R/R_0)^{-N} \quad (1)$$

$$\text{or } S = \exp(-(R-R_0)/A) \quad (2)$$

distance and R_0 is the length of a bond of 1 valence strength. The empirical constants are normally determined from a series of curves based on a known set of compounds, particularly O, F, S and other halogen complexes, although the use of a pair of values for whole series of complexes does not significantly affect the resultant bond valences.³¹ There are two criticisms of this approach. Firstly, the $(S/S_0)^{-N}$ or $\exp(-(R-R_0)/A)$ curves do not go to zero at the van der Waals limit so that small bond valencies are still calculated for very long contacts which when summed represents an appreciable valence. Secondly, the calculated valences are completely non-directional. However, the model does calculate sums of the bond valences around each atom which are very close to the atomic valence in a large number of crystal structures, and specific bond valencies can be associated with what had previously been imprecisely defined as strong, weak and intermediate bonds A-X. Similarly, the correlation between bond angles X-A-X and the average bond valence $\langle S \rangle$ of the A-X bond is only valid for the strong primary bonds. It is notably that when a lone pair is opposite a primary bond so that the trans bond is replaced by several weaker bonds, the bond angle correlation breaks down (e.g. E configuration).³ A model combining the principles of bond valence with those of Galy *et al.* may be of some use.

VI. 5. Correlations between distances A-X and A...Y

If we accept that the majority of secondary bonded systems contain linear triatomic arrangements in which the bonding can be described using 3c-4e MO's, then there must be some correlation between the interatomic distances A-X and A...Y. For the ideal arrangement, there would be a linear correlation between A-X and A...Y. The systems which are very nearly ideal are the simple trihalides (I_3^- , Br_3^-) and the $\sigma - \sigma^*$ 'charge transfer' adducts of iodine or the iodine monohalides, ICl or IBr, with other bases. Using the available data on these complexes, Hassel and Romming have, in fact, arrived at a linear correlation,[†] and this has been discussed in Chapter V in relation to the ion $[Me_2N(ICl)_2]^-$.³² In these simple examples, second order effects are relatively small. However, in the majority of secondary bonded systems, the second order effects, which are non-linear, act to restrict any linear correlations to large A...Y separations when the effects on A-X distances are likely to be masked by observational errors. A smooth curve is then likely to be a better fit to the data on any particular system. A typical correlation between A-X and A...Y distances to be expected is shown for a series of antimony(III) complexes, the majority of which are based on the C (Chapter II) arrangement of 3 primary and 3 secondary bonds.³³ It should be noted, however, that the correlations found will vary considerably from system to system and from compound to compound due to significantly different second order effects. A large number of different examples of roughly the same type with a large spread of A-X and A...Y distances are required before reasonable accurate conclusions about the correlations can be drawn.

The second order effects which are responsible for the non-linear correlations are both steric and electronic in origin, and may be completely inter-related. Broadly speaking, the electronic effects can arise from either the involvement of d-orbitals on A (or X and Y) at short distances and/or rehybridisation of the central atom concurrent with a change in the geometry of the surrounding ligands due to steric

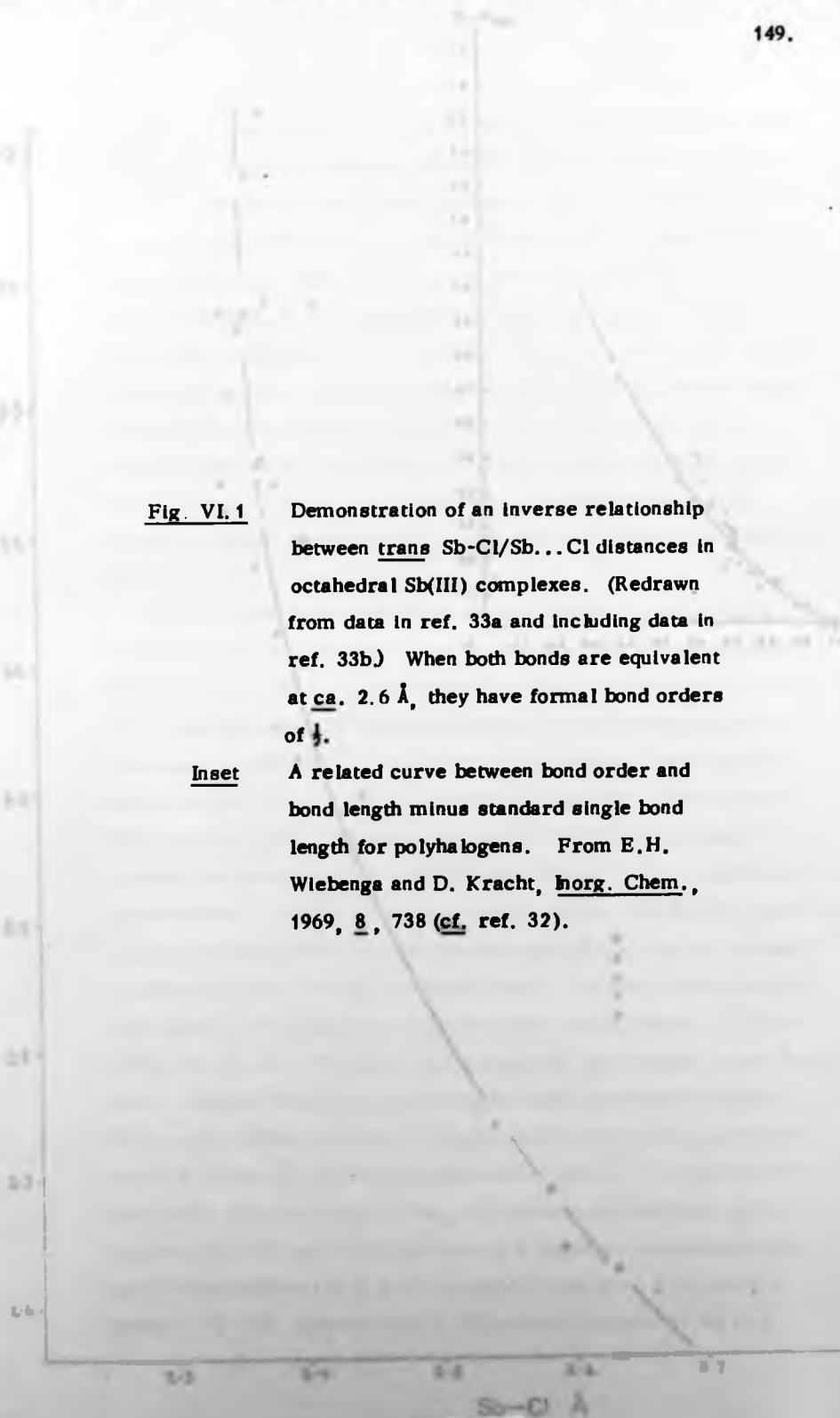
[†] Compare, however, the theoretical curve of Wiebenga and Kracht, also shown in Fig. VI. 4.

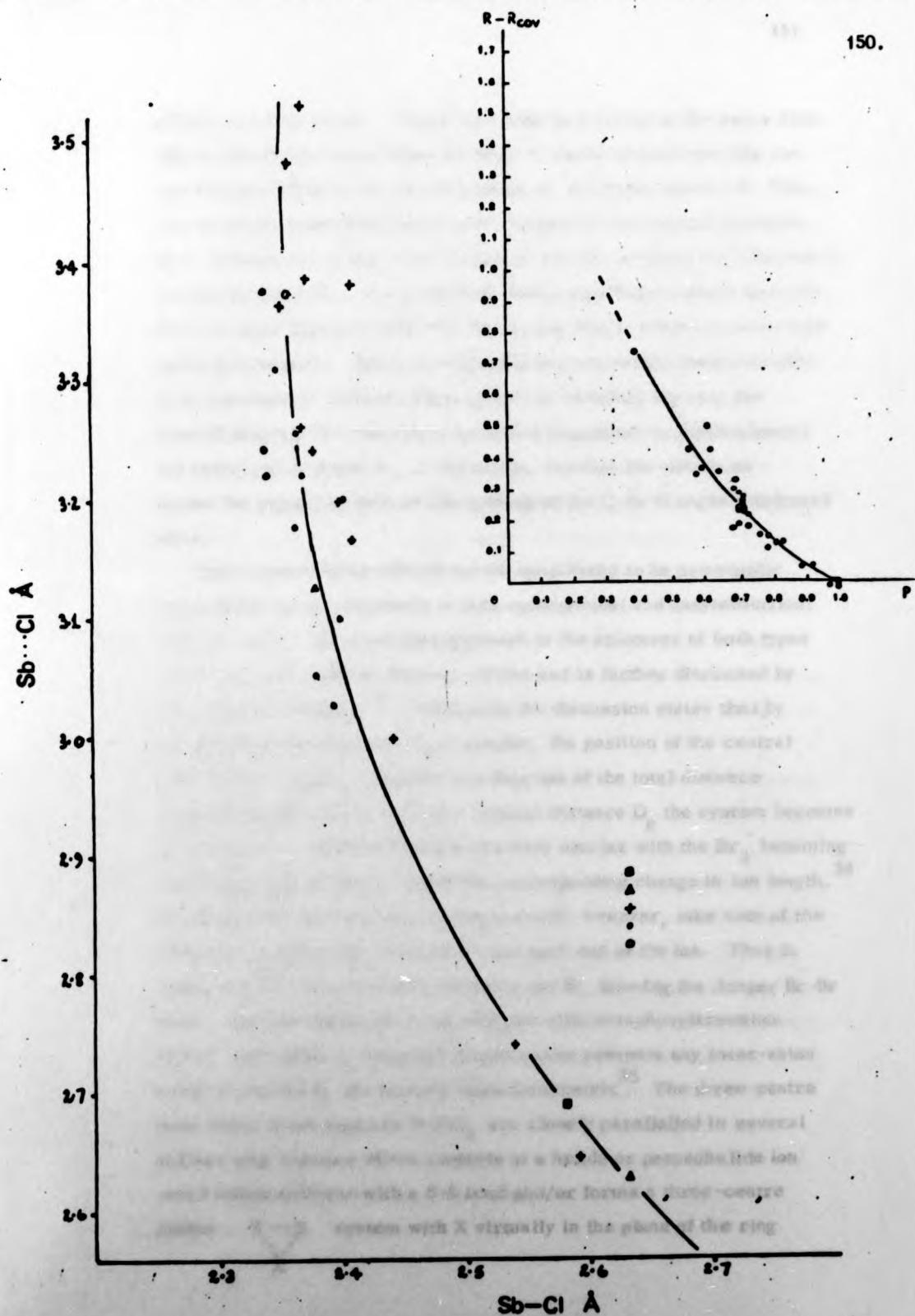
Fig. VI. 1

Demonstration of an inverse relationship between trans Sb-Cl/Sb...Cl distances in octahedral Sb(III) complexes. (Redrawn from data in ref. 33a and including data in ref. 33b) When both bonds are equivalent at ca. 2.6 Å, they have formal bond orders of $\frac{1}{2}$.

Inset

A related curve between bond order and bond length minus standard single bond length for polyhalogens. From E.H. Wiebenga and D. Kracht, Inorg. Chem., 1969, 8, 738 (cf. ref. 32).





effects and vice versa. These may both be involved at the same time. The steric effects arise when the atom Y begins to penetrate the van der Waals surface of the atomic groups or lone pairs around A. This can be partly relieved by geometric changes in the original molecule (e.g. opening out of the C-Sn-C angle in the tin compounds of Chapter I) or else by the X-A...Y approach deviating significantly from linearity. This is especially true when the interacting atoms Y have to avoid lone pairs (see below). Again in evaluating any secondary bond strengths it is important to consider several factors including not only the overall length of the secondary bonded arrangement or (equivalently) the individual A-X and A...Y distances, but also the effects on molecular geometry such as the opening of the C-Sn-C angle mentioned above.

Again second order effects can be considered to be principally responsible for the existence of both symmetrical and unsymmetrical trihalide ions. An empirical approach to the existence of both types of ion has been given by Mooney-Slater and is further discussed by Breneman and Willett.³⁴ Principally the discussion states that by analogy with the triatomic $H_2 \cdot H$ system, the position of the central $I(Br)$ atom in $I_3^-(Br_3^-)$ systems is a function of the total distance between the end atoms until at a critical distance D_c the system becomes symmetrical. The two systems are very similar with the Br_3^- becoming more asymmetric than I^- under the corresponding change in ion length.³⁴ An alternative bond valence approach would, however, take note of the difference in inter-ion contacts around each end of the ion. Thus in $CsBr_3$ the Cs^+ ions are much closer to the Br , forming the longer Br-Br bond. Similar effects occur in CaI_3 , but with tetraphenylarsonium Ph_4As^+ tri-iodide I_3^- the much larger cation prevents any inter-anion contacts and the I_3^- are strictly centrosymmetric.³⁵ The three-centre inter-anion short contacts in CaI_3 are closely paralleled in several sulphur ring systems where contacts to a halide or pseudohalide ion occur either collinear with a S-S bond and/or forms a three-centre planar



system with X virtually in the plane of the ring

containing the S-S bond. Ref. 36 contains data on several compounds containing these types of interactions.

The stereochemical models discussed in the previous sections have all noted the significant effect lone pairs have on the primary geometry. It follows therefore that the presence of lone pair electrons will also considerably affect the positions of the atoms overlapping with the σ^* orbitals of the primary bonds. In some cases the presence and the angles between secondary bonds which are nearly collinear with primary bonds can be especially useful in demonstrating an inactive lone pair (or pairs) of electrons on the central atom (see Chapter II). However, as has already been noted above, the effects of stereoactive (defined as non-bonding) lone pairs is to split a secondary bonding interaction into several contacts which then adopt positions which avoid the lone pair(s), but still overlap to a lesser extent the σ^* orbital. Obviously in these examples the correlation of A-X and A...Y distances is extremely difficult, and the calculation of bond valencies may be the best approach to correlate particular compounds. The situation in a series of xenon halide ions XeF^+ , XeF_3^+ , XeF_5^+ and Xe_2F_3^+ demonstrates well these effects.³⁷

The geometries of the xenon atom in these four ions are described by Gillespie as AXE_3 , AX_3E_2 , AX_5E and AX_2E_3 respectively.¹ In the crystal, however, all four of these ions possess further inter-ionic contacts which are presumably useful in stabilising the unusual oxidation states of Xe. Furthermore, the directions in which these contacts are formed are dictated by the arrangement of the lone pair orbitals as shown in Fig. VI.3. The actual number and detailed arrangement of the inter-ion contacts is however very variable, which is not unexpected owing to the flexibility with which the contacts can form, avoiding the lone pairs. The xenon atoms in the fourth ion Xe_2F_3^+ are, however, completely surrounded by bonding and lone pairs so that the bridging fluorine atom is now unusually charged and becomes involved in several inter-cation contacts.³⁷

Fig. VI.2

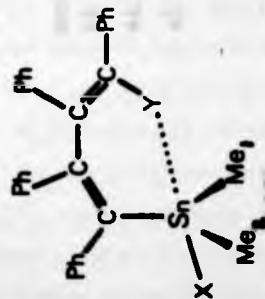
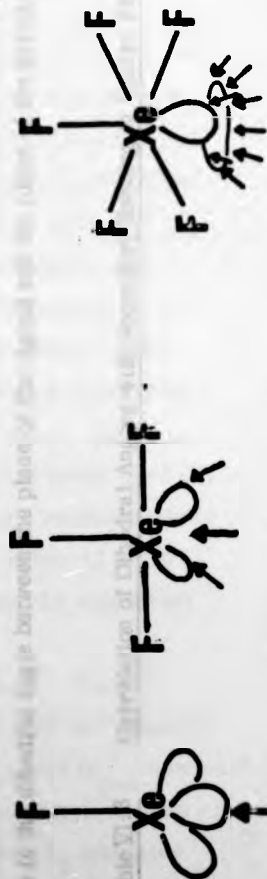


TABLE VI.2 Geometrical parameters for some cis-tetraphenylbutadienyltin complexes.

X	Y	C(Sn...Y)	Sn...Y	C(Bu)-Sn-C(Me1)	C(Bu)-Sn-X	C(Me)-Sn-C(Me)	X...Sn-Y	X-Sn-C(Me1)	X-Sn-C(Me2)
Br	Br	3.774(5)	129.0	105.9(8)	100.7(5)	112.7	149.5(1)	100.0(7)	105.1(7)
Ph	Br	4.284(3)	117.1(5)	109.5(4)	108.4(5)	104.5(6)	143.4(3)	110.9(5)	105.8(5)
Ph	Cl	4.346(2)	116.5(4)	109.4(5)	109.3(3)	105.5(4)	142.3(2)	110.5(4)	104.9(4)

Fig. VI.3 Shapes of XeF_x^+ ions with arrows indicating directions in which secondary bonding interactions would have to form to avoid the stereoactive lone pairs.

Compound ^b	Dihedral Angle 1 (phenyl) ^c	Dihedral Angle 2 (ligand) ^d	Secondary Bonding
PhTe(etu)I	60-61°	small	None
PhTe(esu)I	60-61°	small	None
PhTe(etu)Br	64.6°	small	None
form 1 (C2/c)	87.0°	44.1°	Te...Br 3.8313(10) Å C-Te...Br 162.29°
form 2 (P2 ₁ /c)	87.24°	44.9°	Te...Cl 3.7401(10) Å C-Te...Cl 162.51(7)°
PhTe(etu)Cl	87.25°	45.5°	Te...Br 3.8490(16) Å C-Te...Br 163.31(19)°
PhTe(esu)Br	83.2°	-	No Te...S < 4 Å
PhTe(SCN) ₂ ⁻	85.7°	-	Te...Se 3.965(2) Å C-Te...Se 159.6(2)°
PhTe(SeCN) ₂ ⁻	85°	89° and 46°	Te...Cl 3.606(11) Å C-Te...Cl 163.4(8)°
PhTe(tu) ₂ ⁺ Cl ⁻	52°	69°	Te...Cl 3.71(2) Å C-Te...Cl 164.4(10)°
PhTe(tu)Cl	55°	70°	Te...Br 3.77(1) Å C-Te...Br 164.2(10)°
PhTe(tu)Br			

^a System consists of 3 primary bonds forming a T, and a fourth secondary bond trans to the phenyl which completes a square planar arrangement of bonds.

^b etu = ethylenethiourea; esu = ethyleneselenourea; tu = thiourea

^c This is the dihedral angle between the phenyl ring and the plane of the primary bonds.

^d Similarly, this is the dihedral angle between the plane of the ligand and the plane of the primary bonds.

Table VI.3 Correlation of Dihedral Angles with Secondary Bonding in Square Planar Tellurium Compounds^a

Finally, the presence of phenyl rings in compounds has both steric as well as electronic effects on secondary bonds. These effects have been already noted in Chapter I in regard to cis cis tetraphenylbutadienyl dimethyl tin X (X = Ph, Cl) compounds, and the results are summarised in Table VI. 2.³⁸ The difference in Sn-Br distances when X = Br is replaced by phenyl is 0.57 Å. In the series of phenyltellurium(II) compounds in Table VI.3 the phenyl ring appears to be again partly responsible for the presence of the secondary bond completing the square planar arrangement as can be seen from the dihedral angles when no 4th bond forms. This appears to be due to the phenyl ring at certain orientations being able to engage any available trans orbitals on the tellurium in mesomeric interactions as well as influence a steric effect. A cis effect of the other ligands can possibly be observed from the other dihedral angles in that Table.³⁹ A quantitative measure of related cis - trans effects on primary geometry has been made by Shustorovich and Buslaev, using LCAO calculations based on hypervalent orbital structures. Among their conclusions are: in complexes AXL_m where the central atom preserves the ns^2 "lone pair", the influence of the σ -bonded ligand X is trans, hypervalent I bonds (X-A-X) of Musher are stable only if the ligands X are of greater electronegativity than the central atom and in C_{4v} complexes AL_5 , with either 12 or 10 valence σ -electrons, the axial bond must be shorter than the equatorial ones.⁴⁰

In concluding this section, it appears that approximately linear correlations between the distances A-X and A...Y will hold for systems where the central atom, A, is surrounded only by lone pairs ($D_{\infty h}$ systems), octahedral systems of type C or AX_3Y_3E where the lone pair, E, is inert or very nearly so, and square planar and trigonal planar AX_3E_2 examples where the linear arrangements are relatively free from steric influences and the likelihood of any rehybridisation effects.

(VI.6.) Application of Secondary Bonds

Identification of the important areas in which the inclusion of secondary bonding interactions can greatly help in the understanding of chemical properties of compounds is not always clear cut. However, there appear to be five main areas.

- (1) Secondary bonds are useful in predicting chemical reactions and the likely transition state(s) through which the reaction will proceed.
- (2) Somewhat similarly, the photochemical behaviour of several systems is explained using secondary bonds.
- (3) Some systems which include secondary bonds are good models of the short range ordered arrangements likely to occur in the liquid state or in solutions.
- (4) They may also be of significance in stabilising unusual valence states of the central atom.
- (5) They are useful in explaining other physical properties of the system in the solid state.

Of these five areas, (2) has already been discussed in relation to the behaviour of the benziodoxole compounds in Chapter III, and further information may be obtained from the work of Gougoutas and Etter.⁴¹ Similarly (4) was mentioned in Chapter II with regard to the solid solvate of Me_3NCl with SeOCl_2 in which a centrosymmetric cluster $(\text{Cl} \cdot 5\text{SeOCl}_2)_2^{2-}$ occurs.⁴² Again, this area will not be discussed further.

(VI.6.1.) Reaction Routes

Although chemical reactions are dictated by both kinetic and thermodynamical factors, the extent of reaction is normally measured in terms of relatively few parameters in the molecular structure(s) under consideration. Clearly some of the short inter- and intra-molecular contacts observed in some of the secondary bonded systems must represent very likely reaction co-ordinates along which reactions, notably decomposition or rearrangement reactions, can proceed although actual reaction will require external stimulus (heat, radiation, etc.) A few varied examples will serve to illustrate this point.

The crystal structures of both aluminium iodate nitrate $\{Al[NO_3]_2 \cdot [NO_3] \cdot 6H_2O\}$ and the acid salt aluminium iodate-hydrogen iodate-water $\{[Al(OH_2)_6]^{3+} [IO_3^-] [HIO_3]\}$ have recently been published. The decomposition patterns of these two salts are markedly different. The acid salt in particular loses six water molecules at $135^\circ C$ and a seventh, resulting from the decomposition of $2HIO_3$ to H_2O and I_2O_5 , at $195^\circ C$. This decomposition reaction appears to be related to short I...O contacts in the crystal structure of the latter compound.⁴³

Similarly, both 2-biphenyl tellurium halides and the analogous selenium compounds on heating to the melting (decomposition) point eliminate hydrogen halides in forming a dibenzotellurophene or dibenzoselenophene derivative, and this chemical reaction can be related to short Te...C(12) [Se...C(12)] contacts.⁴⁴ In the iodide this contact has a distance of 3.37 \AA [compared with values of $> 3.83 \text{ \AA}$ for other Te...C (aromatic) contacts] and is $\sim 0.7 \text{ \AA}$ above the equatorial plane and, if included, would give a roughly octahedral geometry for the tellurium. The corresponding bromide has considerably fewer intermolecular Te...Br and Br...Br contacts, but the Te...C(12) contact is much stronger than the iodide [2.945 \AA] and is virtually in the equatorial plane [deviates by 0.035 \AA]. In both these compounds the C(1)-Te...C(12) angles of 68.1° (iodide) and 71.5° (bromide) should be compared to C(1)-Te - C(12) bond angles of 81.7° and 81.8° in dibenzotellurophene and dibenzotellurophene di-iodide respectively.⁴⁴

(VI.6.2.) Stabilisation of unusual valence states

Whilst the above reaction routes can be related to kinetic factors, it may also be tentatively argued that in the majority of cases secondary bonds are more important to the thermodynamics of a system in that they stabilise unusual higher valence states of the central atom. For example, both I^+ and Br^+ species are quite reactive. In the structure of 4,5-dicyano-2-imidazolyl(phenyl) bromonium ylide, however, the bromine atom (Br^+) has a square planar arrangement of two primary bonds and two secondary bonds to the nitrogen atoms of an imidazolyl ring and a cyano group, both

techniques for the stronger inter-molecular and particular intra-molecular

of which are negatively charged and could be expected to stabilise the charge on the bromine.⁴⁵ Similarly, the fact that all trivalent iodine compounds (formally I^{3+}) have square planar or pentagonal planar arrangements of primary and secondary bonds, unless strongly electro-negative groups are bonded to iodine (Chapter III) can be related to the stabilising influence of the secondary bonds. Even when lone pairs prevent a secondary bonding interaction collinear with a primary bond, it is still noticeable that this interaction is then split into several weaker contacts which avoid the lone pair(s). The xenon fluorides (see above), again with an unusual valence state of the central atom, are examples of this. Similarly, the structure of the diaryl dialkoxysulfurane $Ph_2S(OC(CF_3)_2Ph)_2$ is based on a trigonal bipyramidal arrangement with the two phenyl rings and a lone pair in the equatorial plane. The unusual sulfur valence state is then stabilised by 3 short intra-molecular S...F contacts of 2.87, 2.93 and 3.09 Å.⁴⁶ It is noticeable that in the analogous compounds $(p-ClC_6H_4)_2SCl_2$ the S-Cl axial bonds are considerably longer than single bond lengths and are involved in S-Cl...Cl-S-Cl...Cl contacts. Presumably the use of $p-Cl-C_6H_4$ groups and the lengthening of the S-Cl bonds all help stabilise the sulfur valency.⁴⁷

Finally, in 1-acetonyl-1-thionia-5-thia cyclooctane a transannular S...S contact of 3.12 Å ($C-S...S = 179^\circ$) is important in the transition state for reactions of this compound. Similarly, it can also be viewed as stabilising the charge on the sulfur atom (along with a short intra-molecular S...O contact of 2.81 Å [$C'-S...O = 156^\circ$]).⁴⁸

The influence of short inter-molecular contacts is not, however, restricted to secondary bonds, and electrostatic contacts are presumably responsible for stabilising unusual ionic complexes such as the oxo-carbenium ions of ref. 49 and ions such as $Sb_2F_4^{2+}$.⁵⁰

(VI.6.3.) Other physical measurements

In the majority of cases, the secondary bonding is confined to the solid state. In solution for some cases, the effects of molecular association should be observable by spectroscopic (i.r., n.m.r., etc.) or cryoscopic techniques for the stronger inter-molecular and particular intra-molecular

interactions whilst the increased molecular motions associated with the liquid state will prevent the weakest interactions from forming permanently. Any gas phase measurements are unlikely to find any intermolecular interactions other than van der Waals forces. However, gas phase electron diffraction and microwave determinations of molecular structure do serve as good comparisons of the unperturbed structure with that in the solid state involving the secondary bonds.

Since the majority of the effects of charge transfer interactions can be observed by a variety of methods and since secondary bonds are a particular class of σ - σ charge transfer compounds. In making these observations, separation of the complexes into the 3 types σ - σ , σ - π and π - π is readily apparent from their different effects.⁵¹ The presence of secondary bonding can readily be seen from shifts in i.r.,^{41,52} n.q.r.,⁵³ n.m.r.⁵⁴ and other physical measurements, made in both liquid and solid phases, as described for some examples in the previous chapters. The conductivity of several semiconductors, however, is especially related to secondary bonds.⁵⁵ However, one readily observable property which is indicative of secondary bonded systems is the colour of the crystals.

Although principally only applicable to compounds containing the heavier elements (Te, I, etc.), the colouration of the crystals of a compound can indicate not only the presence but also the type of secondary bonding present in that compound. McCullough has noted that the organotellurium diiodides display a range of colours from red-orange through to dark violet with the red crystals being associated with Te...I secondary bonds, and that the dark violet colour results when I...I inter-molecular secondary bonds are present.^{44,56} In other tellurium compounds, inter-molecular Te...Te contacts account for the crystal colour: 1,3-dimethylacetylacetone tellurium(II), for example, is connected into a one dimensional polymeric chain with Te...Te contacts of 4.04 Å and forms bright yellow crystals, although smaller Te...Te separations result in darker colourations.⁵⁷

Similarly, NI_3 , diiodomethylamine and $\text{N,N}'$ -tetraiodoethylene-diamine are all assumed to have very closely related polymeric structures based on corner shared nitrogen tetrahedra. All 3 compounds and some of their base adducts are soluble with difficulty in available solvents and all have very deep or black colours consistent with extensive I...I contacts ($\sim 3.6 \text{ \AA}$) between the chains of tetrahedra. If these contacts are disturbed by adduct formation with N bases, as in $(\text{NI}_3 \cdot 3\text{NH}_3)_n$ or in the adducts of diiodomethylamine with pyridine, trimethylamine or methylamine the colour of the products becomes lighter. Iododimethylamine by comparison is also lighter in colour and fairly soluble, so that I...I contacts are unlikely and the proposed structure is probably monomeric or linked into chains by N...I contacts only.⁵⁸

Finally α - α' -diselenobisformamidine dichloride is significantly different from related sulfur derivatives and forms a secondary bonded Cl...Se-Se...Cl system [$\text{Se} \dots \text{Cl} 3.19 \text{ \AA}$, $\text{C} \dots \text{Se-Se} 169.4^\circ$] which is responsible for the yellow colour of the crystals.⁵⁹

A theoretical treatment relating the crystal colour to the intermolecular interactions and which can also be used to explain the electrical properties of some of these compounds has been given by Donaldson and Silver.⁶⁰ In this, the compounds are assumed to form energy 'bands' by interactions between the non-bonding lone pair orbitals. The colouration of the compounds can then be related to the difference in energy between the band edges. Clearly, as the interacting atoms come closer, or as larger halogen and other heavy atoms are introduced into the structure, the band widths will increase so that the energy separation of the band edges decreases, and the colour of the compound darkens. This treatment is thus related to the band theories of metallic bonding and to the interpretation of the interactions in semiconductors.

18. G.C. Pimentel and J.L. McClellan, "The Hydrogen Bond", W.H. Freeman, 1960.

19. G.V. Fouts and J.D. Wright, *Angew. Chemie*, 1968, 7, 659, and refs. therein.

20. Chapter IV, ref. 16.

(VI.7.) References

1. (a) R.J. Gillespie and R.S. Nyholm, Quart. Rev., 1957, 11, 339;
(b) R.J. Gillespie, J. Chem. Educ., 1970, 47, 18; (c) R.J. Gillespie, 'Molecular Geometry', van Nostrand-Reinhold (London), 1972.
2. H.D.B. Jenkins and T.C. Waddington, Nature, 1975, 255, 623.
3. Chapter II, ref. 17.
4. J. Galy, G. Meunier, S. Andersson and A. Åstrom, J. Solid State Chem., 1975, 13, 142.
5. M.B. Ducourant, R. Fourcade, E. Philippot and G. Mascherpa, Rev. Chim. Miner., 1976, 13, 433; R. Astier, E. Philippot, J. Moret and M. Maurice, ibid., 1976, 13, 359. See also Chapter II, refs. 17 and 22.
6. Chapter II, ref. 21.
7. R.J. Hack and R.E. Rundle, J. Am. Chem. Soc., 1951, 73, 4321.
8. R.J. Gillespie, Can. J. Chem., 1961, 39, 318.
9. For example, K.S. Pitzer, Science, 1963, 139, 414; R.J. Gillespie, Angew. Chem., 1967, 6, 819 and ref. 1(a).
10. R. Gleiter and R. Hoffmann, Tetrahedron, and refs. therein.
11. J. Sletten, Acta Chem. Scand., 1976, A30, 397.
12. J.I. Musher, Angew. Chem. Int. Ed., 1969, 8, 54; also T.B. Brill, J. Chem. Edn., 1973, 50, 392.
13. A. Kitaigorodskii, 'Molecular Crystals and Molecules', Academic Press, 1973.
14. B. Chu, 'Molecular Forces', Interscience, 1967.
15. A.R. Denaro, 'A Foundation for Quantum Chemistry', Butterworths, 1975, Chs. 5 and 6.
16. A. Bondi, J. Phys. Chem., 1964, 68, 441.
17. L. Pauling, 'The Nature of the Chemical Bond', 3rd Ed., Cornell University Press, 1960.
18. G.C. Pimentel and A.L. McClellan, 'The Hydrogen Bond', W.H. Freeman, 1960.
19. C.K. Prout and J.D. Wright, Angew. Chemie, 1968, 7, 659, and refs. therein.
20. Chapter IV, ref. 16.

21. M.J.S. Dewar, *Bull. Soc. Chim. France*, 1951, 18, C71;
J. Chatt, *J. Chem. Soc.*, 1953, 2939. See also M. Orchin
and H.H. Jaffé, 'The Importance of Antibonding Orbitals',
Houghton Mifflin Co., (Boston), 1967.
22. R. Mason, *Nature*, 1968, 217, 543.
23. R.S. Mulliken, *J. Am. Chem. Soc.*, 1952, 74, 811. See also
O. Kh. Poleshchuk and Yu. K. Maksyutln, *Russian Chem. Rev.*,
1976, 12, 1077.
24. J.G. Wijnhoven, W.P.J.H. Bosman and P.T. Beurskens, *J. Cryst.
Mol. Str.*, 1972, 2, 7.
25. A.J. Edwards and K.O. Christie, *J. Chem. Soc. Dalton*, 1976,
175. In the centrosymmetrically bridged structures of the
diphenyl iodonium halides $(C_6H_5)_2IX$ ($X = Cl, Br$ or I), the
bridging I-X distances are much longer than single bond lengths
with the difference $(I-X)_{obs} - (I-X)_{single}$ surprisingly being
constant for the three compounds. This difference is roughly
equivalent to a bond order of ca. 0.35, N.W. Alcock and R.M.C.
Countryman, *J. Chem. Soc. Dalton*, 1977. See also N.J. Brondino,
S. Esperas and S. Husebye, *Acta Chem. Scand.*, 1975, A29, 93.
26. Chapter I, ref. 54.
27. D.L. Kepert, *J. Organometal Chem.*, 1976, 107, 49.
28. Yu. V. Zefirov and P.M. Zorkil, *Zh. Strukt. Khim.*, 1976, 17,
994 (C.A. 86:131510).
29. Yu. V. Zefirov, *Zh. Obshch. Khim.*, 1976, 46, 2636 (C.A.
86:49348).
30. I.D. Brown, *Acta Cryst.*, 1977, B33, 1305; compare this procedure
with that of W.L. Jolly and W.B. Perry, *Inorg. Chem.*, 1974, 13,
2686.
31. I.D. Brown and R.D. Shannon, *Acta Cryst.*, 1973, A29, 266.
32. Chapter V, ref. 22.
33. (a) Trinh-Toan and L.F. Dahl, *Inorg. Chem.*, 1976, 15, 2953;
(b) F.W.B. Einstein and A.C. MacGregor, *J. Chem. Soc. Dalton*,
1974, 778; and refs. therein.

34. G.L. Breneman and R.D. Willett, Acta Cryst., 1969, B25, 1073; R.C.L. Mooney-Slater, ibid., 1959, 12, 187.
35. J. Runsink, S. Swen-Walstra and T. Migchelsen, Acta Cryst., 1972, B28, 1331.
36. O. Andreasen, A.C. Hazell and R.G. Hazell, Acta Cryst., 1977, B33, 1109; G.A. Heath, P. Murray-Rust and J. Murray-Rust, Acta Cryst., 1977, B33, 1209.
37. D.E. McKae, A. Zalkin and N. Bartlett, Inorg. Chem., 1973, 12, 1713; K. Leary, D.H. Templeton, A. Zalkin and N. Bartlett, ibid., 1973, 12, 1726; N. Bartlett, B.G. de Boer, F.J. Hollander, F.O. Sladky, D.H. Templeton and A. Zalkin, ibid., 1974, 13, 780; K. Leary, A. Zalkin and N. Bartlett, ibid., 1974, 13, 775; N. Bartlett, M. Gennis, D.D. Gibling, B.K. Morrell and A. Zalkin, ibid., 1973, 12, 1717.
38. Chapter I, refs. 13 and 58.
39. Based on examination of data in O. Vikane, Acta Chem. Scand., 1975, A29, 787, and earlier papers from the same group. See also A. Hordvik, Acta Chem. Scand., 1966, 20, 1885.
40. E.M. Shustorovich and Yu. A. Buslaev, Inorg. Chem., 1976, 15, 1142.
41. Chapter III, ref. 6.
42. Chapter II, ref. 8.
43. P.D. Cradwick and A.S. de Endredy, J. Chem. Soc. Dalton, 1977, 146; ibid., 1975, 1926.
44. C. Knobler and J.D. McCullough, Inorg. Chem., 1977, 16, 612; ibid., 1976, 15, 2728, and refs. therein.
45. Chapter IV, ref. 23.
46. I.C. Paul, J.C. Martin and B.F. Perozzi, J. Am. Chem. Soc., 1972, 94, 5010.
47. N.C. Baenziger, R.E. Buckles, R.J. Maner and T.D. Simpson, J. Am. Chem. Soc., 1969, 91, 5749.
48. S.M. Johnson, C.A. Maler and I.C. Paul, J. Chem. Soc. (B), 1970, 1603.

49. B. Chevrier and R. Weiss, Angew. Chemie, 1974, 13, 1.
50. Chapter II, ref. 20.
51. See for example, V. Gutmann, Co-ord. Chem. Rev., 1975, 15, 207.
52. Chapter I, ref. 33; Chapter III, ref. 29; E.R. Clark and M.A. Al-Turaihi, J. Organometal. Chem., 1977, 124, 391; W.R. McWhinnie and P. Thavornyutikarn, J. Chem. Soc. Dalton, 1972, 551.
53. G.K. Semin, V.V. Saatsazov, T.A. Babushkina and T.L. Khotsyanova, Izv. Akad. Nauk. SSSR, 1975, 39, 2450; Yu. K. Maksyutin, E.N. Gur'yanova and G.K. Semin, Russ. Chem. Rev., 1970, 39, 334. T.L. Khotsyanova, T.A. Babushkina, V.V. Saatsazov, T.P. Tolstaya, I.N. Lisichkina and G.K. Semin, Koord. Khim., 1976, 2, 1567, demonstrate from the Br 79, Br 81 and I 127 nqr parameters of diphenyl iodonium bromide that the number of unbalanced p-electrons for I (0.95) and Br (0.07) is consistent with an incomplete transfer of an electron $I \rightarrow Br$ so that the ionic bond $I^+ Br^-$ must have some covalent secondary bond character.
54. Chapter II, ref. 14b and 16.
55. T.E. Phillips, T.J. Kistenmacher, A.N. Bloch, J.P. Ferraris and D.O. Cowan, Acta Cryst., 1977, B33, 427; M. Mellini and S. Merlino, ibid., 1976, B32, 1074.
56. J.D. McCullough, Inorg. Chem., 1975, 14, 1143.
57. J.C. Dewan and J. Silver, J. Organometal. Chem., 1977, 125, 125.
58. Chapter V, ref. 21.
59. A.C. Villa, M. Nardelli and M.E.V. Tani, Acta Cryst., 1970, B26, 1504.
60. J.D. Donaldson and J. Silver, J. Solid State Chem., 1976, 18, 117, and earlier work.

CHAPTER VII

Hypho Boranes

(VII.1.) Introduction; n centre - m electron bonding

Since the initial discovery of the boranes by Stock in the 1920-1930's,¹ the chemistry and physical properties of these compounds, their anions and the closely related carboranes has been extensively investigated. Part of the considerable interest in these compounds is that they were and still are structurally novel.² Attempts to describe their structures in terms of normal valence structures with two-centre two-electron bonds met with failure resulting in the introduction of three-centre two electron delocalised bonding and other multi-centre interactions. The term 'electron deficient' was similarly introduced to describe this and other classes of compounds where there are too few valence electrons available to provide a pair of electrons between every pair of atoms close enough to be regarded as covalently bonded.³

The hydrogen bridged structure of the first member of the series, diborane, was initially recognised by infra-red vibrational analysis although several workers favoured an ethane-like structure. The results of an electron-diffraction study, however, served as confirmation of the hydrogen bridged structure (Fig. VII. 1).⁴ This structure is also the first in the borane series with a three-centre hydrogen bridge bond formed when each of the hydrogen 1s orbitals interact with two sp^3 hybrid orbitals from the two borons, so that overall there are two three-centre two electron molecular orbitals above and below the B_2H_4 plane. This represents a convenient MO picture of the bonding although alternative valence bond structures have been formulated including structures where the hydrogen atoms (as H^+) interact with the π -orbitals of a B-B 'ethylenic type' double bond - the protonated double bond model.⁴

The structures of other members of the borane series (B_4H_{10} , B_5H_9 , B_5H_{11} , B_6H_{10} , etc.) were established unambiguously by Lipscomb using low temperature X-ray data.^{4,5} Recently this structural work has

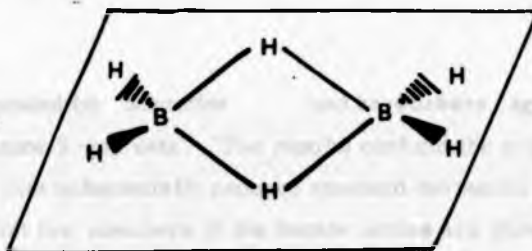


Fig. VII.1

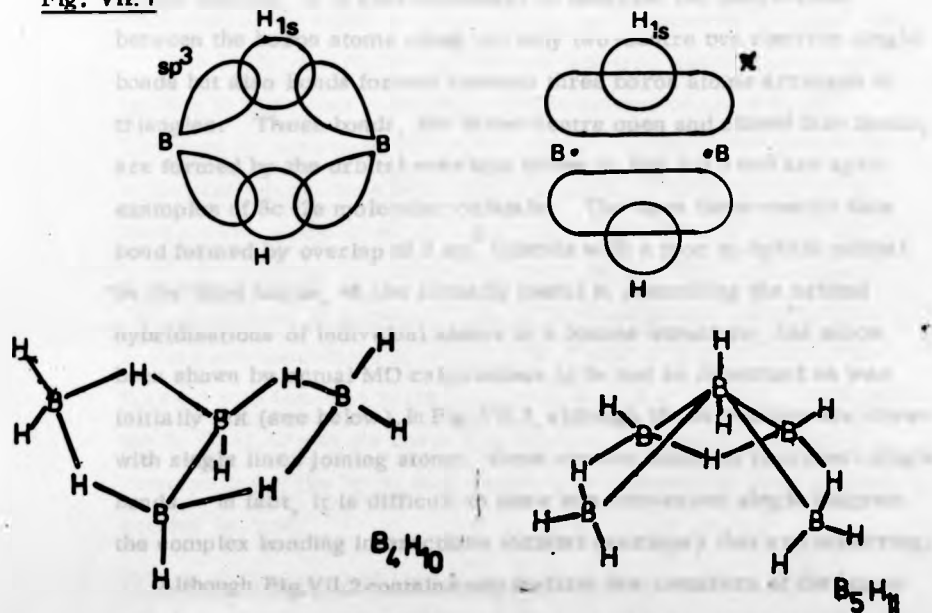


Fig. VII.2

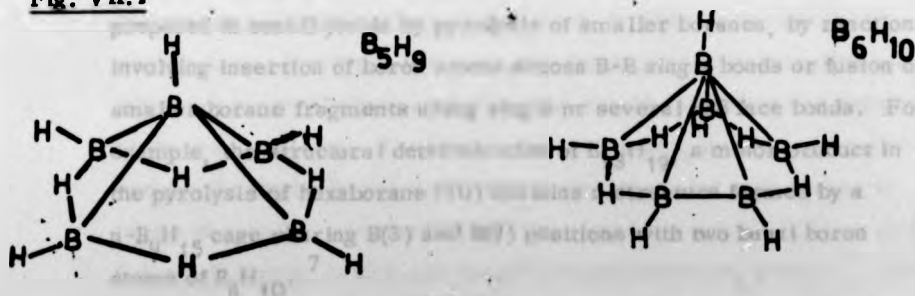
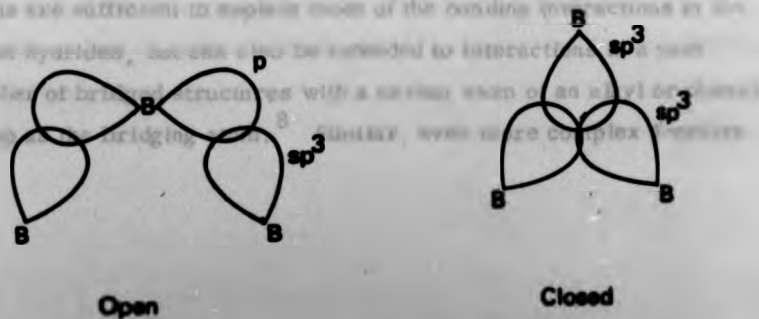


Fig. VII.3



been repeated by Schaeffer and co-workers, again using low temperature X-ray data. The results confirm the original structures but now with substantially reduced standard deviations.⁶ The structures of the first few members of the borane series are shown schematically in Fig.VII.2. In these structures, as well as three-centre hydrogen bridge bonding, it is also necessary to describe the interactions between the boron atoms using not only two-centre two electron single bonds but also bonds formed between three boron atoms arranged in triangles. These bonds, the three-centre open and closed face bonds, are formed by the orbital overlaps shown in Fig.VII.3 and are again examples of 3c-2e molecular orbitals. The open three-centre face bond formed by overlap of 2 sp^3 hybrids with a p or sp hybrid orbital on the third boron, whilst initially useful in describing the orbital hybridisations of individual atoms in a borane structure, has since been shown by actual MO calculations to be not as important as was initially felt (see below). In Fig.VII.2, although the structures are drawn with single lines joining atoms, these are not meant to represent single bonds. In fact, it is difficult to show in a convenient single diagram the complex bonding interactions (orbital overlaps) that are occurring.

Although Fig.VII.2 contains only the first few members of the boron hydride series, numerous higher members of the series have been prepared in small yields by pyrolysis of smaller boranes, by reactions involving insertion of boron atoms across B-B single bonds or fusion of smaller borane fragments using single or several BBB face bonds. For example, the structural determination of $B_{13}H_{19}$, a minor product in the pyrolysis of hexaborane (10) contains a structure formed by a $n-B_9H_{15}$ cage sharing B(3) and B(9) positions with two basal boron atoms of B_6H_6 .⁷

The 3c-2e molecular orbitals of the hydrogen bridge and boron face bonds are sufficient to explain most of the bonding interactions in the boron hydrides, but can also be extended to interactions in a vast number of bridged structures with a carbon atom of an alkyl or phenyl group as the bridging atom.⁸ Similar even more complex 4-centre


2 electron M.O. schemes have been postulated in one example of a carbaborane and in structures from other groups of the Periodic Table, especially the lithium alkyls.⁹ The carbaborane involved is B_5CH_7 ¹⁰ which from a microwave study is reported to possess a hydrogen bridging a BBB face resulting in three long B...B 'bonds' which may be described using either 4c-2e M.O.'s or as a protonated BBB face bond.

The 3c-2e (and higher n-centre m-electron where appropriate) bonding interactions in the boranes and related compounds can therefore be seen to be related to the multi-centre inter- and intra-molecular interactions described in Section I where the secondary bond model uses 3c-4e M.O.'s to explain the linearity of systems X-A...Y where A...Y is the secondary bond. Also in the case of the iodobenzene diacetates (Chap. III) the secondary bonding interactions are considered to parallel the 3-centre face bonding of the boranes with two lone pairs interacting with a σ^* orbital. Although the 3c-2e M.O.'s in the boron hydrides are well established and in common usage, the 3c-4e description of the secondary bonding interactions is not.

(VII.2.) Topological Models

From the previous it can be seen that the bonding in the boranes and electron-deficient compounds is complex in nature and description. However, there are two topological models in particular which are a great help in describing the structure, bonding and geometries of these compounds. The first, Lipscomb's styx notation, describes various theoretically possible valence structures for each borane in terms of possible combinations of three- and two-centre BBB face and B-B single bonds, bridging hydrogens and terminal BH_2 groups.⁴ This notation cannot, however, describe the spacial distribution of the boron atoms which is the important feature of Wade's (and Rudolph's) notation. These models are described in more detail in the following sections.

(VII.2.1.) Lipscomb's styx notation⁴

This is a purely empirical set of simple equations which are based on the assumption that each boron atom provides four orbitals, and therefore is involved in precisely four bonds, whether these be two-centre or three-centre. Thus, in the simplest case of a neutral boron hydride $B_p H_{p+q}$ it is assumed that in any likely valence structure there will be s hydrogen bridges ($3c-2e$), t closed (or open) three-centre  bonds ($3c-2e$), y B-B single bonds and x extra hydrogen atoms on the p B-H groups, i.e. BH_2 groups. For each valence structure the following equations of balance must hold:

$$s + x = q \quad (1)$$

$$s + t = p \quad (2)$$

$$p + q/2 = s + t + y + x \quad (3)$$

$$\text{Using (1), } p = t + y + q/2 \quad (4)$$

Equation (1) balances hydrogen atoms, (2) equates the number of three-centre bonds to the number of boron atoms (p) since each boron provides four orbitals but only 3 electrons and (3) equates the $p + q/2$ electron pairs to the $s + t + y + x$ bonds in the structure which reduces to equation (4). The equations as derived for a neutral boron hydride $B_p H_{p+q}$ are readily modified to include anion or cation charges or the substitution of BH groups by carbon to give the carbaboranes.¹¹

Similarly, for the higher boranes it is possible that the basic assumption that each boron atom forms at least one exoskeletal $2c-2e$ B-H bond will be broken. Again the basic equations are readily modified.¹²

Using the simple equations (1-4) for B_5H_9 gives $s + x = 4$; $s + t = 5$ and $t + y = 3$, from which three solutions, [4120], [3211] and [2302], written in styx order, are obtained.

The possible solution with $s = 1$ or 5 are not allowed, as they would give negative values for y and x respectively.¹³ Clearly, as p and q increase the number of possible valence structures with sets of styx values also increases, although only a few of these structures are actually found and isomeric forms of a particular hydride are not

normally isolable. However, all of these possible structures have to be considered in any MO computations on the orbital structure of a particular hydride. In correlating the observed structure with likely styx values, several simple principles are of use in eliminating the majority of the likely structures. These principles are based on observations of symmetry or restricted inter-orbital angles.¹⁴

Before discussing Wade's notation which deals with the spatial arrangement of the boron atoms, it is important to discuss how styx structures with localised two- and three-centre bonds can be obtained from the results of accurate self-consistent field (SCF) or other MO calculations. These localised chemical bonds are in fact obtained by mixing together MO's of different symmetries, a process which maximises the sum of the repulsions between electrons within the same MO while at the same time minimising the exchange energy and the inter-orbital electron repulsion energy. Using this procedure, Lipscomb was able to derive a series of localised molecular orbitals (LMO) from accurate SCF-MO calculations which in bonding terms are directly comparable to the elements of the styx notation. A quantity d [Equation 5] calculated for each orbital (LMO) is a good indicator of the number of centres over which each bond forms.

$$d = 100 \left[\frac{1}{2} \int (\varphi_L - \varphi_T)^2 dv \right]^{\frac{1}{2}} \quad (5)$$

The calculation of d therefore defines a percentage delocalisation for each orbital, where φ_L is the calculated LMO and φ_T is a truncated LMO obtained by omitting relatively small contributions (less than about 0.2 electrons) to φ_L from other atoms in the structure and then renormalising the remaining orbital. The value of d can, therefore, vary from zero if the LMO is completely localised on the assumed atomic centres to 100% if φ_L and φ_T are completely orthogonal. The results of this type of analysis enabled a few basic bonding principles to be formulated. These may be summarised as follows:

- (1) No open three-centre bonds have been found to be important in the localised molecular orbitals of boranes although carboranes may

have open three centre bonds providing a C atom is central. Similarly, carboranes may have an adjacent pair of C atoms (or an adjacent boron and carbon) joined by both a single bond and also a central three-centre bond. This is not possible for adjacent borons.

(2) Unique preferred three-centre bonds exist in valence structures of B_2H_6 , B_4H_{10} , B_5H_{11} , B_6H_{10} and $1,2-C_2B_4H_6$.

(3) Structures for which three-centre bonds can be drawn are preferred over those which cannot be so expressed.

(4) In comparing isomeric structures, that with the larger number of nearly equivalent three-centre bond structures is preferred. This argument takes precedence over which choice has the more favourable charge distribution.

(5) Unique fractional three-centre bond descriptions exist for $4,5-C_2B_4H_8$ and probably also for $B_{10}H_{14}$, $B_{10}H_{14}^{2-}$ and B_9H_{13} whilst fractional three-centre bonds will replace an open three-centre bond and a single bond from the central atom to a fourth atom, except when C is the central atom.

(6) It is probable that valence structures having a vacant orbital which can easily be incorporated into three-centre bond structures are preferred over those which cannot.¹⁵

(VII.2.2.) Wade's rules¹⁶ (Hypoh systems)

Wade's rules were originally developed for the boron hydrides by considering the number of electrons required to fill all the bonding molecular orbitals (MO's) associated with each boron polyhedron, although their use can also be extended to other metal cluster systems. In the case of the boron hydrides the number of bonding orbitals in each polyhedron is obtained by considering each boron to be sp hybridised. Each exoskeletal BH bond is formed by the overlap of $H(1s)$ with one $B(sp)$ orbital, thus leaving the remaining sp orbital pointing into the polyhedron. A strongly bonding orbital results when all of these sp hybrids have the same phase. The p_x and p_y orbitals on each boron can similarly be combined to produce orbitals delocalised over the

whole polyhedron, half of which will be expected to be bonding and half anti-bonding. Therefore for a closed polyhedron $B_n H_n$ there will be $(n + 1)$ bonding orbitals available, all of which must be filled to produce a stable species. However, for $B_n H_n$, after the electrons associated with each exoskeletal B-H have been considered, there are only n electron pairs available for polyhedron orbitals so that stability results when the species bears a double negative charge. Theoretical calculations have confirmed that for $n = 6$ or 12 the stable species is in fact $B_6 H_6^{2-}$ and $B_{12} H_{12}^{2-}$.

Wade's approach then was to consider the effect of removing vertices from the closed structure. The significant finding was that for a structure of $(n - 1)$ boron atoms (based on an n -polyhedron with one vertex missing); stability, i.e. the filling of all bonding MO's, still requires $(n + 1)$ skeletal electron pairs. Similarly for the structure of $(n - 2)$ boron atoms (based on the closed n polyhedron with two vertices missing), $(n + 1)$ skeletal electron pairs are again required to fill all bonding MO's. Some of the missing electrons may be provided either as negative charges on the polyhedra or by the replacement of BH by CH. In the majority of structures the additional electrons are obtained by adding hydrogen atoms along open edges of the incomplete polyhedron as hydrogen bridges or BH_2 (BH_3) groups.[†]

The implementation of Wade's rules for borane and carbaborane systems is achieved by the following procedure:-

- (1) The system is written as $[(BH)_m (CH)_x H_y]^{z-}$
- (2) The number of skeletal electrons are counted (i.e. excluding the electrons in the exoskeletal B-H bonds). Each B-H unit contributes 2 electrons, each CH unit contributes 3 electrons, the extra hydrogen atoms each contribute 1 electron and finally z electrons are included for the charge. This process is summarised in the following equation:

$$\frac{1}{2}(2m + 3x + y + z) = n + \frac{1}{2}(x + y + z) = \text{no. of skeletal electron pairs where } n = m + x = \text{no. of basic (B+C) skeletal atoms.}$$

[†] The absence of open edges means that the closed polyhedral boranes only occur as di-negative species.

(3) The expected geometry of the boron polyhedra and ^{their} classification are then assigned on the basis of the above formula for the number of skeletal electron pairs. The results are summarised below:

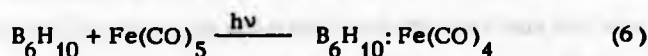
No. of skeletal electron pairs	Boron polyhedron	No. of missing vertices	Nomenclature	Examples [‡]
(n + 1)	n-polyhedron	0	<u>closo</u>	B ₆ H ₆ ²⁻ -octahedron all vertices occupied.
(n + 2)	(n+1)-polyhedron	1	<u>nido</u>	B ₅ H ₉ -square pyramid but based on octahedron with 1 vertex missing.
(n + 3)	(n+2)-polyhedron	2	<u>arachno</u>	B ₄ H ₁₀ -octahedron with 2 missing vertices. B ₃ H ₁₁ -pentagonal bipyramid with 2 missing vertices.
(n + 4)	(n+3)-polyhedron	3	<u>hypho</u> (Gk. net)	See below.

[‡] See also ref. 16. Table 1.


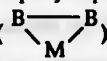
The majority of the boron hydrides, carboranes or related systems can be described as closo, nido or arachno systems. It is only recently that a fourth system with (n+4) skeletal electron pairs and which was given the name HYPHO (Greek for net) has been discussed in the literature. Such systems are even more open than arachno with the n atoms occupying all but three corners of an (n+3) polyhedron; they would be expected to be very reactive and have been postulated to be important reaction intermediates.¹³

Before concentrating on hypho systems, it is worthwhile to review briefly the other Lewis acid-base adducts of the boron hydrides which have been structurally characterised. Apart from the simple Lewis base adducts of the earlier boranes, several attempts were made to utilise the short B-B bond in hexaborane (10) in nucleophilic and other reactions where it would then act as a Lewis acid.¹⁷ Such reactions were eventually realised in 1968 when in a photolytic

reaction the adduct $B_6H_{10}:Fe(CO)_4$ was obtained (eqn. (6))¹⁸

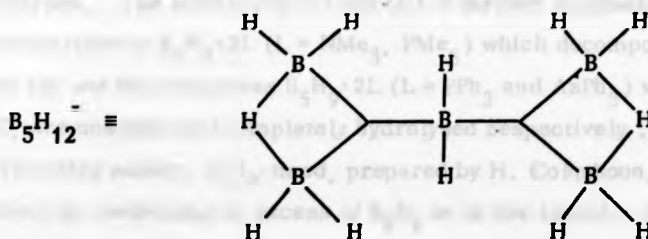


Crystallographic characterisation of this compound and the related adduct $(B_6H_{10})_2PtCl_2$ ¹⁹ both show the transition metals forming three-centre bridging interactions with this short bond. Furthermore, the adduct $[\mu Fe(CO)_4 \cdot B_7H_{12}]^-$ was similarly obtained and its structure is related to that of $\mu-Fe(CO)_4 \cdot B_6H_{10}$ with one of the basal bridging hydrogens of the B_6H_9 group now replaced by a $\mu-BH_3$ group.²⁰

With pentaborane (9) similar μ -bridged structures are likewise known with three-centre  bonding occurring with the remaining B_5H_8 group. However, although B_5H_9 and B_6H_{10} as well as several boron hydrides are now known to act as ligands to a variety of main group and transition metals, no general principles have yet emerged to predict what type of polyhapto bonding - 2e-2c σ bonding (B-M), 2e-3c bridge bonding () or hydrogen bridged structures (B-H-M) will be formed.²¹

None of these complexes are however known to have hypho structures and in fact very little structural data were known for hypho systems when work began on the crystal structures of the diphenylphosphino complexes of B_5H_9 although the crystal structures of both $B_5H_9 \cdot (PMe_3)_2$ and $B_6H_{10} \cdot (PMe_3)_2$ have recently been published by Shore and co-workers.²² Of the other known examples of hypho species many have been prepared and characterised using proton and ¹¹B nmr spectra although this method cannot show the very open nature of the skeletal structure. In some cases (e.g. $B_5H_9 \cdot tmed$) because of poor data or the fluxional behaviour of the open frameworks of these species, several postulated structures could equally well fit the experimental data.²³ One example, fairly well defined by this technique, is $B_5H_{12}^-$ which can be isolated as tetra *n*-butyl ammonium or triphenylmethylphosphonium salts which are white solids stable at low temperatures. The nmr data are consistent with a structure that has four basal atoms in the form of a pyramid. At

elevated temperatures the structure is again fluxional. The 2205 topological representation is consistent with the nmr data and would be even more open than the structure of nido B_5H_9 or arachno B_5H_{11} .²⁴



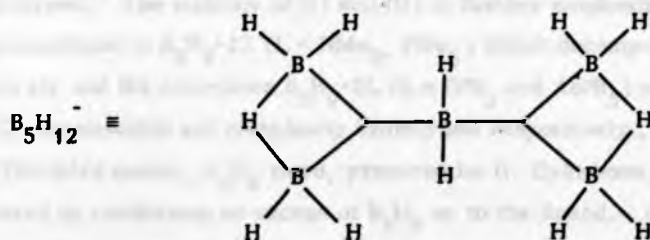
Variable temperature nmr data on the two bis triphenylphosphine adducts of B_5H_9 and B_6H_{10} have similarly been measured and reported with their crystal structures.²² The nmr data on $B_5H_9 \cdot dppm$ (I) and $B_5H_9 \cdot dppe$ (II) were recorded at a single temperature but could still be interpreted in terms of a single apical and four basal boron atoms per molecule.²⁵ The spectra are very similar to those of $B_5H_9(PMe_3)_2$ containing the same broad featureless signals.²⁶ Noise decoupling of the ^{11}B nmr spectra of (I) and (II) only sharpened the signals of the basal atoms which would suggest that (I) and (II) are fluxional in solution like $B_5H_9 \cdot (PMe_3)_2$. In both (I) and (II) the ^{31}P nmr contains two separate signals suggesting that co-ordination is at the apex and base. Furthermore, the methylene resonances in the 1H nmr of (I) is a doublet of doublets and not a triplet showing that the phosphorus atoms are not equivalent.²⁵

(VII.3.) Experimental

(VII.3.1.) Preparation

The colourless adducts (I) (m.p. $185-7^\circ$), and (II) (m.p. $159-60^\circ$) were originally prepared by G. Haran by stirring equimolar ratios B_5H_9 /ligand in THF at $25^\circ C$ for 72 hours. Variations in the conditions can lead to higher m.p. products which were presumed to be cross-linked polymers. Both adducts are stable indefinitely in air, and even in water at $25^\circ C$, and are only slowly hydrolysed by hot water or acid, which is remarkable for B_5H_9 derivatives. The corresponding reactions of

elevated temperatures the structure is again fluxional. The 2205 topological representation is consistent with the nmr data and would be even more open than the structure of nido B_5H_9 or arachno B_5H_{11} .²⁴



Variable temperature nmr data on the two bis triphenylphosphine adducts of B_5H_9 and B_6H_{10} have similarly been measured and reported with their crystal structures.²² The nmr data on $B_5H_9 \cdot dppm$ (I) and $B_5H_9 \cdot dppe$ (II) were recorded at a single temperature but could still be interpreted in terms of a single apical and four basal boron atoms per molecule.²⁵ The spectra are very similar to those of $B_5H_9(PMe_3)_2$ containing the same broad featureless signals.²⁶ Noise decoupling of the ^{11}B nmr spectra of (I) and (II) only sharpened the signals of the basal atoms which would suggest that (I) and (II) are fluxional in solution like $B_5H_9 \cdot (PMe_3)_2$. In both (I) and (II) the ^{31}P nmr contains two separate signals suggesting that co-ordination is at the apex and base. Furthermore, the methylene resonances in the 1H nmr of (I) is a doublet of doublets and not a triplet showing that the phosphorus atoms are not equivalent.²⁵

(VII.3.) Experimental

(VII.3.1.) Preparation

The colourless adducts (I) (m.p. $185-7^\circ$), and (II) (m.p. $159-60^\circ$) were originally prepared by G. Haran by stirring equimolar ratios B_5H_9 /ligand in THF at $25^\circ C$ for 72 hours. Variations in the conditions can lead to higher m.p. products which were presumed to be cross-linked polymers. Both adducts are stable indefinitely in air, and even in water at $25^\circ C$, and are only slowly hydrolysed by hot water or acid, which is remarkable for B_5H_9 derivatives. The corresponding reactions of

pentaborane (9) with the arsenic ligands $\text{Ph}_2\text{As}(\text{CH}_2)_n\text{AsPh}_2$ ($n = 1$ or 2) yielded only high m.p. polymeric materials whilst the anions $\text{B}_5\text{H}_8 \cdot \text{L}^-$ ($\text{L} = \text{dppm}$ or dppe) are similar to B_5H_8^- itself, and are again readily hydrolysed.²⁵ The stability of (I) and (II) is further emphasised by comparison to $\text{B}_5\text{H}_9 \cdot 2\text{L}$ ($\text{L} = \text{NMe}_3, \text{PMe}_3$) which decomposes in moist air and the complexes $\text{B}_5\text{H}_9 \cdot 2\text{L}$ ($\text{L} = \text{PPh}_3$ and AsPh_3) which, at 25°C , are unstable and completely hydrolysed respectively.

The third adduct, $\text{B}_5\text{H}_9 \cdot \text{tmed}$, prepared by H. Colquhoun, was obtained by condensing an excess of B_5H_9 on to the ligand. (III) was found to be air-sensitive and could only be stored or recrystallised without decomposition if an excess of ligand was present. Compounds (I) and (II) are readily recrystallised from tetrahydrofuran, although very slow recrystallisation of (I) over the weekend resulted in the incorporation of a half-molecule of disordered solvent into the lattice.

Methanolysis of $\text{B}_5\text{H}_9 \cdot \text{tmed}$ has similarly produced colourless needle shaped crystals of $\text{B}_4\text{H}_8 \cdot \text{tmed}$. Preliminary work on this compound has shown that contrary to a previous report²³ the crystal class is monoclinic. A data set has been collected, and the structure solution apparently shows the structure of this compound to be disordered in a complex manner although this has yet to be confirmed completely. Attempts to recrystallise the original sample by several methods has also failed to produce better crystals.²⁷

(VII.3.2.) Data collection

Three-dimensional X-ray data for all three compounds were collected on a Syntex P2₁ diffractometer using Mo K_α radiation ($\lambda = 0.71069 \text{ \AA}$). In each case, the cell constants were obtained by least squares refinement of the diffracting positions of up to 15 high angle reflections.

(VII.3.2(i)) $\text{B}_5\text{H}_9 \cdot \text{dppm}$

For the data collection, a needle shaped crystal measuring $.12 \times .20 \times .98 \text{ mm}$ was obtained by cleaving a larger crystal perpendicular to its needle axis.

Crystal data

$C_{25}H_{31}P_2 \cdot \frac{1}{2}C_4H_4O$, $M = 481.5$, orthorhombic, $a = 7.931(4)$, $b = 16.816(5)$, $c = 23.271(8)$ Å, $V = 3105(2)$ Å³, $D_c = 1.03$ g/cm³ for $Z = 4$. Mo K_{α} radiation ($\lambda = 0.71069$ Å), $F(000) = 1016.0$. Systematic absences $h0l$, $h \neq 2n$, $0k0$, $k \neq 2n$ and $00l$, $l \neq 2n$ indicates space group $P2_12_12_1$ (No. 17). Data were collected out to a maximum 2θ of 50° . Reflections were measured using $\theta - 2\theta$ scans using scan ranges which varied from $(K_{\alpha_1} - 0.7)$ to $(K_{\alpha_2} + 0.7)$ at low $\sin \theta$ to $(K_{\alpha_1} - 0.8)$ to $(K_{\alpha_2} + 0.7)$ at higher angles. A variable scan rate of $1^\circ/\text{min}$ to $29.3^\circ/\text{min}$, depending on the intensity of a preliminary 2 sec count, was used. Background counts were recorded at each end of the scan, each for one quarter of the scan time. The intensities of three standard reflections were monitored every 100 reflections. A large drop in the values of the standards at one point was due to a generator failure and 124 reflections were later edited from the data set (not recollected). Apart from this sudden drop there are only statistical fluctuations in the standards.

Of 3031 data collected 1850 were considered observed ($I/\sigma(I) \geq 3.0$) and used in refinement.

(VII.3.2(II)) $B_5H_9 \cdot dppe$

For this compound, two data sets were collected. The structure was initially solved and refined using the first data set collected with Cu radiation ($\lambda = 1.5418$ Å). However, during this first data collection the crystal moved several times and required frequent re-centring. At a late stage in the refinement ($R = 17.6\%$ - all non-hydrogen atoms anisotropic) the listed reflections clearly fell into groups with alternating ΔF positive and negative due to crystal movement and the data set was rejected.

The second data set was collected with the same crystal but this time using Mo radiation ($\lambda = 0.71069$ Å). The following crystal data refers to this 2nd data collection.

Crystal data

$C_{26}B_5H_{33}P_2$, $M = 461.6$, orthorhombic, $a = 14.297(4)$, $b = 16.492(6)$ and $c = 22.280(9)$ Å, $V = 5253(3)$ Å³, $D_c = 1.17$ g/cm³ for $Z = 8$. Mo K_α radiation ($\lambda = 0.71069$ Å), $F(000) = 1952.0$. Systematic absences $Ok1$, $k \neq 2n$, hOl , $l \neq 2n$ and hkO , $h \neq 2n$ indicates space group $Pbca$ (No. 61).

For the second data collection, reflections were measured to a 2θ max of 50° , using θ - 2θ scans over a scan range ($K_{\alpha_1} - 1.0^\circ$) to ($K_{\alpha_2} + 1.0^\circ$) and a variable scan rate of $1 - 29.3^\circ/\text{min}$. Three standards were measured after every 75 reflections and showed only statistical fluctuations. In this second data collection the pre-scan count was increased to 8 secs after 284 reflections had been collected, and a reflection was subsequently collected if this count exceeded 50 c.p.s.

Of the total of 3700 data collected using this method 2643 reflections were considered observed ($I/\sigma(I) > 3.0$).

(VII.3.2(III)) $B_5H_9 \cdot tmed$

Crystals of $B_5H_9 \cdot tmed$ are clear colourless platelets when first exposed but which gradually decompose over a period of an hour or two if left in moist air. Preliminary work on the diffractometer using a thin crystal mounted in a Lindemann capillary revealed a possible tetragonal solution. Since the crystal was not scattering too well, further work was by precession photographs. These again showed $a \approx b$ but fail to show the required tetragonal 4-fold symmetry and the crystal class is orthorhombic.

From a recrystallised sample a larger hexagonal plate was selected and mounted on a fibre in a Lindemann capillary in a period of 15 - 20 min. No decomposition was evident overnight and this crystal was used for the data collection.

Crystal data

$C_6H_{25}B_5N_2$, $M = 179.3$, orthorhombic, $a = 12.940(2)$, $b = 12.911(3)$, $c = 15.046(2)$ Å, $V = 2513.9(8)$ Å³, $D_c = 0.95$ g/cm³ for $Z = 8$ (two independent molecules). Mo K_α radiation ($\lambda = 0.71069$ Å), $F(000) = 800.0$. Systematic absences hOO , $h \neq 2n$; OkO , $k \neq 2n$; and OOl , $l \neq 2n$ indicates space group $P2_12_12_1$ (No. 17).

TABLE VII. 1

Starting reflection sets for multiresolution direct methods program MULTAN

(a) $B_5H_9 \cdot dppm$

Σ_1		0	0	8		180°
origin	{	0	6	17		360°
		5	0	4		360°
		5	15	0		90°
other reflections	{	0	1	24	90,	270
		1	5	9	45,	315

Enantiomorph fixed by (0, 1, 24)

(b) $B_5H_9 \cdot dppe$

Σ_1	{	0	0	8	180°
		0	0	14	360°
		0	0	20	360°
		0	0	24	360°
		0	2	14	360°
		0	14	0	180°
		10	0	0	180°
origin	{	2	15	16	360°
		5	16	16	360°
		4	14	17	360°
other	{	1	2	8	180° or 360°
		5	18	5	180° or 360°

(c) $B_5H_9 \cdot tmed$

origin fixing	{	0	3	11	90°
		1	2	0	90°
		2	0	1	90°
other reflections	{	4	4	2	45°, 135°
		6	3	10	±45°, ±135°
		7	6	5	±45°, ±135°

Enantiomorph fixed by (4, 4, 2)

Data were collected using θ - 2θ scans over a scan range ($K_{\alpha_1} - 0.9^\circ$) to ($K_{\alpha_2} + 0.9^\circ$) to a maximum 2θ of 50° . A variable scan rate of $1 - 29.3^\circ/\text{min}$ depending on a preliminary 2 sec count was used. Three standards collected every 70 reflections showed only statistical fluctuations. Other conditions were the same as in (VII.3.2.(1)). Of 2858 data collected 1200 were considered observed ($I/\sigma(I) \geq 3.0$).

In all three compounds Lorentz and polarisation were applied. All three compounds were eventually solved using direct methods.
 (VII.3.3) Structure Solutions
 (VII.3.3(1)) $\text{B}_5\text{H}_9 \cdot \text{dppm}$

The structure of (I) was solved using NORMAL and MULTAN. Using rigid phenyl groups in the calculation of normalised structure factors for the 3031 data collected, the final statistics and the distribution of the E's clearly showed that the acentric space group $P2_12_12_1$ was correct. In MULTAN, using 295 reflections with $E > 1.55$, 1500 phase relationships with a minimum abs ($E(\underline{h})E(\underline{k})E(\underline{h}-\underline{k})$) of 7.21 were found. The starting set of reflections after the convergence mapping is shown in Table VII.1. In the case of an acentric space group, the 'hand' or enantiomorph has to be specified by restricting the possible phases of the starting reflections. In $P2_12_12_1$ with two general reflections, the enantiomorph is fixed by giving one reflection values of $\pm \pi/4$ and the other values of $\pm \pi/2$. These two general reflections, therefore, gave four phase sets with absform indices: 0.9295, 0.9302, 1.3255 and 0.9864. The third phase set was given by $(1, 5, 9) = 315^\circ$ and $(0, 1, 24) = 90^\circ$ and 19 atoms of the expected structure were immediately visible in the resulting E-map. These atoms gave $R = 34.4\%$ after 2 cycles of least squares refinement and the remaining non-hydrogen atoms were located in the subsequent Fourier. These non-hydrogen atoms were refined for several cycles of least squares, first with isotropic then anisotropic temperature factors, so that the R factor dropped to 15.3%. At this point the difference Fourier contained several peaks attributable to hydrogen atoms and several elongated peaks of sufficient height to be half-weight carbon atoms. These peaks were also found to be present in the initial E-map and the subsequent F_o Fourier. These peaks were attributed to a half-molecule of tetrahydrofuran solvent on a general position, and the best agreement was given when the molecule was

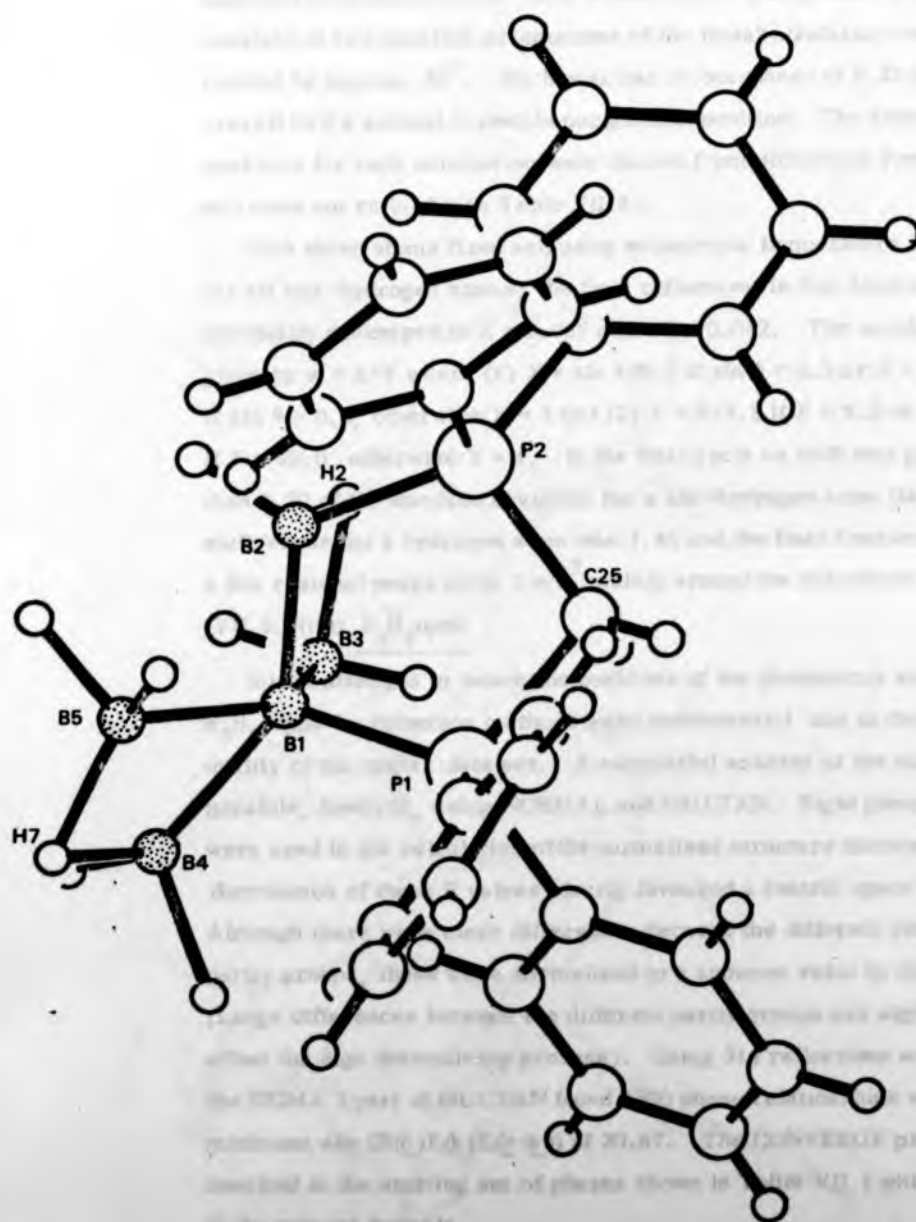


Fig. VII. 4 General view of molecule of $B_5H_9 \cdot dppm$

assumed to be disordered. The model chosen to represent the disorder consists of two separate orientations of the tetrahydrofuran molecule rotated by approx. 36° . Each peak has an occupancy of 0.25 giving overall half a solvent molecule per general position. The atomic positions for each orientation were chosen from difference Fourier's and were not refined (see Table VII. 8).

With these atoms fixed and using anisotropic temperature factors for all non-hydrogen atoms, the final refinement in five blocks eventually converged to $R = 0.069$ and $wR = 0.082$. The weights w were given by $w = X \cdot Y$ where (1) $X = \sin \theta / 0.3$ if $\sin \theta < 0.3$ or $X = 0.4 / \sin \theta$ if $\sin \theta > 0.4$, otherwise $X = 1$ and (2) $Y = F / 9.5$ if $F < 9.5$ or $Y = 20.0 / F$ if $F > 20.0$, otherwise $Y = 1$. In the final cycle no shift was greater than 0.50 of its standard deviation for a non-hydrogen atom (largest shift/error for a hydrogen atom was 1.4) and the final Fourier contained a few residual peaks up to $1 \text{ e}/\text{\AA}^3$ mainly around the disordered solvent. (VII.3.3(II)) $B_5H_9\text{-dppe}$

Initial attempts to locate the positions of the phosphorus atoms in $B_5H_9\text{-dppe}$ by Patterson methods were unsuccessful due to the poor quality of the initial data set. A successful solution of the structure was possible, however, using NORMAL and MULTAN. Rigid phenyl groups were used in the calculation of the normalised structure factors and the distribution of these E values clearly favoured a centric space group. Although there were clear differences between the different reflection parity groups, these were normalised to a common value by the program. (Large differences between the different parity groups can significantly affect the sign determining process). Using 314 reflections with $E > 2.0$, the SIGMA 2 part of MULTAN found 1500 phase relationships with a minimum $\text{abs}(E(\underline{h})E(\underline{k})E(\underline{h}-\underline{k}))$ of 20.67. The CONVERGE process resulted in the starting set of phases shown in Table VII. 1 which was used in the tangent formula.

The ABSFOM indices of the four resulting phase sets had the values 0.6221, 1.0399, 0.6414 and 0.5034. The second of these phase sets

was given by $(1, 2, 8) = '-'$ and $(5, 18, 5) = '+'$. The resulting E-map from this phase set had two large peaks but with significantly different heights (559 and 271, arbitrary units). However, least squares resulted in an R-factor of 54.5% for these two phosphorus positions and the following Fourier synthesis revealed several phenyl rings. Eventually, when all the non-hydrogen atoms had been located, several cycles of least squares, even with all atoms anisotropic did not lower R below 17.7%. At this point, the data set was rejected.

Using the second data set collected with Mo-radiation, 66 atoms (including hydrogens) were loaded and two cycles of least squares with all temperature factors isotropic reduced R to 8.5%. Anisotropic temperature factors for all non-hydrogen atoms reduced this further to 5.4%. After repositioning several hydrogen atoms (ring hydrogens in calculated positions, $C-H = 0.95 \text{ \AA}$), and including corrections for extinction and dispersion effects, the refinement in 5 blocks eventually converged to $R = 0.047$ and $wR = 0.063$. The weights used were given by $w = \sqrt{A + B + C \cdot F^2}$ where $A = 14.6$ and $B = 0.0073$.

(VII.3.3(III)) $B_5H_9 \cdot tmed$

Compound (III) was also solved by direct methods. Normalised structure factors for the 2858 reflections collected were calculated using the X-RAY link NORMSF. The distribution of the E_{hkl} 's was consistent with the acentric space group $P2_12_12_1$. Initially direct methods were applied using MULTAN on 298 reflections with $E > 1.50$. 2000 phase relationships with a minimum abs ($E(h)E(k)E(h-k)$) of 6.42 were found, but the sigma 1 formula failed to fix the signs of any reflections. The convergence mapping resulted in the starting set of reflections shown in Table VII.1 with the enantiomorph being fixed by the (4, 4, 2) reflection. With 3 general reflections, 32 phase sets were expected. However, the program ran out of process time after 22 phase sets had been calculated and was not re-run because it was discovered that at that time the link FOURR was missing the necessary code to calculate E-maps. Of the 22 phase sets calculated, the highest absform of 1.0988 was given by the first calculated set of phases with (4, 4, 2), (6, 3, 10) and (7, 6, 5) with

phase angles of 45° . This phase set was investigated further using the direct method links in the program SHELX.²⁷ For acentric structures this program requires the starting set of reflections to be input by the user from a previously calculated convergence map. In the present case, the origin fixing reflections from MULTAN and the above three values (45°) of the general reflections were input and the other phases of the 230 reflections with $E > 1.55$ were determined. From the resulting E-map, 25 of the expected 26 non-hydrogen atoms were found amongst the most prominent peaks (several peaks spurious). Including all these peaks as carbon atoms and refining for two cycles of least squares on all reflections resulted in an R of 0.333. From the resultant temperature factors and chemical intuition the atoms were correctly re-assigned and the missing carbon atom in one of the tmed ligands was found in the subsequent Fourier.

All subsequent calculations were performed using the XRAY system. After repositioning atoms B13 and B23 and refining with isotropic temperature factors for all atoms, the R-factor decreased to 15.3%. The temperature factors of the second tmed were in general high ($U = 0.06 - 0.13$). After locating and including several hydrogen atoms in the structure factor calculations, the R factor decreased to 12.4%, at which point it became clear that the carbon atoms of the second tmed were disordered, existing in two separate conformations of equal weight. Adopting this model enabled the hydrogen atoms attached to this tmed to be located, some with unit population parameters. Keeping these atoms fixed during the final refinement cycles and allowing anisotropic temperature factors for all atoms except the carbon atoms of the disordered tmed, the least squares refinement in five blocks eventually converged to $R = 0.055$ and $wR = 0.049$. The weights used were given by $w = X \cdot Y \cdot (1/\sigma(F))^2$ where (1) $X = \sin\theta/0.245$ if $\sin\theta < 0.245$, otherwise $X = 1$ and (2) $Y = F/5.0$ if $F < 5.0$ or $Y = 18.0/F$ if $F > 18.0$, otherwise $Y = 1$. Six reflections with large $w(\Delta F)^2$ after the application of this scheme were rejected from subsequent refinement cycles. In the final refinement cycle

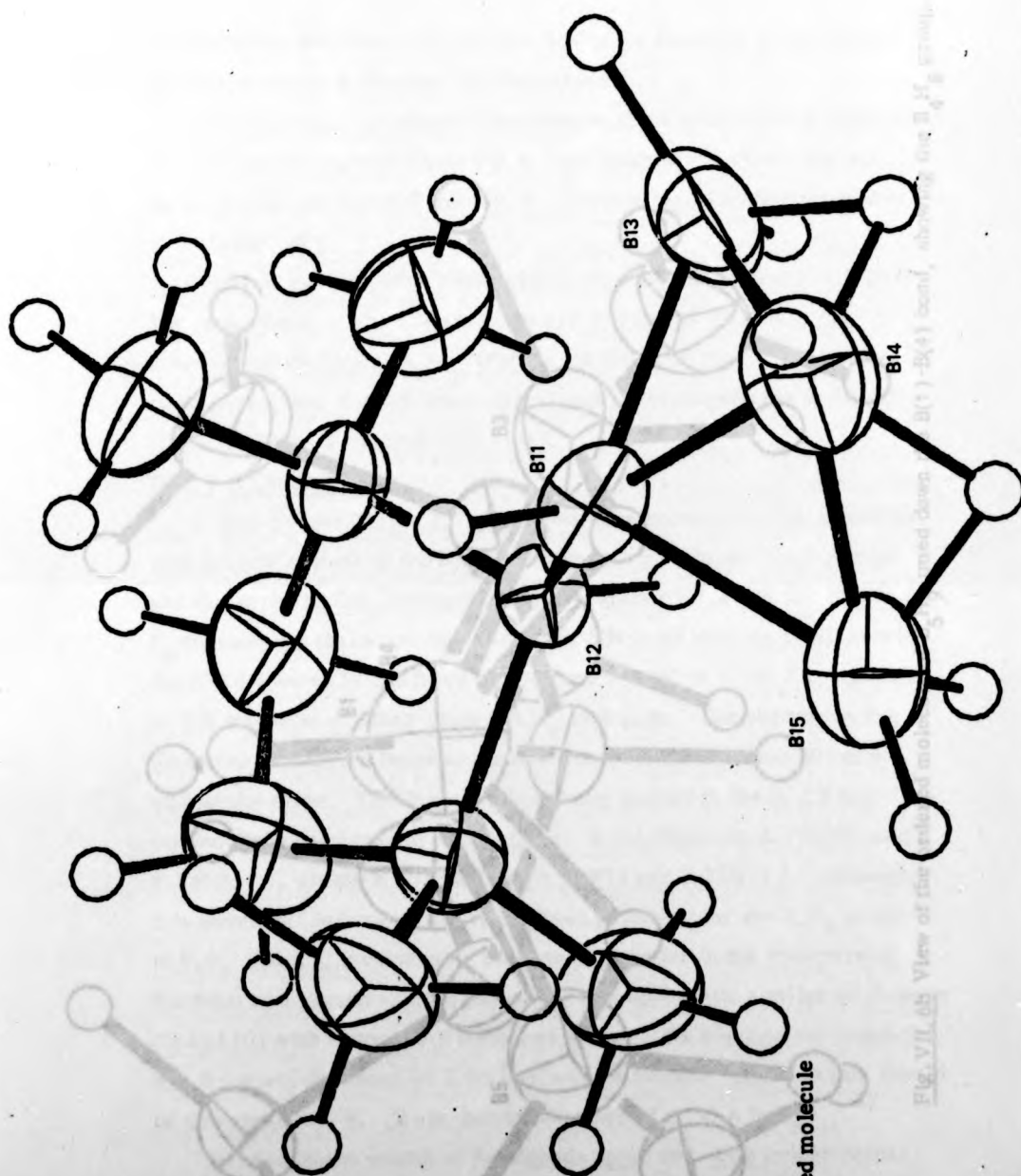


Fig. VII. 6a

General view of ordered molecule
of B₅H₉·tmed.

Fig. VII. 6b View of the molecule along the B(1)-B(4) bond, showing the B(1)-B(4) bond.

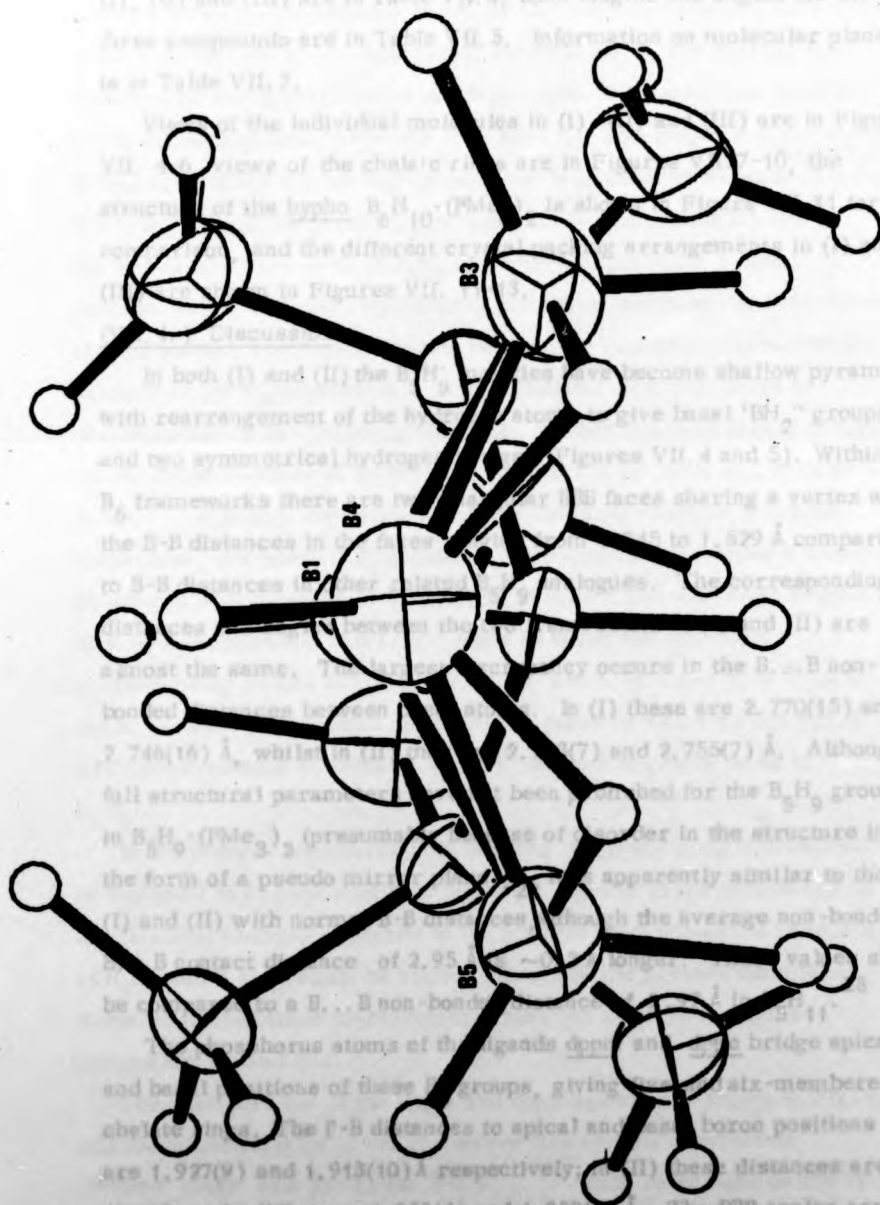


Fig. VII. 6b View of the ordered molecule of B_5H_9 viewed down the B(1)-B(4) bond, showing the B_4H_9 group.

no parameter shift was greater than 33% of its standard deviation and the final difference Fourier was featureless.

Final positional parameters and temperature factors for all atoms in (I), (II) and (III) are in Table VII. 4, bond lengths and angles for all three compounds are in Table VII. 5. Information on molecular planes is in Table VII. 7.

Views of the individual molecules in (I), (II) and (III) are in Figures VII. 4-6, views of the chelate rings are in Figures VII. 7-10, the structure of the hypho $B_6H_{10} \cdot (PMe_3)_2$ is shown in Figure VII. 11 for comparison, and the different crystal packing arrangements in (I) and (III) are shown in Figures VII. 11-13.

(VII. 4.) Discussion

In both (I) and (II) the B_5H_9 moieties have become shallow pyramids with rearrangement of the hydrogen atoms to give basal 'BH₂' groups and two symmetrical hydrogen bridges (Figures VII. 4 and 5). Within the B_5 frameworks there are two triangular BBB faces sharing a vertex with the B-B distances in the faces ranging from 1.745 to 1.829 Å comparable to B-B distances in other related B_5H_9 analogues. The corresponding distances and angles between the two frameworks in (I) and (II) are almost the same. The largest discrepancy occurs in the B...B non-bonded distances between basal atoms. In (I) these are 2.770(15) and 2.746(16) Å, whilst in (II) they are 2.723(7) and 2.755(7) Å. Although full structural parameters have not been published for the B_5H_9 group in $B_5H_9 \cdot (PMe_3)_2$ (presumably because of disorder in the structure in the form of a pseudo mirror plane),²² it is apparently similar to those in (I) and (II) with normal B-B distances, although the average non-bonded B...B contact distance of 2.95 Å is ~0.2 Å longer. These values should be compared to a B...B non-bonded distance of 2.97 Å in B_5H_{11} .²⁸

The phosphorus atoms of the ligands dppm and dppe bridge apical and basal positions of these B_5 groups, giving five- and six-membered chelate rings. The P-B distances to apical and basal boron positions in (I) are 1.927(9) and 1.913(10) Å respectively; in (II) these distances are significantly different, 1.953(4) and 1.939(4) Å. The BBP angles are within the range 107-117°. The difference in distances in (II) was

similarly found in $B_5H_9 \cdot (PMe_3)_2$ where the P-B distances to apical and basal positions are 1.90(1) and 1.98(1) Å.^{22a} In $B_6H_{10} \cdot (PMe_3)_2$, however, the P-B distances are the same (1.887 Å ave.).^{22b} In other adducts involving phosphorus-boron bonds, the P-B distances have varied from 1.83 to 1.96 Å.²⁹ Apart from steric factors, the shorter P-B distance for the apical bond presumably reflects the electron densities at the apical and basal positions (see later). The longer P-B distances in (II) are needed for the formation of the 6-membered as opposed to the 5-membered ring in (I). In forming the skeletal arrangements in compounds (I) and (II), the apical hydrogen atom of B_5H_9 must have migrated to a basal position during the rearrangement of the boron atoms on the introduction of four bonding electrons from the phosphorus atoms into the molecular orbitals of the B_5 polyhedron. With 9 skeletal electron pairs to accommodate in the *hypho*- B_5 skeleton, the boron atoms should occupy all but three vertices of an 8-vertex polyhedron by Wade and Rudolph's rules.¹⁶ Although the dodecahedron is the most common 8-vertex polyhedron, the present B_5 geometry more closely resembles a hexagonal bipyramid with a centre to apex height of 0.64 Å and with edge lengths of 1.81 Å (equatorial) and 1.77 Å (apex to base) for (I); the corresponding values in (II) are 0.645 Å, and 1.82 Å and 1.78 Å. The angle between the opposite triangular B_3 faces is 130.4° (I) and 126.5° (II) compared with an angle of 90 - 91° between opposite faces in B_5H_9 .

In the present structures, the bridging *dpmm* and *dppe* ligands would be expected to impose a certain degree of rigidity to the structures so that the fluxional changes observed in the bis(trimethyl phosphine) adducts of B_5H_9 and B_6H_{10} would be slightly slower in the present complexes. Variable temperature measurements have yet to be made on the compounds (I) and (II).

The configuration of the *dpmm* and *dppe* ligands are shown in Fig. VII. 10 and the torsion angles in the respective five and six membered chelate rings are in Table VII. 5. Both these ligands are very

Fig. VII. 7 View of the dodecahedral molecule of B_5H_9 -model

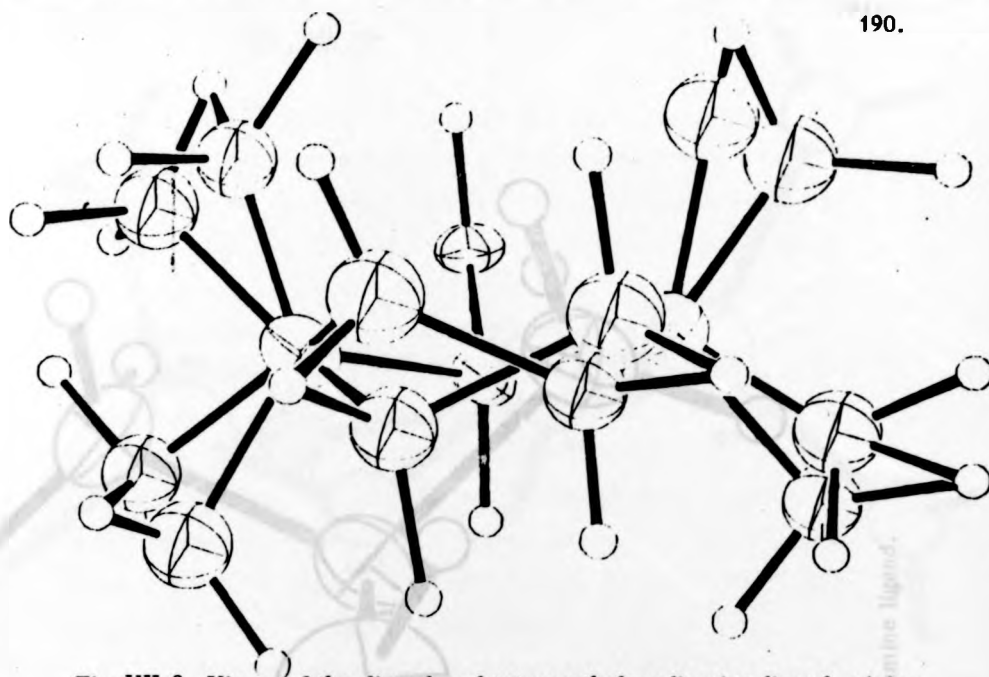


Fig. VII. 8 View of the disordered tetramethylenediamine ligand, giving the arrangement of hydrogen atoms.

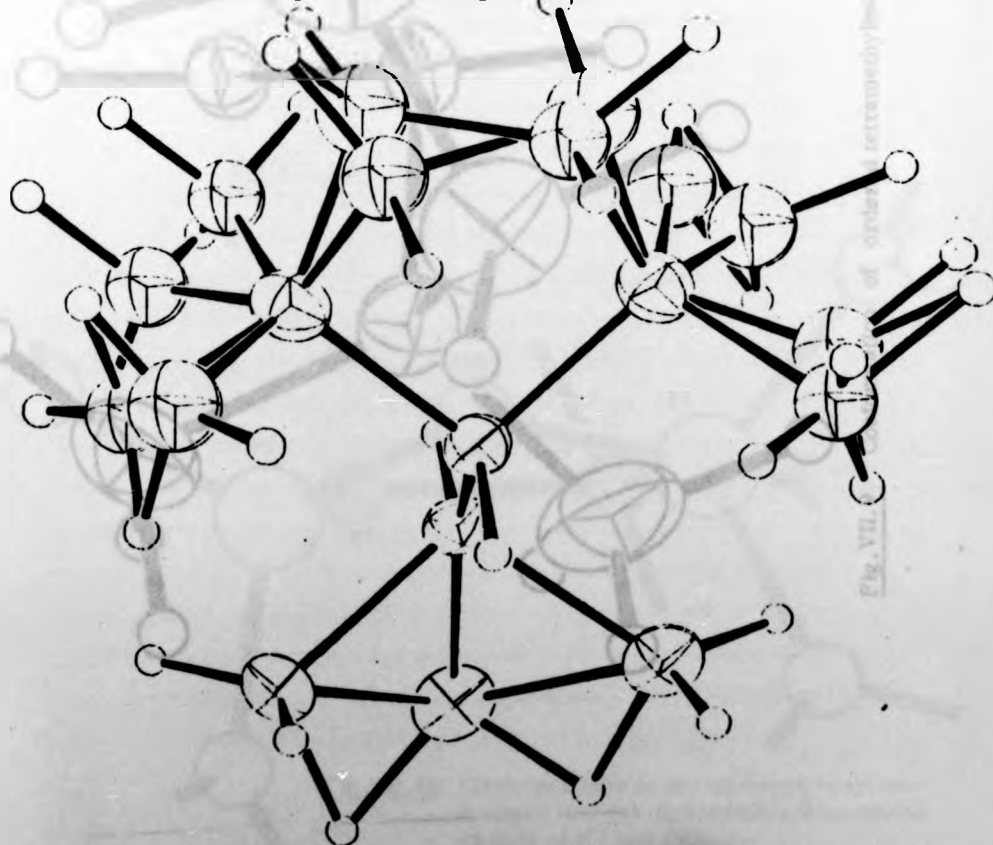


Fig. VII. 7 View of the disordered molecule of $B_5H_9 \cdot tmed$

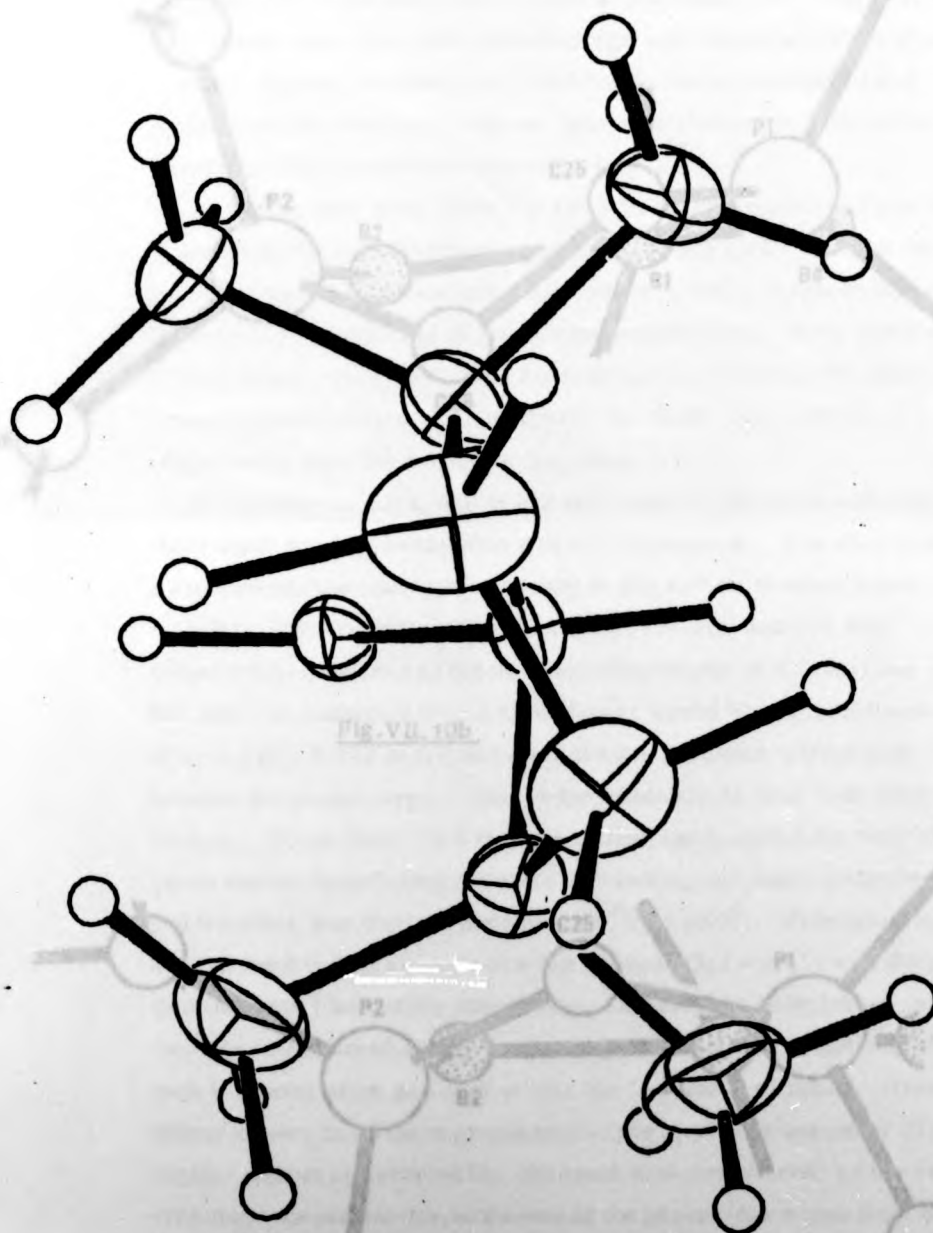


Fig. VII. 9 Conformation of ordered tetramethylene diamine ligand.

Fig. VII. 10 Conformations of (a) diphenylphosphino-
methane and (b) diphenylphosphinoethane
ligands of (I) and (II).

Fig. VII. 10a

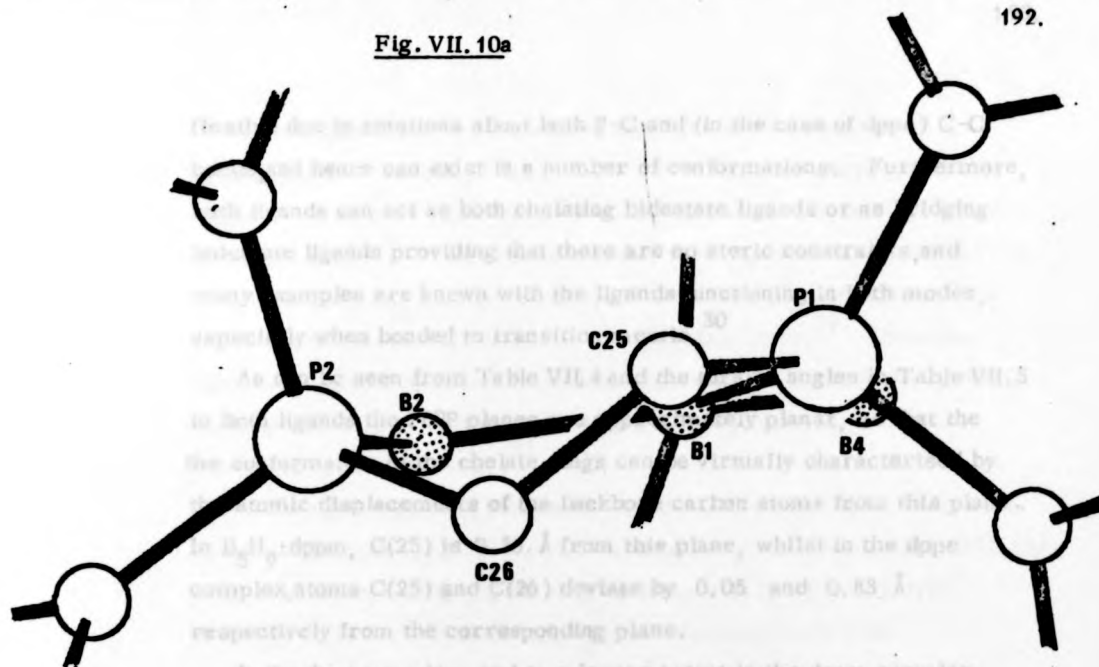


Fig. VII. 10b

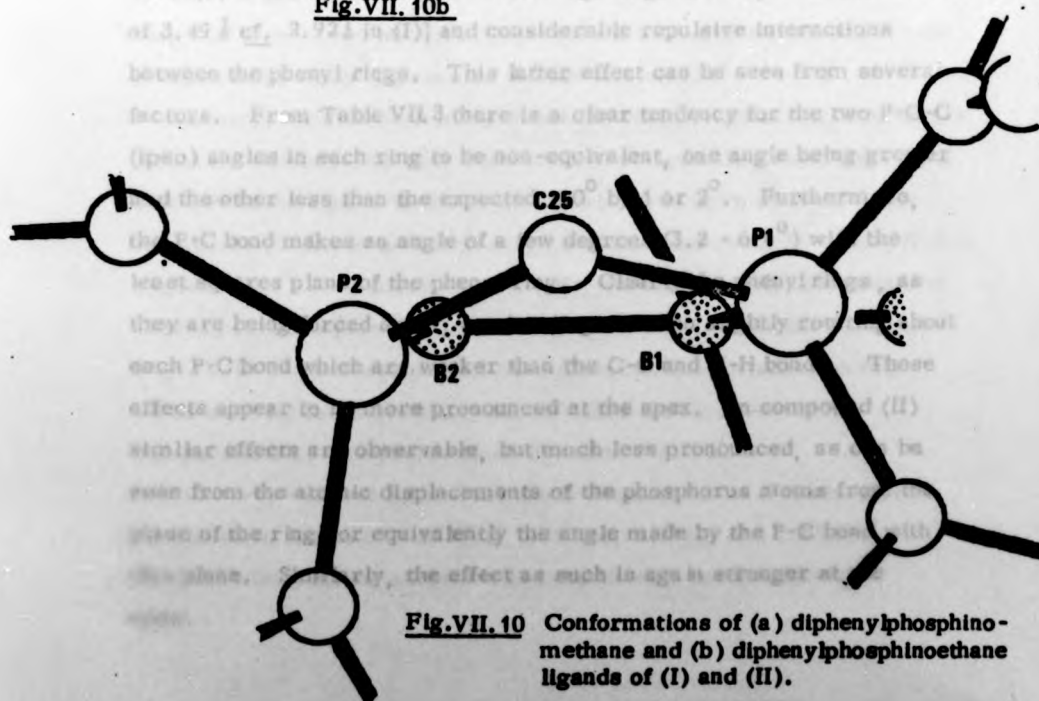


Fig. VII. 10 Conformations of (a) diphenylphosphinoethane and (b) diphenylphosphinoethane ligands of (I) and (II).

flexible due to rotations about both P-C and (in the case of dppe) C-C bonds, and hence can exist in a number of conformations. Furthermore, both ligands can act as both chelating bidentate ligands or as bridging bidentate ligands providing that there are no steric constraints, and many examples are known with the ligands functioning in both modes, especially when bonded to transition metals.³⁰

As can be seen from Table VII.4 and the torsion angles in Table VII.5 in both ligands the PBBP planes are approximately planar, so that the the conformation in the chelate rings can be virtually characterised by the atomic displacements of the backbone carbon atoms from this plane. In $B_5H_9 \cdot dppm$, C(25) is 0.56 Å from this plane, whilst in the dppe complex, atoms C(25) and C(26) deviate by 0.05 and 0.83 Å respectively from the corresponding plane.

In the dppe complex, and to a lesser extent in the dppm complex, there appears to be considerable strain in the ligands. The need to form a strained six membered chelate ring in (II) results in much larger P(1)-B(1)-B(2) and P(2)-B(2)-B(1) angles [117.2(3) and 115.9(3)° respectively compared to the corresponding angles of 107.7(6) and 107.4(6)° in compound (I)], a much larger ligand bite [P...P distance of 3.49 Å *cf.* 2.92 Å in (I)] and considerable repulsive interactions between the phenyl rings. This latter effect can be seen from several factors. From Table VII.3 there is a clear tendency for the two P-C-C (ipso) angles in each ring to be non-equivalent, one angle being greater and the other less than the expected 120° by 1 or 2°. Furthermore, the P-C bond makes an angle of a few degrees (3.2 - 6.6°) with the least squares plane of the phenyl ring. Clearly the phenyl rings, as they are being forced apart, are bending and also slightly rotating about each P-C bond which are weaker than the C-C and C-H bonds. These effects appear to be more pronounced at the apex. In compound (II) similar effects are observable, but much less pronounced, as can be seen from the atomic displacements of the phosphorus atoms from the plane of the rings or equivalently the angle made by the P-C bond with this plane. Similarly, the effect as such is again stronger at the apex.

These effects are not uncommon and have been extensively investigated by Coulson, Domenicano and Vacilago for phenylphosphino ligands and several other examples with second row non-metals attached to phenyl rings.³¹ The results of these investigations show that the use of a rigid body $D_{6h}(6/mmm)$ model for the substituted phenyl rings in these ligand classes will result in systematic errors.³² These and similar inductive effects may also be apparent in cyclohexylphosphine ligands resulting in systematic changes in bond angles and bond distances around the rings.³³

In the dppm ligand of compound (I), the C-C distances in the phenyl rings range from 1.326(18) to 1.408(15) Å (weighted average is 1.375(25) Å) with the corresponding angles varying from 116.7(10) to 122.1(8)^o (average 119.18). For the dppe ligand of compound (II) the corresponding C-C distances and CCC angles range from 1.346(8) to 1.407(6) Å (average 1.385(14) Å) and from 117.9(4) to 121.5(5)^o (average 119.99) respectively. The corresponding P-C(Ph) distances in (I) average 1.821 Å; in (II) they average 1.828 Å. These should be compared to the normal range of P-C(sp²) distances of 1.807(3) to 1.839(6) Å³¹ found in phosphines. Possibly because of the strains in the chelate ring and between the phenyl rings, there is no distinct difference in the P-C(Ph) and P-C(sp³) distances in both compounds.

In compound (III) both independent molecules contain a B₅ framework which is markedly different from those in compounds (I) and (II). Both nitrogen atoms donate to the same 'basal' boron atom forming a five membered chelate ring with average B-N distance of 1.673 Å and N-B-N angle of 97.1^o. In molecule 2 of (III), the chelate ring is disordered existing in two separate conformations with equal weight as shown in Fig. VII.7. The arrangement of the hydrogen atoms attached to this disordered ligand is similarly shown with a similar view of the conformation of the ordered tmed ligand in Fig. VII.8.

The ave. value of 1.673 Å for the B-N distances in (III) should be compared to values of 1.636(4), 1.610(6), 1.60(2) and 1.58(3) Å in the trimethylamine adducts with respectively boron trifluoride

Fig. VII. 11 Two views ((a) and (b)) of the hypho $B_6H_{10} \cdot (PMe_3)_2$ adduct. (Redrawn from co-ordinates in ref. 22b).

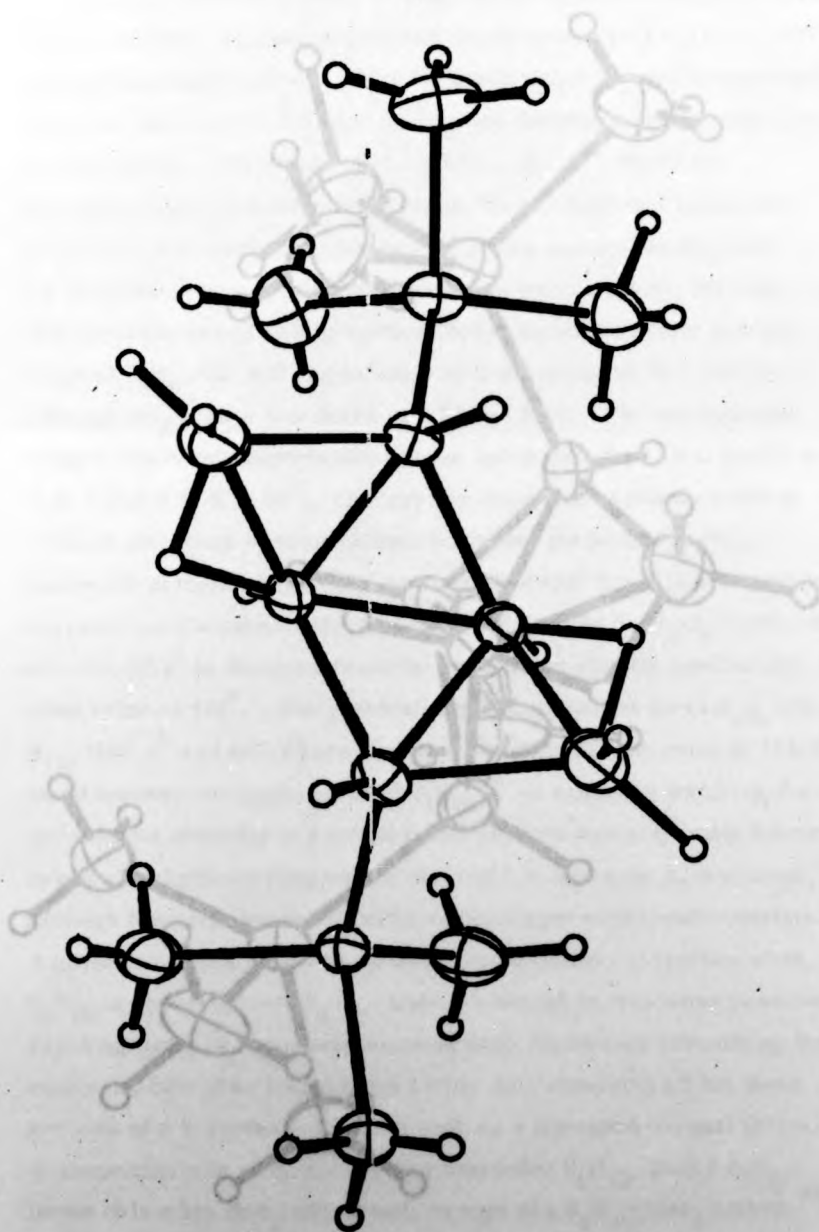


Fig. VII. 11a.

trichloride, -trifluoride and -tri-iodide and values of 1.609 Å and 1.878(2) Å [B-OH₂] in BH₃-PMe₃ and ammonia-trimethoxyborane, [Me₃-OH₂]-BMe₃ respectively.³⁵ Other examples of B-N distances are also in ref.35.

In both molecules of (III) the basal boron atoms bonded to the mixed ligands become, on rearrangement, singly bonded [B(1)-B(2) = 1.609 Å ave.] to the apical boron atom of the remaining B₅ unit. It is separated from the basal atoms B(3) and B(5) by one bonded distance of 2.704 Å [B(2)...B(3)] and 2.721 Å [B(2)...B(5)]. Within the triangular faces of the B₅ group the distances range from 1.699 to 1.835 Å with the shortest B(1)-B(4) [1.700 Å ave.] and the longest B(3)-B(4) [1.835 Å]. The arrangement of hydrogen atoms bears some similarity with the original B₅H₉ with B-H single bonds still occurring at B(1) and B(4) although BH₂ groups now occur at B(3) and B(5). The two hydrogen bridges are within experimental error symmetrical (B-H bridge is 1.32 Å and B-H-B is 64°), although the individual B-H bonds seem to indicate that there is some difference between the bridges (B-H(5) compared to that to H(4)). The B₅ unit is regarded as a hexagonal bipyramid with angles B₁B₄B₃ = 107.9(6)° and 107.8(5)° in the two independent molecules, slightly smaller than the ideal value of 120°. The dihedral angles between the faces B₁B₃B₅ and B₁B₄B₅ (129.4° and 127.4°) are, however, smaller than the value of 118.1° found between analogous faces of B₅H₉. A structure involving the bridging and chelating at a single boron atom was previously favoured over other possibilities on the basis of the *in vacuo* deviation, although the positions of boron and hydrogen atoms was uncertain.²³ A gross movement of the basal boron atoms also occurs when B₅H₉ is complexed with Me₃P, although in this latter case the resulting hydroborane forms an open framework resembling the equatorial belt of an icosahedron rather than occupying all but three vertices of a 9-vertex polyhedron with a tricapped trigonal prism.¹² In connection with this it should be noted that B₅H₉, unlike B₅H₇, forms only a *dis* PMe₃ adduct with no sign of a B₅H₉ PMe₃ adduct.²²

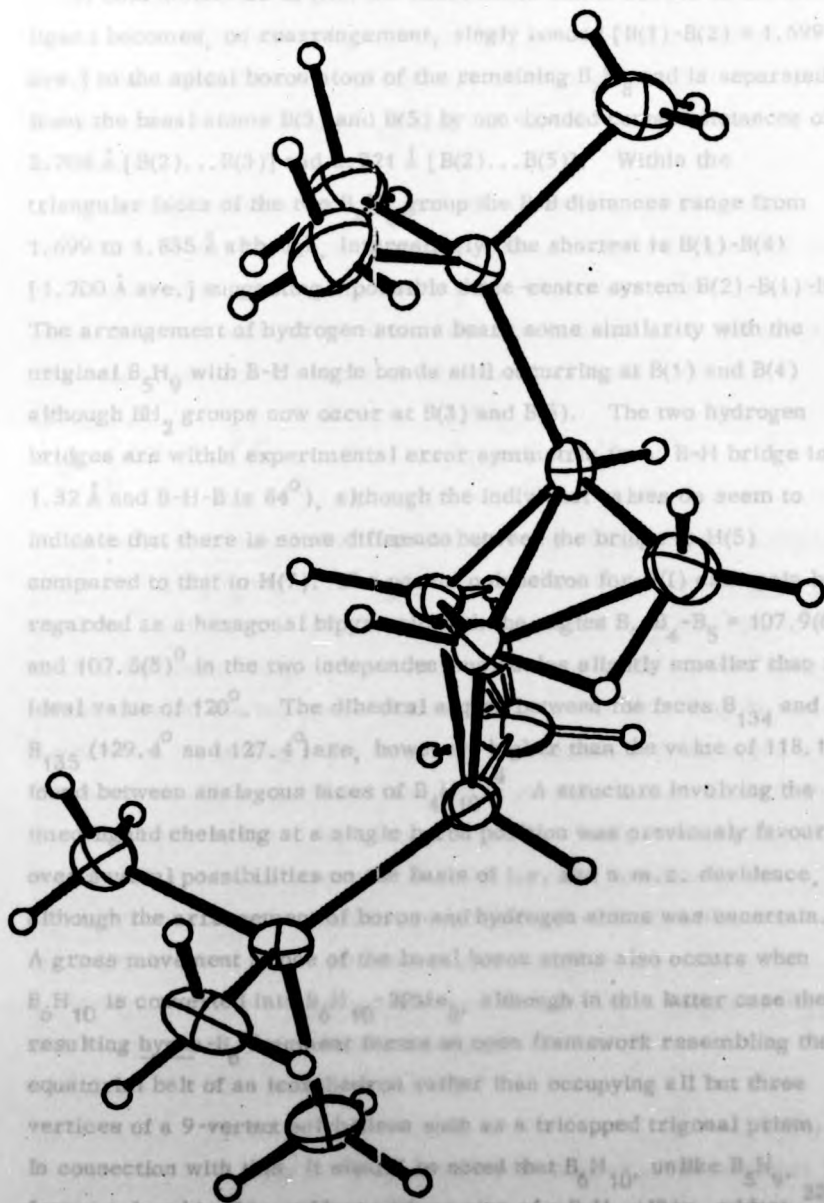


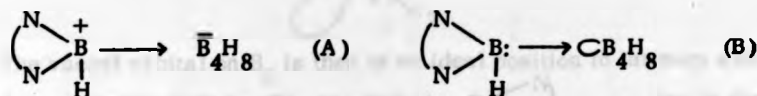
Fig. VII. 11b

-trichloride, -tribromide and -tri-iodide³⁴ and values of 1.609 Å and 1.578(8) Å [B-NH₃] in BH₃·NMe₃ and ammonia-isothiocyanatoborane, NH₃·BH₂·NCS respectively.³⁵ Other examples of B-N distances are also in ref.35.

In both molecules of (III) the basal boron atoms bonded to the tmed ligand becomes, on rearrangement, singly bonded [B(1)-B(2) = 1.699 Å ave.] to the apical boron atom of the remaining B₄H₈ and is separated from the basal atoms B(3) and B(5) by non-bonded contact distances of 2.708 Å [B(2)...B(3)] and 2.721 Å [B(2)...B(5)]. Within the triangular faces of the two B₄H₈ group the B-B distances range from 1.699 to 1.835 Å although, interestingly, the shortest is B(1)-B(4) [1.700 Å ave.] suggesting a possible three-centre system B(2)-B(1)-B(4). The arrangement of hydrogen atoms bears some similarity with the original B₅H₉ with B-H single bonds still occurring at B(1) and B(4) although BH₂ groups now occur at B(3) and B(5). The two hydrogen bridges are within experimental error symmetric (ave. B-H bridge is 1.32 Å and B-H-B is 84°), although the individual values do seem to indicate that there is some difference between the bridge to H(5) compared to that to H(7). The parent polyhedron for (III) can again be regarded as a hexagonal bipyramid with the angles B₃-B₄-B₅ = 107.9(6)° and 107.5(5)° in the two independent molecules slightly smaller than the ideal value of 120°. The dihedral angles between the faces B₁₃₄ and B₁₃₅ (129.4° and 127.4°) are, however, higher than the value of 118.1° found between analogous faces of B₄H₁₀.⁴ A structure involving the tmed ligand chelating at a single boron position was previously favoured over several possibilities on the basis of i.r. and n.m.r. evidence, although the arrangement of boron and hydrogen atoms was uncertain.²³ A gross movement of one of the basal boron atoms also occurs when B₆H₁₀ is converted into B₆H₁₀·2PMe₃, although in this latter case the resulting hypho-B₆ fragment forms an open framework resembling the equatorial belt of an icosahedron rather than occupying all but three vertices of a 9-vertex polyhedron such as a tricapped trigonal prism.²² In connection with this, it should be noted that B₆H₁₀, unlike B₅H₉, forms only a bis PMe₃ adduct with no sign of a B₆H₁₀·PMe₃ adduct.²²

A rearrangement compatible with this involves attachment of the two P atoms at the two ends of the basal single bond which is broken. A subsequent diamond-square-diamond arrangement is needed to break an apex-base bond before the boron skeleton flattens out to give the arrangement in Fig. VII.11 with the two PMe_3 groups well separated. What effect the fact that the phosphorus atoms are constrained in dppm and dppe may have on any $\text{B}_6\text{H}_{10} \cdot \text{dppe}$ (or dppm) adducts is open to speculation.

The overall atomic arrangement of the borons in (III) is still believed to be an example of the hypho class, although the structure might be interpreted in several different ways. In particular, zwitterionic canonical forms such as (A) or a valence structure such as (B) probably make significant contributions to the overall molecular orbitals.



The valence structure (A) in fact shows strong similarities to adducts of the type $\text{L} \cdot \text{B}_4\text{H}_8$ where the B_4H_8^- fragment would then be an arachno species.³⁵ However, the present arrangement of tmed and hydrogen atom at the 'basal' boron atom B(2) in each molecule appears to be unique amongst the boranes and their ions, so that there may be some justification for putting some weight on the suggestion that a truer representation of the present structure is given by the canonical form (B), especially as the ' B_4H_8 ' fragment can be written in terms of a 2112 vacant orbital valence structure.³⁶ Examples of possible vacant orbital valence structures are again given by modification of the rules for calculating normal neutral valence structures.

Using Lipscomb's styx notation for a neutral boron hydride B_pH_{p+q} with v vacant orbitals, the rules become:

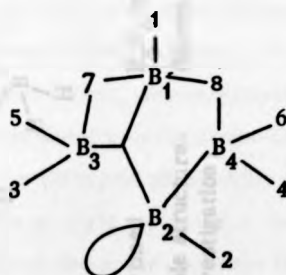
$$s + x = q$$

$$s + t = p - v$$

$$t + y = p - q/2 \quad \text{where the number of three-centre bonds}$$

$(s + t)$ is reduced by the number of vacant orbitals, but the number of

hydrogens ($s + x + p$) and the number of framework bonds ($t + y$) remain constant. The normal styx structures for B_4H_8 are [4020], [2202] and [3111]; those for valence structures with one vacant orbital ($v = 1$) are [3021], [2122] and [1203]. Of these latter structures, the C_s 2112 structure is a resonance hybrid between a structure having a single B_2B_4 bond and a central three-centre $B_1B_2B_3$ bond, and a valence structure with a single B_2B_3 bond and central three-centre $B_1B_2B_4$ bond.³⁶



The vacant orbital on B_2 is then in an ideal position to interact with a donor species such as $:BH_3$ to which the $:B \begin{smallmatrix} \nearrow N \\ \searrow N \\ | H \end{smallmatrix}$ species is formally equivalent. Assuming that all hypho tmed structures contain the ligand chelating at a single boron position, it is possible to postulate a closed series for these tmed complexes as shown in Table VII.2. Of the structures in this Table, $B_5H_9 \cdot tmed$ and $[BH_4]^- [tmedBH_2]^+$ ³⁷ are well characterised, and $B_4H_8 \cdot tmed$ is currently under investigation. It is assumed that the series is completed with $B_6H_{10} \cdot tmed$ because there are then no more H-atoms remaining on the apical boron atom, although this criterion is somewhat arbitrary and may be incorrect if similar vacant orbital structures to those in $B_5H_9 \cdot tmed$ have some significance for the higher ($>B_6$) boranes. Each structure in the Table can therefore be written as a neutral valence structure analogous to (B) above, and the styx vacant orbital structures for the fragments with which each

$L(= \begin{smallmatrix} \nearrow N \\ \searrow N \\ | H \end{smallmatrix} B:)$ group interacts are shown below each entry in the Table,

with the favoured styx structure noted. For $B_6H_{10} \cdot tmed$, this favoured structure requires a further modification to the equations for calculating

TABLE VII. 2
Known or postulated structures for tetramethylene diamine adducts of the boron hydrides.

Formulation	Structure	Full formula	No. of H atoms on apical boron	Vacant orbital valence structure for 'BH' group	Alternatives
BH_5L		$tmedBH_2^+BH_4^-$ (known as individual ions)	[4]	-	
B_2H_6L		$B_3H_7 \cdot tmed$	2 terminal + 1 bridge	[1003] _{v=1}	
B_3H_7L		$B_4H_8 \cdot tmed$ (probable structure under investigation)	2 terminal	[1103] _{v=1}	[2012] _{v=1}
B_4H_8L		$B_5H_9 \cdot tmed$ (known)	1 terminal	[2112] _{v=1}	[1203] _{v=1} [3021] _{v=1}
B_5H_9L		$B_6H_{10} \cdot tmed$ (postulated)	0	[3122] _{v=1}	

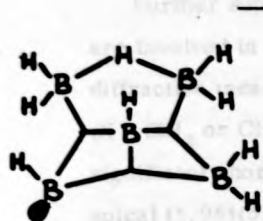
See Table VII.3

styx values to allow the vacant orbital to occur on a bare boron atom, i.e. without an exoskeletal BH bond. In Table VII.3 some of the alternative styx vacant orbital structures not shown in Table VII.6 are depicted.

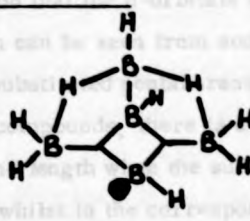
In comparing compounds (I) and (II) with (III), it could be expected that an open hypho framework would be rather flexible and might not correspond precisely to the rigid geometry of the corresponding closed parent polyhedron. It is somewhat unexpected to find it capable of the gross rearrangements observed here. In discussing some of the reasons for this isomerism, any mechanism for delocalising some of the excess electron density in the boron framework will be of importance. In this respect, the ability of phosphorus to accept electron density into its empty 3d orbitals might account for the preferential co-ordination of a phosphorus atom at the apical position (especially as in B_5H_9 there is a residual negative charge at the apical boron atom⁴) and the bridging mode of the phosphine ligands. Since any electron density removed by the phosphorus atoms can then be effectively further delocalised in phenyl ring orbitals, this process could be very effective. The fact that $B_5H_9 \cdot (PPh_3)_2$ is completely decomposed at 25°C may be attributed to the fact that electron delocalisation from the hypho structures is so effective that the resultant boron framework is unstable with respect to dissociation into stable products such as $(Ph_3P)_2BH_2$.

Since nitrogen has no low-lying d-orbitals, no π -character can be associated with the B-N bonds. Hence the co-ordination of the ligand tned into a chelating mode at a basal position could be predicted. The different framework arrangement in (III) then reflects a need to delocalise effectively a greater electron density left on the B_5 skeleton by the ineffective tned. Part of this electron density is effectively localised in the short B(1)-B(2) bond which is close to a 2c-2e bond rather than the 3c-2e bonds in the triangular faces of the frameworks in (I) and (II). The retention of an integral B_4 unit in (III) may again be fractionally better at delocalising the remaining framework electrons than the two three-centre systems in (I) and (II) connected via the apical atom.

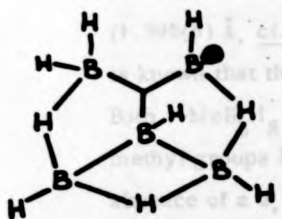
TABLE VII.3

Some B_5H_9 vacant orbital species

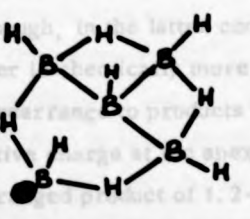
1303



2212



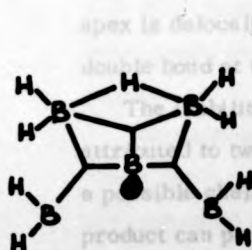
3121



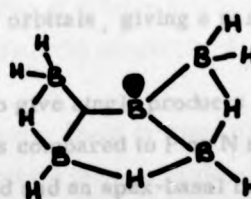
4030

Some B_5H_9 vacant orbital species with the vacant orbital on an

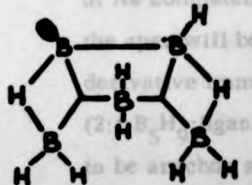
apical boron



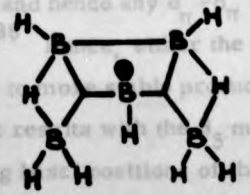
1304



3122



2213



4031

● = vacant orbital

Further support for the suggestion that the d-orbitals on phosphorus are involved in charge delocalisation can be seen from some electron diffraction measurements on mono-substituted pentaboranes, B_5H_8X ($X = SiH_3$ or CH_3). With the silyl compounds, there is a very significant shortening of the B-Si bond length when the substituent is apical (1.981(5) Å, *cf.* 2.006(4) Å) whilst in the corresponding methyl substituted derivatives there is no difference in B-C bond lengths (1.595(5) Å, *cf.* 1.592(5) Å) even though, in the latter compounds, it is known that the 2-substituted isomer is chemically more stable. Both 1-MeB₅H₈ and 1,2-(Me)₂B₅H₇ rearrange to products with the methyl groups basal due to the negative charge at the apex. The absence of a 2,4 isomer in the rearranged product of 1,2-(Me)₂B₅H₇ is attributable to H(methyl)...H(bridge) repulsions in the likely intermediate for the rearrangement.³⁷ The shortening of the apical B-Si bond is consistent with the suggestion that the negative charge at the apex is delocalised into the empty Si 3d orbitals, giving a partial double bond at the apical position.⁶

The inability of the arsino ligands to give single products can be attributed to two factors; the size of As compared to P or N rules out a possible chelating mode for this ligand and an apex-basal bridged product can possibly be ruled out because the phenyl substituents on the As atom are ineffectual in contracting the more diffuse 4d orbitals of As compared to 3d orbitals on P, and hence any $d_{\pi}-p_{\pi}$ overlap at the apex will be very small for As.³⁸ Hence, either the hypho derivative immediately decomposes to more stable products or else a (2:1 B₅H₉:ligand) polymeric product results with the B₅ moieties likely to be arachno and the ligand bridging basal positions of these groups.

The reaction of pentaborane (9) with other ligands and other metal complexes similarly results in basal co-ordination, either via two-centre M-B or three-centre $B \begin{array}{c} \text{---} \\ \diagup \text{M} \diagdown \end{array} B$ bridging interactions regardless of whether the starting borane had been apical or basal substituted. As noted already in the Introduction, there are no rules regarding

whether the result bond is M-B or $B \begin{array}{c} \diagup \\ M \\ \diagdown \end{array} B$ at present, although the common feature is the co-ordination of the metal at the base. Any rules for these co-ordination modes must take into consideration the excess electron density at the B_5H_9 apical atom, which presumably is forcing poor π -acceptor metals into their basal co-ordination.

Finally, the presence of a chelate effect is apparent in all the adducts, the monodentate ligand species being much less stable, so that, for example, $B_5H_9 \cdot 2PPh_3$ is completely decomposed at $25^\circ C$. Of the three compounds, (III) is the least stable (cf. I and II), presumably decomposing to give $[tmedBH_2]^-$ and other ionic products. Part of the chemical stability of complexes (I) and (II) must also be attributed to the size of the extremely bulky diphos ligands compared to the B_5H_9 , preventing any approach from nucleophiles, etc. Furthermore, the three hypho structures must be considered to be electron rich compared with B_5H_9 itself, so that a greater number of valence structures for these hypho derivatives can be formulated with single (2c-2e) bonds present.

The packing of the three compounds are shown in Figs. VII. 12 and 13. There are no close inter-molecular contacts between molecules which are separated by typical van der Waals contacts.

VII. 5. References

1. A. Stock, E. Wiberg and W. Mathing, Ber., 1936, 69B, 2811 and earlier papers in series.
2. See for example, E. Wiberg, Ber., 1936, 69B, 2816 and S.H. Bauer and L. Pauling, J. Am. Chem. Soc., 1936, 58, 1403.
3. 'Electron deficient compounds', K. Wade, Nelson (London), 1971.
4. W.N. Lipscomb, 'Boron Hydrides', W.A. Benjamin, New York, 1963, and refs. therein.
5. C.E. Nordman and W.N. Lipscomb, J. Chem. Phys., 1953, 21, 1856; W.J. Dulmage and W.N. Lipscomb, J. Am. Chem. Soc., 1951, 73, 3539; L. Lavine and W.N. Lipscomb, J. Chem. Phys., 1954, 22, 614;

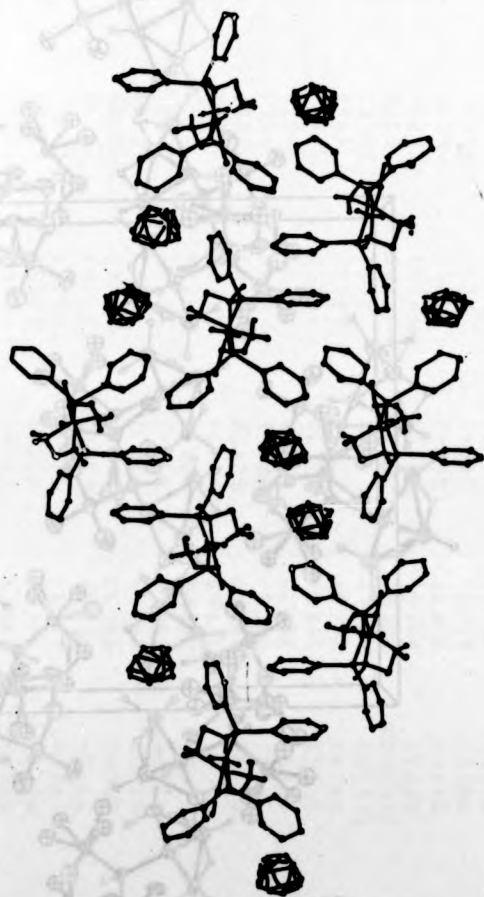


Fig. VII.12 Packing arrangement in B₅H₉·dppm viewed down a.

Fig. VII.13 Packing diagram for B₅H₉·dppm viewed down c.

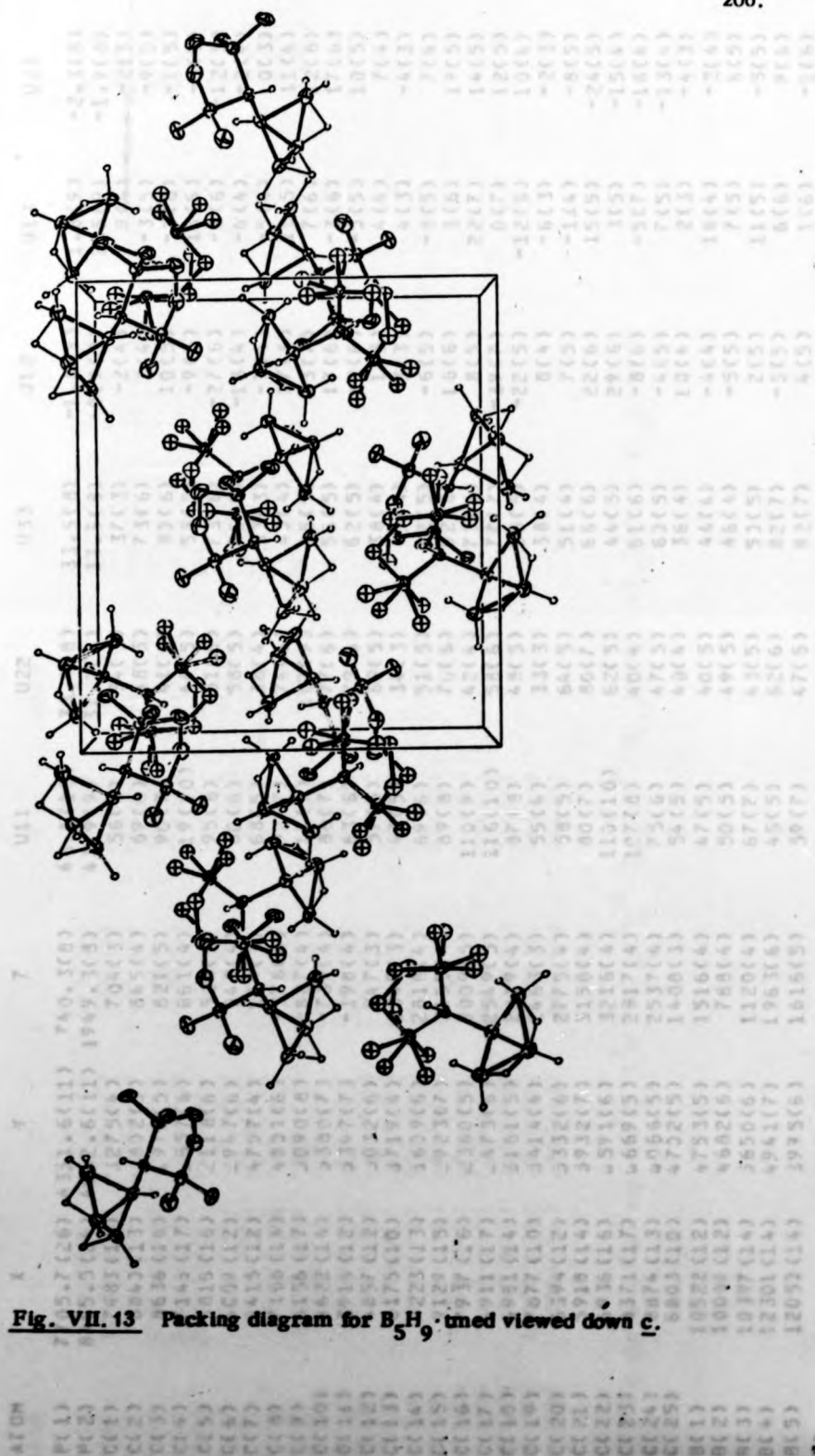


Fig. VII. 13 Packing diagram for B_5H_9 dimer viewed down c .

TABLE VII.4
Atomic co-ordinates ($\times 10^{-4}$) and temperature factors ($\times 10^{-3}$), with standard deviations in parentheses.
(a) B_5H_9 · dppm

ATOM	X	Y	Z	U11	U22	U33	U12	U13	U23
P(1)	7705.7(26)	4351.6(11)	740.3(8)	48.1(10)	39.4(8)	33.5(8)	-1.0(9)	1.6(9)	-2.3(8)
P(2)	8465.5(24)	4642.6(11)	1949.3(8)	42.9(9)	31.2(8)	33.5(8)	-0.9(9)	2.5(9)	-1.9(8)
C(1)	7483(11)	5275(4)	704(3)	56(5)	34(3)	37(3)	-2(4)	9(4)	-2(3)
C(2)	8843(13)	5802(5)	845(4)	69(6)	48(5)	73(6)	2(4)	-3(5)	-9(5)
C(3)	8636(16)	5972(5)	821(5)	90(7)	41(4)	82(6)	10(5)	-2(6)	-1(5)
C(4)	7145(17)	5657(6)	661(4)	119(10)	44(5)	55(5)	-9(6)	13(6)	-5(5)
C(5)	5815(16)	5211(8)	528(5)	95(8)	51(6)	73(6)	-27(6)	-6(6)	-12(5)
C(6)	6009(12)	5947(6)	542(4)	60(6)	58(5)	55(5)	-13(4)	-6(4)	-2(4)
C(7)	6415(12)	4757(4)	169(3)	68(5)	38(4)	33(3)	-7(4)	-5(4)	0(3)
C(8)	7168(14)	4801(6)	-376(4)	92(7)	74(6)	43(4)	27(6)	10(5)	11(4)
C(9)	6156(17)	5090(8)	-827(4)	111(9)	107(9)	45(5)	13(7)	7(6)	12(6)
C(10)	4622(14)	5380(7)	-739(4)	88(7)	77(6)	55(5)	17(6)	-3(6)	17(6)
C(11)	3915(12)	5347(7)	-198(4)	63(6)	79(6)	62(5)	-8(6)	-5(5)	10(5)
C(12)	4857(12)	5032(6)	247(3)	59(5)	69(5)	38(4)	1(5)	4(4)	7(4)
C(13)	8175(10)	5719(4)	2349(3)	47(5)	34(3)	45(4)	3(3)	4(3)	-4(3)
C(14)	9223(13)	5609(6)	2818(4)	69(6)	51(5)	52(5)	-6(5)	-8(5)	7(4)
C(15)	9129(15)	5923(7)	3155(4)	89(8)	70(6)	62(6)	16(6)	3(6)	19(5)
C(16)	7937(16)	5236(5)	3009(5)	110(9)	42(4)	73(6)	8(5)	22(7)	14(5)
C(17)	6911(17)	5473(6)	2549(5)	116(10)	58(6)	77(7)	-39(7)	0(7)	12(5)
C(18)	6981(14)	5161(5)	2219(4)	87(8)	48(5)	55(5)	-22(5)	-12(5)	10(4)
C(19)	7877(10)	5414(4)	2463(3)	55(4)	33(3)	38(4)	8(4)	-6(3)	-2(3)
C(20)	6394(12)	5332(6)	2775(4)	58(5)	64(5)	51(4)	7(5)	-1(4)	-8(5)
C(21)	5919(14)	5932(7)	3158(4)	80(7)	80(7)	65(6)	22(6)	15(5)	-24(5)
C(22)	6935(16)	5591(6)	3216(4)	110(10)	62(5)	44(5)	29(6)	3(5)	-15(4)
C(23)	8371(17)	5669(5)	2917(4)	107(8)	40(4)	61(6)	-8(6)	-5(7)	-18(4)
C(24)	8874(13)	5066(5)	2537(4)	75(6)	47(5)	63(5)	-4(5)	7(5)	-13(4)
C(25)	6803(10)	4722(5)	1408(3)	54(5)	40(4)	36(4)	10(4)	2(3)	-4(3)
B(1)	10522(12)	4753(5)	1516(4)	47(5)	40(5)	44(4)	-4(4)	18(4)	-2(4)
B(2)	10009(12)	4682(6)	788(4)	50(5)	49(5)	46(4)	-5(5)	7(5)	6(5)
B(3)	10397(14)	5650(6)	1120(4)	67(7)	43(5)	52(5)	2(5)	11(5)	-5(5)
B(4)	12301(14)	4941(7)	1963(6)	45(5)	62(6)	82(7)	-3(5)	6(6)	9(6)
B(5)	12052(14)	5995(6)	1616(5)	59(7)	47(5)	82(7)	4(5)	1(6)	-1(6)

TABLE VII.4 (cont.)

(a) $B_H \cdot \text{dppm}$											
ATOM	X	Y	Z	U	ATOM	K	Y	Z	U		
H(1)	9568(88)	5416(45)	593(29)	42(20)	H(161)	6973(113)	1234(49)	696(37)			70(35)
H(2)	10856(115)	4422(58)	529(38)	84(28)	H(171)	5148(157)	1736(70)	358(48)			70(31)
H(3)	9343(75)	9005(37)	1197(25)	21(15)	H(181)	4984(174)	3138(78)	490(51)			70(44)
H(4)	11612(114)	5952(53)	1016(34)	58(23)	H(201)	7723(247)	4283(112)	-474(75)			70(93)
H(5)	13063(87)	4269(43)	1968(30)	45(19)	H(211)	6817(129)	5168(61)	-1225(39)			70(43)
H(6)	11898(95)	5138(46)	2482(33)	50(22)	H(221)	3514(313)	5533(138)	-867(95)			70(120)
H(7)	9796(189)	2908(82)	3578(56)	70(15)	H(231)	2849(132)	5648(60)	-148(42)			70(33)
H(8)	11672(127)	5500(56)	1694(40)	68(27)	H(241)	3933(235)	4938(112)	500(71)			70(86)
H(9)	13098(131)	5945(65)	1254(45)	93(33)	H(251)	6413(94)	5231(48)	1373(30)			70(24)
H(21)	10649(171)	4006(72)	2843(52)	70(35)	H(252)	5875(165)	4368(80)	1520(51)			70(51)
H(31)	3226(95)	3317(47)	1771(31)	46(20)							
H(41)	7433(125)	2920(53)	3213(36)	70(28)							
H(51)	5951(122)	2422(55)	2545(39)	70(41)							
H(61)	6271(122)	2201(54)	1905(39)	70(23)							
H(81)	5593(146)	4984(68)	2654(45)	70(38)							
H(91)	4891(140)	3887(60)	3332(42)	70(35)							
H(101)	6373(146)	5951(64)	3498(43)	70(31)							
H(111)	9137(157)	7038(74)	3104(52)	70(45)							
H(121)	245(109)	1113(49)	2728(32)	70(37)							
H(141)	10673(128)	-930(56)	988(38)	70(26)							
H(151)	9555(146)	1737(68)	886(46)	70(23)							

In the form: $U = \exp[-2\pi^2(U_{11}^2 a^2 + U_{22}^2 b^2 + U_{33}^2 c^2 + 2U_{12}^2 hka^*b^* + 2U_{13}^2 hla^*c^* + 2U_{23}^2 klb^*c^*)]$

Table VII. 4(cont.)

(b) $B_5H_9 \cdot (Ph_2PCH_2)_2$, (II)

Atom	<u>X</u>	<u>Y</u>	<u>Z</u>
P(1)	0.35387(6)	0.01975(6)	0.28206(4)
P(2)	0.25323(6)	0.04436(6)	0.41652(4)
C(1)	0.3875(2)	0.0423(2)	0.2168(2)
C(2)	0.3373(3)	0.0346(3)	0.1632(2)
C(3)	0.3539(3)	0.0865(3)	0.1156(2)
C(4)	0.4207(3)	0.1475(3)	0.1212(2)
C(5)	0.4707(3)	0.1559(2)	0.1730(2)
C(6)	0.4556(2)	0.1028(2)	0.2208(2)
C(7)	0.3406(3)	-0.1215(2)	0.2499(2)
C(8)	0.4155(3)	-0.1540(3)	0.2174(2)
C(9)	0.4127(4)	-0.2339(3)	0.1972(2)
C(10)	0.3352(4)	-0.2815(3)	0.2074(2)
C(11)	0.2614(4)	-0.2499(3)	0.2367(2)
C(12)	0.2628(3)	-0.1700(2)	0.2589(2)
C(13)	0.2229(2)	0.1235(2)	0.4703(2)
C(14)	0.1608(3)	0.1857(2)	0.4565(2)
C(15)	0.1439(3)	0.2474(3)	0.4974(2)
C(16)	0.1885(3)	0.2470(3)	0.5520(2)
C(17)	0.2490(3)	0.1858(3)	0.5665(2)
C(18)	0.2673(3)	0.1237(3)	0.5261(2)
C(19)	0.1754(2)	-0.0409(2)	0.4282(2)
C(20)	0.2100(3)	-0.1186(2)	0.4256(2)
C(21)	0.1499(3)	-0.1848(3)	0.4285(3)
C(22)	0.0552(3)	-0.1734(3)	0.4335(2)
C(23)	0.0197(3)	-0.0960(3)	0.4367(2)
C(24)	0.0785(3)	-0.0297(3)	0.4336(2)
C(25)	0.2323(2)	0.0149(2)	0.2951(2)
C(26)	0.2217(2)	0.0816(2)	0.3420(2)
B(1)	0.4350(3)	-0.0159(3)	0.3525(2)
B(2)	0.3846(3)	0.0156(3)	0.4201(2)

Table VII, 4(cont.)

B(3)	0.4603(3)	0.0837(3)	0.3773(2)
B(4)	0.5502(3)	-0.0494(3)	0.3297(3)
B(5)	0.4763(3)	-0.1151(3)	0.3740(2)
H(1)	0.4173(26)	0.0859(22)	0.4296(16)
H(2)	0.4030(25)	-0.0125(22)	0.4615(16)
H(3)	0.4262(29)	0.1316(27)	0.3543(19)
H(4)	0.5305(31)	0.0985(25)	0.3935(18)
H(5)	0.5493(31)	-0.1285(28)	0.3433(20)
H(6)	0.6127(27)	-0.0214(22)	0.3550(17)
H(7)	0.5585(28)	-0.0517(24)	0.2782(18)
H(8)	0.5003(25)	-0.1244(23)	0.4191(17)
H(9)	0.4299(27)	-0.1659(23)	0.3583(16)
H(21)	0.2878(27)	-0.0057(22)	0.1591(18)
H(31)	0.3232(31)	0.0741(25)	0.0768(19)
H(41)	0.4324(25)	0.1795(21)	0.0883(16)
H(51)	0.5194(28)	0.1980(24)	0.1792(17)
H(61)	0.4871(22)	0.1071(19)	0.2555(15)
H(81)	0.4695(31)	-0.1222(28)	0.2078(20)
H(91)	0.4592(29)	-0.2557(25)	0.1735(18)
H(101)	0.3379(34)	-0.3390(30)	0.1898(21)
H(111)	0.2112(30)	-0.2724(27)	0.2438(21)
H(121)	0.2081(21)	-0.1460(19)	0.2818(13)
H(141)	0.1324(20)	0.1839(17)	0.4195(13)
H(151)	0.1094(24)	0.2890(20)	0.4884(16)
H(161)	0.1777(29)	0.2869(23)	0.5811(17)
H(171)	0.2779(31)	0.1816(27)	0.6019(20)
H(181)	0.3086(26)	0.0877(22)	0.5339(16)
H(201)	0.2772(31)	-0.1272(28)	0.4222(19)
H(211)	0.1753(33)	-0.2349(28)	0.4238(21)
H(221)	0.0117(28)	-0.2205(25)	0.4341(17)
H(231)	-0.0463(34)	-0.0828(28)	0.4415(21)
H(241)	0.0571(29)	0.0181(25)	0.4394(19)

Table VII. 4 (cont.)

H(251)	0.1985(22)	-0.0272(20)	0.3113(14)
H(252)	0.2057(25)	0.0305(22)	0.2558(18)
H(261)	0.2573(23)	0.1290(20)	0.3340(14)
H(262)	.1581(26)	0.0988(22)	0.3436(16)

TABLE VII. 4 (cont.)

Anisotropic Temperature Factors ($\times 10^3$)[†] for B₅H₉.dppe

Atom	U ₁₁	U ₂₂	U ₃₃	U ₁₂	U ₁₃	U ₂₃
P(1)	28.2(5)	32.0(5)	41.8(5)	-2.3(4)	1.4(4)	1.5(4)
P(2)	29.6(5)	33.7(5)	41.1(5)	1.4(4)	1.0(4)	3.2(4)
C(1)	36.0(19)	34.2(20)	44.2(21)	6.0(16)	9.5(17)	1.3(17)
C(2)	51.6(25)	50.9(26)	51.8(24)	2.6(20)	0.7(20)	4.4(20)
C(3)	59.7(27)	72.9(31)	49.8(26)	10.2(26)	-3.0(22)	9.2(24)
C(4)	64.9(29)	59.7(29)	60.5(30)	20.2(24)	19.7(25)	27.0(24)
C(5)	51.1(24)	39.3(23)	66.9(29)	3.3(19)	17.4(23)	12.1(22)
C(6)	38.7(20)	41.6(22)	49.3(23)	-0.2(17)	6.4(18)	-0.9(18)
C(7)	48.4(22)	33.7(18)	39.7(20)	-2.1(17)	-7.7(18)	3.4(17)
C(8)	59.2(26)	43.8(24)	64.3(29)	4.9(20)	3.9(23)	-3.2(22)
C(9)	94.6(36)	43.2(25)	61.2(29)	9.7(26)	6.5(27)	-4.0(22)
C(10)	106.5(42)	36.4(23)	55.2(28)	-1.5(28)	-16.6(29)	1.7(21)
C(11)	81.4(34)	47.4(27)	72.9(33)	-23.1(29)	-18.1(29)	8.6(23)
C(12)	54.6(25)	42.6(23)	63.4(26)	-11.2(21)	-1.1(22)	0.5(21)
C(13)	35.9(19)	37.2(20)	43.0(21)	-3.7(17)	3.3(16)	0.3(17)
C(14)	36.5(20)	45.5(22)	46.4(22)	3.0(17)	-0.5(17)	-2.2(18)
C(15)	45.7(21)	37.9(20)	68.9(27)	0.5(20)	11.4(21)	0.0(20)
C(16)	60.1(26)	49.7(25)	57.3(27)	-4.6(24)	17.8(23)	-13.1(22)
C(17)	63.0(28)	72.8(33)	49.0(25)	1.6(27)	-2.6(23)	-10.7(22)
C(18)	54.4(26)	54.6(25)	49.3(23)	5.0(21)	0.1(20)	-2.1(21)
C(19)	29.5(17)	39.1(21)	43.6(21)	-1.5(16)	2.5(16)	3.0(17)
C(20)	33.3(20)	38.7(24)	95.6(35)	1.5(16)	5.1(22)	12.2(23)
C(21)	46.2(25)	37.0(23)	127.5(47)	-1.1(21)	6.4(28)	10.6(26)
C(22)	47.2(25)	48.5(26)	81.7(34)	-12.5(22)	3.8(23)	5.5(24)
C(23)	30.9(21)	66.8(32)	92.3(37)	-5.0(21)	9.7(22)	-4.1(27)
C(24)	36.9(21)	43.8(25)	81.8(32)	2.4(19)	13.0(21)	-6.0(22)
C(25)	29.5(18)	49.5(22)	40.9(20)	2.6(17)	-2.6(15)	3.2(18)
C(26)	31.9(18)	41.3(21)	45.3(22)	6.3(16)	0.8(16)	3.1(18)

TABLE VII.4 (continued)

Atom	U ₁₁	U ₂₂	U ₃₃	U ₁₂	U ₁₃	U ₂₃
B(1)	27.0(19)	40.0(22)	47.3(25)	-2.4(18)	-1.1(19)	3.2(20)
B(2)	31.1(21)	41.4(24)	48.0(25)	-4.2(19)	-2.4(18)	7.6(21)
B(3)	36.4(24)	51.0(28)	57.7(30)	-15.3(22)	6.0(22)	-3.4(24)
B(4)	30.7(23)	59.8(32)	67.2(34)	5.7(22)	7.9(22)	-3.1(27)
B(5)	40.2(25)	51.3(30)	59.4(31)	9.5(23)	0.2(24)	7.4(25)

Atom	U	Atom	U	Atom	U
H(1)	47(10)	H(41)	41(10)	H(171)	64(14)
H(2)	44(10)	H(51)	58(12)	H(181)	49(11)
H(3)	64(13)	H(61)	37(9)	H(201)	74(14)
H(4)	64(12)	H(81)	73(14)	H(211)	76(15)
H(5)	70(13)	H(91)	77(13)	H(221)	54(12)
H(6)	51(11)	H(101)	84(16)	H(231)	83(15)
H(7)	53(12)	H(111)	81(14)	H(241)	58(13)
H(8)	43(10)	H(121)	26(8)	H(251)	34(9)
H(9)	47(11)	H(141)	19(7)	H(252)	43(10)
H(21)	56(12)	H(151)	41(10)	H(261)	31(8)
H(31)	67(13)	H(161)	53(12)	H(262)	45(11)

† In the form

$$U = \exp \left\{ -2\pi^2 \left(U_{11} h^2 a^{*2} + U_{22} k^2 b^{*2} + U_{33} l^2 c^{*2} + 2U_{12} hka^*b^* + \right. \right. \\ \left. \left. 2U_{13} hla^*c^* + 2U_{23} klb^*c^* \right) \right\}$$

TABLE VII.4 (cont.)

Atomic co-ordinates (* 10 ** 4) and temperature factors (* 10 ** 3), with standard deviations in parentheses.

(c) B_{3H_9} med

ATOM	X	Y	Z	U11	U22	U33	U12	U13	U23
N(11)	3718(3)	4102(3)	4543(3)	48(3)	39(3)	44(2)	-4(3)	1(2)	8(2)
N(12)	3129(3)	4865(3)	5991(3)	40(3)	41(3)	57(3)	4(2)	1(2)	-2(3)
N(21)	2180(3)	840(3)	-1546(3)	43(3)	47(3)	56(3)	-2(2)	1(2)	8(3)
N(22)	1353(3)	706(3)	-45(3)	44(3)	50(3)	48(3)	2(3)	-3(2)	6(3)
C(11)	3432(6)	3014(5)	4257(4)	69(5)	77(5)	316(4)	-24(4)	-3(4)	-13(4)
C(12)	4553(5)	4471(5)	3941(4)	91(5)	89(5)	42(3)	-42(4)	10(3)	1(3)
C(13)	2766(5)	4769(6)	4456(4)	84(5)	86(5)	63(4)	36(4)	-19(4)	13(4)
C(14)	2767(5)	5472(5)	5213(5)	64(4)	57(4)	86(5)	35(3)	-3(4)	4(4)
C(15)	2295(5)	4199(6)	6371(6)	49(4)	83(5)	82(6)	-3(5)	19(4)	2(5)
C(16)	3477(5)	5618(5)	6687(4)	88(5)	70(5)	96(5)	25(4)	12(4)	-28(4)
O(11)	4304(5)	3053(5)	6106(4)	39(4)	42(4)	52(4)	1(3)	10(4)	-1(4)
O(12)	4119(4)	4200(5)	5599(4)	32(3)	30(3)	41(4)	0(3)	-6(3)	1(3)
O(13)	4860(6)	3475(7)	7173(5)	54(5)	72(6)	61(6)	-9(5)	-18(5)	8(5)
O(14)	5298(6)	2364(7)	6662(5)	65(5)	56(6)	187(7)	6(4)	-14(5)	14(5)
O(15)	5566(5)	2668(6)	5533(5)	54(4)	50(5)	156(5)	8(4)	-2(5)	-4(5)
O(21)	164(5)	1721(5)	-1380(4)	44(4)	32(4)	48(4)	-8(3)	1(3)	-9(3)
O(22)	1339(4)	1515(5)	-913(4)	37(3)	33(4)	43(4)	-7(3)	11(3)	-3(3)
O(23)	509(6)	2694(6)	-2208(5)	66(5)	50(4)	50(5)	2(5)	2(4)	11(4)
O(24)	-688(6)	2661(6)	-1678(5)	44(4)	64(5)	66(5)	-1(4)	-9(4)	-12(4)
O(25)	-454(6)	2506(6)	-513(5)	41(4)	49(4)	67(5)	-14(4)	5(4)	-10(4)
ATOM	X	Y	Z	U	ATOM	X	Y	Z	U
C21A	1715(9)	22(10)	-2049(8)	54(3)	N(123)	5150(67)	3766(69)	3903(57)	207(36)
C22A	2780(10)	1527(10)	-2122(8)	55(4)	N(131)	2677(39)	5063(42)	3883(32)	87(17)
C23A	2900(9)	416(10)	-84(8)	57(3)	N(132)	2105(37)	4081(39)	4644(29)	81(16)
C24A	2145(13)	-63(13)	-112(11)	69(6)	N(141)	2104(27)	5831(30)	5317(21)	34(11)
C25A	1533(10)	1492(11)	807(9)	51(5)	N(142)	3467(43)	6128(43)	4874(34)	105(19)
C26A	400(11)	130(11)	200(10)	71(5)	N(151)	2028(45)	3676(52)	5963(40)	88(25)
C21B	1761(9)	517(11)	-2451(8)	63(4)	N(152)	2516(37)	3904(37)	6912(33)	43(18)
C22B	3103(10)	1592(11)	-1752(9)	68(4)	N(153)	1735(39)	4780(41)	6613(31)	87(17)
C23B	2541(10)	-105(11)	-1072(9)	70(4)	N(161)	3006(33)	6101(31)	6792(25)	51(13)
C24B	2470(11)	185(11)	-129(10)	50(5)	N(162)	3597(50)	5190(54)	7091(39)	128(23)
C25B	1308(12)	1154(13)	781(11)	62(5)	N(163)	4019(38)	6151(36)	6377(32)	74(16)
C26B	528(11)	-128(11)	-164(10)	70(5)	N21AB	1188	49	-2396	80

TABLE VII.4 (cont.)

(c) B ₅ H ₉ -tmed									
ATOM	X	Y	Z	U	ATOM	X	Y	Z	U
MC(11)	3773(33)	2451(35)	6085(28)	47(13)	H22A(1)	3486	1100	-2044	80
MC(12)	4702(24)	4784(26)	5530(20)	10(9)	H22A(2)	2805	2185	-2024	80
MC(13)	5182(41)	4175(46)	7090(31)	67(18)	H23A	3362	-175	-1164	80
MC(14)	4385(41)	3445(41)	7851(36)	74(17)	H24A	2531	-289	482	80
MC(15)	5704(40)	2806(38)	7331(32)	62(15)	H25A	719	1797	768	80
MC(16)	5198(34)	4608(44)	6854(27)	53(15)	H26A(1)	-109	438	98	80
MC(17)	6116(47)	2473(43)	6213(40)	86(18)	H26A(2)	369	-599	-158	80
MC(18)	5576(36)	2034(38)	5109(32)	57(15)	H21A(1)	2347	-347	-2394	80
MC(19)	6071(34)	3505(41)	5326(28)	63(15)	H21A(2)	1256	-640	-1813	80
MC(21)	-203(33)	1058(36)	-1601(27)	48(14)	H22A(3)	2401	1370	-2736	80
MC(22)	1757(28)	2225(32)	-720(24)	27(11)	H23A(2)	3369	1074	-514	80
MC(23)	1171(30)	3100(30)	-1896(23)	22(11)	H24A(2)	1877	-850	-355	80
MC(24)	436(28)	2473(28)	-2934(28)	26(11)	H25A(1)	1560	959	1445	80
MC(25)	-90(38)	3492(42)	-2082(28)	63(15)	H25A(2)	2180	1921	593	80
MC(26)	-1390(37)	2436(35)	-1954(27)	42(13)	H26A(3)	424	-116	934	80
MC(27)	-851(35)	3221(39)	-1013(32)	58(14)	H21B(1)	2494	137	-2786	80
MC(28)	37(42)	2966(38)	-147(33)	74(18)	H21B(3)	1446	1196	-2820	80
MC(29)	-1126(35)	2185(32)	-85(29)	47(13)	H22B(3)	3442	1929	-1187	80
MC(111)	3221(24)	3026(25)	3682(20)	18(10)	H23B(2)	2342	-724	-1436	80
MC(112)	2893(37)	2718(37)	4726(30)	56(17)	H24B(1)	2994	667	132	80
MC(113)	4138(43)	2650(39)	4266(34)	60(17)	H25B(1)	1108	629	1298	80
MC(121)	4920(37)	5186(38)	4097(30)	80(15)	H25B(3)	1972	1388	960	80
MC(122)	4326(31)	4293(33)	3347(24)	49(12)					

In the form: $U = \exp\{-2\pi^2(U_{11}^h a^{*2} + U_{22}^k b^{*2} + U_{33}^l c^{*2} + 2U_{12}^h ka^*b^* + 2U_{13}^h la^*c^* + 2U_{23}^k lb^*c^*)\}$

Table VII. 5a

Bond distances (\AA) and bond angles ($^\circ$) with the standard deviations in parentheses for $\text{B}_5\text{H}_9 \cdot (\text{Ph}_2\text{P})_2\text{CH}_2$ (I) and $\text{B}_5\text{H}_9 \cdot (\text{Ph}_2\text{PCH}_2)_2$ (II)

(a) Distances

(i) B_5H_9 moiety

	I	II		I	II
P(1)-B(1)	1.927(9)	1.953(4)	B(2)-H(1)	1.36(8)	1.27(4)
P(2)-B(2)	1.913(10)	1.939(4)	B(3)-H(1)	1.45(7)	1.32(4)
B(1)-B(2)	1.745(13)	1.747(6)	B(2)-H(2)	0.11(9)	1.06(4)
B(1)-B(3)	1.769(14)	1.768(6)	B(3)-H(3)	1.04(6)	1.06(4)
B(1)-B(4)	1.781(15)	1.810(6)	B(3)-H(4)	1.12(9)	1.09(4)
B(1)-B(5)	1.774(14)	1.804(6)	B(4)-H(5)	1.28(7)	1.34(5)
B(2)-B(3)	1.827(14)	1.829(7)	B(5)-H(5)	1.24(7)	1.27(4)
B(4)-B(5)	1.794(16)	1.806(7)	B(4)-H(6)	1.29(8)	1.15(4)
B(2)...B(5)	2.770(15)	2.723(7)	B(4)-H(7)	1.07(8)	1.16(4)
B(3)...B(4)	2.746(16)	2.755(7)	B(5)-H(8)	0.90(10)	1.07(4)
			B(5)-H(9)	1.14(11)	1.12(4)

(ii) Ligand

	I	II		I	II
P(1)-C(1)	1.825(7)	1.841(4)	C(25)-C(26)	-	1.525(5)
P(1)-C(7)	1.826(8)	1.834(4)	C(25)-H(251)	0.94	0.92(3)
P(2)-C(13)	1.821(7)	1.824(4)	C(25)-H(252)	0.96	0.99(4)
P(2)-C(19)	1.811(8)	1.812(4)	C(26)-H(261)	-	0.95(3)
P(1)-C(25)	1.827(8)	1.853(4)	C(26)-H(262)	-	0.95(4)
P(2)-C(25)	1.809(8)	-			
P(2)-C(26)	-	1.827(4)			

(iii) Phenyl rings I $\text{B}_5\text{H}_9 \cdot \text{dppm}$

	Ring 1		Ring 2
C(1)-C(2)	1.384(13)	C(7)-C(8)	1.389(12)
C(2)-C(3)	1.398(14)	C(8)-C(9)	1.397(14)
C(3)-C(4)	1.381(16)	C(9)-C(10)	1.378(16)
C(4)-C(5)	1.358(17)	C(10)-C(11)	1.340(17)
C(5)-C(6)	1.390(14)	C(11)-C(12)	1.403(13)
C(6)-C(1)	1.367(12)	C(12)-C(7)	1.362(12)

Table VII. 5a (cont.)

Ring 3		Ring 4	
C(13)-C(14)	1.378(13)	C(19)-C(20)	1.404(12)
C(14)-C(15)	1.406(13)	C(20)-C(21)	1.408(15)
C(15)-C(16)	1.347(17)	C(21)-C(22)	1.326(18)
C(16)-C(17)	1.346(17)	C(22)-C(23)	1.377(14)
C(17)-C(18)	1.402(14)	C(23)-C(24)	1.383(13)
C(18)-C(13)	1.346(13)	C(24)-C(19)	1.332(13)

II $B_5H_9 \cdot dppe$

Ring 1		Ring 2	
C(1)-C(2)	1.399(5)	C(7)-C(8)	1.399(6)
C(2)-C(3)	1.384(6)	C(8)-C(9)	1.394(6)
C(3)-C(4)	1.392(7)	C(9)-C(10)	1.377(8)
C(4)-C(5)	1.366(7)	C(10)-C(11)	1.346(8)
C(5)-C(6)	1.396(6)	C(11)-C(12)	1.407(6)
C(6)-C(1)	1.397(5)	C(12)-C(7)	1.386(6)

Ring 3		Ring 4	
C(13)-C(14)	1.392(5)	C(19)-C(20)	1.374(6)
C(14)-C(15)	1.387(6)	C(20)-C(21)	1.390(5)
C(15)-C(16)	1.374(6)	C(21)-C(22)	1.372(6)
C(16)-C(17)	1.368(6)	C(22)-C(23)	1.376(7)
C(17)-C(18)	1.388(6)	C(23)-C(24)	1.380(6)
C(18)-C(13)	1.395(6)	C(24)-C(19)	1.402(5)

(b) Angles(l) B_5H_9 moiety

	I	II
P(1)-B(1)-B(2)	107.7(6)	117.2(3)
P(1)-B(1)-B(3)	107.9(6)	113.7(3)
P(1)-B(1)-B(4)	112.4(6)	107.8(3)
P(1)-B(1)-B(5)	116.1(6)	112.2(3)
P(2)-B(2)-B(1)	107.4(6)	115.9(3)
P(2)-B(2)-B(3)	116.4(6)	113.7(3)
B(2)-B(1)-B(3)	62.6(6)	62.7(3)
B(4)-B(1)-B(5)	60.6(6)	60.0(3)

Table VII, 5a (cont.)

B(2)-B(1)-B(5)	103.8(7)	100.1(3)
B(3)-B(1)-B(4)	101.3(7)	100.6(3)
B(2)-B(1)-B(4)	139.7(8)	135.0(3)
B(3)-B(1)-B(5)	136.0(8)	133.8(3)
B(1)-B(2)-B(3)	59.3(5)	59.2(3)
B(1)-B(3)-B(2)	58.0(5)	58.1(3)
B(1)-B(4)-B(5)	59.5(6)	59.9(3)
B(1)-B(5)-B(4)	59.9(6)	60.2(3)
P(2)-B(2)-H(1)	89.9(30)	98.0(17)
P(2)-B(2)-H(2)	118.5(54)	112.4(19)
B(1)-B(2)-H(1)	108.8(30)	105.3(17)
B(1)-B(2)-H(2)	117.2(52)	121.1(20)
B(3)-B(2)-H(1)	51.5(30)	46.2(17)
B(3)-B(2)-H(2)	122.0(55)	125.0(19)
H(1)-B(2)-H(2)	111.5(62)	99.3(26)
B(1)-B(3)-H(1)	103.6(30)	101.8(16)
B(1)-B(3)-H(3)	116.3(34)	116.6(24)
B(1)-B(3)-H(4)	117.0(44)	119.8(22)
B(2)-B(3)-H(1)	47.4(30)	43.9(16)
B(2)-B(3)-H(3)	116.6(34)	115.9(23)
B(2)-B(3)-H(4)	117.4(43)	120.4(22)
H(1)-B(3)-H(3)	86.4(44)	100.9(28)
H(1)-B(3)-H(4)	109.4(50)	97.3(27)
H(3)-B(3)-H(4)	117.9(56)	114.6(32)
B(2)-H(1)-B(3)	81.1(38)	89.9(23)
B(1)-B(4)-H(5)	102.9(32)	103.1(19)
B(1)-B(4)-H(6)	113.3(34)	116.5(19)
B(1)-B(4)-H(7)	114.0(41)	112.4(20)
B(5)-B(4)-H(5)	43.6(32)	44.6(19)

Table VII.5a (cont.)

B(5)-B(4)-H(6)	128.3(35)	115.2(19)
B(5)-B(4)-H(7)	114.5(42)	125.7(20)
H(5)-B(4)-H(6)	109.5(47)	106.7(27)
H(5)-B(4)-H(7)	101.7(53)	101.1(27)
H(6)-B(4)-H(7)	114.1(53)	114.8(28)
B(1)-B(5)-H(5)	105.3(34)	106.5(21)
B(1)-B(5)-H(8)	117.5(64)	118.9(20)
B(1)-B(5)-H(9)	114.3(54)	113.5(20)
B(4)-B(5)-H(5)	45.6(33)	47.8(21)
B(4)-B(5)-H(8)	139.8(61)	114.3(20)
B(4)-B(5)-H(9)	108.9(55)	128.4(19)
H(5)-B(5)-H(8)	115.3(70)	102.6(28)
H(5)-B(5)-H(9)	94.9(62)	100.8(28)
H(8)-B(5)-H(9)	107.6(83)	112.0(28)
B(4)-H(5)-B(5)	90.9(46)	87.7(28)
(II) <u>Ligand</u>		
B(1)-P(1)-C(1)	117.1(4)	117.4(2)
B(1)-P(1)-C(7)	119.4(4)	113.9(2)
B(1)-P(1)-C(25)	104.1(4)	114.9(2)
C(1)-P(1)-C(7)	103.8(3)	103.1(2)
C(1)-P(1)-C(25)	107.9(4)	101.4(2)
C(7)-P(1)-C(25)	103.2(4)	104.2(2)
B(2)-P(2)-C(13)	112.6(4)	112.3(2)
B(2)-P(2)-C(19)	118.2(4)	113.5(2)
B(2)-P(2)-C(25)	103.5(4)	-
B(2)-P(2)-C(26)	-	111.0(2)
C(13)-P(2)-C(19)	106.6(4)	108.3(2)
C(13)-P(2)-C(25)	109.0(4)	-
C(13)-P(2)-C(26)	-	107.4(2)

Table VII.5a (cont.)

C(19)-P(2)-C(25)	106.5(4)	-
C(19)-P(2)-C(26)	-	103.9(2)
P(1)-C(1)-C(2)	116.1(6)	119.3(3)
P(1)-C(1)-C(6)	123.9(6)	121.9(3)
P(1)-C(7)-C(8)	119.2(6)	118.3(3)
P(1)-C(7)-C(12)	120.4(6)	123.7(3)
P(2)-C(13)-C(14)	119.2(7)	122.2(3)
P(2)-C(13)-C(18)	120.3(7)	118.6(3)
P(2)-C(19)-C(20)	116.3(7)	119.7(3)
P(2)-C(19)-C(24)	123.7(6)	121.1(3)
P(1)-C(25)-P(2)	106.8(4)	-
P(1)-C(25)-C(26)	-	115.0(2)
P(2)-C(26)-C(25)	-	110.9(3)
P(1)-C(25)-H(251)	110.2	108.8(20)
P(1)-C(25)-H(252)	109.4	107.6(21)
P(2)-C(25)-H(251)	111.2	-
P(2)-C(25)-H(252)	110.2	-
H(251)-C(25)-H(252)	108.9	110.1(29)
P(2)-C(26)-H(261)	-	108.4(19)
P(2)-C(26)-H(262)	-	107.6(22)
C(26)-C(25)-H(251)	-	102.8(20)
C(26)-C(25)-H(252)	-	112.4(21)
C(25)-C(26)-H(261)	-	114.3(19)
C(25)-C(26)-H(262)	-	109.5(22)
H(261)-C(26)-H(262)	-	105.8(30)
C(19)-C(1)-C(6)	123.9(6)	121.9(3)
C(19)-C(7)-C(8)	119.2(6)	118.3(3)
C(19)-C(7)-C(12)	120.4(6)	123.7(3)
C(19)-C(13)-C(14)	119.2(7)	122.2(3)
C(19)-C(13)-C(18)	120.3(7)	118.6(3)
C(19)-C(19)-C(20)	116.3(7)	119.7(3)
C(19)-C(19)-C(24)	123.7(6)	121.1(3)
C(19)-C(25)-P(2)	106.8(4)	-
C(19)-C(25)-C(26)	-	115.0(2)
C(19)-C(26)-C(25)	-	110.9(3)
C(19)-C(25)-H(251)	110.2	108.8(20)
C(19)-C(25)-H(252)	109.4	107.6(21)
C(19)-C(25)-H(251)	111.2	-
C(19)-C(25)-H(252)	110.2	-
C(19)-H(251)-C(25)	108.9	110.1(29)
C(19)-H(261)-C(26)	-	108.4(19)
C(19)-H(262)-C(26)	-	107.6(22)
C(19)-C(25)-H(251)	-	102.8(20)
C(19)-C(25)-H(252)	-	112.4(21)
C(19)-C(26)-H(261)	-	114.3(19)
C(19)-C(26)-H(262)	-	109.5(22)
C(19)-H(261)-C(26)	-	105.8(30)

Table VII.5a (cont.)

(III) Phenyl rings

(I) $B_5H_9 \cdot dppm$

Ring 1		Ring 2	
C(6)-C(1)-C(2)	120.0(8)	C(12)-C(7)-C(8)	120.4(8)
C(1)-C(2)-C(3)	121.4(9)	C(7)-C(8)-C(9)	119.3(9)
C(2)-C(3)-C(4)	117.7(10)	C(8)-C(9)-C(10)	119.0(10)
C(3)-C(4)-C(5)	120.6(9)	C(9)-C(10)-C(11)	121.7(9)
C(4)-C(5)-C(6)	121.9(10)	C(10)-C(11)-C(12)	119.8(10)
C(5)-C(6)-C(1)	118.5(9)	C(11)-C(12)-C(7)	119.8(9)
Ring 3		Ring 4	
C(18)-C(13)-C(14)	120.5(8)	C(24)-C(19)-C(20)	120.0(8)
C(13)-C(14)-C(15)	118.3(9)	C(19)-C(20)-C(21)	116.7(10)
C(14)-C(15)-C(16)	120.1(10)	C(20)-C(21)-C(22)	122.3(10)
C(15)-C(16)-C(17)	121.6(9)	C(21)-C(22)-C(23)	120.0(10)
C(16)-C(17)-C(18)	118.8(11)	C(22)-C(23)-C(24)	118.7(9)
C(17)-C(18)-C(13)	120.6(9)	C(23)-C(24)-C(19)	122.1(8)

(II) $B_5H_9 \cdot dppe$

Ring 1		Ring 2	
C(6)-C(1)-C(2)	118.5(3)	C(12)-C(7)-C(8)	117.9(4)
C(1)-C(2)-C(3)	120.7(4)	C(7)-C(8)-C(9)	120.5(4)
C(2)-C(3)-C(4)	119.7(4)	C(8)-C(9)-C(10)	120.6(5)
C(3)-C(4)-C(5)	120.5(4)	C(9)-C(10)-C(11)	119.3(4)
C(4)-C(5)-C(6)	120.1(4)	C(10)-C(11)-C(12)	121.5(5)
C(5)-C(6)-C(1)	120.5(4)	C(11)-C(12)-C(7)	120.1(4)
Ring 3		Ring 4	
C(18)-C(13)-C(14)	119.1(4)	C(24)-C(19)-C(20)	118.8(3)
C(13)-C(14)-C(15)	120.4(4)	C(19)-C(20)-C(21)	120.5(4)
C(14)-C(15)-C(16)	119.8(4)	C(20)-C(21)-C(22)	120.4(4)
C(15)-C(16)-C(17)	120.4(4)	C(21)-C(22)-C(23)	119.7(4)
C(16)-C(17)-C(18)	120.7(4)	C(22)-C(23)-C(24)	120.4(4)
C(17)-C(18)-C(13)	119.6(4)	C(23)-C(24)-C(19)	120.1(4)

TABLE VII.5b

Bond distances (\AA) and bond angles ($^\circ$) with standard deviations in parentheses for $\text{B}_5\text{H}_9 \cdot \text{tmed}$

(a) Distances(1) B_5H_9 moiety

	Molecule 1	Molecule 2		Molecule 1	Molecule 2
N(11)-B(12)	1.677(7)	1.689(7)	B(1)-H(1)	1.111(45)	1.033(46)
N(2)-B(2)	1.651(7)	1.673(7)	B(2)-H(2)	1.071(33)	1.102(40)
B(1)-B(2)	1.700(9)	1.697(8)	B(3)-H(3)	1.003(59)	1.109(39)
B(1)-B(3)	1.804(10)	1.824(10)	B(3)-H(4)	1.192(54)	1.133(42)
B(1)-B(4)	1.701(10)	1.699(10)	B(3)-H(5)	1.418(51)	1.303(53)
B(1)-B(5)	1.825(10)	1.835(10)	B(4)-H(5)	1.271(50)	1.456(51)
B(3)-B(4)	1.723(13)	1.742(11)	B(4)-H(6)	1.026(56)	1.040(47)
B(4)-B(5)	1.778(11)	1.789(11)	B(4)-H(7)	1.264(61)	1.252(49)
B(2)...B(3)	2.720(10)	2.696(10)	B(5)-H(7)	1.272(60)	1.297(49)
B(2)...B(5)	2.726(10)	2.716(9)	B(5)-H(8)	1.038(49)	1.029(52)
B(3)...B(5)	2.830(12)	2.848(11)	B(5)-H(9)	1.301(51)	1.160(45)

(11) Ligand

	Molecule 1	
N(11)-C(11)	1.515(8)	C(13)-H(131) 0.95(5)
N(11)-C(12)	1.488(7)	C(13)-H(132) 1.27(5)
N(11)-C(13)	1.508(8)	C(14)-H(141) 0.99(4)
N(12)-C(14)	1.485(8)	C(14)-H(142) 1.34(6)
N(12)-C(15)	1.494(9)	C(15)-H(151) 0.97(16)
N(12)-C(16)	1.499(8)	C(15)-H(152) 0.94(5)
C(13)-C(14)	1.457(9)	C(15)-H(153) 1.10(5)
C(11)-H(111)	1.06(5)	C(16)-H(161) 0.89(4)
C(11)-H(112)	1.03(5)	C(16)-H(162) 0.84(6)
C(11)-H(113)	0.91(3)	C(16)-H(163) 1.09(5)
C(12)-H(121)	1.06(5)	
C(12)-H(122)	0.97(4)	
C(12)-H(123)	1.19(9)	

TABLE VII.5b continued

(II) Ligand (cont.)

Molecule 2			
N(21)-C(921a)	1.432(13)	N(21)-C(21b)	1.524(13)
N(21)-C(22a)	1.464(13)	N(21)-C(22b)	1.570(14)
N(21)-C(23a)	1.511(13)	N(21)-C(23b)	1.488(15)
N(22)-C(24a)	1.430(17)	N(22)-C(24b)	1.599(15)
N(22)-C(25a)	1.652(15)	N(22)-C(25b)	1.372(17)
N(22)-C(26a)	1.486(15)	N(22)-C(26b)	1.526(15)
C(23a)-C(24a)	1.596(20)		
C(21a)...C(21b)	0.882(18)	C(23b)-C(24b)	1.471(20)
C(21a)...C(23b)	1.825(17)	C(24a)...C(23b)	1.534(21)
C(22a)...C(21b)	1.919(18)	C(24a)...C(24b)	0.529(22)
C(22a)...C(22b)	0.701(19)	C(25a)...C(25b)	0.526(21)
C(23a)...C(23b)	0.887(19)	C(26a)...C(25b)	1.973(22)
C(23a)...C(24b)	1.247(19)	C(26a)...C(26b)	0.662(21)

(b) Angles(1) B₅H₉ moiety

	Molecule 1		Molecule 2		Molecule 1		Molecule 2	
N(1)-B(2)-N(2)	97.9(4)	96.3(4)	H(3)-B(3)-H(5)	104.5(37)	91.4(30)			
N(1)-B(2)-N(1)	115.0(4)	115.1(4)	H(4)-B(3)-H(5)	103.5(33)	106.8(27)			
N(2)-B(2)-B(1)	116.7(4)	115.5(4)	B(1)-B(4)-H(5)	116.3(23)	107.0(20)			
B(2)-B(1)-B(3)	101.8(5)	99.9(4)	B(1)-B(4)-H(6)	123.2(25)	118.2(22)			
B(2)-B(1)-B(4)	144.7(5)	143.3(5)	B(1)-B(4)-H(7)	105.2(27)	108.2(22)			
B(2)-B(1)-B(5)	101.2(4)	100.5(4)	B(3)-B(4)-H(5)	53.8(23)	47.1(20)			
B(3)-B(1)-B(4)	58.8(4)	59.1(4)	B(3)-B(4)-H(6)	128.7(25)	126.8(24)			
B(3)-B(1)-B(5)	102.5(5)	102.2(5)	B(3)-B(4)-H(7)	115.0(26)	120.1(22)			
B(4)-B(1)-B(5)	60.4(4)	60.7(4)	B(5)-B(4)-H(5)	125.3(23)	113.7(18)			
B(1)-B(3)-B(4)	57.6(4)	56.9(4)	B(5)-B(4)-H(6)	120.2(25)	120.5(24)			
B(1)-B(4)-B(3)	63.6(5)	64.0(4)	B(5)-B(4)-H(7)	45.7(27)	46.5(22)			
B(1)-B(4)-B(5)	63.2(4)	63.4(4)	H(5)-B(4)-H(6)	104.9(33)	120.1(30)			
B(1)-B(5)-B(4)	56.3(4)	55.9(4)	H(5)-B(4)-H(7)	91.6(36)	89.9(29)			
B(3)-B(4)-B(5)	107.9(6)	107.5(5)	H(6)-B(4)-H(7)	111.2(36)	109.4(32)			

TABLE VII.5b continued

B(2)-B(1)-H(1)	116.2(23)	114.5(25)		
B(3)-B(1)-H(1)	120.3(22)	117.6(23)	B(3)-H(5)-B(4)	79.7(28) 78.1(29)
B(4)-B(1)-H(1)	99.0(23)	102.1(25)		
B(5)-B(1)-H(1)	112.4(23)	119.1(24)	B(1)-B(5)-H(7)	98.2(28) 98.9(22)
N(1)-B(2)-H(2)	100.9(17)	105.2(19)	B(1)-B(5)-H(8)	121.1(26) 115.5(30)
N(2)-B(2)-H(2)	102.2(18)	108.0(20)	B(1)-B(5)-H(9)	107.9(21) 121.6(22)
B(1)-B(2)-H(2)	120.7(18)	114.8(20)	B(4)-B(5)-H(7)	45.3(28) 44.4(22)
B(1)-B(3)-H(3)	107.7(28)	103.0(20)	B(4)-B(5)-H(8)	114.6(27) 124.4(28)
B(1)-B(3)-H(4)	125.2(26)	117.7(19)	B(4)-B(5)-H(9)	120.6(20) 117.2(23)
B(1)-B(3)-H(5)	103.3(20)	107.5(21)	H(7)-B(5)-H(8)	109.3(37) 98.3(35)
B(4)-B(3)-H(3)	123.9(30)	120.3(20)	H(7)-B(5)-H(9)	94.4(32) 106.2(30)
B(4)-B(3)-H(4)	121.6(26)	111.2(19)	H(8)-B(5)-H(9)	120.1(33) 111.8(36)
B(4)-B(3)-H(5)	46.5(20)	54.9(22)		
H(3)-B(3)-H(4)	110.4(39)	126.2(27)	B(4)-H(7)-B(5)	89.1(39) 89.1(31)

(II) LigandMolecule 1

B(12)-N(11)-C(11)	114.5(4)	H(121)-C(12)-H(123)	112.5(50)
B(12)-N(11)-C(12)	101.1(4)	H(122)-C(12)-H(123)	88.4(48)
B(12)-N(11)-C(13)	107.0(4)	N(11)-C(13)-H(131)	114.0(31)
C(11)-N(11)-C(12)	107.5(4)	N(11)-C(13)-H(132)	97.6(23)
C(11)-N(11)-C(13)	107.8(5)	C(14)-C(13)-H(131)	117.4(32)
C(12)-N(11)-C(13)	111.0(4)	C(14)-C(13)-H(132)	105.2(21)
B(12)-N(12)-C(14)	103.8(4)	H(131)-C(13)-H(132)	113.7(37)
B(12)-N(12)-C(15)	113.5(5)	N(12)-C(14)-H(141)	113.4(20)
B(12)-N(12)-C(16)	110.8(4)	N(12)-C(14)-H(142)	114.8(23)
C(14)-N(12)-C(15)	112.2(5)	C(13)-C(14)-H(141)	114.5(21)
C(14)-N(12)-C(16)	107.6(4)	C(13)-C(14)-H(142)	95.6(23)
C(15)-N(12)-C(16)	108.8(5)	H(141)-C(14)-H(142)	110.6(33)
N(11)-C(13)-C(14)	106.7(5)	N(12)-C(15)-H(151)	114.4(36)
N(12)-C(14)-C(13)	106.7(5)	N(12)-C(15)-H(152)	110.1(30)

TABLE VII.5c continued

(II) Ligand: Molecule 1 cont.

N(11)-C(11)-H(111)	109.2(21)	N(12)-C(15)-H(153)	102.1(27)
N(11)-C(11)-H(112)	101.8(29)	H(151)-C(15)-H(152)	111.8(48)
N(11)-C(11)-H(113)	107.8(26)	H(151)-C(15)-H(153)	116.5(44)
H(111)-C(11)-H(112)	116.1(33)	H(152)-C(15)-H(153)	100.9(39)
H(111)-C(11)-H(113)	106.7(35)	N(12)-C(16)-H(161)	112.0(27)
H(112)-C(11)-H(113)	114.2(39)	N(12)-C(16)-H(162)	97.7(45)
N(11)-C(12)-H(121)	117.9(26)	N(12)-C(16)-H(163)	107.7(25)
N(11)-C(12)-H(122)	105.4(24)	H(161)-C(16)-H(162)	117.6(51)
N(11)-C(12)-H(123)	104.8(42)	H(161)-C(16)-H(163)	94.4(37)
H(121)-C(12)-H(122)	122.9(35)	H(162)-C(16)-H(163)	127.6(52)

Molecule 2

Conformation		Conformation	
a	b	a	b
B(22)-N(21)-C(21)	114.1(5)	B(22)-N(22)-C(25)	102.9(6)
B(22)-N(21)-C(21)	111.3(6)	B(22)-N(22)-C(26)	119.8(6)
B(22)-N(21)-C(23)	101.0(5)	C(24)-N(22)-C(25)	112.3(8)
C(21)-N(21)-C(22)	110.9(7)	C(24)-N(22)-C(26)	105.4(9)
C(21)-N(21)-C(23)	111.2(7)	C(25)-N(22)-C(26)	103.4(8)
C(22)-N(21)-C(23)	107.8(7)	N(21)-C(23)-C(24)	104.2(9)
B(22)-N(22)-C(24)	112.8(7)	N(22)-C(24)-C(23)	102.6(11)
C(21a)-N(21)-C(21b)	34.5(7)	C(25a)-N(22)-C(24b)	101.1(7)
C(21a)-N(21)-C(22b)	132.1(7)	C(25a)-N(22)-C(25b)	17.0(8)
C(21a)-N(21)-C(23b)	177.3(7)	C(25a)-N(22)-C(26b)	128.5(8)
C(22a)-N(21)-C(21b)	79.9(7)	C(26a)-N(22)-C(24b)	124.0(8)
C(22a)-N(21)-C(22b)	26.4(7)	C(26a)-N(22)-C(25b)	87.2(9)
C(22a)-N(21)-C(23b)	127.9(8)	C(26a)-N(22)-C(26b)	25.3(8)
C(23a)-N(21)-C(21b)	138.2(7)	N(21)-C(23a)-C(24b)	114.5(11)
C(23a)-N(21)-C(22b)	83.9(7)	N(21)-C(23b)-C(24a)	108.5(11)
C(23a)-N(22)-C(23b)	34.4(7)	N(22)-C(24a)-C(23b)	109.3(12)
C(24a)-N(22)-C(24b)	19.1(8)	N(22)-C(24b)-C(23a)	111.7(11)
C(24a)-N(22)-C(25b)	112.7(10)		
C(24a)-N(22)-C(26b)	90.2(9)		

TABLE VII.6

Equations of the least squares mean planes $PI + QJ + RK = S^\dagger$, interplanar angles and some significant atomic displacements from these planes.

(a) $B_5H_9 \cdot dppm$

Plane	Defining atoms	P	Q	R	S
1	B(1) B(2) B(3)	0.9708	-0.0754	-0.2279	6.6940
2	B(1) B(4) B(5)	-0.5084	-0.3378	0.7921	-4.1488
3	B(1) B(2) B(5)	0.7268	0.6508	-0.2199	10.4894
4	B(1) B(3) B(4)	-0.6020	0.3866	0.6987	0.5307
5	B(2) B(3) B(4) B(5)	-0.8123	-0.1486	0.5639	-6.6117
6	P(1) P(2) B(1) B(2)	-0.2311	0.9687	-0.0907	5.5597
7	C(1 - 6)	-0.6649	0.4496	0.5965	1.7744
8	C(7 - 12)	0.4995	-0.4586	0.7350	3.1659
9	C(13 - 18)	-0.2955	-0.0028	0.9553	-0.2077
10	C(19 - 24)	0.3640	0.9107	0.1954	9.2242

Lines

11. P(1)-C(1) 12. P(1) - C(7) 13. P(2) - C(13) 14. P(2) - C(19)

Angles ($^\circ$) between planes or lines:-

(1) - (2) 130.43 (2) - (3) 40.23 (3) - (5) 35.80 (7) - (8) 84.27
 (1) - (3) 45.05 (2) - (4) 43.21 (3) - (6) 61.16 (9) - (10) 85.61
 (1) - (4) 39.40 (2) - (5) 24.51 (4) - (5) 34.35 (7) - (11) 0.31
 (1) - (5) 25.06 (2) - (6) 73.64 (4) - (6) 63.24 (8) - (12) 1.59
 (1) - (6) 73.94 (3) - (4) 109.85 (5) - (6) 89.58 (9) - (13) 0.75
 (10) - (14) 0.35

Significant atomic displacements from plane above:-

Plane 5: B(1) by 0.635 Å	Plane 7: P(1) by -0.022 Å
P(1) by 1.532 Å	Plane 8: P(1) by -0.059 Å
P(2) by 2.902 Å	Plane 9: P(2) by -0.027 Å
Plane 6: C(25) by 0.556 Å	Plane 10: P(2) by 0.001 Å

(b) $B_5H_9 \cdot dppe$

Plane	Defining atoms	P	Q	R	S
1	B(1) B(2) B(3)	0.7692	-0.3426	0.4988	8.9581
2	B(1) B(4) B(5)	0.3873	0.3854	0.8375	8.8858
3	B(1) B(2) B(5)	0.8734	0.3978	0.2809	7.5339
4	B(1) B(3) B(4)	0.1678	-0.3462	0.9230	8.3836
5	B(2) B(3) B(4) B(5)	0.6551	0.0295	0.7550	10.6862
6	P(1) P(2) B(1) B(2)	0.2443	0.9456	-0.2149	-0.4200
7	C(1) - C(6)	-0.6943	0.6251	0.3567	-1.6957
8	C(7) - C(12)	0.3965	-0.3198	0.8606	7.3501
9	C(13) - C(18)	0.7537	0.5299	-0.3888	-0.5953
10	C(19) - C(24)	0.0867	-0.0121	0.9962	9.7295

Lines

11. P(1) - C(1) 12. P(1) - C(7) 13. P(2) - C(13) 14. P(2) - C(19)

Angles ($^\circ$) between planes or lines:-

(1) - (2)	126.45	(2) - (3)	43.38	(3) - (5)	37.25	(7) - (8)	80.32
(1) - (3)	45.64	(2) - (4)	45.20	(3) - (6)	58.05	(9) - (10)	70.83
(1) - (4)	44.55	(2) - (5)	26.18	(4) - (5)	37.19	(7) - (11)	6.65
(1) - (5)	27.38	(2) - (6)	73.79	(4) - (6)	61.01	(8) - (12)	4.86
(1) - (6)	76.31	(3) - (4)	105.55	(5) - (6)	88.52	(9) - (13)	3.19
		(10) - (14)	5.67 $^\circ$				

Significant atomic displacements from planes above:-

Plane 5:	B(1) by -0.690 Å	Plane 7:	P(1) by 0.221 Å
	P(1) by -2.637 Å	Plane 8:	P(1) by 0.168 Å
	P(2) by -1.287 Å	Plane 9:	P(2) by 0.104 Å
Plane 6:	C(25) by 0.050 Å	Plane 10:	P(2) by -0.180 Å
	C(26) by 0.829 Å		

(c) B_5H_9 - med

No.	Defining atoms	P	Q	R	S
1	N(1) B(2) N(2)	0.4706 [0.7605	0.8542 0.5120	-0.2212 0.3994	5.2767 1.7711]
2	B(1) B(2) B(4)	-0.3369 [-0.4271	0.3681 -0.0551	0.8666 0.9025	7.5010 -2.0874]
3	B(1) B(3) B(4)	0.7178 [0.3569	0.5273 0.5908	-0.4546 0.7236	1.9746 -0.1147]
4	B(1) B(4) B(5)	0.4380 [0.7492	0.8524 0.6601	0.2858 0.0544	8.4696 1.7385]
5	B(1) B(3) B(5)	0.1023 [0.8866	0.9294 0.1263	-0.3548 0.4449	0.9840 -0.4554]
6	B(2) B(3) B(4)	0.8779 [0.2409	0.4437 0.8251	-0.1801 0.5111	5.5679 1.3299]
7	B(2) B(4) B(5)	0.7017 [0.4859	0.6495 0.8739	0.2928 0.0155	9.7291 2.5307]
8	B(3) B(4) B(5)	0.9390 [0.0286	0.2395 0.9937	0.2467 0.1083	9.6423 3.1152]

Angles ($^\circ$) between planes:-

(1)-(2) 87.9[89.6] (2)-(7) 75.1[76.0] (3)-(8) 46.5[47.5] (5)-(7) 55.1[56.8]
 (2)-(3) 63.8[62.1] (2)-(8) 89.2[88.2] (4)-(5) 42.6[43.7] (5)-(8) 76.6[78.5]
 (2)-(4) 65.6[66.1] (3)-(4) 129.3[128.2] (4)-(7) 19.2[19.9] (6)-(7) 148.4[147.8]
 (2)-(5) 90.0[89.1] (3)-(5) 43.6[44.5] (4)-(8) 46.7[47.8] (6)-(8) 27.6[28.1]
 (2)-(6) 73.2[71.8] (3)-(6) 18.9[19.4] (5)-(6) 55.5[57.0] (7)-(8) 27.5[27.9]

Significant atomic displacements from planes above:-

Plane 1: C(3) 0.18 Å [a, 0.85; b, 0.02 Å] Plane 2: B(3) 1.38 Å [-1.38 Å]
 C(4) 0.71 Å [a, 0.23; b, 0.70 Å] B(5) -1.45 Å [1.46 Å]
 Plane 2: N(1) -1.26 Å [-1.28 Å] Plane 5: B(2) 1.61 Å [1.63 Å]
 N(2) 1.26 Å [1.23 Å] B(4) -1.00 Å [-1.02 Å]
 C(3) -0.63 Å [a, -0.69; b, -0.77 Å] Plane 8: B(1) -1.11 Å [-1.13 Å]
 C(4) 0.69 Å [a, 0.75; b, 0.53 Å] B(2) -1.26 Å [-1.27 Å]

† With the orthogonal unit vector I parallel to a, K perpendicular to a in the ac plane and J perpendicular to the ac plane.

Defined as in R. Buncick, *Thermal Expansion*, 1974, p. 136.

TABLE VII.7

Torsion angles * in the Chelate Rings ($^{\circ}$)

(a) $B_5H_9 \cdot dppm$		
P(1)-C(25)-P(2)-B(2)		+32.98
C(25)-P(2)-B(2)-B(1)		-26.23
P(2)-B(2)-B(1)-P(1)		-9.46
B(2)-B(1)-P(1)-C(25)		-10.51
B(1)-P(1)-C(25)-P(2)		+27.42
(b) $B_5H_9 \cdot dppe$		
P(1)-C(25)-C(26)-P(2)		-66.10
C(25)-C(26)-P(2)-B(2)		+64.74
C(26)-P(2)-B(2)-B(1)		-28.48
P(2)-B(2)-B(1)-P(1)		-0.76
B(2)-B(1)-P(1)-C(25)		-2.34
B(1)-P(1)-C(25)-C(26)		+56.70
(c) $B_5H_9 \cdot tmed$		
Molecule 1		
B(2)-N(1)-C(3)-C(4)		-17.82
N(1)-C(3)-C(4)-N(2)		-39.28
C(3)-C(4)-N(2)-B(2)		+43.82
C(4)-N(2)-B(2)-N(1)		-29.42
N(2)-B(2)-N(1)-C(3)		+7.34
Molecule 2		
B(2)-N(1)-C(3a)-C(4a)	-48.56	C(3a)-C(4a)-N(2)-B(2) -17.50
B(2)-N(1)-C(3a)-C(4b)	-35.32	C(3a)-C(4b)-N(2)-B(2) +9.28
B(2)-N(1)-C(3b)-C(4a)	+8.12	C(3b)-C(4a)-N(2)-B(2) +15.99
B(2)-N(1)-C(3b)-C(4b)	+28.42	C(3b)-C(4b)-N(2)-B(2) +47.28
N(1)-C(3a)-C(4a)-N(2)	+42.46	C(4a)-N(2)-B(2)-N(1) -10.11
N(1)-C(3a)-C(4b)-N(2)	+17.04	C(4b)-N(2)-B(2)-N(1) -26.79
N(1)-C(3b)-C(4a)-N(2)	-14.98	N(2)-B(2)-N(1)-C(3a) +34.97
N(1)-C(3b)-C(4b)-N(2)	-46.75	N(2)-B(2)-N(1)-C(3b) +0.63

* Defined as in R. Bucourt, Topics Stereochem., 1974, 8, 159.

TABLE VII.8

Atomic co-ordinates ($\times 10^3$), bond distances (\AA) and bond angles ($^\circ$) for the disordered tetrahydrofuran solvent in compound (1)[†]. The estimated standard deviations in these measurements are shown beneath each section.

Atomic Co-ordinates			
Atom	X	Y	Z
C(261)	495	289	457
C(271)	398	229	425
C(281)	347	274	374
C(291)	450	347	379
C(301)	463	363	439
C(262)	494	233	439
C(272)	371	251	393
C(282)	356	334	378
C(292)	458	361	413
C(302)	523	326	448
Estimated standard deviation:	± 10	± 5	± 4

Bond distances and angles

(a) Distances (\AA)

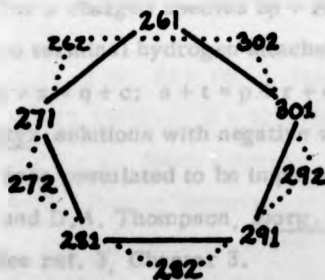
C(261)-C(271)	1.46	C(262)-C(272)	1.48
C(271)-C(281)	1.47	C(272)-C(282)	1.44
C(281)-C(291)	1.47	C(282)-C(292)	1.23
C(291)-C(301)	1.41	C(292)-C(302)	1.11
C(301)-C(261)	1.34	C(302)-C(262)	1.60
C(261)-C(262)	1.02	C(291)-C(282)	0.77
C(261)-C(302)	0.70	C(291)-C(292)	0.83
C(271)-C(262)	0.83	C(301)-C(292)	0.59
C(271)-C(272)	0.86	C(301)-C(302)	0.80
C(281)-C(272)	0.62		
C(281)-C(282)	1.01		

(b) Angles ($^{\circ}$)

C(301)-C(261)-C(271)	112	C(302)-C(262)-C(272)	89
C(261)-C(271)-C(281)	102	C(262)-C(272)-C(282)	115
C(271)-C(281)-C(291)	102	C(272)-C(282)-C(292)	98
C(281)-C(291)-C(301)	106	C(282)-C(292)-C(302)	127
C(291)-C(301)-C(261)	98	C(292)-C(302)-C(262)	110
C(302)-C(261)-C(262)	136	C(261)-C(262)-C(271)	103
C(262)-C(271)-C(272)	123	C(271)-C(272)-C(281)	167
C(272)-C(281)-C(282)	121	C(281)-C(282)-C(291)	110
C(282)-C(291)-C(292)	101	C(291)-C(292)-C(301)	167
C(292)-C(301)-C(302)	105	C(301)-C(302)-C(262)	126

† The estimated standard deviations in the bond distances and angles quoted are $\approx \pm 0.10$ Å and $\pm 10^{\circ}$ respectively.

†† Numbering of the atoms in the disordered solvent is:-



- K. Eriks, W.N. Lipscomb and R. Schaeffer, ibid., 1954, 22, 754; F.L. Hirshfield, K. Eriks, R.E. Dickenson, E.L. Lippert, Jr., and W.N. Lipscomb, ibid., 1958, 28, 56.
6. R. Schaeffer, D.C. Moody and P.J. Dolan, 'Recent Advances in the Chemistry of Boron Hydrides', Second International Meeting on Boron Chemistry, Leeds, 1974.
 7. J.C. Huffman, D.C. Moody, J.W. Rathke and R. Schaeffer, J. Chem. Soc. Chem. Comm., 1973, 308. See also J. Rathke and R. Schaeffer, J. Am. Chem. Soc., 1973, 95, 3402 for preparation of $B_{15}H_{23}^+$.
 8. J.C. Calabrese and L.F. Dahl, J. Am. Chem. Soc., 1971, 93, 6042 and refs. therein.
 9. R. Zerger, W. Rhine and G. Stucky, J. Am. Chem. Soc., 1974, 96, 6048 and refs. therein.
 10. G.L. McKown, B.P. Don, R.A. Beaudet, T.G. Vergamini and L.H. Jones, J. Chem. Soc. Chem. Comm., 1974, 765.
 11. For a charged species $BpHp^C + q + c$, the equations become $s + x = q + c$; $s + t = p + c$; $t + y = p - c - q/2$.
 12. For a charged species $Bp + rHp^C + q + c$ in which r boron atoms have no terminal hydrogen attached, the equations become $s + x = q + c$; $s + t = p + r + c$; $s + r = 2y + 3c + x$
 13. Styx solutions with negative values [sty(-1) especially] have, however, been postulated to be important reaction intermediates, R.W. Rudolph and D.A. Thompson, Inorg. Chem., 1974, 13, 2779.
 14. See ref. 3, Chapter 3.
 15. W.N. Lipscomb, Acc. Chem. Research, 1973, 6, 257.
 16. K. Wade, Advan. Inorg. Chem. Radiochem., 1976, 18, 1.
 17. J. Rathke and R. Schaeffer, Inorg. Chem., 1974, 13, 3008.
 18. A. Davison, D.D. Traficante and S.S. Wreford, J. Chem. Soc. Chem. Comm., 1972, 1155.
 19. J.P. Brennan, R. Schaeffer, A. Davison and S.S. Wreford, J. Chem. Soc. Chem. Comm., 1973, 354.

20. O. Hollander, W.R. Clayton and S.G. Shore, J. Chem. Soc. Chem. Comm., 1974, 604; M. Mangion, W.R. Clayton, O. Hollander and S.G. Shore, Inorg. Chem., 1977, 16, 2110.
21. N.N. Greenwood, J.A. Howard and W.S. McDonald, J. Chem. Soc. Dalton, 1977, 37; D.F. Gaines and J. Ulman, Inorg. Chem., 1974, 13, 2792; M.R. Churchill, J.J. Hackbarth, A. Davison, D.D. Traficante, S.S. Wreford, J. Am. Chem. Soc., 1974, 96, 4041.
22. (a) A.V. Fratini, G.W. Sullivan, M.L. Denniston, R.K. Hertz and S.G. Shore, J. Am. Chem. Soc., 1974, 96, 3013; (b) M. Mangion, R.K. Hertz, M.L. Denniston, J.R. Long, W.R. Clayton and S.G. Shore, J. Am. Chem. Soc., 1976, 98, 449.
23. N.E. Miller, H.C. Miller and E.L. Muetterties, Inorg. Chem., 1964, 3, 867.
24. R.J. Remmel, H.D. Johnson II, I.S. Jaworlowsky and S.G. Shore, J. Amer. Chem. Soc., 1975, 97, 5395.
25. C.G. Savory and M.G.H. Wallbridge, unpublished results.
26. C.G. Savory and M.G.H. Wallbridge, J. Chem. Soc. Dalton, 1973, 179.
27. $C_6H_{24}B_4N_2$, $M = 167.5$, monoclinic, $a = 7.654(2)$, $b = 12.937(3)$, $c = 12.536(3)$ Å, $\beta = 107.78(2)^\circ$, $U = 1182.0(5)$, $\rho = 0.94$ g/cm³ for $Z = 4$. Space group Cc or C2/c. Crystal not scattering very well. Data collected out to $2\theta = 45^\circ$ in two shells, using θ - 2θ scans. Of 853 reflections 575 are observed ($I/\sigma(I) > 3.0$). Distribution of E's favours acentric space group.
28. SHELX (G.M. Sheldrick, 1975): a multisolution direct method technique utilising Σ_2 sign expansion along a pre-determined pathway with selective rejection tests based on M_{abs} (Chapter VIII) and $NQT = -\Sigma E_{h+k} E_{h-k} (2E_h^2 E_k^2 - E_h^2 - E_k^2)$ values. The latter is related to the probability of the sign of the product E_{h+k}^* E_{h-k} being correct when E_h , E_{h+k} , E_{h-k} are large and E_k small (or E_k large and E_h small). For a comparison of SHELX with MULTAN (and XCSD) see Z. Shakked and O. Kennard, Acta Cryst., 1977, B33, 516.

29. D.L. Black and R.C. Taylor, Acta Cryst., 1975, B31, 1116.
30. F.A. Cotton and J.M. Troup, J. Am. Chem. Soc., 1974, 96, 4422; M.G.B. Drew, J. Chem. Soc. Dalton, 1972, 1329;
J.C. Jeffries, Ph. D. thesis, Univ. of Warwick, 1975.
31. A. Domenicano, A. Vaciago and C.A. Coulson, Acta Cryst., 1975, B31, 1630.
32. A. Domenicano and A. Vaciago, Acta Cryst., 1975, B31, 2553.
33. See for example D.J. Brauer and C. Krüger, Inorg. Chem., 1977, 16, 884.
34. P.H. Clippard, J.C. Hansen and R.C. Taylor, J. Cryst. Mol. Str., 1971, 1, 363.
35. C. Glidewell, Inorg. Chlm. Acta, 1974, 11, 257 and refs. therein.
36. W.N. Lipscomb, 'Effects of Orbital Vacancies in Boron Compounds', Third International Meeting on Boron Chemistry, München and Ettal, July, 1976.
37. L.B. Friedman and W.N. Lipscomb, Inorg. Chem., 1966, 5, 1752.
38. K.A.R. Mitchell, Chem. Rev., 1969, 69, 157; C.A. Coulson, Nature, 1969, 221, 1106.

CHAPTER VIII

Crystallographic Methods

(VIII.1.) X-Ray Diffraction

The basis of X-ray crystallography is the property of a crystal, whose internal dimensions are of the same order of magnitude as the wavelength of X-rays, to act as a three dimensional diffraction grating for X-rays. The data collected are the intensities of an X-ray beam which is diffracted only when the crystal is at particular orientations to the incident beam. The pattern of these diffracted intensities depends on the distribution of electron density within the crystal and, of course, electron density is concentrated around the atomic nuclei and its maxima will indicate atomic positions. It is, however, the square root of the intensity, the structure factor with which the crystallographer works. These structure factors can be expressed as a series of Fourier coefficients, and related to the pattern of electron density within the crystal as explained later. There is one major problem in this procedure. Whilst the experimental intensity of each reflection can be directly measured and reduced to a structure factor, there is at present no method available to directly measure the phase angle associated with each reflection. It is this loss of phase information - the phase problem - which is central to all the different methods used in crystallographic studies.

Much has been written about the general background and mathematical principles involved in X-ray crystallography.¹ In the following paragraphs a few of the most important principles and equations used throughout the present work are summarised.

(VIII.2.) Structure Determination

The course of a single structure determination consists of the following main stages:

- (a) Collecting and processing of the raw X-ray data, the experimental intensity measurements, to give structure factors, $F(hkl)$, which are proportional to the square root of the measured intensities.

- (b) Solving the phase problem, usually by statistical methods or interpretation of the Patterson function. This latter is a Fourier summation performed with intensity rather than $\sqrt{\text{intensity}}$ as coefficients, and it reveals all the vectors between atoms in the structure, a peak being approximately of height $Z_1 \cdot Z_2$, where Z_1 and Z_2 are the atomic numbers of the two atoms. This means that vectors associated with a heavy atom normally dominate the map.
- (c) A Fourier inversion of the phased $F(hkl)$ values (a complex number) to yield an electron density map of the structure in which atoms can be identified.
- (d) Least squares or further Fourier refinement to find the atomic positions which give best agreement between the observed and calculated data.
- (e) Calculation of derived parameters, that is bond lengths, bond angles and conformations, together with the assignment of their chemical importance and explanation of other physical and chemical properties of the substance.

During each determination there are, therefore, a large number of computations involved. Most of these are of the number crunching variety, and efficient programs are essential. The majority of the structures described in this thesis have been solved using the X-RAY suite of crystallographic programs² and the details relating to each of the steps enumerated above are discussed with particular reference to individual program links of that system.

(VIII.3.) Data Collection

In the first step the amount of data collected for each crystal is large; typically 2000 to 5000 diffracted intensities for a structure of moderate size. The actual quantity depends on the symmetry and volume of the unit cell. Each diffracted intensity is a function of both the number of electrons involved and the distribution of atoms in the plane of the crystal which is in position to diffract according to Bragg's law. Whilst the maximum amount of data (number of planes) is finite but exceedingly large, and the accuracy of derived parameters can be related to the size of the data set collected, practical considerations normally limit the amount of data collected. All data

sets for the compounds discussed were collected using a Syntex P2₁ four circle diffractometer by the use of graphite monochromatised radiation.³ The diffractometer is controlled on-line by a Data General Nova computer and all data is recorded on 7-track magnetic tape before processing to paper tape and/or disk files on the computer.

A distinct advantage with the Syntex P2₁ is the ability to work with a randomly orientated crystal. Once the crystal has been centred, so that it is rotating about an arbitrary axis, a φ rotation photograph is taken. From this photograph the co-ordinates of several (max.15) reflections are accurately centred. In the centring process the 2θ and χ angles are calculated for each reflection and, with ω assumed to be zero, the φ circle is rotated at low speed until a reflection with an intensity greater than a specified default is encountered. The program will then home in on the refined angular co-ordinates until consecutive refinements give angles within specified tolerances. In each refinement step the angles are refined in the order, first ω , then 2θ , ω again and then χ . If default parameters are used, each iteration will scan at $\sim 5^\circ/\text{min}$ in ω over a maximum range of $\pm 1^\circ$, recording the position of the half-height peak intensity, then at $\sim 5^\circ/\text{min}$ in $2\theta \pm 2^\circ$, again at $\sim 5^\circ/\text{min}$ in $\omega \pm 1^\circ$ and finally at $30^\circ/\text{min}$ in $\chi \pm 20^\circ$. Normally φ is held fixed (but would be scanned at $\sim 5^\circ/\text{min}$ if refined). At the end of each iteration 2θ , ω , φ , χ and the peak intensity are printed. The procedure is the same for refining approximate angular values except the preliminary ω scan can sometimes be omitted, and for the weaker higher angle reflections it is necessary to slow the scan speeds in the refinement to a half or a quarter of their normal values.

Once all the reflections have been refined, their refined angular co-ordinates are used to generate sets of possible axial vectors which would give integer ± 0.1 values for all the hkl indices of the refined reflections. This program can be used a priori for determining the unit cell although it is better to have some form of photographic confirmation. The choice of the best axial vectors is based on axial lengths and the cosine of the inter-vector angles. In an a priori

situation where no preliminary precession or Weissenberg photographs have been taken, it is essential to take axial photographs about the chosen axial vectors from which the spacing of the layer lines will give approximate axial lengths and the presence or absence of mirror symmetry about the horizontal line in the photograph indicates the presence or absence of a symmetry axis.⁴ Any spots lying off layer lines probably indicate twinning or the presence of satellite subcrystals. Thus, if the auto-indexing shows three vectors with their inter-vector cosines zero, then this solution would require mirror symmetry to be found in all three axial photographs before the unit cell could be accepted as being orthorhombic or of higher symmetry. The choice of Laue and space group symmetries can similarly be found by performing rapid data collections over specified reflections (see below).⁴

From the chosen set of axial vectors, the auto-indexing program assigns indices to all reflections in the reflection array and calculates a unit cell volume. If negative, the choice of axes has given a left handed cell. Interchange of two axes or making one axis negative will solve this problem. Similar interchanges are necessary in the triclinic and monoclinic cases to give the correct cell with angles $> 90^\circ$. For any triclinic cell it is necessary to reduce it to its most primitive form, a process named after Delauney.

From the assigned indices and the refined values of 2θ , ω , φ and λ an orientation matrix relating the crystal unit cell to the diffractometer reference axes can be determined by least squares methods. This orientation matrix can then be used to reverse the process and calculate the angles with (1) φ held constant and (2) ω constrained to be $\frac{1}{2}(2\theta)$. Finally the indices of each reflection are calculated from the orientation matrix and the observed angles. The least squares refined unit cell parameters are also printed along with a measure of the standard deviation in each value. Although in the calculation of the unit cell parameters from the refined angular co-ordinates the crystal system is always treated as if it was triclinic, it is found that, providing the crystal is well centred, the calculated unit cell

parameters are normally within three standard deviation (typically 0.02°) of the crystallographically correct values.⁵ Such differences are considered insignificant and in subsequent programs mean axial lengths and/or angles of 90° , 120° , etc. where appropriate to the lattice symmetry are used.⁴ In the data collection, the values calculated do allow for instrumental and other alignment errors.

The accuracy of the orientation matrix can be improved by centring (at slow speeds if necessary) on up to 15 higher angle (2θ) reflections determined either from previous photographs or else by collecting a shell of data at higher scan speeds. It is good practice to avoid axial reflections and ensure all regions of reciprocal space are investigated.

Once a satisfactory orientation matrix has been obtained, the data collection can proceed. The conditions associated with the collection of each data set are listed in the individual chapters. However, data sets were normally collected using the $2\theta:\theta$ method in which both the counter (2θ circle) and crystal (ω circle) are rotated at relative angular rates given by

$$\Delta 2\theta = 2 \Delta \omega$$

In the course of a data collection the data are collected out to a maximum practical 2θ (in shells if required), each peak being scanned over a specified range above and below the α_1 and α_2 peaks. The scan speed over the peak depends on the intensity of a preliminary count. The count rates for collection at the extreme speeds are pre-set by the user, and intermediate speeds are determined by the program. A coincidence correction is applied automatically to particularly intense reflections with a number of counts exceeding 12,000 cps. Backgrounds for each reflection are measured for a specified amount (normally, a quarter on each side) of the time taken to measure each peak.

Several standard reflections at various 2θ values are remeasured at regular intervals to check for variations in intensity due to decomposition or crystal movement (corrected by re-centring the crystal at intervals or after a specified drop in the intensity of the standards).

Generally, the intensities of the standard reflections will show only statistical fluctuations due to small variations in temperature and in the intensity of the incident beam. These fluctuations will be in opposite directions, preventing any valid corrections. This procedure is different from that used by some crystallographers who scale individual measurements of a single standard to a common value.

However, when there is a significant drop in the intensities of the standards due to decomposition, the effects of this decomposition can be reduced by scaling the intensities or more particularly the calculated structure factors, using a scaling equation of the form

$$F_{\text{corr}} = F_{\text{calc}} * (1 + \alpha * t)(1 + \beta * t * \sin \theta / \lambda) \quad (1)$$

where F_{corr} = corrected structure factor,

F_{calc} = structure factor calculated from the observed intensity for that reflection collected at time t (hrs) and at a particular $\sin \theta / \lambda$.⁶

The co-efficients α and β in the above equation are determined by plotting the values of F_{calc} for each standard against the times of measurement. Assuming this graph shows a linear decay for the whole data on a particular standard, then a second graph of F_{t_1} / F_{t_2} ($t_1 < t_2$) against $\sin \theta / \lambda$ is plotted for all of the standards. The gradients of the second graph give two values of the F_{t_1} / F_{t_2} ratio at two values of $(\sin \theta) / \lambda = 0$ and $(\sin \theta) / \lambda = x$ from which α and β are calculated from

$$\alpha = [1 - (F_{t_1} / F_{t_2} \text{ at } (\sin \theta) / \lambda = 0)] \div \text{Exposure time} \quad (2)$$

$$\beta = \left[1 - \frac{(F_{t_1} / F_{t_2} \text{ at } (\sin \theta) / \lambda = x)}{(F_{t_1} / F_{t_2} \text{ at } (\sin \theta) / \lambda = 0)} \right] \div [\text{Exposure time}] * x \quad (3)$$

This correction is applied after the observed intensities have been reduced to structure factors F_{hkl} using the program SYNDAT.⁷ The relationship between F_{hkl} and intensity I is given in equation (4).

$$F_{hkl} = \sqrt{\frac{KI_{hkl}}{Lp}} \quad (4)$$

where p , the polarisation factor is a simple function of 2θ given by

$$p = \frac{1 + \cos^2 2\theta}{2} \quad (5)$$

and the Lorentz factor L for the diffractometer is given by

$$L = \frac{1}{\sin 2\theta} \quad (6)$$

In fact, for the present monochromator geometry the parallel vector of the incident radiation is affected more than the perpendicular vector so that the actual polarisation factor used is

$$p = \frac{1 + \cos^2 2\theta_m \cos^2 2\theta}{2(1 + \cos^2 2\theta_m)} \quad (7)$$

$$\text{where } \cos 2\theta_m = (1.0 - 0.4447\lambda^2) \quad (8)$$

λ = wavelength of incident radiation.

The program SYNDAT applies these factors, corrects any affects of crystal decay, and finally prints out a list of h , k , l , F and $\sigma(F)$ values. Normally a reflection is considered observed if $I/\sigma(I) \geq 3.0$ ($F/\sigma(F) \geq 6.0$).^{8a} The program also flags any reflections with

$B_l - B_r > 3\sqrt{B_l + B_r}$ (B_l and B_r are the left and right backgrounds of each reflection) as faulty but does not exclude them.^{7, 8b}

Whilst the calculated structure factors F_{hkl} are associated with real atoms and hence are dependent on atomic scattering factors which fall off as a function of $\sin \theta$, it is necessary in direct methods and in some Patterson methods to use structure factors which do not have any $\sin \theta$ dependence. These, the normalised structure factors E_{hkl} 's, are associated with ideal point atoms and can be calculated from equation (9)

$$|E_{hkl}|^2 = \frac{|F_{hkl}|_{\text{abs}}^2}{\epsilon \sum_{j=1}^N f_j^2} \quad (9)$$

where ϵ is a weighting factor, f_j is the atomic scattering factor for atom j and thus includes the thermal vibration of the atom and the

$|F_{hkl}|_{\text{abs}}$ values are corrected for any scale or temperature effects. The form of this correction can be calculated by two methods - the Wilson plot (equation 10 and ref. 9) and by the K-curve method (ref. 10). Details of these two methods are given elsewhere. One important use of the final E-values is that their final statistical distribution is an important discriminatory test between possible centric and acentric space groups.¹¹

$$\ln \left(\frac{I_{\text{rel}}}{\sum_{l=1}^n f_o^2} \right) = \ln C - 2B \left(\frac{\sin^2 \theta}{\lambda^2} \right) \quad (10)$$

where K is related to C by $K = \frac{1}{\sqrt{C}} = \left| \frac{F_{\text{abs}}}{F_{\text{rel}}} \right|$

(VIII. 4.) Structure Solution

The determination of the part of the structure - the phasing model - which is approximately correct and will reveal further information about the structure can be approached using two main methods:-

(VIII. 4.1.) The Patterson method.¹²

As mentioned above, Patterson in 1935 defined a function $P(u, v, w)$ given by equation (11)

$$P(u, v, w) = v \int_0^1 \int_0^1 \int_0^1 \rho(x, y, z) \cdot \rho(x+u, y+v, z+w) dx dy dz \quad (11)$$

$$\{\rho(x, y, z) = \frac{1}{v} \sum_h \sum_k \sum_{l=-\infty}^{+\infty} |F(hkl)| \exp[-2\pi i(hx + ky + lz)]\} \quad (12)$$

On substituting expressions for $\rho(x, y, z)$ and $\rho(x+u, y+v, z+w)$ given by equation (12) and rearranging, the expression for $P(u, v, w)$ can eventually be written

$$P(u, v, w) = \frac{1}{v} \sum_h \sum_k \sum_{l=-\infty}^{+\infty} |F(hkl)|^2 \cos 2\pi^2(hu + kv + lw) \quad (13)$$

from which it can be seen that $P(u, v, w)$ is real for all u, v and w , and is independent of any phase information for the individual reflections. Hence a Fourier synthesis using $|F|^2$ as coefficients describes vectors between the electron densities at the points (x, y, z) and

$(x + u, y + v, z + w)$ so that vectors will appear as peaks with weights given by $A(x, y, z) \cdot \rho(x + u, y + v, z + w)$, i.e. $Z_i \cdot Z_j$, where Z_i and Z_j are the atomic numbers of the atoms concerned for an interatomic vector. Clearly if one atom is heavier than the rest, then the vectors associated with that atom will dominate the Patterson map.

In interpreting any Patterson maps there are several general principles which are of importance and these have been discussed in detail elsewhere.¹

In particular, Harker planes or lines in the Patterson map can be of considerable use. The Harker lines and planes are concentrations of vector points on certain planes or lines produced by symmetry related atoms. Every atom, heavy or light, will produce a peak on these lines or planes with enhanced weights. The position(s) of these lines or planes can, therefore, provide valuable information on atomic positions, as well as providing a useful check on the space group symmetry.

In some space groups, the information gained from the Harker lines or planes may not be sufficient to assign all of the heavy atom(s) co-ordinates, in which case one or more of the co-ordinates may be assigned arbitrarily, but once assigned cannot be refined. This can then result in additional symmetry in the resulting Fourier phased by the heavy atom(s). To give an example, in the monoclinic space group $P2_1$, the equivalent positions are x, y, z and $\bar{x}, \frac{1}{2} + y, \bar{z}$. The heavy atom vectors between symmetry related atoms, therefore, are to be found on the Harker plane $u, \frac{1}{2}, w$ with $u = 2x$ and $w = 2z$. For a single heavy atom the dominant peak on this plane allows the x and z co-ordinates to be calculated and the y co-ordinate may be assigned arbitrarily to determine the origin point with respect to the polar b axis in the space group. However, the two heavy atoms in this space group will then be centrosymmetrically related ($x, \frac{1}{2}, z$ and $\bar{x}, \frac{1}{2}, \bar{z}$ if y is assigned the value $\frac{1}{2}$) although the space group is non-centrosymmetric. As a result, the phase angles calculated for all reflections will be 0 or π resulting in a Fourier containing both

the true structure and its mirror image. This additional symmetry is normally broken by including the position of a second atom or several atoms from a molecular fragment in the calculation of the phase angles and re-examining the Fourier to see which peaks have remained and hence belong to the 'true' structure. It is important in the early stages to ensure atoms all come from the same molecule and to avoid false peaks due to the overlap of mirror related images of a peak. In some cases, even when a molecular fragment such as a phenyl ring has been located and refined, the false symmetry may still be present and chemical intuition could be useful in sorting out the remaining atoms from their mirror images. A case in point is the structure of Iodoxybenzene described in Chapter II.

(VIII.4.2.) Direct methods

For structures where no one atom is much heavier than the rest, statistical methods may be needed to find the correct phases for the data. These methods are all based on an original equation developed by Sayre.¹³ In these cases one attempts to set up an initial subset of data with signs/phases which in all probability are correct. The Sayre equation and triple product relationships are used in a bootstrap operation until all the data have been assigned a phase and a probability that that phase is correct. This procedure involves setting up many thousands of relationships between the h, k, l indices associated with each datum, normally in the form of triplets as in equation (14) below, where $S(h_1, k_1, l_1)$ means the sign of the datum identified by the indices h_1, k_1, l_1 .

$$S(h_1, k_1, l_1) \cdot S(h_2, k_2, l_2) = S(h_1 + h_2, k_1 + k_2, l_1 + l_2) \quad (14)$$

The procedures involved in applying direct methods to light atom structures have been the subject of several computer programs. In the X-RAY system, the program links NORMSF, SINGEN and PHASE (or APhase) are available and are single solution methods. Alternatively MULTAN,¹⁴ which is available as a link in XRAY76 (with NORMSF) or as

a separate program (along with a program NORMAL¹⁵ to calculate normalised structure factors), is a multi-solution program which has been successfully applied in all the light atom structures in this thesis and will be described in some detail.

The program MULTAN¹⁴ is based on the tangent formula of Karle and Hauptmann¹⁶ and consists of three parts; SIGMA2, CONVERGE and FASTAN. SIGMA2 sets up all phase relationships of the form

$$\varphi_{\underline{h}} \approx \varphi_{\underline{h}'} + \varphi_{\underline{h}-\underline{h}'} \quad (15)$$

where $\varphi_{\underline{h}}$ is the phase of $F_{\underline{h}}$ after "standardising" the reflection indices so that they all lie in the same part of the reciprocal lattice, a process that may involve a phase shift on standardisation. Each relationship is assigned a weight $K_{hh'}$, defined as

$$K_{hh'} = 2\sigma_3 \sigma_2^{-3/2} |E_{\underline{h}} E_{\underline{h}'} E_{\underline{h}-\underline{h}'}| \quad (16)$$

where $\sigma_n = \sum_{j=1}^N Z_j^n$ and $E_{\underline{n}}$ is the normalised structure factor

associated with reflection \underline{h} ($= h, k, l$). Only a specified number of these relationships with the highest $K_{hh'}$ values are retained for use in the tangent formula.

The second part of the program, CONVERGE, uses the phase relationships from SIGMA2 to determine a starting set of reflections which are involved in the most important phase relationships and enable the origin and enantiomorph of the cell to be accurately defined. Included in the starting set are any reflections which the sigma 1 (Σ_1) formula has determined with a reasonably high probability of being correct as well as several starting reflections. In a centric space group there would be assigned values of ± 1 ; in an acentric space group values of $\pm \pi/2$ if they are special reflections or else all combinations of the values $\pm \pi/4$ or $\pm 3\pi/4$ if they are general reflections. Normally only two or three of these starting reflections are chosen, and their various combinations of values provide a multiple starting point for the tangent formula.

The actual application of the tangent formula occurs in the third part of the program, FASTAN, and results in several sets of phases for all the reflections being calculated from the convergence mapping of the phase relationships. Output with each set of phases are several figures of merit which are measures of the internal consistency of the set of phases.

The actual tangent formula used in FASTAN is given in equation (17) where the weight w_h associated with each phase φ_h is given by equation (18)

$$\tan \varphi_h \approx \frac{\sum_{h'} w_{h'} w_{h-h'} \left| E_{h'} E_{h-h'} \right| \sin (\varphi_{h'} + \varphi_{h-h'})}{\sum_{h'} w_{h'} w_{h-h'} \left| E_{h'} E_{h-h'} \right| \cos (\varphi_{h'} + \varphi_{h-h'})} = \frac{T_h}{B_h} \quad (17)$$

$$\text{and } w_h = \tanh \left\{ N^{-\frac{1}{2}} \left| E_h \right| (T_h^2 + B_h^2)^{\frac{1}{2}} \right\} \quad (18)$$

The initial weights for the starting set of phases are taken as unity, except for the \sum_1 phases where, if the sign is determined with a probability P , the weight used is $2P-1$, based on an expectation value for the sign. The specification of the four alternative values $\pm \pi/4$, $\pm 3\pi/4$ for a general acentric starting reflection gives a maximum error of 45° for any reflection and an expectation error of $22\frac{1}{2}^\circ$.

In MULTAN, three figures of merit are normally used. The absolute figure of merit ABSFORM is related to $\sum_h \alpha_h$, where α_h is defined by

$$\alpha_h = 2N^{-\frac{1}{2}} \left| E_h \right| (T_h^2 + B_h^2)^{\frac{1}{2}} \quad (19)$$

so that (18) can be rewritten

$$w_h = \tanh \left(\frac{1}{2} \alpha_h \right)$$

The actual value for ABSFORM is

$$\text{ABSFORM} = \frac{\sum_h \alpha_h - \sum_r \alpha_r}{\sum_e \alpha_e - \sum_r \alpha_r} = M_{\text{abs}}$$

where $\sum_e \alpha_e$ is the sum of the expected values of α_h^2 as given by equations (20) and (21).

$$\sum \alpha_e = \sum_{\underline{h}}' < \alpha_{\underline{h}}^2 >_{\text{exp}}^{\frac{1}{2}} \quad (20)$$

where

$$< \alpha_{\underline{h}}^2 >_{\text{exp}} = \sum_{\underline{h}'} \kappa_{\underline{h}, \underline{h}'}^2 + 2 \sum_{\underline{h}'} \sum_{\underline{h}''} \kappa_{\underline{h}, \underline{h}'} * \kappa_{\underline{h}, \underline{h}''} * \frac{I_1(\kappa_{\underline{h}, \underline{h}'})}{I_0(\kappa_{\underline{h}, \underline{h}'})} * \frac{I_1(\kappa_{\underline{h}, \underline{h}''})}{I_0(\kappa_{\underline{h}, \underline{h}''})} \quad (21)$$

where the $I_0(\kappa)$ and $I_1(\kappa)$ are modified Bessel functions,¹⁷ and $\sum \alpha_r$ is a random expectation value assuming no internal consistency in the contributions to α

$$\sum \alpha_r = \sum_{\underline{h}} < \alpha_{\underline{h}}^2 >_{\text{rand}}^{\frac{1}{2}} = \sum_{\underline{h}} \left(\sum_{\underline{h}'} \kappa_{\underline{h}, \underline{h}'} \right)^{\frac{1}{2}} \quad (22)$$

For a set of phases with almost no self-consistency, the value of M_{abs} will be zero, whilst for the correct set of phases $\sum \alpha_{\underline{h}} \approx \sum \alpha_e$ and correct phase sets normally have values of $\text{ABSFORM} \approx 1.2 \pm 0.2$. Other figures of merit are related to ABSFORM except PSI ZERO which is also a valuable discriminator between phase sets. The PSI ZERO test uses selected weak reflections, below a specified $E_{\text{min}}^{\text{18}}$.

(VIII, 5.) Electron Density Maps

Whether the structure is solved by the Patterson method or by direct methods, each approach eventually requires the calculation of a density map. For the Patterson map, the peaks in the map will represent inter-atomic vectors and the expression relating the Patterson function $P(u, v, w)$ to the structure factors has already been given. However, once heavy atom positions are known, further refinement proceeds using F_o Fourier's to locate further atoms in the structure. The Fourier expression for a F_o Fourier is given in equation (12) where the coefficients, the $F(h, k, l)$ values are not merely the moduli of the structure factors, which are readily available as $|F_o|$'s calculated from the observed intensities, but also require a knowledge of the phase associated with each reflection.

Equation (4) contains the various

$$F(hkl) = |F(hkl)| e^{i\alpha} = |F(hkl)| \cos \alpha + i |F(hkl)| \sin \alpha \\ = A(hkl) + i B(hkl) \quad (23)$$

computational expressions used. In the direct methods, equation (12) is modified to use normalised structure factors $E(hkl)$'s instead of $F(hkl)$'s and the phase angles associated with each $E(hkl)$ are of course calculated by the tangent formula of MULTAN or the appropriate direct methods program. If the process is reasonably efficient, these phase angles will be reasonably accurate and the majority of the structure will be located in the resulting E-map. However, the majority of E-maps contain many spurious peaks, with the result that perhaps only a molecular fragment may be located.

In both Patterson and the direct methods, an electron density map calculated using the measured structure factors and the trial calculated phases as Fourier co-efficients (a F_o Fourier), usually reveals more of the structure and enables the shifts in the atoms of the partial structure to be calculated. Incorporating the new atoms and the new positions for the atoms of the phasing model enables the process to be repeated. Several such steps normally converge to the correct structure.

At later stages in the refinement (or earlier stages if a really heavy atom that dominates the scattering is present), it is necessary to continue refinement using difference Fouriers. These are essential in locating hydrogen atoms in the structure since they are too small relatively to show up in an F_o Fourier. Even in a difference Fourier, the relative scattering power of the hydrogen atom may be of the same order as the observational errors in $|F_{obs}|$ unless very accurate data is available.

For a difference Fourier, the heavy atom contributions are subtracted out by using equation (24)

$$\rho(x,y,z) = \sum_h \sum_k \sum_l |F(h,k,l) - F_{calc}(h,k,l)| e^{i\varphi_{calc}(hkl)} \quad (24)$$

Since a Fourier synthesis with co-efficients $\left| F_{\text{calc}}(hkl) \right| \cdot e^{i\varphi_{\text{calc}}(hkl)}$ generates only the electron density due to the heavy atoms, the equation (24) will generate the difference between the actual electron density and that due to the phasing model. Therefore, if the phases of the partial model are correct, then the synthesis provides a measure of the difference between the partial model and the true structure. If the phases are in some error, the difference Fourier is still of considerable use. Apart from indicating missing atoms (hydrogen or otherwise) as positive peaks, the difference in $\rho_0 - \rho_c$ at each heavy atom position can either be positive or negative due to site occupancy errors caused by wrongly identified atoms or, if a characteristic pattern of positive peaks and negative holes appears round an atomic site, this can be taken to indicate an anisotropically vibrating atom and its temperature factor components U_{ij} appropriately refined. In the most accurate analyses, it may even be possible to gain some information on the positions of the valence electrons associated with each bonding or lone pair orbital.¹⁹

At the end of the refinement, the few residual peaks remaining will probably be close to the heaviest atom in the structure. In a good analysis these peaks, if present, will be small. The rest of the final difference map should also be featureless.

(VIII.6.) Least Squares Refinement

Although improved atomic positions can be obtained by calculation of the peak positions in electron density maps, the positional and thermal parameters associated with each atom can also be subjected to least squares refinement, which is unfortunately non-linear in the X-ray program CRYLSQ. The function minimised is a formalised difference between the observed structure factors and the structure factors calculated from the trial or approximate atomic positions. A full matrix refinement of a structure containing 20 atoms all of whose positional and isotropic thermal parameters together with a scaling factor can vary independently would require the setting up of 81 normal

equations to be solved for the 81 variables. This problem, although relatively small in crystallographic terms, obviously involves immense calculations.

Normally several cycles of least squares refinement are required at each step in the structure solution and it is this calculation that accounts for the bulk of the computer time expended on each structure. For reasons of economy, in the earlier stages of refinement it may be better to use a subset of the data. However, the estimates of the standard deviations which are obtained from least squares refinement are unreliable unless the process is carried to completion with the full data set.

At each stage of the refinement, a measure of the accuracy of the current structural model is given by a Reliability Index or Residual R given by

$$R = \frac{\sum w \cdot ||F_o| - |F_c||}{\sum w \cdot |F_o|}$$

This R-factor decreases as the trial structure is refined towards the true structure. In the early stages it also is a good indicator of whether the starting phasing model is likely to result in the rest of the structure being found, as it has been calculated that a random distribution of atoms in an acentric space group will give a R-factor of 0.59 (0.83 in a centric space group).¹ In the early stages it is also advisable to give each reflection hkl a weight w of unity. However, towards the end of the refinement the weights are normally chosen to remove any intrinsic errors in the data set (see below).

For diffractometer collected data, a well refined structure will normally give a R factor < 0.05 . It may be necessary during certain refinements to remove correlations between various group parameters by refining that group as a rigid body.²⁰ This procedure is best suited to tetrahedral groups and phenyl rings, although the use of a rigid $6/mmm$ model of a phenyl ring may introduce

equations to be solved for the 81 variables. This problem, although relatively small in crystallographic terms, obviously involves immense calculations.

Normally several cycles of least squares refinement are required at each step in the structure solution and it is this calculation that accounts for the bulk of the computer time expended on each structure. For reasons of economy, in the earlier stages of refinement it may be better to use a subset of the data. However, the estimates of the standard deviations which are obtained from least squares refinement are unreliable unless the process is carried to completion with the full data set.

At each stage of the refinement, a measure of the accuracy of the current structural model is given by a Reliability Index or Residual R given by

$$R = \frac{\sum w \cdot ||F_o| - |F_c||}{\sum w \cdot |F_o|}$$

This R-factor decreases as the trial structure is refined towards the true structure. In the early stages it also is a good indicator of whether the starting phasing model is likely to result in the rest of the structure being found, as it has been calculated that a random distribution of atoms in an acentric space group will give a R-factor of 0.59 (0.83 in a centric space group).¹ In the early stages it is also advisable to give each reflection hkl a weight w of unity. However, towards the end of the refinement the weights are normally chosen to remove any intrinsic errors in the data set (see below).

For diffractometer collected data, a well refined structure will normally give a R factor < 0.05 . It may be necessary during certain refinements to remove correlations between various group parameters by refining that group as a rigid body.²⁰ This procedure is best suited to tetrahedral groups and phenyl rings, although the use of a rigid $6/mmm$ model of a phenyl ring may introduce

errors and in the final refinement cycles it may be better to remove the rigid body constraints on phenyl-rings (see Section VII.4) For further details see ref. 21.

(VIII.7.) Systematic Errors²⁷

Whilst a very good idea of most structures can be obtained using data simply corrected for Lorentz and polarisation effects, there are a number of systematic errors which are likely to affect the data set. These can be relatively easily identified, and a correction applied. However, at the end of any determination there will still remain a number of intrinsic errors in the data set and the calculated model which a good weighting scheme can minimise. The following sections summarise two of these systematic errors, their effects and how they are corrected for.

(VIII.7.1.) Absorption

As the beam of radiation passes through the crystal, it is attenuated by absorption effects to an extent given by the equation

$I = I_0 e^{-\mu\tau}$, where I = measured intensity; I_0 = incident intensity, τ = total distance travelled through the crystal and μ = a linear absorption co-efficient given by the equation

$$\mu = \rho \sum_n (P_n/100) \left(\frac{\mu}{\rho} \right)_{En, \lambda} \quad (25)$$

where P_n = percentage of element n in compound and μ/ρ = mass absorption co-efficient for the element n at wavelength λ .⁴ Obviously μ/ρ can be roughly related to the atomic number of the elements and the wavelength (penetrating power) of the radiation, so that absorption effects are most serious for compounds with odd shaped crystals containing a high percentage of a heavy element. Previously crystals with large absorption factors had to be ground into spheres or cylinders so that absorption factors could be calculated. Nowadays exact absorption corrections are calculated, using programs such as ABSCOR, providing the crystal faces can be measured exactly.²² A method for describing and measuring the crystal has been given.²³ Once the crystal has been accurately described, the program ABSCOR works by dividing the crystal into Howell's polyhedra so that rays are entering or leaving via one face only. Within these polyhedra the loci

of constant absorption are planes; these may lie in any direction, but their position is determined from the absorption of rays diffracted at the corners of the polyhedra. For each of the polyhedra, the contribution to the total diffracted intensity (A_T) is found. The transmission is then given by A_T/V (V = crystal volume).²²

VIII.7.2.) Extinction

There are two forms of extinction called primary and secondary. The mathematical treatment of extinction was originally given in the work of Darwin.²⁴ Both primary and secondary extinction lower the intensity of the diffracted beam because of interactions between the incident and diffracted rays inside the sample. Primary extinction relates to an interference process whereby an incident ray is multiply reflected by a particular series of planes. As on each reflection a phase change of $\pi/2$ occurs, a ray multiply reflected n times within a crystal will interact with a reflection which has been multiply reflected $(n-2)$ times since there will be a phase difference of π between them. Hence the net result is that the diffracted ray is proportional to $|F|$ not $|F|^2$ assuming the crystal is ideally perfect. However, Darwin's treatment of extinction recognised that a crystal is not ideally perfect but consists of small mosaic blocks which are slightly misaligned to each other so that the perfect planes required for primary extinction do not extend over appreciable regions in the crystal. The effect of primary extinction in a real crystal with some mosaic spread causes the diffracted intensity to be proportional to $|F|^n$ where $1 \ll n < 2$. The value of n for most crystals is near 2, so that primary extinction effects can normally be neglected.

However, secondary extinction is more important and several mathematical models relating to extinction effects have resulted in approximate equations which can be readily implemented. The effect is important when the mosaic blocks are fairly well aligned

since, for reflections of appreciable intensity, the effect occurs when an appreciable amount of the incident radiation is reflected by the initial planes encountered so that deeper planes receive less incident intensity and therefore reflect less. The effects of secondary extinction are more pronounced at lower $(\sin \theta)/\lambda$ values because the general level of intensities is higher in this region. The effect is clearly observed in intense reflections which are systematically less than their calculated values. Unlike absorption which can be corrected for exactly (as far as theory permits) the effects of extinction are determined by least squares refinement of the appropriate parameters in the relevant expressions relating observed data to the calculated intensities including extinction effects. In the X-RAY system, the form of the extinction correction is a modified equation from Zachariasen's²⁵ mathematical treatment of Darwin's early work due to Larson.²⁶ This equation (26) is again based on a mosaic model for the crystal with the term r^* related to both the size (r) and spread (g) of the individual domains in the crystal by equation (28).

$$|F_c^*| = K \cdot |F_c| \cdot [(1 + 2r^* |F_c|^2 \delta)]^{-\frac{1}{2}} \quad (26)$$

$$\text{where } \delta = \frac{e^2}{mc^2} \cdot \frac{1}{v} \cdot \frac{\lambda^3}{\sin 2\theta} \cdot \left(\frac{P_2}{P_1} \right) \cdot \bar{T} \quad (27)$$

$P_n = (1 + \cos^{2n} 2\theta)/2$ are polarisation factors and \bar{T} transmission factors (set as 0.03 cm if no values given)

$$r^* = \theta(1 + (\theta/g)^2)^{-\frac{1}{2}} \quad (28)$$

and $\theta = r/\lambda$ r is radius of a single domain. The magnitude of r^* is useful because it enables the crystal to be classified as Type I or II.²⁵

(VIII.7.3.) ²⁷Other factors; weighting schemes

The above absorption and extinction are the principal sources of error in the measured data. There are other sources of systematic

errors in the data, but their effects are increasingly smaller and are normally calculated a posteriori only in the most accurate work. The most important use of these calculations is in experiments designed to show the valence electron density distribution around atoms. However, the majority of the calculations involve numerous approximations. The effects covered include contributions from the anisotropy of the extinction effect, thermal diffuse scattering, multiple wave interference effects, etc.²⁷

Whether these effects are allowed for or not, there still remains small errors in the molecular model even after introducing atomic scattering factors for charged atoms and the allowing for anomalous dispersion effects.⁴ These are normally the result of small but systematic biases introduced by the least squares refinements using unit weights for all reflections. A careful statistical analysis of the data in ranges of F and $\sin \theta$ at this stage is likely to have a distribution similar to that in Fig. 1. By careful selection of an appropriate weighting scheme, it is possible to produce an even distribution of $w \cdot \Delta F^2$ values and refinement with these calculated weights will reduce any bias in the data (the extinction factor should be fixed at the value at the end of the refinement with unit weights). Although the use of $(1/\sigma(F))^2$ as weights is common, the X-RAY system offers a choice of weighting schemes. It has, however, been found that a modified scheme that downweights reflections at the extreme F and $\sin \theta$ ranges has been useful in the majority of the later structures. The scheme gives a reflection a weight of \approx zero if $A \cdot F_{\text{obs}}$ is greater than $|F_c|$, otherwise the weights for the reflection are given by $w = X \cdot Y \cdot Z$ where $Z = 1.0$ or $Z = (1/\sigma(F))^2$. The values of X and Y are given as follows.

If $\sin \theta < B$ then $X = \sin \theta / B$ or if $\sin \theta > D$ then $X = D / \sin \theta$, otherwise $X = 1.0$. Similarly, if $F_{\text{obs}} < E$ then $Y = F_{\text{obs}} / E$ or if $F_{\text{obs}} > C$ then $Y = C / F_{\text{obs}}$, otherwise $Y = 1.0$. It has been found that this scheme is extremely flexible and weights can be calculated

using just a few parameters which effectively divide Fig. 1 up into 3 sections with straight lines approximating the curves. A good weighting scheme should eventually result in $w \cdot \Delta F$ values being as equivalent as possible and in particular not greater than twice the minimum $w \cdot \Delta F$.

Although no such correction has been applied to any of the tables of bond distances and angles in this thesis, it should be mentioned that a correction can be made to final tables of atomic parameters calculated from the positional co-ordinates to include correlations between the thermal motions of individual atoms of each bond which has a foreshortening effect on bond lengths. Such effects can be removed if a rigid-body model is assumed in which all inter-atomic separations remain fixed. For further details the reader is referred to ref. 28.

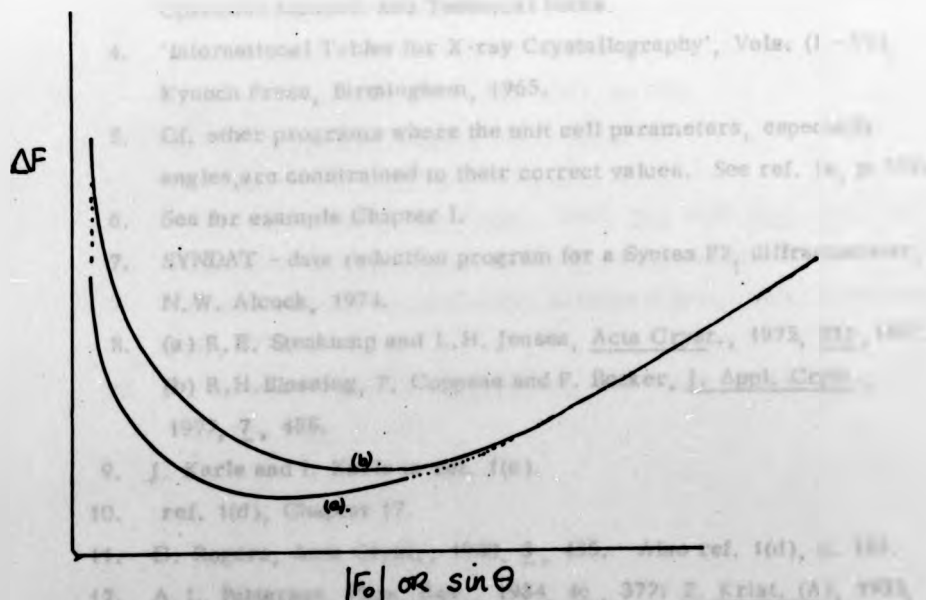


Fig. VIII.1 Typical $|\Delta F|$ vs. $P(\sin \theta)$ curves for diffractometer data before the application of any weighting scheme.
(a) Large crystal. (b) Small crystal.

(VIII.8.) References

1. (a) M.J. Buerger, 'Crystal Structure Analysis', J. Wiley & Sons, 1960; 'X-Ray Crystallography', J. Wiley & Sons, 1965.
 (b) C.W. Bunn, 'Chemical Crystallography' Oxford University Press, 1961.
 (c) M.M. Woolfson, 'Direct Methods in Crystallography', Oxford University Press, 1961.
 (d) 'Computing Methods in Crystallography', ed. J.S. Rollett, Pergamon, 1965.
 (e) 'Crystallographic Computing', ed. F.R. Ahmed, Munksgaard, Copenhagen, 1970.
 (f) G.H. Stout and L.H. Jensen, 'X-Ray Structure Determination', MacMillan (London), 1968.
2. The X-RAY system - versions of June, 1972 and 1976 - Technical Reports TR-192 and TR-446 of the Computer Science Centre, University of Maryland.
3. Description of operating procedures for Syntex P2₁ diffractometer and program documentation given in Syntex Analytical Instruments Operation Manuals and Technical Notes.
4. 'International Tables for X-ray Crystallography', Vols. (I - VI), Kynoch Press, Birmingham, 1965.
5. Cf. other programs where the unit cell parameters, especially angles, are constrained to their correct values. See ref. 1e, p.319.
6. See for example Chapter I.
7. SYNDAT - data reduction program for a Syntex P2₁ diffractometer, N.W. Alcock, 1974.
8. (a) R.E. Stenkamp and L.H. Jensen, *Acta Cryst.*, 1975, **B31**, 1507.
 (b) R.H. Blessing, P. Coppens and P. Becker, *J. Appl. Cryst.*, 1972, **7**, 488.
9. J. Karle and I. Karle in ref. 1(e).
10. ref. 1(d), Chapter 17.
11. D. Rogers, *Acta Cryst.*, 1950, **3**, 455. Also ref. 1(d), p. 123.
12. A.L. Patterson, *Phys. Rev.*, 1934, **46**, 372; *Z. Krist. (A)*, 1935, **90**, 517.
13. D. Sayre, *Acta Cryst.*, 1952, **5**, 60.

14. MULTAN (1972) - system of computer programs for the automatic solution of crystal structures, P. Main and M.M. Woolfson, (Physics Dept., Univ. of York); see also J. Karle, Acta Cryst., 1968, B24, 182; J.P. Declercq, G. Germain and M.M. Woolfson, Acta Cryst., 1975, A31, 367.
15. NORMAL - computer program for calculating normalised structure factors (E's) from observed structure amplitudes (F's), P. Main, Physics Dept., Univ. of York).
16. J. Karle and H. Hauptman, Acta Cryst., 1956, 9, 635.
17. Lecture notes, 'Direct and Patterson methods of solving Crystal Structures', University of York, 1971.
18. A combined figure of merit using both Mabs and psizero indices is a very useful discriminator between phase sets. Note also that in space groups without any translational symmetry, the correct phase set normally has the lowest figures of merit.
19. P. Coppens, Angew. Chem., 1977, 16, 32.
20. RGBOD - a program for the generation of rigid groups, N.W. Alcock.
21. Chapter VII, refs. 31 and 32.
22. N.W. Alcock, G.S. Pawley, C.P. Rourke, M.R. Levine, Acta Cryst., 1972, A28, 440. Ref. 1(d), p. 271.
23. N.W. Alcock, Acta Cryst., 1970, A26, 437.
24. C.G. Darwin, Phil. Mag., 1922, 43, 800.
25. W.H. Zachariasen, Acta Cryst., 1963, 16, 1139; ibid., 23, 558.
26. A.C. Larsen, Acta Cryst., 1967, 23, 664, and ref. 1(e).
27. Lecture notes, Electron Density Summer School, Univ. of Warwick, July, 1975.
28. V. Schomaker and K.N. Trueblood, Acta Cryst., 1968, B24, 63; also ref. 1(d), p. 220.

Appendix A

Final Structure Factor Tables

Final structure factor tables for the diethyl tin dihalides are available as Supplementary Publication No. SUP 21983 (14 pp., 1 microfiche); those for (Z, Z)-2,4-Dibromo-1,5-diphenyl-penta-1,4-dien-3-one as Supplementary Publication No. SUP 31357 (16 pp., 1 microfiche). Due to the size of the tables for the other compounds, and since they will eventually be deposited when details of the individual structures are finally published, the other structure factor tables have been omitted from this thesis but are available on request.

APPENDIX B

Published Papers

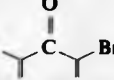
(Z, Z)-2,4-Dibromo-1,5-diphenylpenta-1,4-dien-3-one

BY N. W. ALCOCK AND J. F. SAWYER

Department of Molecular Sciences, University of Warwick, Coventry CV4 7AL, England

(Received 4 August 1975; accepted 11 September 1975)

Abstract. $C_{17}H_{12}OBr_2$, monoclinic, $P2_1/c$, $a=41.080$ (11), $b=6.527$ (2), $c=11.118$ (3) Å, $\beta=97.77$ (2)°, $V=2953$ (1) Å³ at 18°C, $Z=8$, $D_x=1.76$ g cm⁻³. There are two essentially identical molecules in the asymmetric

unit both having approximately planar  unit both having approximately planar Br-C-Br conformations with Br and O adjacent. Intramolecular repulsions result in substantial deviations from planarity.

Introduction. The title compound (m.p. 97–98°C), recrystallized from ethanol, was prepared and supplied by Professor Shoppee. The crystals appear as chunky needles (needle axis c). Systematic absences $h0l$, $l \neq 2n$; $0k0$, $k \neq 2n$, indicate space group $P2_1/c$ with two independent molecules in the asymmetric unit. The crystals also display pseudo-absences $hk0$, $h \neq 2n$.

Data were collected on a Syntex P2₁ diffractometer with graphite-monochromatized Mo K α radiation to $2\theta_{max}$ of 50° in two shells with $\omega/2\theta$ scans over the range $(K_{a1}-0.9)-(K_{a2}+0.8)^\circ$. In the first shell ($0^\circ <$

Table 1. Atomic coordinates ($\times 10^4$) and anisotropic temperature factors ($\times 10^4$) with standard deviations in parentheses

$$T = \exp \{ -2\pi^2 (U_{11}h^2a^{*2} + U_{22}k^2b^{*2} + U_{33}l^2c^{*2} + 2U_{12}hka^*b^* + 2U_{13}hla^*c^* + 2U_{23}klb^*c^*) \}.$$

	x	y	z	U_{11}	U_{22}	U_{33}	U_{12}	U_{13}	U_{23}
Br(11)	1573 (1)	-1534 (4)	3388 (3)	88 (2)	30 (2)	78 (2)	19 (2)	27 (2)	4 (2)
Br(12)	917 (1)	4886 (5)	5324 (2)	124 (3)	75 (2)	39 (1)	56 (2)	32 (2)	10 (2)
O(1)	1190 (4)	776 (24)	4988 (14)	74 (13)	29 (9)	42 (9)	1 (9)	18 (9)	10 (8)
C(11)	1581 (5)	2553 (34)	2564 (20)	18 (14)	26 (10)	39 (13)	6 (11)	-5 (11)	-15 (11)
C(12)	1449 (6)	1279 (39)	3262 (20)	20 (14)	50 (17)	42 (13)	12 (12)	-12 (11)	10 (13)
C(13)	1223 (6)	1899 (35)	4102 (20)	42 (15)	34 (13)	49 (14)	4 (12)	23 (12)	-32 (13)
C(14)	1024 (5)	3721 (30)	3849 (18)	23 (13)	20 (12)	28 (11)	16 (10)	8 (10)	-10 (10)
C(15)	894 (5)	4363 (32)	2773 (16)	40 (16)	31 (14)	11 (10)	0 (11)	14 (10)	14 (9)
C(111)	1825 (5)	2373 (39)	1725 (21)	4 (13)	53 (15)	51 (14)	12 (12)	1 (11)	-5 (14)
C(112)	2025 (7)	4138 (39)	1561 (21)	40 (18)	64 (16)	37 (14)	-8 (14)	-7 (13)	6 (12)
C(113)	2264 (9)	4079 (59)	701 (30)	65 (28)	113 (29)	60 (20)	4 (21)	14 (20)	-19 (20)
C(114)	2292 (7)	2315 (52)	94 (22)	55 (19)	76 (23)	41 (15)	-7 (17)	-1 (13)	-5 (16)
C(115)	2124 (7)	610 (39)	276 (23)	43 (19)	60 (16)	47 (15)	27 (14)	16 (15)	-6 (13)
C(116)	1894 (6)	575 (43)	1063 (22)	46 (18)	70 (20)	35 (14)	4 (14)	-4 (13)	-10 (14)
C(121)	660 (5)	6054 (33)	2421 (20)	7 (12)	42 (13)	38 (13)	6 (10)	-8 (10)	21 (11)
C(122)	445 (6)	5732 (40)	1282 (23)	43 (16)	56 (17)	53 (16)	10 (14)	18 (13)	25 (14)
C(123)	201 (8)	7149 (44)	922 (28)	45 (22)	53 (19)	67 (21)	5 (15)	23 (17)	15 (16)
C(124)	169 (6)	8876 (46)	1625 (29)	24 (16)	71 (20)	90 (22)	14 (13)	24 (16)	37 (18)
C(125)	395 (7)	9236 (42)	2716 (27)	57 (20)	61 (18)	66 (20)	13 (16)	28 (17)	23 (15)
C(126)	643 (7)	7840 (41)	3096 (21)	84 (24)	37 (17)	49 (14)	4 (15)	22 (14)	-10 (13)
Br(21)	4084 (1)	9898 (5)	4436 (2)	119 (3)	70 (2)	28 (1)	-46 (2)	1 (1)	-6 (2)
Br(22)	3445 (1)	3329 (4)	1931 (3)	96 (3)	35 (2)	69 (2)	-16 (2)	-9 (2)	7 (2)
O(2)	3804 (5)	5763 (24)	3900 (13)	107 (15)	34 (10)	31 (8)	-15 (9)	15 (9)	6 (7)
C(21)	4112 (6)	9277 (44)	1912 (23)	19 (19)	56 (20)	61 (16)	16 (14)	6 (14)	-24 (14)
C(22)	3970 (5)	8677 (34)	2892 (20)	10 (12)	48 (14)	37 (13)	13 (11)	1 (10)	-6 (12)
C(23)	3776 (6)	6793 (36)	2928 (21)	32 (14)	24 (12)	59 (15)	-4 (11)	13 (12)	-15 (13)
C(24)	3542 (6)	6133 (30)	1830 (22)	49 (18)	6 (10)	59 (15)	-9 (10)	26 (14)	-2 (11)
C(25)	3401 (6)	7260 (35)	1013 (20)	60 (20)	35 (12)	24 (12)	11 (12)	-4 (12)	-25 (12)
C(211)	4344 (6)	10955 (31)	1752 (20)	40 (16)	16 (11)	38 (12)	-22 (11)	-9 (12)	-6 (10)
C(212)	4549 (6)	10647 (38)	824 (19)	17 (14)	65 (16)	43 (12)	23 (13)	11 (11)	3 (12)
C(213)	4791 (7)	12076 (42)	697 (22)	39 (19)	68 (19)	46 (16)	-4 (15)	32 (14)	17 (15)
C(214)	4823 (8)	13850 (38)	1428 (23)	89 (25)	42 (16)	37 (16)	9 (14)	-14 (16)	24 (14)
C(215)	4593 (7)	14167 (39)	2339 (24)	53 (19)	35 (16)	75 (18)	-3 (14)	32 (15)	12 (13)
C(216)	4379 (5)	12745 (31)	2455 (18)	2 (12)	29 (13)	37 (12)	-5 (9)	-6 (10)	0 (10)
C(221)	3166 (6)	7070 (39)	-71 (19)	21 (14)	52 (19)	35 (13)	7 (12)	5 (11)	16 (13)
C(222)	2987 (7)	8737 (42)	-531 (27)	31 (19)	61 (19)	90 (22)	13 (14)	10 (17)	21 (16)
C(223)	2753 (7)	8807 (40)	-1569 (27)	50 (18)	56 (18)	80 (20)	10 (14)	-38 (17)	-9 (16)
C(224)	2701 (7)	6778 (62)	-2137 (23)	45 (20)	110 (29)	32 (15)	-16 (22)	-4 (14)	-17 (20)
C(225)	2896 (8)	5114 (44)	-1717 (25)	73 (21)	51 (17)	62 (17)	-44 (17)	-4 (16)	14 (17)
C(226)	3115 (8)	5260 (38)	-663 (28)	49 (22)	36 (15)	60 (22)	-15 (14)	-17 (18)	-2 (16)

$2\theta \leq 35^\circ$) all reflexions were collected; in the second ($35^\circ < 2\theta \leq 50^\circ$) a reflexion was only collected if the intensity of an 8s preliminary count was greater than 40 c.p.s. A variable scan rate, $1.0\text{--}29.3^\circ \text{ min}^{-1}$ depending on the intensity of the preliminary count was used. Cell constants and errors were obtained by least-squares refinement of the positions of 15 reflexions (Mo K α , $\lambda = 0.71069 \text{ \AA}$).

The positions of the four Br atoms were located with *NORMAL* and *MULTAN* (Germain & Woolfson, 1968) applied to the 274 reflexions with $E > 1.50$ in the first shell of data. Fourier and least-squares refinement with the 1865 observed [$I/\sigma(I) > 3.0$] reflexions in both shells located the remaining non-hydrogen atoms. The final refinement was with Br, C and O with anisotropic temperature factors to an R of 0.081. Scattering factors were from Cromer & Mann (1968). The weighting scheme was $w = 1.0/(186 - 335 \sin \theta)$. H atoms were not included and no correction for absorption was performed. Computing was carried out with the X-RAY system (1972) on a CDC 7600 computer.

Fig. 1 shows the atomic numbering, bond lengths and angles; Fig. 2 gives views of the two molecules. Atomic coordinates and temperature factors are given in Table 1, and molecular planes in Table 2.*

Discussion. The primary aim of the investigation was to determine the conformation of the compound [regarded to have the *Z,Z* configuration (Shopee & Cooke, 1973)]. There was also the possibility of intermolecular Br...O secondary bonds (Alcock, 1972), important in many brominated steroids (Peck, Duax, Eger &

* A list of structure factors has been deposited with the British Library Lending Division as Supplementary Publication No. SUP 31357 (16 pp., 1 microfiche). Copies may be obtained through The Executive Secretary, International Union of Crystallography, 13 White Friars, Chester CH1 1NZ, England.

Table 2. Least-squares planes

(a) Equations of the least-squares mean planes $PI + QJ + RK = S^*$ in orthogonal space. Deviations of atoms forming these planes are insignificant and are not shown.

Plane	Defining atoms	P	Q	R	S
1	Br(11), C(11), C(12), C(13)	0.6583	0.2039	0.7246	6.4071
2	Br(12), C(13), C(14), C(15)	0.8072	0.5902	0.0119	4.3591
3	Br(21), C(21), C(22), C(23)	0.7768	-0.5879	0.2257	13.6357
4	Br(22), C(23), C(24), C(25)	0.8316	-0.1868	-0.5230	11.2415
5	C(12), C(13), C(14), O(1)	0.6604	0.5265	0.5354	5.9584
6	C(22), C(23), C(24), O(2)	0.7835	-0.5312	-0.3223	11.8726
7	C(111)-C(116)	0.6055	-0.2893	0.7414	5.3629
8	C(121)-C(126)	0.7137	0.4736	-0.5161	2.1855
9	C(211)-C(216)	0.5654	-0.4721	0.6764	10.9384
10	C(221)-C(226)	0.7973	0.2218	-0.5614	10.0034

(b) Angles ($^\circ$) between planes or lines

(1)-(2)	48.7	(3)-(4)	50.4
(1)-(5)	21.6	(3)-(6)	32.0
(1)-(7)	28.7	(3)-(9)	29.6
(2)-(5)	31.8	(4)-(6)	23.2
(2)-(8)	31.8	(4)-(10)	23.8

* With the orthogonal unit vector I parallel to A , K perpendicular to A in the AC plane and J perpendicular to the AC plane.

Norton, 1970). The independent molecules are virtually identical. Both approximate to a planar Br-C=O-Br

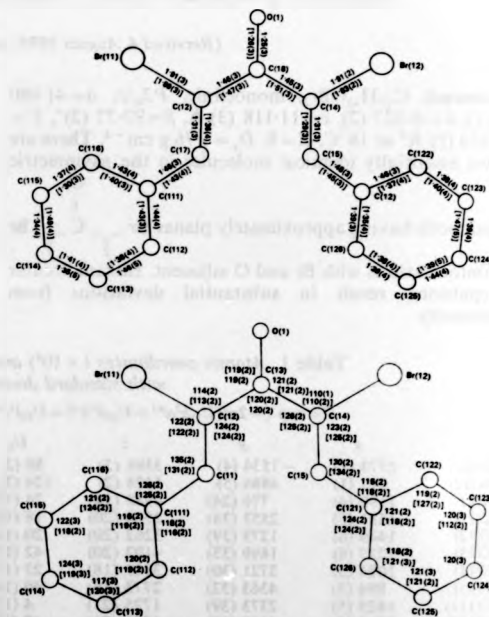
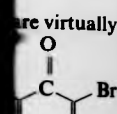


Fig. 1. Atomic numbering, bond lengths and angles (in square brackets for the second molecule) with standard deviations in parentheses. For the second molecule, the initial digit in each atom's number is (2) instead of (1).



are virtually

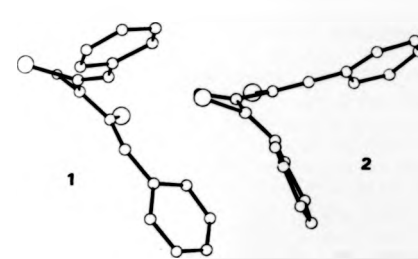
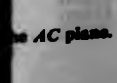
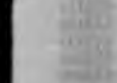
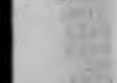
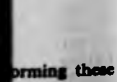
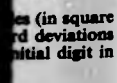
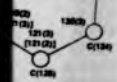
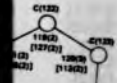
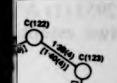
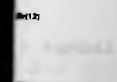
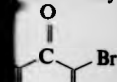


Fig. 2. Views of the two molecules showing the deviations from planarity.

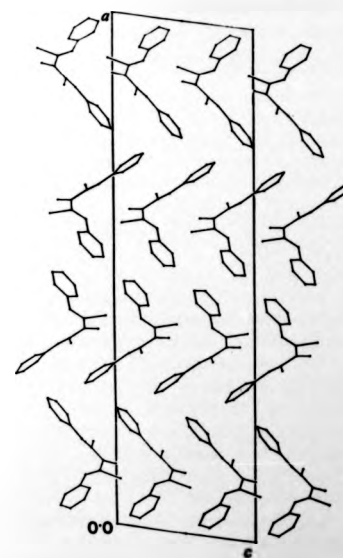


Fig. 3. Packing diagram, viewed down b . The rows contain respectively (from the bottom) molecules 1, 2, 1, 2, those in each row being related by the glide plane.

conformation with Br and O adjacent. This probably arises because rotation by 180° about either C-C bond would lead to Br-H or Br-Br repulsion. Maximum π -

conjugation requires the molecule to be completely planar,* but intramolecular repulsions lead to large deviations from this. Each C=O is twisted out of the

plane on either side of it by angles of between 22 and 32° , with the Br atoms on opposite sides of the

plane. This still leaves comparatively short O-Br contacts of $2.93\text{--}2.95 \text{ \AA}$. Further, the phenyl rings are twisted out of plane by between 24 and 32° to increase the Br-H(*ortho*) contact distances resulting in values between 2.61 and 2.78 \AA (H in calculated posi-

tions). The (Ph)C-C angles are also substantially larger than expected, presumably for the same reason. Other bond lengths and angles have normal values.

The molecular packing (Fig. 3) proved not to be controlled by Br...O secondary bonds. Instead, the phenyl rings take up the typical herring-bone arrangement.

We thank Professor Shoppee for drawing our attention to this problem, and the S. R. C. for a research studentship (J.F.S.) and a grant for the diffractometer (N.W.A.).

* This is found in 1,5-diphenylpenta-1,4-dien-3-one itself [investigated as its uranyl complex (Alcock, Herron, Kemp & Shoppee, 1975)].

References

- ALCOCK, N. W. (1972). *Advanc. Inorg. Radiochem.* **15**, 1-58.
- ALCOCK, N. W., HERRON, N., KEMP, T. J. & SHOPPEE, C. W. (1975). To be published.
- CROMER, D. T. & MANN, J. B. (1968). *Acta Cryst.* **A24**, 321-324.
- GERMAIN, G. & WOOLFSON, M. M. (1968). *Acta Cryst.* **B24**, 91-96.
- PECK, D. N., DUAX, W. L., EGER, C. & NORTON, D. A. (1970). *Amer. Cryst. Assoc. Abstracts*, Summer 1970, 71 (L6).
- SHOPPEE, C. W. & COOKE, B. J. A. (1973). *J. Chem. Soc. Perkin I*, pp. 2197-2199.
- X-RAY system (1972). Technical Report TR-192 of the Computer Science Center, Univ. of Maryland, June 1972.

Secondary Bonding. Part 2.¹ Crystal and Molecular Structures of Diethyltin Dichloride, Dibromide, and Di-iodide

By Nathaniel W. Alcock and Jeffery F. Sawyer, Department of Molecular Sciences, University of Warwick, Coventry CV4 7AL

Reprinted from

JOURNAL
OF
THE CHEMICAL SOCIETY

DALTON TRANSACTIONS

1977

Secondary Bonding. Part 2.¹ Crystal and Molecular Structures of Diethyltin Dichloride, Dibromide, and Di-iodide

By Nathaniel W. Alcock and Jeffery F. Sawyer, Department of Molecular Sciences, University of Warwick, Coventry CV4 7AL

The crystal and molecular structures of the diethyltin dihalides, R_2SnX_2 [(1) $X = Cl$, (2) $X = Br$, (3) $X = I$], have been determined from diffractometer data. Crystal parameters are: (1), monoclinic, space group $P2_1/c$, $a = 9.677(3)$, $b = 9.835(2)$, $c = 9.243(3)$ Å, $\beta = 102.73(2)^\circ$, $Z = 4$, 811 observed reflections, $R = 0.047$; (2), orthorhombic, space group $C222_1$, $a = 9.786(2)$, $b = 10.006(3)$, $c = 9.494(2)$ Å, $Z = 4$, 289 observed reflections, $R = 0.058$; (3), orthorhombic, space group $Pbcn$, $a = 13.469(4)$, $b = 5.385(2)$, $c = 13.733(4)$ Å, $Z = 4$, 342 observed reflections, $R = 0.049$. In (2) and (3), the individual molecules have crystallographic symmetry 2. All three compounds form chains of interacting molecules with each tin atom forming four primary and two secondary bonds such that the geometry may be described as intermediate between tetrahedral and octahedral. The lengths of the secondary bonds in (1) and (2) are 3.461(4) and 3.777(4) Å, 0.39 and 0.17 Å less than the sum of the respective van der Waals radii, with C-Sn-C angles opened to 134.0(6) and 135.9(10)°. For (3) the secondary bond distance is 4.284(5) Å, longer than the sum of the van der Waals radii, although the C-Sn-C angle [130.2(11)°] shows that the interaction is still stereochemically important. The packing in (3) also differs from that in (1) and (2).

The lengths of these secondary bonds are compared with other known examples in organotin(IV) chemistry, and factors influencing the strength of the interactions are discussed.

THERE have been a wealth of physical measurements made on organotin(IV) compounds since Sn is readily adaptable to many physical techniques. In particular, their crystal chemistry has been extensively investigated,² and there has been much discussion of molecular association.

This discussion concerns the significance of certain inter- and intra-molecular contact distances in the crystal, which are less than the sum of the relevant van der Waals radii. Furthermore, these interactions appear to be stereochemically important in affecting the primary geometry at the tin atom and the packing in the crystal. The name 'secondary bonds'³ has been suggested by us for these interactions, although other terms have been used.

These long bonds have been discussed in terms of electrostatic interactions between the atoms, but a more satisfactory description is in terms of three-centre four-electron ($3c-4e$) molecular orbitals.⁴ In a system of the type $Y-A \cdots X$, the secondary bond $A \cdots X$ is formed by donation from a lone pair on X into the σ^* orbital of the $Y-A$ primary bond. Alternatively (and equivalently), the interaction of the three σ -symmetry atomic orbitals (on Y, A, and X) gives a filled bonding molecular orbital concentrated between A and Y, a filled non-bonding or weakly bonding orbital concentrated between A and X, and an empty antibonding orbital. The overall scheme is identical to the MO description of the hydrogen bond.

This paper forms part of a systematic investigation of secondary bonding. Here the effect of the halogen and

organo-groups on the degree of association in the diorganotin dihalides are studied.

Previous Results.—Of the four diorganotin(IV) dihalides whose crystal structures are known, Me_2SnF_2 has the Sn atoms octahedrally co-ordinated by forming two *trans*-bonds to methyl groups and four equal Sn-F bonds (2.14 Å), giving a regular two-dimensional layer lattice.⁵ In both Me_2SnCl_2 (ref. 5) and $(CH_3Cl)_2SnCl_2$ (ref. 6) the tin atoms can be regarded as being four-co-ordinate, but it is also possible to distinguish infinite chains in the crystal held together by weak intermolecular interactions. The tin atoms are strongly distorted from the expected tetrahedrally co-ordinated arrangement by further secondary bonds to chlorine atoms of other molecules. In the crystal structure of Ph_2SnCl_2 , the original authors described the structure in terms of isolated molecules without any intermolecular tin-chlorine bridging.⁷ This has been criticised by Bokii *et al.*⁸ who point out that the Sn-Cl bond lengths are different, and that the chlorine atoms involved in the longer of the Sn-Cl bonds are also involved in short intermolecular interactions of 3.77–3.78 Å with the tin atoms of neighbouring molecules. These interactions produce linear groups of four molecules, the two terminal tin atoms remaining four-co-ordinate while the central tin atoms can be viewed as six-co-ordinate.

As well as the diorganotin(IV) dihalides, the crystal structures are known of several nominally four-co-ordinate dialkyltin(IV) compounds containing pseudo-halides⁹ and many trialkyl- and triaryl-tin(IV) halides

¹ Part 1, N. W. Alcock and R. M. C. Countryman, *J.C.S. Dalton*, 1977, 217.

² For reviews see R. Okawara and M. Wada, *Adv. Organometallic Chem.*, 1967, 8, 137; N. G. Bokii and Yu. T. Struchkov, *J. Struct. Chem.*, 1968, 9, 643; B. Y. K. Ho and J. J. Zuckerman, *J. Organometallic Chem.*, 1973, 69, 1; P. J. Smith, 'A Bibliography of Organotin X-ray Crystal Structures', No. 484, London, T.R.I., 1975.

³ N. W. Alcock, *Adv. Inorg. Chem. Radiochem.*, 1972, 15, 1.

⁴ E. O. Schlemper and D. Britton, *Inorg. Chem.*, 1966, 5, 995.

⁵ (a) J. D. Graybeal and D. A. Berta, U.S. Nat. Bur. Stand., Spec. Publ. No. 301, 1967, p. 393 (This structural analysis was based upon an incorrect space group); A. G. Davies, H. J. Milledge, D. C. Puxley, and P. J. Smith, *J. Chem. Soc. (A)*, 1970, 2802.

⁶ N. G. Bokii, Yu. T. Struchkov, and A. K. Prokofev, *J. Struct. Chem.*, 1972, 13, 619.

⁷ P. T. Greene and R. F. Bryan, *J. Chem. Soc. (A)*, 1971, 2549.

⁸ Y. M. Chow, *Inorg. Chem.*, 1970, 9, 794; 1971, 10, 673.

⁹ R. A. Forder and G. M. Sheldrick, *J. Organometallic Chem.*, 1970, 22, 611; J. Konnert, D. Britton, and Y. M. Chow, *Acta Cryst.*, 1972, B28, 190.

and pseudohalides.⁹ Three review articles¹⁰ have discussed the intermolecular bonding in the organometallic pseudohalides of several heavy atoms including tin in terms of donor-acceptor bonding. Most of these compounds are also associated in the crystal, and the secondary bonds to the O, S, and N ligands appear to be much stronger than those to chlorine. It also appears that some compounds which are not associated by secondary bonding at room temperature may be associated at lower temperatures. This is seen in triphenyltin(IV) chloride whose room-temperature crystal structure shows discrete molecules with the valence angles about the tin being very close to normal tetrahedral values.¹¹ The authors suggested that the significant difference in the ^{119}Sn n.q.r. spectra at 303 and 77 K (ref. 12) was due to the appearance of a polymeric structure with trigonal-bipyramidal tin and a weak secondary bond $Sn \cdots Cl$ (as has been suggested¹³ for Me_2SnCl_2) at the lower temperature. However, a recent series of Mössbauer measurements over a range of temperatures has failed to discover any gross structural changes in Ph_2SnCl_2 , whilst the association in Me_2SnCl_2 becomes stronger at lower temperatures.¹⁴

EXPERIMENTAL

The title compounds were recrystallised from dry isopentane, and to prevent air-moisture hydrolysis were sealed under nitrogen in Lindemann capillary tubes which had been baked *in vacuo* for several hours.

Crystal Data.—Unit-cell and space-group data are listed in Table 1. Unit-cell constants and their standard deviations were obtained from least-squares refinement of the

$\times 0.48$ mm bounded by the faces {001}, {010}, {100}. Systematic absences $h0l$, $l \neq 2n$; $0k0$, $k \neq 2n$, indicate space group $P2_1/c$. Reflections were measured using a θ - 2θ scan and scan range ($K_{\alpha_1} - 0.95$) to ($K_{\alpha_2} + 0.95$), to $2\theta_{max}$ of 50° . A variable scan-rate of 1.3 – $29.6^\circ \text{ min}^{-1}$ was used, depending on the intensity of a preliminary 2-s count. Background counts were recorded at each end of the scan. The intensities of 3 standard reflections monitored every 80 reflections showed a steady loss of intensity and the collected data were rescaled according to the equation $F = F_0(1 + 0.00065d)(1 + 0.00254 \sin \theta/\lambda \cdot t)$. The maximum rescale factor was 1.1458. 1709 Data were collected, of which 811 were considered observed having $I/\sigma(I) \geq 3.0$.

(b) Et_2SnBr_2 , Compound (2). Data were collected from a crystal of dimensions $0.211 \times 0.260 \times 0.343$ mm bound by the faces {110} and {001}. Systematic absences hkl , $h + k \neq 2n$; $00l$, $l \neq 2n$, indicate space group $C222_1$, with the Sn on special positions, symmetry 2. Reflections were measured as in (a), scan range ($K_{\alpha_1} - 0.9$) to ($K_{\alpha_2} + 0.9$), and variable scan rate of 1.5 – $29.3^\circ \text{ min}^{-1}$ to $2\theta_{max}$ of 55° . The intensities of 4 standard reflections recorded after every 50 reflections again showed a steady loss in intensity, and collected data were rescaled according to the equation $F = F_0(1 + 0.0004204d)(1 + 0.0012724 \sin \theta/\lambda \cdot t)$; maximum rescale factor 1.0524. Of 1263 data measured, including systematic absences due to the centering condition, 289 were considered observed.

(c) Et_2SnI_2 , Compound (3). Data were collected from a needle-shaped crystal, needle axis a (dimensions unknown). Systematic absences $0kl$, $k \neq 2n$; $h0l$, $l \neq 2n$; $hk0$, $h + k \neq 2n$, indicate space group $Pbcn$ with the Sn on special positions, symmetry 2. Reflections were measured as before, scan range ($K_{\alpha_1} - 0.9$) to ($K_{\alpha_2} + 0.9$), variable scan rate of 3 – $29.3^\circ \text{ min}^{-1}$ to $2\theta_{max}$ of 52° . The intensities

TABLE 1
Unit-cell data for the diethyltin(IV) dihalides

Compound	System	Space group	a/Å	b/Å	c/Å	$\beta/^\circ$	U/Å ³	Z	D_x	$\mu(\text{Mo-K}\alpha)/\text{cm}^{-1}$
Et_2SnCl_2	Monoclinic	$P2_1/c$	9.677(3)	9.835(2)	9.243(3)	102.73(2)	858.1(4)	4	1.92	35.35
Et_2SnBr_2	Orthorhombic	$C222_1$	9.786(2)	10.006(3)	9.494(2)		929.7(4)	4	2.40	117.70
Et_2SnI_2	Orthorhombic	$Pbcn$	13.469(4)	5.385(2)	13.733(4)		996.0(6)	4	2.87	97.61

diffracting positions of 15 reflections on a Syntex $P2_1$ diffractometer, by use of $Mo-K_{\alpha}$ radiation ($\lambda = 0.71069$ Å). D_x measurements were not made because of the moisture sensitivity of the crystals and their solubility in most organic solvents, although D_c values are in reasonable agreement with the values quoted for Me_2SnCl_2 and Ph_2SnCl_2 . All reflection data were collected on a Syntex $P2_1$ diffractometer under the following conditions, by use of graphite-monochromated Mo radiation.

(a) Et_2SnCl_2 , Compound (1). Data were collected from a needle-shaped crystal of dimensions 0.052×0.052

of 3 standard reflections recorded after every 80 reflections showed a steady drop in intensity, and collected data were rescaled in two sections according to the equations: $F = F_0(1 + 0.007655d)(1 - 0.004628 \sin \theta/\lambda \cdot t)$ for $t \leq 15.18$, and $F = F_0(1 + 0.0028323d)(1 - 0.0009808 \sin \theta/\lambda \cdot t)$ for $t > 15.18$; maximum rescale factor 1.0682. Of 1187 data measured, 342 were considered observed.

For compounds (1) and (2) Lorentz, polarisation, and absorption corrections were applied, the last with the program ABCOR.¹⁵ For (3) Lorentz and polarisation corrections were made, but crystal decomposition prevented

¹⁰ R. A. Forder and G. M. Sheldrick, *J.C.S. Dalton*, 1968, 1128; *J. Organometallic Chem.*, 1970, 21, 115; R. Hulme, *J. Chem. Soc.*, 1963, 1524; N. Kasai, K. Yasuda, and R. Okawara, *J. Organometallic Chem.*, 1968, 8, 172; E. O. Schlemper and D. Britton, *Inorg. Chem.*, 1966, 5, 507; Y. M. Chow and D. Britton, *Acta Cryst.*, 1971, B27, 866; H. C. Clark, R. J. O'Brien, and J. Trotter, *J. Chem. Soc.*, 1964, 2232; J. B. Hall and D. Britton, *Acta Cryst.*, 1972, B28, 1123; A. M. Domingos and G. M. Sheldrick, *J. Organometallic Chem.*, 1974, 67, 287.

¹¹ J. S. Thayer and R. West, *Adv. Organometallic Chem.*, 1967, 15, 169; M. F. Lappert and H. Pyun, *Adv. Inorg. Chem. Radiochem.*, 1966, 8, 123; D. Britton, *Perspectives in Structural Chem.*, 1967, 1, 109.

¹² N. G. Bokii, G. N. Zhabkova, and Yu. T. Struchkov, *Zh. strukt. Khim.*, 1970, 11, 895.

¹³ P. Green and J. Graybeal, *J. Amer. Chem. Soc.*, 1967, 89, 4305; T. Srivastava, *J. Organometallic Chem.*, 1967, 10, 373.

¹⁴ H. A. Stöckler, personal communication, quoted in *J. Amer. Chem. Soc.*, 1968, 90, 3224; A. G. Davies, H. J. Milledge, and D. C. Puxley, unpublished work, quoted in M.T.P. Internat. Rev. Sci., 1972, 4, 290.

¹⁵ G. M. Bancroft, K. D. Bulter, and T. K. Sham, *J. Chem. Soc. (A)*, 1975, 1463.

¹⁶ N. W. Alcock, 'The Analytical Method for Absorption Correction,' in 'Crystallographic Computing,' ed. F. Ahmed, Munksgaard, Copenhagen, 1970.

any measurement of the dimensions of the crystal for absorption correction.

In all three cases, structure solution was attempted successfully, using three-dimensional Patterson maps to

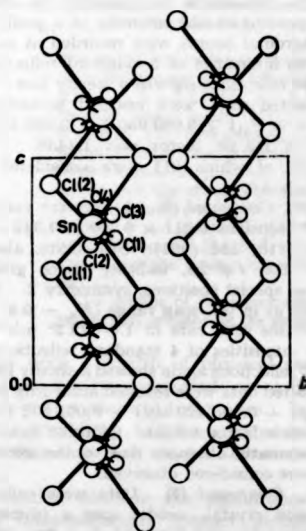


FIGURE 1 Et_3SnCl , projected down a ; primary bonds are shown closed; secondary bonds open

locate the heavy atoms and Fourier maps to locate the other non-hydrogen atoms. Block-diagonal least-squares refinement with anisotropic temperature factors for all atoms, with correction for the effects of anomalous dispersion, produced final R factors of 0.047 (1), 0.058 (2), and

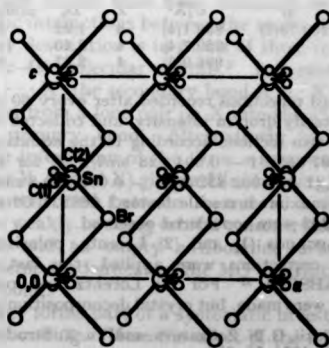


FIGURE 2 Et_3SnBr , projected down a

0.049 (3). The weights used were based on counting statistics. Scattering factors for neutral non-hydrogen atoms were taken from ref. 16. Computing was on an ICL 4130 computer with the programs of Dr. D. Russell. Final co-ordinates are listed in Table 2, significant bond

* See Notice to Authors No. 7, in *J.C.S. Dalton*, 1976, Index issue.

lengths and angles in Table 3. Structure factors and anisotropic thermal parameters for the three compounds are listed in Supplementary Publication No. SUP 21983

TABLE 2

Atomic co-ordinates ($\times 10^4$) with standard deviations in parentheses

Atom	X	Y	Z
(1) Et_3SnCl			
Sn	2 788(1)	2 312(1)	7 006(1)
Cl(1)	2 774(5)	705(4)	5 071(4)
Cl(2)	2 738(4)	672(4)	8 898(4)
C(1)	751(14)	3 238(15)	6 542(16)
C(2)	-413(20)	2 217(25)	6 152(34)
C(3)	4 912(16)	3 100(15)	7 494(18)
C(4)	6 028(16)	2 021(18)	7 800(20)
(2) Et_3SnBr			
Sn	431(3)	0(0)	5 000(0)
Br	2 100(3)	49(21)	3 002(3)
C(1)	-420(26)	1 956(25)	4 745(31)
C(2)	393(28)	3 001(31)	5 366(61)
(3) Et_3SnI			
I	1 245(1)	965(5)	1 531(1)
Sn	0(0)	4 080(6)	2 500(0)
C(1)	904(19)	5 829(54)	3 644(15)
C(2)	1 501(21)	3 739(77)	4 220(17)

(14 pp., 1 microfiche). * Views of the compounds are in Figures 1–3.

DISCUSSION

In all three compounds, the individual molecules interact to form chains. Probably as a result, there are significant angular distortions from tetrahedral values in the individual molecules. The values of the angles C-Sn-C and X-Sn-X are respectively $134.0(6)$ and

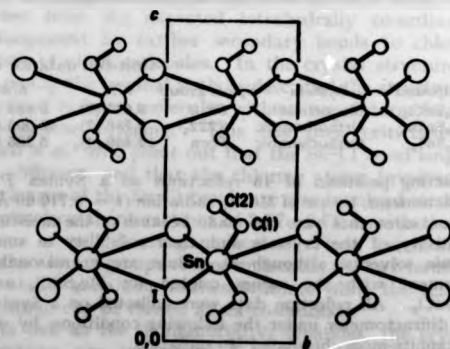


FIGURE 3 Et_3SnI , projected down a

96.0(1) for (1), 135.9(10) and 98.5(1) for (2), and 130.2(11) and 104.0(2)° for (3).

Although there are few other Sn-C(Et) bond distances available for comparison, there should be little difference between Sn-C(Me) and Sn-C(Et) . The Sn-C(Et) bond in dichloro(ethyl)hydroxotin¹⁷ is 2.90(3) Å and a large number of Sn-C(Me) distances in the solid state for a

¹⁶ 'International Tables for X-Ray Crystallography', vol. 3, Kynoch Press, Birmingham, 1962.

¹⁷ P. C. Lacombe, J. Protas, and M. Devaud, *Acta Cryst.*, 1976, B22, 922.

variety of distorted geometries at tin give Sn-C from 2.07 to 2.22 Å.¹⁸ The Sn-C distance in SnMe_4 has been determined most recently by gas-phase electron diffraction as 2.144(3) Å.¹⁹ The present values are quite close to those quoted, but they do seem to show a slight systematic increase from (1) to (3). For Sn-Cl bonds, electron diffraction has shown a regular contraction in the bond length with increasing halogen

The present mean Sn-Cl bond length 2.384 Å does not differ significantly from those for the other two dialkyltin dichlorides listed in Table 3 although it is ca. 0.04 Å longer than that in Ph_2SnCl_2 . It is clearly considerably longer than that in Me_4SnCl_2 in the gas phase.²⁰

Examples of Sn-Br and Sn-I bond distances are less numerous. The observed values [Sn-Br 2.505(4) and Sn-I 2.719(4) Å] are again longer than the gas-phase

TABLE 3

Bond distances (Å) and bond angles (°) with standard deviations in parentheses

(a) Distances	Sn-X	Sn-C	C-C	Sn...X	Δ^a	Sn...X ^b	X...X
Compound							
Me_4SnCl_2 ^c	2.40(4)	2.21(8)		3.54(5)	1.14	3.85	
$(\text{CH}_3\text{CH}_2)_2\text{SnCl}_2$ ^d	2.37(2)	2.18(7)		3.71 (3.21) ^e	1.34(0.84)		
Et_3SnCl ^f	2.386(3)	2.132(13)	1.452(25)	3.493(4)			
	2.384(4)	2.167(15)	1.471(22)	3.440(4)	1.08		3.544(6)
Et_3SnBr ^f	2.505(4)	2.162(26)	1.456(46)	3.777(4)	1.27	3.95	3.795(4)
Et_3SnI ^f	2.719(4)	2.178(27)	1.573(49)	4.284(5)	1.565	4.08	
Ph_2SnCl_2 (1) ^g	2.353(2)	2.119(5)		3.78	1.44		4.284(3)
(2)	2.336(2)	2.105(5)				3.85	
(3)	2.357(2)	2.118(5)		3.77	1.44		
(4)	2.336(2)	2.112(5)					
(b) Angles							
Compound	X-Sn-X	C-Sn-C	C-Sn-X	Sn-C-C	X...Sn-X	Sn...X-Sn	
Me_4SnCl_2	93.0(20)	123.5(45)	109.0(45)				
$(\text{CH}_3\text{CH}_2)_2\text{SnCl}_2$	97.0(20)	135.0(60)	105.0(20)				
Et_3SnCl	96.0(1)	134.0(6)	106.3(4)	112.1(12)	173.0(1)	104.0(1)	
			105.4(4)	113.6(10)	172.0(1)	102.8(1)	
Et_3SnBr	98.5(1)	135.9(10)	97.5(9)	114.0(20)	179.5(5)	98.2(1)	
Et_3SnI	104.0(2)	130.2(11)	106.6(8)	110.0(21)	158.0(1)	98.0(1)	
Ph_2SnCl_2 (1)	101.7(1)	123.9(2)	106.0(2)	108.8(2)			
(2)	97.8(1)	127.0(2)	106.5(2)	107.8(2)			
(3)			110.1(2)	105.0(2)			
(4)			107.1(2)	105.9(2)			

^a $\Delta = (\text{Sn} \cdots \text{X})$ minus (Sn-X) . ^b van der Waals distance, from A. Bondi, *J. Phys. Chem.*, 1964, 68, 441. ^c Ref. 5. ^d Ref. 6. ^e Value in parenthesis is Sn-Cl intramolecular distance. ^f This work. ^g Ref. 7.

substitution in the series Me_4SnCl_2 ($n = 1-4$). The Sn-Cl distances are 2.351(7) (Me_4SnCl_2), 2.327(3) (Me_3SnCl_2), 2.304(3) (Me_2SnCl_2), and 2.281(4) Å (SnCl_4). The Sn-C distances are essentially constant (2.104–2.108 Å).²⁰ The Sn-Cl distance in (chloromethyl)trichlorostannane is 2.340 Å, intermediate between those for Me_3SnCl and Me_4SnCl_2 , presumably owing to the inductive effect of the chloromethyl group.²¹

Crystallographic determinations of the Sn-Cl bond length have generally fallen in the range from 2.318 to 2.584 Å,²² with the length of the Sn-Cl bond increasing as the co-ordination of the tin changes from tetrahedral to octahedral. The longest recorded Sn-Cl distance is 2.696(3) Å in $[\text{Me}_3\text{SnCl}_2]^-$,²³ although bridging $\text{Sn} \cdots \text{Cl}$ distances of 2.805, 2.96, and 2.78 Å occur in the transition-metal complexes $[(\text{bipy})\text{Mo}(\text{CO})_2(\text{SnMeCl}_2)\text{Cl}]$, $[(\text{dth})\text{W}(\text{CO})_2(\text{SnMeCl}_2)\text{Cl}]$, and $[(\text{dth})\text{Mo}(\text{CO})_2(\text{SnCl}_2)\text{Cl}]$ ²⁴ ($\text{bipy} = \text{cis-bipyridyl}$, $\text{dth} = 2,5$ -dithiahexane).

¹⁸ T. K. Sham and G. M. Bancroft, *Inorg. Chem.*, 1975, 14, 2281.

¹⁹ M. Nagashima, H. Fujii, and M. Kimura, *Bull. Chem. Soc. Japan*, 1975, 48, 3708.

²⁰ B. Bagley, K. McAloon, and J. M. Freeman, *Acta Cryst.*, 1974, B30, 444; H. Fujii and M. Kimura, *Bull. Chem. Soc. Japan*, 1971, 44, 2643.

²¹ I. A. Ronova, N. A. Sinitsyna, Yu. T. Struchkov, and A. K. Prokofiev, *Zhur. strukt. Khim.*, 1973, 13, 18.

²² P. G. Harrison, T. J. King, and J. A. Richards, *J.C.S. Dalton*, 1974, 1723.

bond lengths in SnBr_4 and SnI_4 [2.44(2) and 2.64(4) Å],²⁵ while in crystalline SnBr_4 and SnI_4 the respective values are 2.41 and 2.69(2) Å.²⁶ Electron-diffraction measurements on Me_4SnX_2 ($\text{X} = \text{Br}$ and I) are probably not very accurate as the molecules were assumed to be tetrahedral and no allowance was made for scattering phase shift; in Me_4SnX_2 Sn-Br was 2.45(2) and Sn-I 2.69(3) Å, and for this series a contraction was reported with increasing halogen substitution,²⁷ although the values quoted above for SnX_4 seem not to bear this out.

Considering solid-state values, the observed Sn-Br value is in good agreement with that [2.504(5) Å] in (4-bromo-1,2,3,4-tetraphenyl-*cis,cis*-buta-1,3-dienyl)dimethyltin bromide which is also distorted from tetrahedral geometry by secondary-bond interactions.²⁷ In the two isomers of bis[1,2-bis(ethoxycarbonyl)ethyl]tin dibromide, Sn-Br distances of 2.516(6), 2.588(6), and

²³ P. J. Vergamini, H. Vahrenkamp, and L. F. Dahl, *J. Amer. Chem. Soc.*, 1971, 93, 6237.

²⁴ M. Elder and D. Hall, *Inorg. Chem.*, 1969, 8, 1368, 1373; R. A. Anderson and F. W. B. Einstein, *Acta Cryst.*, 1976, B32, 966.

²⁵ (a) M. W. Lister and L. E. Sutton, *Trans. Faraday Soc.*, 1941, 37, 393; (b) P. Brand and H. Sackmann, *Acta Cryst.*, 1963, 19, 446; F. Mellow and I. Fankuchen, *Acta Cryst.*, 1955, 8, 343.

²⁶ H. A. Skinner and L. E. Sutton, *Trans. Faraday Soc.*, 1944, 40, 164.

²⁷ F. P. Boer, J. J. Flynn, jun., H. H. Freedman, S. V. McKinley, and V. R. Sandel, *J. Amer. Chem. Soc.*, 1967, 89, 5068; F. P. Boer, G. A. Doorkin, H. H. Freedman, and S. V. McKinley, *ibid.*, 1970, 92, 1226.

2.504(5) Å were found in distorted octahedral structures.²² The only other examples of solid-state Sn-Br distances are for organotin-transition-metal compounds, where more complex bonding and packing effects occur, e.g. [(Br₃Sn)Fe(CO)₅(η -C₅H₅)] mean 2.501(2), [(Br₃Sn){Mn(CO)₅}₂] 2.548(2), and [(BrSn){Co(CO)₄}₂] 2.520(5) Å.²³ The mean value for [(Br₃Sn)Mo(η -C₅H₅)Br] is 2.506(8) Å, but this compound also possesses a long bridging Sn-Br distance of 3.411 Å (cf. ref. 24) which results in trigonal-bipyramidal geometry at the tin atom.^{24d}

The observed Sn-I for (3) also agrees with that [2.729(3) Å] in 1,4-bis(iododiphenyl)-1,4-distannabutane which contains a tetrahedral tin atom.²⁵

Intermolecular Interactions.—The strength of the intermolecular interactions can be deduced from the length of the secondary bonds and the angles around tin (especially C-Sn-C). In Et₃SnCl₂ and Et₃SnBr₂ the lengths of the secondary bonds (see Table 3) are 0.39 and 0.17 Å less than the sum of their appropriate van der Waals radii. The weakest interaction occurs in Et₃SnI₂, where the Sn...I secondary-bond distance [4.284(5) Å] is greater than the sum of the tin and iodine van der Waals radii. However, it can be argued that the interaction is still present since the value of the C-Sn-C angle of 130.2(11)° is much larger than the tetrahedral value. Taking into account only the difference between the secondary-bond distance and the sum of the van der Waals radii, it would appear that the strength of the secondary bonding is in the order Cl > Br > I. However, if the apparent difference in the C-Sn-C angle is genuine, then the order may be Cl \approx Br > I. It has also been suggested, from n.q.r. measurements, that bromine bridging is stronger than chlorine bridging.²¹ Zahrobaky,²⁶ by use of a simple stereochemical model which optimises the van der Waals forces between the bonded and neighbouring atoms (regarded as spheres), has predicted intermolecular distances of 3.81 and 4.11 Å for Me₃SnBr₂ and Me₃SnI₂. The distances quoted are reasonable although the steric requirements of the larger ethyl group might affect these results. However, this model only calculates the C-Sn-C angles as being 125 and 124° respectively.

The mode of bridging in the Et₃SnCl₂ and Et₃SnBr₂ chains is also different from that in Et₃SnI₂ where both bridging secondary bonds Sn...I involve the halogen atoms on the same neighbouring molecule (Figure 3). In Et₃SnCl₂ and Et₃SnBr₂ the distorted octahedral arrangement around each tin is completed by two secondary bonds involving the halogen atoms of two neighbouring molecules (Figures 1 and 2). Both

(CH₃Cl)₂SnCl₂ and Ph₃SnCl₂ associate in the same chelating manner as does Et₃SnI₂; Me₃SnCl₂, however, has the second bridging-type of association. It is not readily apparent which type of bridging arrangement a system containing secondary bonds will adopt, but the chelating bridges seems to be favoured with the longer weaker bonds. Brown and Shannon²⁸ have attempted to classify the bridging environments in certain inorganic structures using the bond valences of the bridging atoms, and this method may be applicable to secondary-bonded systems.

The lengths of the Sn...Cl secondary bonds (Table 3) can be compared to that [3.496(7) Å] for quinolinium trichlorodimethylstannate(IV) where this bond links two Me₃SnCl₂⁻ ions into dimeric units.²⁴ The cation here is very important since in [Me₃Sn(terpyridyl)]⁺[Me₃SnCl₂]⁻ the anion shows no Sn...Cl contacts < 3.7 Å;²⁵ nor does the ion [Me₃SnCl₂]⁻ in [Mo₃(η -C₅H₅)S₄][Me₃SnCl₂], although it does contain a very long Sn-Cl distance (2.696 Å).²⁵

The Sn...Br secondary bond in Et₃SnBr₂ has the same length [3.774(5) Å] as the intramolecular interaction of bromine with tin in (4-bromo-1,2,3,4-tetraphenyl-*cis,cis*-buta-1,3-dienyl)dimethyltin bromide (resulting in an axially substituted trigonal bipyramid with equatorial organic groups).²⁷ In that compound also, the C(butadienyl)-Sn-Me angle has opened to 129.0° and Me-Sn-Me to 112.7°. A series of analogous 4-chloro- and 4-bromo-compounds has been investigated in which Sn-Ph replaces Sn-Br. In these compounds, the interaction is drastically weakened so that the Sn...Cl (4.28) and Sn...Br distances (4.35 Å) are both greater than the sum of the two corresponding van der Waals radii. The difference in the two Sn...Br distances is 0.57 Å. Similarly the C(butadienyl)-Sn-Me angles are reduced to 116.5 (4-chloro) and 117.1° (4-bromo).²⁸

Factors affecting Intermolecular Interactions.—A CNDO calculation of the valence-electron distribution in a series of Sn^{IV} compounds has shown that for isolated halogeno(dimethyl)stannanes the 5s and 5p orbital occupancies are strongly dependent on the electronegativity of the halogen.²⁷ Although the methyl groups donate electrons to the tin, they are unable to replace all the electron density removed by the halogen atoms, leaving a slightly electron-deficient tin atom which can then form secondary bonds. The decreasing electronegativity of the halogens and decreasing overlap with the more diffuse orbitals on bromine and iodine would then qualitatively explain the observed strengths of the secondary interactions. There is also a clear

²² T. Kimura, T. Ueki, N. Yasuoka, N. Kasai, and M. Kakudo, *Bull. Chem. Soc. Japan*, 1966, **41**, 1113.

²³ (a) H. Probst, W. Wolfes, and H. J. Haupt, *Z. anorg. Chem.*, 1975, **413**, 131; (b) G. A. Melson, P. F. Stohely, and R. F. Bryan, *J. Chem. Soc. (A)*, 1970, 2247; R. D. Hall and D. Hall, *J. Organometallic Chem.*, 1973, **88**, 293; (c) T. S. Cameron and C. K. Probst, *J.C.S. Dalton*, 1973, 1447.

²⁴ V. Cody and E. Corey, *J. Organometallic Chem.*, 1966, **19**, 359.

²⁵ D. F. van de Vordel, H. Willemsen, and G. P. van der Kelen, *J. Organometallic Chem.*, 1973, **82**, 205.

²⁶ R. F. Zahrobaky, *J. Solid-State Chem.*, 1973, **8**, 101.

²⁷ I. D. Brown and R. D. Shannon, *Acta Cryst.*, 1975, **A30**, 266; I. D. Brown, *J. Solid-State Chem.*, 1974, **11**, 214.

²⁸ A. J. Buttenschaw, M. Duchene, and M. Webster, *J.C.S. Dalton*, 1975, 2320.

²⁹ F. W. B. Einstein and B. R. Penfold, *J. Chem. Soc. (A)*, 1968, 2010.

³⁰ F. P. Boer, F. P. van Ramoortere, P. P. North, and G. N. Reche, *Inorg. Chem.*, 1971, **10**, 539.

³¹ P. G. Furkine and D. H. Wall, *J. Chem. Soc. (A)*, 1971, 2630.

connection between secondary-bond strength and the nature of the organic group.

In Me_2SnCl_2 , Et_2SnCl_2 , and Et_2SnBr_2 the secondary bonding is considerably stronger than in Ph_2SnCl_2 . The effect of replacing methyl by ethyl in R_2SnCl_2 is to strengthen the intermolecular bonding by shortening the secondary bond from 3.54(5) to 3.461(4) (mean) Å with the corresponding C-Sn-C angle opening out from 123(4) to 134.0(6)°. These angles are still considerably less than in the more-associated dimethyltin pseudohalide compounds $\text{Me}_2\text{Sn}(\text{CN})_2$ [148.7(3.5)°] and $\text{Me}_2\text{Sn}(\text{NCS})_2$ [145.9(1.4)°]. The phenyl group produces a significant weakening of the secondary interaction as can be seen from Table 3 and from the dimethyl(tetraphenylbutadienyl)tin compounds already mentioned. This is presumably due to the ability of the phenyl group to involve available orbitals on the tin atom in inductive and mesomeric interactions so that they cannot overlap effectively with further orbitals. Similarly, the chloromethyl-group, with a reasonably strong inductive effect, also weakens the secondary bonding. However, the C-Sn-C angle of 135(6)° in $(\text{CH}_2\text{Cl})_2\text{SnCl}_2$ compared with 123.9(2) and 127.0(2)° in the two crystallographically independent Ph_2SnCl_2 molecules suggests a stronger interaction in the former. If the viewpoint of Bokii *et al.*⁶ is accepted, the difference of 4° between the C-Sn-C angles in the two Ph_2SnCl_2 molecules is directly attributable to secondary-bonding effects.

Hybridisation Models and Other Physical Measurements.

—The C-Sn-C angle is important when describing any tin hybridisation model and in interpreting other physical measurements made on tin. Sham and Bancroft,¹⁰ using a simple theoretical model, have correlated the ^{119}Sn Mössbauer quadrupole splittings with the C-Sn-C angle in a number of distorted $\text{Me}_2\text{Sn}^{\text{IV}}$ compounds. They find that Me_2SnCl_2 and $\text{Me}_2\text{Sn}(\text{NO}_2)_2$ lie in intermediate positions between the two predicted curves for Me_2SnL_2 and Me_2SnL_4 . Recent Mössbauer results have also shown that the amount of tin 5s character in the bonds from tin to transition metals and organic groups in the series of compounds $\text{X}_n\text{R}_{3-n}\text{SnM}$ [X = Cl, Br, or C_6F_5 ; R = Me or Ph; M =

$\text{Mn}(\text{CO})_5$ or $\text{Fe}(\text{CO})_5(\eta\text{-C}_5\text{H}_5)$] decreases in the order: $\text{Sn-Fe}(\text{CO})_5(\eta\text{-C}_5\text{H}_5) > \text{Sn-Mn}(\text{CO})_5 > \text{Sn-Me} > \text{Sn-Ph} > \text{Sn-C}_6\text{H}_5 > \text{Sn-Cl} \approx \text{Sn-Br}$. By use of this series they have rationalised the known distortions from tetrahedral geometry in several tin compounds.³⁰

The values of the coupling constants $J(^{119}\text{Sn-CH}_3)$ also indicate that the s character in the Sn-Me bonds decreases substantially as the C-Sn-C angle decreases.³⁰ There should be a corresponding increase in the Sn-C distance, which is not always readily seen owing to the difficulty of determining this distance accurately. The idea of a linear relationship between the $J(^{119}\text{Sn-CH}_3)$ values and the percentage s character in the Sn-C bonds was advanced by Holmes and Kesz⁴⁰ but has been criticised by McFarlane,⁴¹ van den Berghe and van der Kelen⁴² have since suggested that the coupling constants are proportional to the percentage s character of sp^2 hybrid orbitals only, since any d orbital involvement in bonding would increase orbital overlap and hence bond strength, whilst not increasing the amount of s character of the hybrid orbital.

In *trans*-octahedral complexes, the bonding may, therefore, be described in terms of sp^2 hybridisation of the tin with p_z and p_x orbitals used in the equatorial bonds.⁴³ The resulting equatorial bonds should then be longer than those observed for tetrahedral compounds as is generally found (*cf.* Ph_2SnCl_2 and Et_2SnCl_2). In the present compounds (1)–(3), which are clearly intermediate between tetrahedral and *trans*-octahedral, the tin hybridisation must be intermediate between sp^3 and sp and involvement of the 3d orbitals is possible. The Mössbauer parameters and other physical measurements have been made on the present compounds as well as on a series of related mixed-halogen species.⁴⁴

We thank Dr. D. A. Armitage for samples of the diethyltin halides, and the S.R.C. for a research studentship (to J. F. S.) and a grant for the diffractometer (to N. W. A.).

[6/1562 Received, 9th August, 1976]

¹⁰ G. M. Bancroft, K. D. Butler, A. T. Rake, and B. Dale, *J. C. S. Dalton*, 1972, 2025.

³⁰ R. C. Poller, 'Chemistry of Organotin Compounds,' Academic Press, New York, 1970.

⁴⁰ J. R. Holmes and H. D. Kesz, *J. Amer. Chem. Soc.*, 1961, **83**, 3903.

⁴¹ W. McFarlane, *J. Chem. Soc. (A)*, 1967, 528.

⁴² E. V. van den Berghe and G. P. van der Kelen, *J. Organometallic Chem.*, 1968, **11**, 479.

⁴³ First suggested by M. M. McGrady and R. S. Tobias, *J. Amer. Chem. Soc.*, 1965, **87**, 1909, although equatorial bonding has been discussed in terms of 3c-4e orbitals by e.g. E. O. Schlemper, *Inorg. Chem.*, 1967, **6**, 2012 and 1973, **12**, 677. See also E. M. Shustorovich and Yu. A. Buslaev, *Inorg. Chem.*, 1976, **15**, 1142, and refs. therein, for a discussion of the mutual *cis-trans* influences of ligands and the application of hypervalent bonding theory in main-group co-ordination compounds. This paper also contains an energy-level diagram showing the relative energy positions that organo- and halogen atoms adopt in relation to the energy levels of the main-group elements.

⁴⁴ D. A. Armitage, to be published.

**Preparation and X-Ray Structure of a Novel Pseudo-polyhalide
Anion $[\text{Me}_2\text{N}(\text{ICl})_2]^-$**

By NATHANIEL W. ALCOCK, STEINAR ESPERÅS, and JEFFERY F. SAWYER
(*Department of Molecular Sciences, University of Warwick, Coventry CV4 7AL*)

and NEIL D. COWAN, CLIFFORD J. LUDMAN, and THOMAS C. WADDINGTON
(*Department of Chemistry, University of Durham, South Road, Durham DH1 3LE*)



Reprinted from

**Journal of The Chemical Society
Chemical Communications
1977**

The Chemical Society, Burlington House, London W1V 0BN

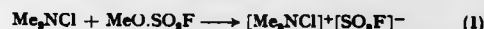
Preparation and X-Ray Structure of a Novel Pseudo-polyhalide Anion $[\text{Me}_2\text{N}(\text{ICl})_2]^-$

By NATHANIEL W. ALCOCK, STEINAR ESPERÅS, and JEFFERY F. SAWYER
(Department of Molecular Sciences, University of Warwick, Coventry CV4 7AL)

and NEIL D. COWAN, CLIFFORD J. LUDMAN, and THOMAS C. WADDINGTON
(Department of Chemistry, University of Durham, South Road, Durham DH1 3LE)

Summary The reaction of dimethylchloramine with an excess of iodomethane at room temperature gives a yellow crystalline material which has been shown by low temperature X-ray analysis to contain the $[\text{Me}_2\text{N}]^+$ cation and the novel anion $[\text{Me}_2\text{N}(\text{ICl})_2]^-$ which can be regarded as having the structure (A), analogous to $[\text{I}_3]^-$ with $[\text{NMe}_2]^-$ as a pseudo-halide ion.

DURING the study of the halogen-substituted ammonium cations, the reactions of dimethylchloramine with a series of potential alkylating agents were investigated and it was found that powerful alkylating agents such as methyl fluorosulphate gave salts of the colourless trimethylchloroammonium ion [equation (1)].

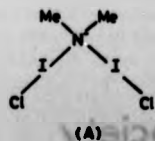


In contrast to this, when dimethylchloramine was dissolved in an excess of iodomethane at room temperature, a fine yellow solid slowly precipitated. The elemental analysis showed the compound to have the empirical formula $\text{C}_2\text{H}_5\text{ClIN}$. The product was formed quantitatively on the dimethylchloramine taken, with respect to equation (2).



The compound represented an isomer of the known adduct of trimethylamine with iodine monochloride,¹ but the i.r. spectrum clearly showed that the compound was of a different structure. Crystals of the compound were obtained by its slow preparation in tetrahydrofuran at 243 K over a number of months.

Crystal data: $\text{C}_2\text{H}_5\text{ClIN}$, M 442.92, monoclinic, $a = 11.233(3)$, $b = 5.773(1)$, $c = 11.087(2)$ Å, $\beta = 98.24(2)^\circ$, $U = 711.6(3)$ Å³, $D_c = 2.067$ for $Z = 4$, $D_m = 2.08$ g cm⁻³, Mo-K α radiation, $\lambda = 0.7107$ Å, space group $P2_1/c$.



The crystals decompose in a few hours at 20 °C, so all X-ray work was performed at -60 °C using a Syntex P2₁ diffractometer with an LT-1 low temperature device. Three-dimensional data were collected to a maximum 2θ of 60° and reduced to 1855 observed reflections ($I/\sigma(I) \geq 3.0$). The structure was solved by Patterson methods. The crystals are invariably twinned ($a' = c$) but the effects

of this were removed by excluding all data with $\sin \theta/\lambda < 0.5$ from the final refinement. Least-squares refinement using the remaining 1045 reflections resulted in an R factor of 0.066 (I and Cl with anisotropic temperature factors).†

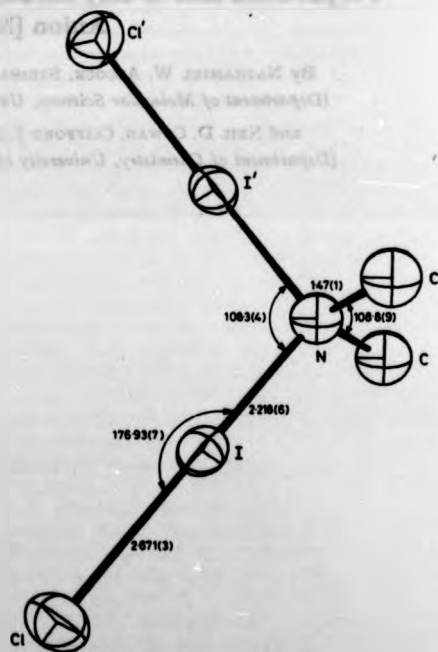


FIGURE 2. Structure of the $[\text{Me}_2\text{N}(\text{ICl})_2]^-$ ion. Primed atoms are related to unprimed ones by the crystallographic 2-fold axis. Bond distances are in Å.

The crystal has been found to consist of $[\text{NMe}_2]^+$ and $[\text{Me}_2\text{N}(\text{ICl})_2]^-$ ions, each with crystallographic two-fold symmetry (Figure). The only possible analogues to the novel anion are the polyhalide anions, in particular $[\text{I}_3]^-$ which exists as a nearly planar V-shaped ion.² In parallel with this, the present anion can be regarded as having the structure (A) with $[\text{Me}_2\text{N}]^-$ considered as a new pseudo-halide. The N-I and I-Cl distances in the anion are 2.918(6) and 2.671(3) Å, respectively, and the N-I-Cl system is very nearly linear [$\angle \text{N-I-Cl} = 176.9(1)^\circ$].

† The atomic co-ordinates for this work are available on request from the Director of the Cambridge Crystallographic Data Centre, University Chemical Laboratory, Lensfield Road, Cambridge CB2 1EW. Any request should be accompanied by the full literature citation for this communication.

Other angles around nitrogen have values close to those for a tetrahedron. The I-Cl bond length is considerably longer than in gaseous ICl (2.321 Å)³ or in the adducts of iodine monochloride with pyridine (2.510 Å),⁴ 2-chloroquinoline (2.446 Å),⁵ and trimethylamine (2.52 Å).¹ The observed N-I distance is shorter than the N-I bond lengths in the same adducts (2.29, 2.43, and 2.30 Å, respectively). However, the N-I distance is longer than the single N-I bond lengths of 2.09 and 2.14 Å observed in the adducts $\text{NI}_3 \cdot \text{C}_2\text{H}_5\text{N}$ and $\text{NI}_3 \cdot \text{L}_3\text{C}_2\text{H}_5\text{N}$,⁶ though the former also has a longer N-I bond of 2.36 Å to a further iodine linking NI_3 tetrahedra together.

If the bonding in the present anion is described in terms of charge transfer interactions between lone pairs of electrons on the nitrogen atom and two iodine monochloride molecules, the short N-I and long I-Cl distances

indicate that these interactions are the strongest so far observed for iodine monochloride adducts.

The study of this and similar compounds is continuing. When dimethylbromamine is treated with methyl iodide, the corresponding bromo-compound is produced, formulated as $[\text{Me}_2\text{N}]^+[\text{Me}_2\text{N}(\text{IBr})_2]^-$, but the interaction of dimethylchloramine with methyl bromide gives the compound Me_2NBrCl . When methyl chloride is used as the alkylating agent, only decomposition products of the chloramine are obtained.

We thank the S.R.C. for a grant for the diffractometer (to N.W.A.), for research studentships (to J.F.S. and N.D.C.), and for postdoctoral support (to S.E.).

(Received, 24th March 1977; Com. 279.)

¹ O. Hassel and H. Hope, *Acta Chem. Scand.*, 1960, 14, 391.

² E. H. Wiebenga, E. E. Havinga, and K. H. Boswijk, *Adv. Inorg. Chem. Radiochem.*, 1961, 3, 148.

³ E. Hulthen, N. Johansson, and U. Pilsäter, *Arkiv Fysik*, 1959, 14, 31.

⁴ C. Remming, *Acta Chem. Scand.*, 1972, 26, 1555; G. Eia and O. Hassel, *ibid.*, 1956, 10, 139.

⁵ G. Bernardinelli and R. Gerdil, *Acta Cryst.*, 1976, B32, 1906.

⁶ H. Hartl and D. Ullrich, *Z. anorg. Chem.*, 1974, 409, 228; H. Pritzkow, *ibid.*, 1974, 409, 237.

Isomeric *Hypho* Borane Structures $B_2H_4 \cdot L$ [$L = (Ph_2P)_2CH_2$, $(Ph_2PCH_2)_2$, or $(Me_2NCH_2)_2$]; X-Ray Crystal and Molecular Structures

By NATHANIEL W. ALCOCK,* HOWARD M. COLQUHOUN, GERALD HARAN, JEFFREY F. SAWYER,
and MALCOLM G. H. WALLBRIDGE†

(Department of Molecular Sciences, University of Warwick, Coventry CV4 7AL)



Reprinted from

**Journal of The Chemical Society
Chemical Communications
1977**

The Chemical Society, Burlington House, London W1V 0BN

Isomeric *Hypho* Borane Structures B_5H_5L [$L = (Ph_2P)_2CH_2$, $(Ph_2PCH_2)_2$, or $(Me_2NCH_2)_2$]; X-Ray Crystal and Molecular Structures

By NATHANIEL W. ALCOCK,* HOWARD M. COLQUHOUN, GERALD HARAN, JEFFREY F. SAWYER, and MALCOLM G. H. WALLBRIDGE†

(Department of Molecular Sciences, University of Warwick, Coventry CV4 7AL)

Summary The X-ray crystal structures of the 1:1 complexes, containing *hypho* boron polyhedra, derived from pentaborane(9) and the ligands bis(diphenylphosphino)methane (dppm), bis(diphenylphosphino)ethane (dppe), and tetramethylethylenediamine (tmed) are reported; the dppm and dppe structures both show the phosphorus atoms bridging the apical and basal atoms of a flattened pyramidal B_5 framework (with rearrangement of the hydrogen atoms), the tmed complex differing markedly, with the ligand chelating one of the originally basal boron atoms, which becomes singly bonded to the apical boron atom and is separated from the remaining basal atoms by typical non-bonded contact distances.

THE boranes and carboranes form *closo*-, *nido*-, *arachno*-, and *hypho*-derivatives,¹ and a knowledge of all these classes is required before their co-operative role in rearrangement reactions of polyhedral frameworks, or as reaction intermediates can be fully rationalised.² Unfortunately, very few examples of the *hypho*-class are known. Such systems should possess $(n+4)$ skeletal electron pairs with the framework atoms occupying n vertices of an $(n+3)$ vertex polyhedron, and some support for this proposal has come from the crystal structures of the adducts $B_5H_5 \cdot 2L$ and $B_5H_5 \cdot 2L$ ($L = PMe_2$).^{3,4} We now report the properties and crystal structures of three further derivatives which are isoelectronic with the hypothetical *hypho*- B_5H_5 ion, viz. $B_5H_5 \cdot L$ [$L = dppm$, (I); $dppe$, (II); and $tmed$, (III)†] and which show significant differences, illustrating the diversity possible within such a related series.

The colourless adducts (I) (m.p. 185–187 °C), and (II) (m.p. 180–182 °C) were prepared by stirring equimolar quantities of B_5H_9 and the ligand in tetrahydrofuran

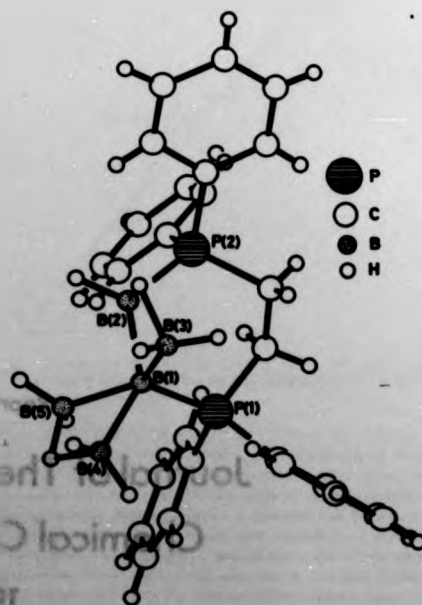


FIGURE 1. General view of molecule of (II). Distances P(1)–B(1) and P(2)–B(5) are 1.963(4) and 1.959(4) Å, respectively.

† dppm = bis(diphenylphosphino)methane, dppe = bis(diphenylphosphino)ethane, tmed = tetramethylethylenediamine.

(THF) at 25 °C for 72 h; variations in the conditions led to high-melting polymeric products. Both adducts are stable in air, and only slowly hydrolysed by hot water or acid, which is remarkable for B_5H_9 derivatives. However, the anions, $B_5H_5 \cdot L^-$ ($L = dppm$ or $dppe$), are similar to B_5H_5 itself, and are readily hydrolysed. The adduct (III), obtained by condensing an excess of B_5H_9 on the ligand, was air-sensitive and could only be stored or recrystallised without decomposition if an excess of ligand was present.

Crystal data: (I), $C_{20}H_{18}B_5P_2$, M_r 481.5, orthorhombic, $a = 7.931(4)$, $b = 16.816(5)$, $c = 23.271(8)$ Å, $U = 3105(2)$ Å³, $D_o = 1.03$ g cm⁻³, $Z = 4$, space group $P2_12_12_1$. (II), $C_{20}H_{20}B_5P_2$, M_r 461.6, orthorhombic, $a = 14.297(4)$, $b = 16.492(6)$, $c = 22.280(9)$ Å, $U = 5243(3)$ Å³, $D_o = 1.17$ g cm⁻³, $Z = 8$, space group Pbc_2 . (III), $C_8H_{12}B_5N_4$, M_r 179.3, orthorhombic, $a = 12.940(2)$, $b = 12.911(3)$, $c = 15.046(2)$ Å, $U = 2513.9(8)$ Å³, $D_o = 0.95$ g cm⁻³, $Z = 8$ (2 independent molecules), space group $P2_12_12_1$.

Three-dimensional X-ray data for all three compounds were collected on a Syntex P2₁ diffractometer using Mo- K_α radiation ($\lambda = 0.71069$ Å). 1850, 2643, and 1200 independent reflections with $I/\sigma(I) > 3.0$ were collected for compounds (I), (II), and (III), respectively. All three structures were solved using the direct methods programs NORMAL and MULTAN. Block diagonal least-squares refinement has produced R factors of 0.070 (I), 0.047 (II), and 0.062 (III), using anisotropic temperature factors for all non-hydrogen atoms except for the disordered THF solvent in (I) and for one of the tmed ligands in (III) which exists in two different conformations.†

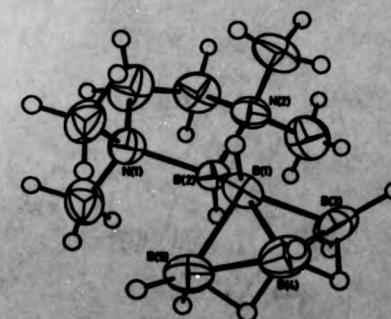
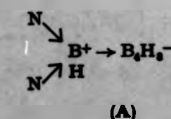


FIGURE 2. ORTEP view of the ordered molecule of (III). Some distances are: N(1)–B(3), 1.994(9); N(2)–B(5), 1.993(9); B(1)–B(3), 1.718(10); B(1)–B(5), 1.823(12); B(1)–B(4), 1.896(12); and B(1)–B(5), 1.806(12) Å. The non-bonded distances B(3) ... B(3) and B(5) ... B(5) are 2.728(12) and 2.718(11) Å, respectively.

In both $B_5H_5 \cdot dppm$ (I) and $B_5H_5 \cdot dppe$ (II) (Figure 1), the B_5H_5 species has become a shallow pyramid with major rearrangements of the hydrogen atoms; the hydrogen at the apex has moved to the base where three BH_2 groups and two symmetrical B–H–B bridges are found. The phosphorus atoms bridge the apical and basal positions, and the angle



similarities to adducts of the type $L \cdot B_5H_5$, where the B_5 fragment would be an *arachno* species.⁵ The parent polyhedron for (III) can again be seen as a hexagonal bipyramid [$\angle B(3)–B(4)–B(5)$ 108.2 and 107.0°] especially as the $B(1), B(3), B(4)–B(1), B(4), B(5)$ dihedral angles (129.4 and 127.4°) are higher than the value of 118.1° in B_5H_9 .⁶ A structure involving the ligand chelating at a single boron position was previously favoured on the basis of i.r. and n.m.r. evidence, although the arrangement of boron and hydrogen atoms was uncertain.⁶ A gross movement of one of the basal boron atoms also occurs when B_5H_9 is converted into $B_5H_5 \cdot 2PMe_2$, although in this case the resulting *hypho*- B_5 fragment forms an open framework resembling the equatorial belt of an icosahedron rather than occupying all but three vertices of a 9-vertex polyhedron such as a tricapped trigonal prism.⁴

The differences between the structures of (I) and (II) compared with (III) are surprising. In B_5H_5 there is residual negative charge at the apical boron atom, and the ability of the phosphine ligands to withdraw electron density through σ -type interactions might account for their preferential co-ordination at the apical position,^{7,8} while the co-ordination of tmed at the basal positions could be predicted since no π -effects are possible. The different

† The atomic co-ordinates for this work are available on request from the Director of the Cambridge Crystallographic Data Centre, University Chemical Laboratory, Lensfield Road, Cambridge CB2 1EW. Any request should be accompanied by the full literature citation for this communication.

framework arrangements in (I) and (II) and (III) could also reflect the need to delocalise the greater electron density placed on the B_3 skeleton by the tmed ligand, and the retention of an integral B_3 unit in (III) is significant in contrast to the two distinct B_3 fragments in (I) and (II). Finally, the presence of a chelate effect is apparent in all the adducts, the monodentate ligand species being much less stable, so that, for example, $B_3H_3 \cdot 2PPh_3$ is completely

dissociated at 25 °C.¹² We are investigating the influence of related ligands on the skeletal atom arrangement.

We thank the S.R.C. for a grant for the diffractometer (N.W.A.), for postdoctoral fellowships (H.M.C. and G.H.), and for a research studentship (J.F.S.).

(Received, 15th March 1977; Com. 252.)

¹ K. Wade, *Adv. Inorg. Chem. Radiochem.*, 1976, 18, 1.

² R. W. Rudolph and D. A. Thompson, *Inorg. Chem.*, 1974, 13, 2779.

³ A. V. Fratini, G. W. Sullivan, M. L. Denniston, R. K. Hertz, and S. G. Shore, *J. Amer. Chem. Soc.*, 1974, 96, 2013.

⁴ M. Mangion, R. K. Hertz, M. L. Denniston, J. R. Long, W. R. Clayton, and S. G. Shore, *J. Amer. Chem. Soc.*, 1976, 98, 449.

⁵ L. R. Lavine and W. N. Lipscomb, *J. Chem. Phys.*, 1954, 22, 614.

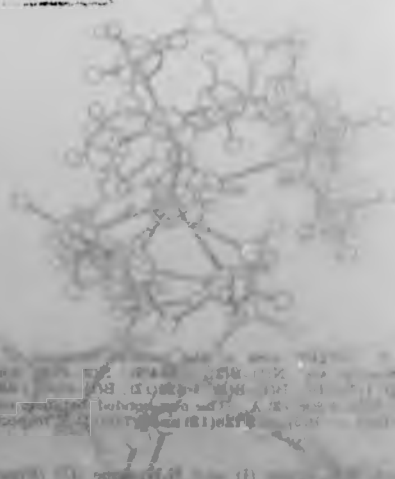
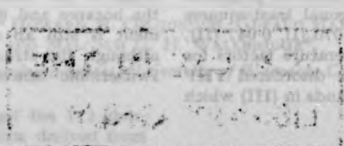
⁶ M. D. LaPrade and C. E. Nordman, *Inorg. Chem.*, 1969, 8, 1649.

⁷ C. E. Nordman and W. N. Lipscomb, *J. Chem. Phys.*, 1963, 21, 1856.

⁸ N. E. Miller, H. C. Miller, and E. L. Muetterties, *Inorg. Chem.*, 1964, 3, 867.

⁹ See however, M. R. Churchill, J. J. Hackbarth, A. Davison, D. D. Traficante, and S. S. Wreford, *J. Amer. Chem. Soc.*, 1974, 96, 4041.

¹⁰ C. G. Savory and M. G. H. Wallbridge, *J.C.S. Dalton*, 1973, 179.



(I) (II) (III)

Figure 3. General structure of the borane adducts.